Enzymology

of gentamicin biosynthesis

Anna Reva

Clare College

University of Cambridge

This dissertation is submitted for the degree of

Doctor of Philosophy.

September 2017

Enzymology of gentamicin biosynthesis

Anna Reva

Thesis summary

Gentamicin C complex is a mixture of five structurally similar aminoglycoside antibiotics, gentamicins C1, C1a, C2, C2a, and C2b, produced by the actinomycete bacterium *Micromonospora echinospora*. It is established in clinical use and despite significant toxicity remains valuable to treat severe Gram-negative bacterial infections. There is a pressing need to develop novel versions of such antibiotics to combat the rise of resistance among pathogens. Engineering of the pathway requires a detailed knowledge of the genes, enzymes, and intermediates involved.

The final steps of gentamicin biosynthesis begin at gentamicin X2, the last common intermediate of the C complex. 6'-*C*-Methylation generates two branches, with analogous reactions happening in both. Candidate genes and enzymes for the steps from the first 6'-*C*-methylated intermediate, G418, to an aminated metabolite JI-20B have already been described, but none for the subsequent loss of two hydroxyl groups from Ring II, or the *N*-methylation that then occurs. A novel separation method using dynamic countercurrent chromatography was successfully applied to the difficult purification of gentamicin metabolites. The first step from JI-20B was shown to be specific phosphorylation by GenP on the 3'-hydroxy group of Ring II. In the presence of the enzyme GenB3 this led to di-dehydroxylated products, including the known aminoglycoside verdamicin and its 6'-keto derivative. Further reaction in the additional presence of recombinant enzyme GenB4 generated gentamicin C2a, and the presence of recombinant enzyme GenB2 processed this in part to gentamicin C2. These results allowed a detailed mechanism to be proposed for almost the entire pathway from G418 to the C complex, and by analogy for the unbranched pathway, too.

The last step of the pathway is 6'-*N*-methylation of gentamicins C1a and C2. Genome mining and cell-free assays were used by the group of Professor Yuhui Sun (Wuhan University) to identify *genL*, a methyltransferase gene encoded elsewhere on the *M. echinospora* genome and capable of this catalysis. Here, *in vitro* reactions with recombinant GenL confirmed its function, and its kinetic parameters were measured with its substrates. The full mechanistic pathway for the late stages of gentamicin C complex biosynthesis has therefore now been elucidated.

Declaration

This dissertation is the result of my own work and includes nothing which is the outcome of work done in collaboration except as declared in the preface and specified in the text.

This work was carried out under the supervision of Professor Peter F. Leadlay in the Department of Biochemistry of the University of Cambridge between October 2013 and September 2017. It is not substantially the same as any I have submitted, or, is being concurrently submitted for a degree or diploma or other qualification at the University of Cambridge or any other University or similar institution except as declared in the Preface and specified in the text. I further state that no substantial part of my dissertation has already been submitted, or, is being concurrently submitted for any such degree, diploma or other qualification at the University of Cambridge or any other University or similar institution except as declared in the Preface and specified in the text.

It does not exceed the prescribed word limit for the Degree Committee for Biology (60,000 words).

Anna Reva

September 2017

Acknowledgements

I would like to take a moment to say Thank You to everyone who has helped me over the years to get to where I am now. Firstly, a great big Thank You to Professor Peter Leadlay for enabling me to join his lab and providing me with support and ideas over the course of my PhD. Thank you also for encouraging my brain to think and for allowing me to develop into a scientist. Thank you to Dr Fanglu Huang for her patience and supervision in teaching me everything I know. For sharing the joys and successes - as well as the hardships - of the gentamicin project with me, and for always sparing me all the time I needed. Thank you to everyone in our Lab for their time, ideas, and support. I have enjoyed my time with you immensely and I wish you all the best in life and science! Thank you for the laughter, the cakes, and the memories. And a special thank you to Oana Sadiq for making us into a fully-functioning lab.

To my parents, Tatjana Reva and Sergejs Reva, Thank You for always having the time to answer my never-ending questions. For bringing me up in love with this world and its beautiful nature, capable of finding the answers to my questions when they went beyond your knowledge, and not once stopping me when I wanted to buy yet another book. Thank You for being strong enough to let me go abroad. You both are truly the inspiration behind my story.

To my dearest Christopher Morton, a Thank You in all the languages of this world and the others. For your encouragements, for your knowledge and suggestions, for your help, advise, and understanding, above all for always being on my side as my better half and as my support. For allowing me to feel strong enough to continue doing science, for helping me feel less worthless at doing it, for knowing exactly how to get me interested again, and for all your love and eternal patience with me. Thank you also for giving me your family and to them for accepting me.

Thank you to Catherine and Martin D'Rozario, as well as Matt and Jonathan, for creating a space in your family for me and giving me the first insight into what life in the UK is about. Thank you for making me feel like I always had a home nearby to come back to.

To my friends Katsiaryna Usachova, Sebastian Walesch, Constance Wu, and Yue Zhang, in different labs all over the world - Thank you for your friendship and the jokes we shared together. To Kat and Helene Mobbs thank you for being friends outside the lab as well as in it.

To the three menaces Anastasija Nikitina, Dr Jana Bjornsone, and Marina Aleksejeva: you have my eternal gratitude for surviving school and adolescence together. Our adventures will forever be legendary and have made me into the woman I am.

To Cassandra Smith for being a great friend and helping with Phylogenetic analysis - Thank You. And for sharing the pain of applying to Cambridge, leaving Sheffield and doing a PhD. Thank you also for our discussions about science, research, and the literature world.

A massive Thank you to our collaborators in Wuhan university, Professor Yuhui Sun and his Lab, especially the gentamicin project scientists, Dr Chuan Huang and Sicong Li, for working on the *in vivo* side of the project, generating the *Micromonospora* mutants, and generous gifts of any substrates and intermediates required. Thank You to Sicong for exchange of ideas and encouragements!

Thank You's to Dr Svetlana Ignatova, Dr Ian Garrard, and Dr Peter Hewitson for having me over at the Brunel university and allowing me to use their Counter-current Chromatography machines. Thank you to Ian for explaining the basics of the science to me. Thank You to Svetlana for looking after me and teaching me the practical aspects of CCC - and on one memorable occasion, for the tastiest bowl of soup ever! Thank You to Peter for allowing me to finally be the one to press the buttons. I really enjoyed my time with you guys.

Thank you to Dr Finian Leeper for explaining NMR to me again, for help with NMR data analysis, for any mechanism ideas explained, and for taking on - along with Emma Thompson - parts of the project that I was not chemically-equipped to do.

Thank You's to Shilo Dickens, Reda Deglau, Nataliya Scott, and Anna Efimova for the best DNA sequencing facility a girl could ever dream of! Thank

you also for the friendship and the lunches together. To Dr Len Packman and Peter Sharratt of the Protein Analysis Facility - thank you for the analysis and help.

Thank you for extensive help with kinetics and analysis of kinetics to Dr Tommaso Moschetti and especially Dr Joseph Maman. You didn't deserve the continuous pestering but you stoically helped me anyway.

Thank you to Dr Dimitry Chirgadze, Dr Simon Quick, and Dr Paul Brear for training and help with crystal set-up. Thank you to our collaborator Dr Marcio Dias for help and advice on crystallography.

Thank you to Dr Katherine Stott for help and advice in the Biophysics lab. And Thank you to Dr Marko Hyvönen for teaching me the ways of the Emulsiflex. Thank you to Dr Peter Grice and Dr Duncan Howe of the Department of Chemistry for their extensive help with the NMR.

Thank you to my Graduate Thesis Panel members: Dr Marko Hyvönen, Dr Hee-Jeon Hong, Professor Ben Luisi, and my advisor Dr Florian Hollfelder for extra supportduring my PhD and ideas.

To all the Support staff, and especially David Plummer and Ian Saunders, Sharon Marshall, Sue Leach, and Christine McLoughlin, thank you for all the challenging work you put in daily to allow this place to continue running. Thank you to Graham Eloff and John Anderson for bringing us into the 21st century with internet and computers. Thank you to Trevor Sawyer for keeping us fire-proofed and for helping me with large-scale fermentations. Thank you to Jonathon Zelos and his team for fixing our equipment. A further Thank You for always having a minute for a smile and a Hello to all you.

Thank you to Elena Blagodarnaja, Marina Ivanova, and Cynthia Sandhu, and all my previous teachers for getting me through the education system with a fully preserved thirst for knowledge. I wish there were more teachers like you in this world.

Finally, I would like to thank Medical Research Council, Herchel Smith Scholarship, and Clare college for the funding to run this project. I hope that the money provided was used wisely, but only time will tell.

Table of Contents

List of Figures

List of Tables

List of Abbreviations

Abbreviation	Abbreviation expansion
2-DOI	2-Deoxyinososе
2-DOS	2-Deoxystreptamine
A_{xxx}	Absorbance at xxx nm wavelength
A	Adenine
AAC	*N*-acetyltransferases
ACAGA	Aminocyclitol-containing aminoglycoside antibiotics
ACP	Acyl carrier protein
AHBA	(*S*)-4-Amino-2-hydroxybutyryl chain
AHPA	(*S*)-3-Amino-2-hydroxypropyl side chain
AIDS	Auto-immune deficiency syndrome
AIM	Auto-inducible medium
ANT	*O*-nucleotidyltransferases
APH	*O*-phosphotransferases
apr	Apramycin cluster
ATCC	American type culture collection
ATP	Adenosine triphosphate
BLAST	Basic local alignment search tool
BSA	Bovine serum albumin
CCC	Counter-current chromatography
CD	Circular dichroism
CFTR	Cystic fibrosis transmembrane conductance regulator
COSY	Homonuclear correlation spectroscopy
DI	Deionised
DMD	Duchenne muscular dystrophy
DMSO	Dimethyl sulfoxide
DNA	Deoxyribonucleic acid
DSM or DSMZ	Deutsche Sammlung von Mikroorganismen und Zellkulturen
DTT	Dithiothreitol
EDTA	Ethylenediaminetetraacetic acid
for	Fortimicin cluster
G	Guanine
GC	Guanine cytosine
gen	Gentamicin cluster
GI	GenInfo identifier
GTP	Guanosine triphosphate
GYM	Glucose, yeast, malt
HIV	Human immunodeficiency virus
HPLC	High-Performance Liquid Chromatography
HSQC	Heteronuclear single quantum coherence spectroscopy
IEX	Ion exchange
IPTG	Isopropyl β-D-1-thiogalactopyranoside
JI-20	Jan Ilavsky-20
kan	Kanamycin cluster
LB	Luria-Broth
LC-MS	Liquid chromatography - mass spectrometry
LLC	Liquid-liquid chromatography

LP	Luca Pellegrini
MDR	Multidrug-resistant
MALDI	Matrix assisted laser desorption/ionization
MIC	Minimum inhibitory concentration
MOPS	3- (*N*-Morpholino)-propanesulfonic acid
MQ	Milli-Q®
mRNA	Messenger ribonucleic acid
MRSA	Methicillin-resistant *Staphylococcus aureus*
MS	Mass spectrometry
NADPH	Nicotinamide adenine dinucleotide phosphate
NHS	*N*-hydroxysuccinimidyl
NMR	Nuclear Magnetic Resonance
NOESY	Nuclear Overhauser Effect spectroscopy
A	Optical density
ORF	Open reading frame
PAGE	Polyacrylamide gel electrophoresis
PCR	Polymerase chain reaction
PEI	Polyethyleneimine
ppm	Parts per million
RBS	Ribosome binding site
RCF	Relative centrifugal force
RNA	Ribonucleic acid
ROS	Reactive oxygen species
rRNA	Ribonucleic acid
SAH	*S*-adenosyl-L-homocysteine
SAM	*S*-adenosyl-L-methionine
SDM	Site-directed mutagenesis
SDS	Sodium dodecyl sulphate
SEM	Scanning electron microscopy
SET	Sodium dodecyl sulphate, EDTA, Tris
SOC	Super optimal broth
TAE	Tris base - Acetic acid - EDTA
TB	Terrific broth
TEMED	Tetramethylethylenediamine
TFS	Trifluoroacetic acid
TLC	Thin layer chromatography
TMOS	Hydrolysed tetramethyl orthosilica
tRNA	Transfer ribonucleic acid
TSB	Tryptic soy broth
TWM	Tap water medium
UV	Ultra-violet
v/v	Volume by volume
w/v	Weight by volume
WHO	World Health Organization
YEME	Yeast extract - malt extract
YT	Yeast tryptone

1

Introduction

1.1 The development of antibiotic therapy

Herbal and fungal ingredients were used even by early humans to treat various ailments. The ancient Chinese, Greeks, and Egyptians knew about the anti-infective properties of plants and mould (Varley et al., 2009a). For example, mouldy soybean curd and cinchona tree bark were used as herbal remedies to treat diseases. Industrial production of drugs started in 1820 with the isolation of anti-malarial compound quinine from cinchona bark. Much later, Louis Pasteur

cured anthrax in animals by injecting them with extracts of soil bacteria in 1877 (Torok et al., 2009).

However, the growth of human population also led to spread of disease. In 1900 in the USA, a third of all deaths were due to pneumonia, tuberculosis, diarrhoea, and enteritis, of which 40% were in children below the age of 5 (Center for Disease Control and Prevention, 1999).

The discovery of antibiotics, starting with penicillin in 1928 and streptomycin in 1943, brought hope for effective treatment of infectious disease and started a new age of pharmaceutical chemistry (Davies, 2006, Aldridge, 1999). The First World War was the last major conflict where more people died from infections of non-lethal wounds than from hostile injuries (Driscoll, 2003). In the 20th century advances in microbiology and chemistry saw rapid progress in the isolation of microbial strains capable of killing human pathogens, and in the characterisation of the active antimicrobial substances, or antibiotics, that they were found to produce.

1.1.1 Antibiotic classification and modes of action

Antibiotics are secondary or specialised metabolites, produced by a wide range of life forms from plants to bacteria. The term was first used in 1889 by Vuillemin to describe an organism which is strictly antagonistic towards the life of another organism.

During what was termed the Golden Age, 1950-1960, more than one half of the currently-used therapeutics and most of the currently-known classes of antibiotics were discovered (Davies, 2006). Based on their chemical structure, antibiotics can be divided into nine main classes (Figure 1.1), within which they tend to have similar biosynthetic pathways, mechanisms of action, and mechanisms of toxicity.

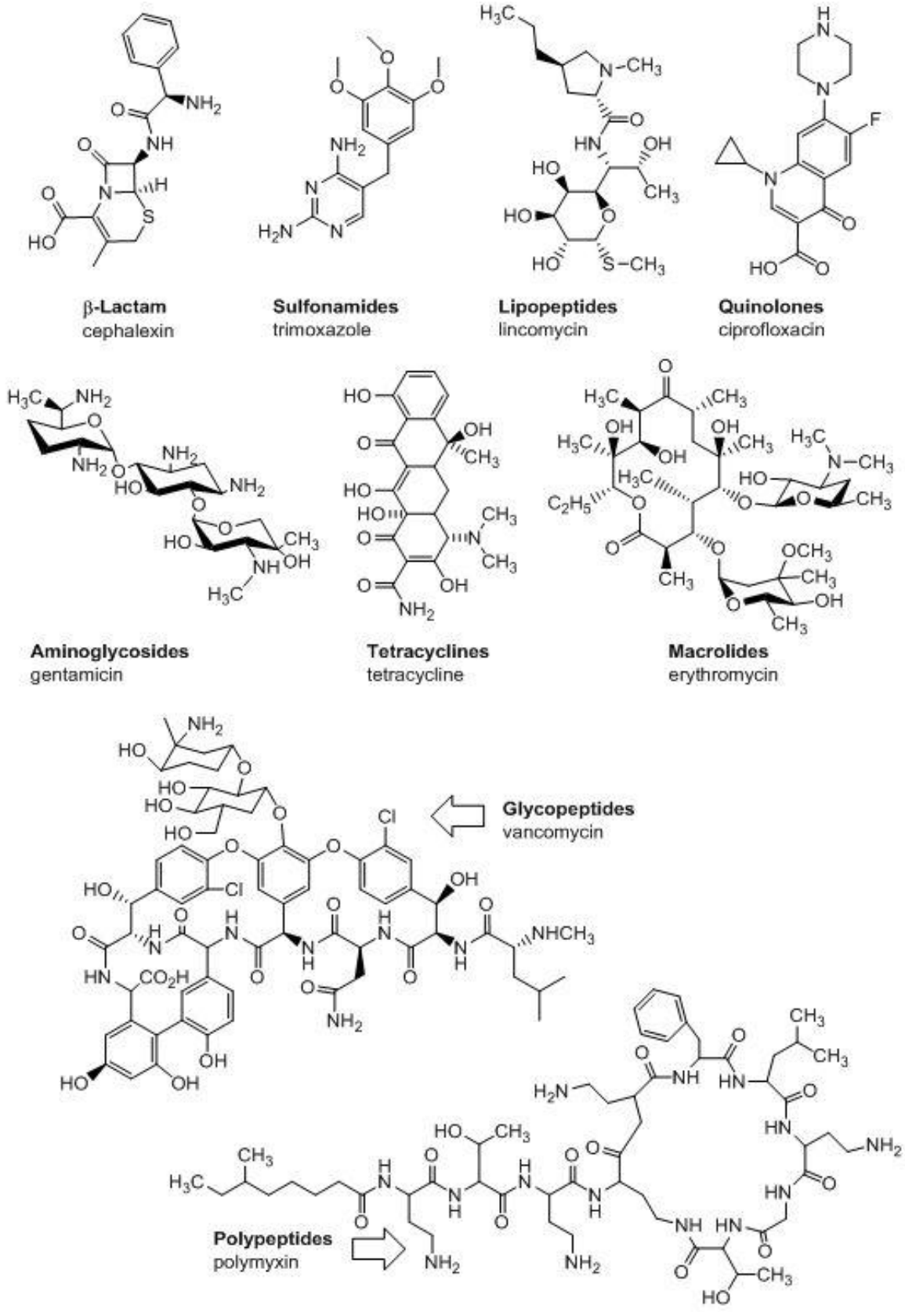

Figure 1.1 Major classes of antibiotics. The structures of typical antibiotics from the nine major classes (in bold).

Antibiotics belonging to the same class tend to inhibit the same essential process within the bacterial cell (Figure 1.2). Inhibitors of cell wall biosynthesis are either β-lactam antibiotics (penicillins, cephalosporins, carbapenems, and monobactams), glycopeptides or polypeptides. Lipopeptides bind to the membrane. Folate biosynthesis is inhibited by sulfonamides. Quinolones prevent DNA replication via inhibition of DNA topoisomerase. Protein synthesis is also a major target, with macrolides binding the 50S ribosomal subunit, and aminoglycosides and tetracyclins binding the 30S ribosomal subunit.

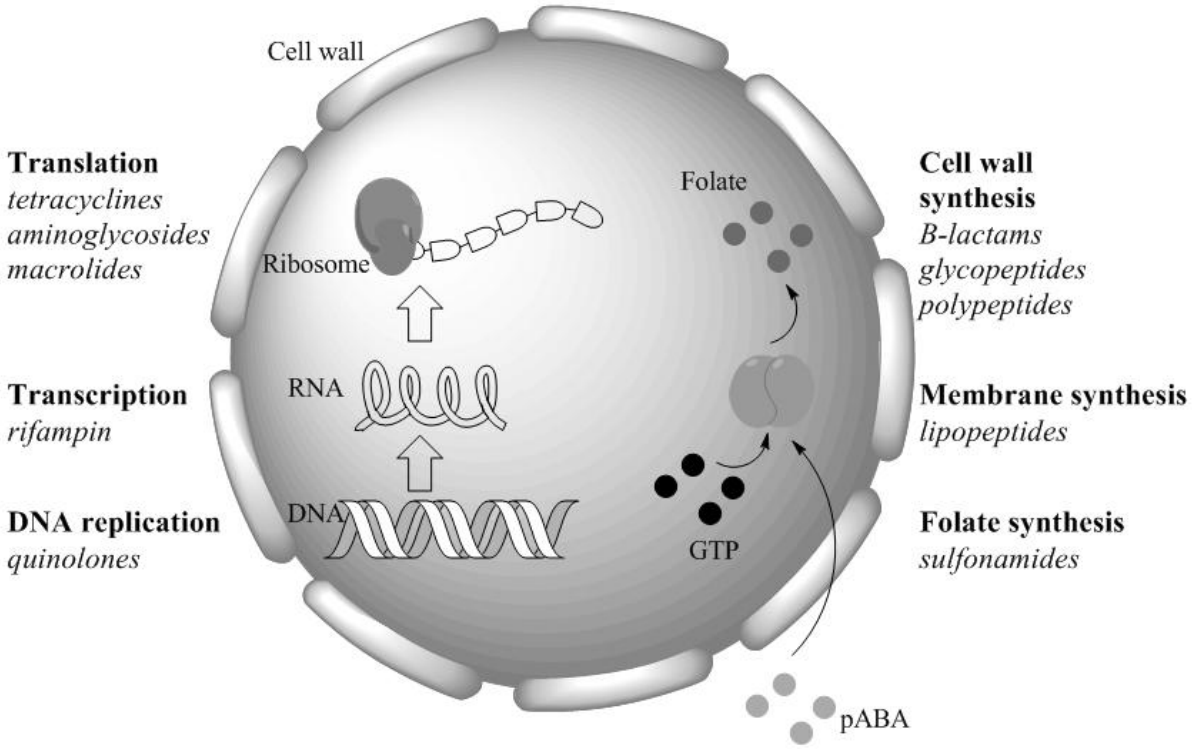

Figure 1.2 Antibiotic targets within the bacterial cell. Antibiotics bind and inhibit essential processes within the bacterial cell. Different groups of antibiotics (in italics) target different processes (in bold).

1.1.2 Function and evolution of antibiotics

The complex biosynthetic pathways to antibiotics require both energy and precursors (Haslam, 1995). The biosynthetic machinery is encoded on substantial portions of DNA, retention and control of which also places significant demand on the organism. Therefore, although the production of antibiotics is not essential for normal growth and division, they must confer other advantages to the organism. Antibiotics may fulfil a variety of roles within

the producing organism. For *Streptomyces, Micromonospora*, and related genera of aerobic filamentous bacteria, antibiotic production is tightly linked to their complex life cycle. When nutrients are abundant, the substrate mycelium forms a highly branched network on the surface of, for example, soil particles. As nutrient supply becomes limiting, this initiates a complex reprogramming of the colony in which, in *Streptomyces*, arial hyphae are formed, which in turn give rise to heat-labile, desiccation-resistant spores, while the substrate mycelium is broken down by a mixture of degradative enzymes to provide a temporary food supply for sporogenesis (Bibb, 2005, Liu et al., 2013). This transitional phase of the life cycle coincides in many cases with the onset of antibiotic production, consistent with a major role for antibiotics in protecting this nutrient supply from competing fungi and bacteria (Barka et al., 2016). The execution of these events is under a complex regulation which is only partly understood (Rigali et al., 2006, Hesketh et al., 2007). For the model organism *Streptomyces coelicolor,* transposon mutagenesis has revealed as many as 348 genes that modulate the production of the tripyrrole antibiotic prodigiosin (Xu et al., 2017).

Antibiotics produced by strains in the environment will generally be present at low concentrations where their action is inhibitory rather than bactericidal or fungicidal. Antibiotics have been shown at low concentration to act as signalling molecules within a microbial community (Yim et al., 2007). Antibiotics have also been shown to interact with over 5% of promoters and to regulate gene expression (Goh et al., 2002).

Many actinomycete species, such as *Micromonospora* live in symbiosis with plants, especially legumes, and can even promote their growth (Martínez-Hidalgo et al., 2014). Antibiotic production in that context may provide protection to both the plant and bacterium, for example defending against fungal infection (Martínez-Hidalgo et al., 2015).

Davies has proposed that the origin and evolution of specialised metabolite biosynthesis lies in their original catalytic roles in the RNA world (Davies et al., 1992). In contrast, it has been argued that the possession of the biosynthetic machinery rather than the evolution of a particular compound confers the real selective advantage to the producer (Firn and Jones, 2000). They

propose that maintenance of biosynthetic genes is selected for to provide the potential for evolution and the ability of the producer to adapt to the changing environment by rapidly producing a novel metabolite. Natural products are often found as mixtures of closely structurally-related compounds, which rather than being evidence for "primitive" less selective enzymology, may instead hint at a flexibility that provides material for further evolution while maintaining production of a useful molecule.

1.1.3 Organisation of the genes governing antibiotic biosynthetic pathways

The observed vast diversity and number of known antibiotic structures arise from primary metabolites in the cell by variation on a limited number of biosynthetic pathways. In general, the initial phase of biosynthesis involves the assembly of a scaffold or template structure, which is then acted upon by tailoring enzymes (often including glycosyltransferases, hydroxylases, and methyltransferases) to create diversity and confer activity. In addition to the enzymes catalysing each step, specific mechanisms are needed to transport the end products out of the cell; and to regulate the timing and extent of production.

Whole-genome DNA sequencing of actinomycetes has transformed our view of the organisation, distribution, and number of genes clusters for specialised metabolites that are present in these large bacterial chromosomes (typically between 7 and 11 Mbp). The chromosome of a typical *Streptomyces* spp. is linear (Bentley et al., 2002, Ikeda et al., 2003) while that of the other genera such as *Micromonospora* spp. (Trujillo et al., 2014) and *Saccharopolyspora* spp. (Oliynyk et al., 2007) is circular, but in each case the genes encoding the essential primary metabolism are located in a core region of roughly half of the chromosome, near the origin of replication. In contrast, genes encoding specialised metabolite biosynthesis are in the region away from the origin of replication. Figure 1.3 shows the distribution of over 20 biosynthetic gene clusters in the complete genome of the model organism *Streptomyces coelicolor* (Bentley et al., 2002). Some strains house additional biosynthetic gene clusters on giant plasmids (Medema et al., 2010). The co-location of pathway genes and pathway-specific regulatory elements within clusters has greatly facilitated the investigation of antibiotic biosynthesis in these bacteria.

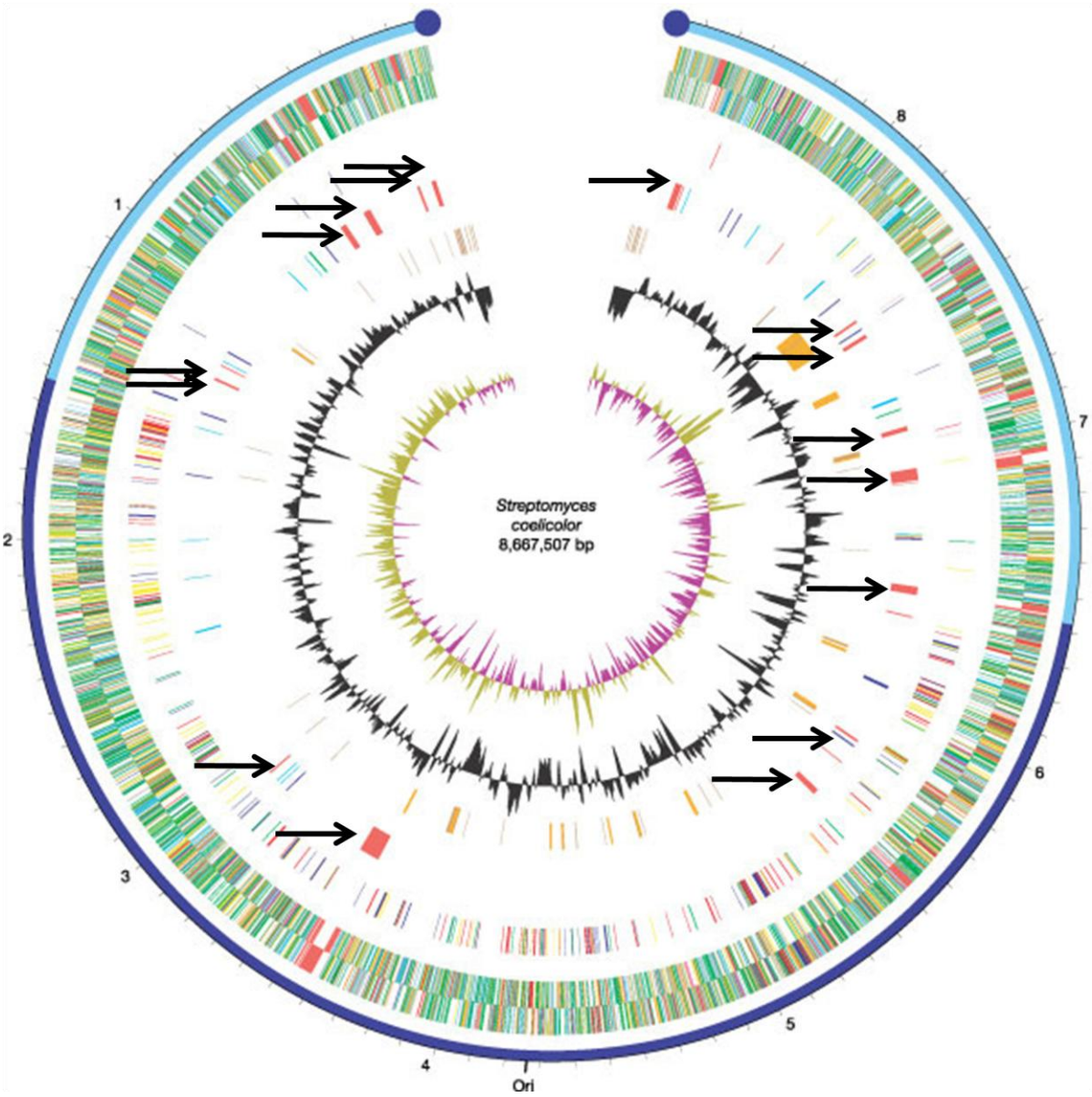

Figure 1.3 Complete genome of *Streptomyces coelicolor*. The complete genome of *Streptomyces coelicolor* is over 8.5 Mbp long (numbering on the outside). From the outside in, circles 1 and 2 show all the annotated genes, circle 3 shows essential primary metabolism genes, while circle 4 shows genes encoding secondary metabolism. The red stretches of DNA indicate biosynthetic clusters (also indicated by black arrows), of which there are over 20. Circle 5 shows mobile elements (Figure 1 from (Bentley et al., 2002)).

1.1.4 Antibiotic producer's self-resistance

The producer must also possess at least one mechanism to protect itself against its own antibiotic. A common strategy is modification of the target of the antibiotic. For antibiotics affecting protein synthesis, this is often achieved by specific methylation of rRNA residues by *S*-adenosylmethionine (SAM)-dependent methyltransferases, for example in the methylation of G1405 in the 16S rRNA of several aminoglycoside-producing *Micromonospora* spp. (Savic et

al., 2009) (see later). For glycopeptides and lantibiotics that target lipid II in cell wall biosynthesis, the strategy is to synthesise modified peptidoglycan (Stegmann et al., 2015). For other antibiotics, like the fatty acid synthase inhibitor thiolactomycin (Tang et al., 2015, Tao et al., 2016) and the aminoacyl tRNA synthetase inhibitor borrelidin (Olano et al., 2004), the biosynthetic gene cluster houses an isoenzyme of the target enzyme that is impervious to the action of the inhibitor.

In some strains that produce inhibitors of protein synthesis, the ribosomes remain un-methylated and sensitive to the antibiotic. Instead, the antibiotic itself is inactivated by phosphorylation, as in streptomycin biosynthesis in *Streptomyces griseus* (Sugiyama et al., 1983), or by acetylation (Sugiyama, 2015). The protective group is enzymatically removed after export. Even more commonly, so-called ABC transporters (Méndez and Salas, 2001) catalyse the active, ATP-driven efflux of antibiotic molecules (Martín et al., 2005), with an inactive precursor often inducing synthesis of the pump protein (Hopwood, 2007). In contrast, a different group of efflux system, the major facilitator superfamily exporters, are driven by chemi-osmotic ion gradient (Martín et al., 2005).

1.1.5 Resistance development in pathogens

Unfortunately, the widespread and often unnecessary use of broad-spectrum antibiotics led to a fast rise of pathogen resistance, causing arguably one of the biggest problems of the 21st century (Hede, 2014). Today one third deaths worldwide is due to infectious disease, with an estimated 50,000 people dying daily. The emergence of resistance has been so rapid that since 2009 several pathogens have been isolated that are resistant to essentially all front-line antibiotics: these include Gram-negative pathogens (Lepape et al., 2009, Palumbi, 2001) such as polymyxin-resistant and/or carbepenem-resistant *Pseudomonas aeruginosa* (Walsh and Amyes, 2004, Liu et al., 2016, Lepape et al., 2009), carbapenem-resistant *Klebsiella pneumoniae* (Fair and Tor, 2014), and multi drug-resistant (MDR) *Mycobacterium tuberculosis* (Velayati et al., 2009).

Mechanisms of resistance to antibiotics mirror three of those involved in self-protection of producing strains: modification of the antibiotic target (cell

wall, cell membrane, or protein), acquisition of efflux pumps capable of removing the antibiotic from the organism, and antibiotic-inactivating enzymes. The latter are especially serious, as the enzymes are normally encoded by a single gene and can be easily transferred between bacterial pathogens. The origin of antibiotic-modifying proteins is often the producers themselves, and often such genes are located on mobile genetic elements, contributing to the spread of resistance by horizontal gene transfer.

Microbial resistance is driven by four main factors: antibiotic overuse, overdose, use of broad-spectrum antibiotics, and non-compliance. Increasing quantities of antibiotics used for non-human applications (estimated 80% of all antibiotics sold in the USA), such as farming and fishing, has also lead to antibiotic-contaminated waste being released into the environment. This creates evolutionary pressure for bacteria to evolve and acquire more resistance genes, and highlights the importance of discovering new antibiotics as well as preventing overuse of existing compounds.

1.1.6 Strategies for antibiotic discovery

The wide emergence of antibiotic-resistant strains and novel infectious agents has coincided with a reduced success in developing novel antimicrobials. Recent decades have seen high rates of re-discovery of known compounds, and increasingly disappointing news from semi-synthetic efforts on established compounds (Butler et al., 2013). This, combined with low prices of most antibiotics, led to vastly reduced interest from big pharmaceutical companies, leaving small companies and academia (Fernandes and Martens, 2017) to consider new ways of generating (or discovering) antibiotics.

Underexplored parts of the global biota are a source of new microorganisms capable of novel modes of action (Kala, 2000). For example, isolation of fungi and actinomycete bacteria from mangrove ecosystems (He et al., 2017) and of actinomycetes from the deep ocean (Kamjam et al., 2017) has revealed new species and new antibiotics. A major limitation of the discovery of novel species has been our inability to culture the clear majority of them in laboratory conditions. Due to advances in DNA technologies, we have the ability to interrogate metagenomic samples from environmental samples by sequencing,

and to clone biosynthetic gene clusters from total DNA into an appropriate *Streptomyces* host strain to attempt heterologous production (Bekiesch et al., 2016). Another interesting approach is the gradual adaptation of a previously unculturable microorganism to laboratory media using iChip technology (Nichols et al., 2010). This technology has recently led to the discovery of teixobactin, claimed to be the first novel-class antibiotic discovered for 30 years (Ling et al., 2015).

It is increasingly clear that powerful novel approaches to the discovery and engineering of novel antibiotics require a detailed knowledge of the biosynthetic pathways that form them. The outlines of all the major biosynthetic pathways, to polyketides, to nonribosomal peptides, to terpenes and alkaloids, were worked out in the second half of the last century using isotopically labelled precursors and isolating the products to localise the label by increasingly sophisticated mass spectrometry (MS)- and nuclear magnetic resonance (NMR)-based methods. Mutant strains specifically blocked in biosynthesis were shown to accumulate intermediates which could likewise be characterised. After 1980, major advances in the molecular microbiology provided the necessary tools to manipulate *Streptomyces* and other actinomycetes. The discovery and sequencing of biosynthetic gene clusters, and recognition of the assembly-line paradigm for polyketide and nonribosomal peptide synthesis (Staunton and Weissman, 2001, Hertweck, 2009, Khosla et al., 2014, Walsh, 2016), together led to a step change in our ability to study and engineer biosynthetic pathways. This in turn led to first attempts at combinatorial biosynthesis (Gregory et al., 2005, Wilkinson and Micklefield, 2007, Weissman, 2016) and has informed genome mining of actinomycete genomes for novel gene clusters. The knowledge gained has also been used to divert synthesis to a single desired component, as in erythromycin fermentation, where integration of an additional copy of the late-acting cytochrome P450-encoding gene *eryK* into *Saccharopolyspora erythraea* increased the yield and purity of the final product erythromycin A (Chen et al., 2008).

Alongside these developments, chemical synthesis has continued to show its power to adapt an antibiotic natural product template to optimise its drug parameters, including reduction of toxicity and give more favourable

pharmacokinetics. For example, semi-synthesis has been used to create a platform of over 400 compounds starting with the natural aminoglycoside sisomicin. One - renamed plazomicin - has recently passed through Phase III clinical trials (Anchaogen, 2017). Similarly, semi-synthesis has led to development of ketolides, fourth generation 14-membered macrolides effective against macrolide-resistant pathogens, such as *Clostridium difficile* (Karpiuk and Tyski, 2015), while omadacycline is a semi-synthetic tetracycline effective against antibiotic-resistant *Streptococcus pneumoniae* (Villano et al., 2016, Macone et al., 2014). Even total synthesis of antibiotics is viable if the binding site of the target is well understood. Fully synthetic fluorocycline compound TP-271 is currently in the advanced preclinical stage as a treatment for bacterial pneumonia (Grossman et al., 2017). However, total synthesis of most antibiotics is limited by the cost of goods, when compared to single-step fermentation (Houghton et al., 2010).

There is a pressing need to develop new and safe antibiotics which can treat multidrug-resistant infections. A recent increase in Gram-negative infections is worrying, as fewer antibiotic classes are active against them. Novel tetracyclines, aminoglycosides, and fluoroquinolones are urgently needed to combat the rise of pathogens.

1.2 Aminoglycoside antibiotics

Aminoglycosides were the first broad-spectrum antibiotic class to be recognised (Table 1.1). Streptomycin, discovered in 1944 by Waksman, was moreover the first antibiotic to be discovered by systematic screening, the first to be produced by a bacterium, and the first antibiotic effective against *M. tuberculosis* (Schatz et al., 1944). Its discovery allowed complex carbohydrates to be recognised as an important class of natural products (Pokrovskaya et al., 2010).

Table 1.1 Aminoglycoside-producing strains

Aminoglycoside	Producer	Cluster	GI number
Apramycin	*Streptomyces tenebrarius*	*apr*	85813519
Butirosin	*Bacillus circulans*	*btr*	70720831
Fortimicin	*Micromonospora olivasterospora*	*for*	85813900
Gentamicin	*Micromonospora echinospora*	*gen*	433287151
Kanamycin	*Streptomyces kanamyceticus*	*gen*	108743311
Neomycin	*Streptomyces fradiae*	*neo*	85813555
Sisomicin	*Micromonospora inyoensis, Micromonospora zionensis*	*sis*	327197283
Streptomycin	*Streptomyces griseus*	*str*	62896300
Tobramycin	*Streptomyces tenebrarius*	*tob*	85813675
Verdamicin	*Micromonospora grisea*	-	-

Most aminoglycoside compounds are produced by actinomycete bacteria, particularly *Streptomyces* (compounds are given a -mycin suffix) and *Micromonospora* (compounds are given a -micin suffix).

1.2.1 The *Micromonosporaceae*

Amongst actinomycete bacteria, *Streptomyces* and *Micromonospora* genera produce, directly or after semi-synthesis, nearly all the antibiotics currently in clinical use. Conventional classification of actinomycetes relies on morphological and ecological characteristics, with cell wall composition being an important criterion (Yamaguchi, 1965). The *Micromonosporaceae* are characterised by an extensive substrate mycelium and the absence of a true aerial mycelium (Figure 1.4). Spore formation occurs directly on the substrate mycelium, unlike the aerial mycelium of *Streptomyces*, and only isolated spores are produced (Kawamoto et al., 1981). Different species of *Micromonospora* either live independently, or exist as legume symbionts within nitrogen-fixing nodules or as plant endophytes (Barka et al., 2016).

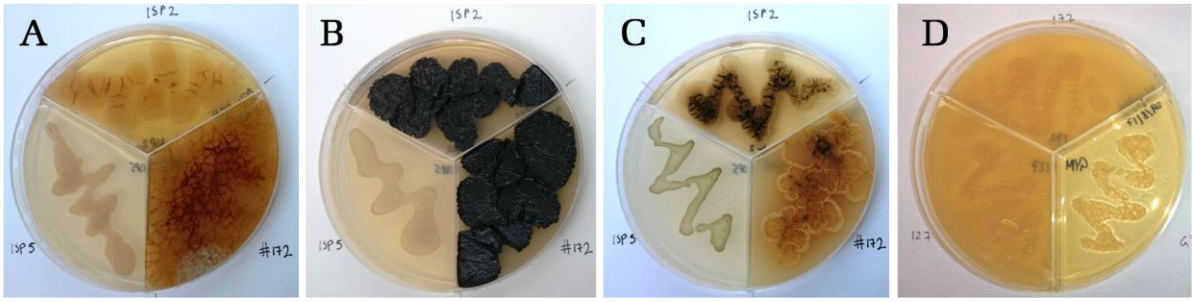

Figure 1.4 Solid cultures of different *Micromonospora* species. (A) Gentamicin producer *Micromonospora echinospora,* ATCC 15835; (B) sisomicin producer *Micromonospora inyoensis*; (C) *Micromonospora olivasterospora* produces fortimicin; (D) verdamicin producer *Micromonospora grisea*.

The cell wall of *Micromonospora* contains glycine, sugars, and *meso*-3-hydroxy-diaminopimelic acid, making it a Type II cell wall, as opposed to no sugars and LL-diaminopimelic acid in the Type I cell wall of *Streptomyces*. The sugar composition of the cell wall can be used to distinguish between different *Micromonospora* species (Table 1.2) (Kawamoto et al., 1981). *M. echinospora* is an actinomycete bacterium producing gentamicin, currently the most widely used aminoglycoside antibiotic. The sugars and amino acids present in its cell wall are similar, in both identity and quantity, to those present in the cell walls of species producing structurally similar compounds, and are very different to other related *Micromonospora* species.

Table 1.2 Cell wall composition of *Micromonospora;* adapted from Table 2 in (Kawamoto et al., 1981)

Species	Antibiotic	Cell wall composition		
		Glucose	Galactose	Mannose
M. olivasterospora	Fortimicin	✓	✓	×
M. zionensis	Sisomicin, G-52	✓	✓	×
M. grisea	Verdamicin	✓	✓	×
M. echinospora	Gentamicins	×	✓	✓
M. sagamiensis	Gentamicin C2b	×	×	✓
M. inyoensis	Sisomicin	×	×	×

1.2.2 Structure and classification of aminoglycosides

Aminoglycosides are a group of related aminosugar-containing antibiotics (Figure 1.5). In the environment, they are predicted to act as cell-signalling molecules (Yim et al., 2006) and as a defence against other microbes. The idea from Julian Davies that they originated as effector molecules in primordial DNA- and RNA-based reactions receives some support from the observation that, in the presence of aminoglycosides, DNA can be used as a template for translation (Bretscher, 1968).

Aminoglycosides are divided into separate classes (Figure 1.5) based on their core aminocyclitol moiety, which can be either streptamine, streptidine, or - for most clinically-used aminoglycosides - 2-deoxystreptamine (2-DOS). The core then becomes decorated with aminosugar units. The relationships between 2-DOS-containing natural products have been greatly clarified by extensive work on their early steps of biosynthesis. Important early findings on the origin of 2-DOS were obtained from feeding studies of blocked mutants with radioactively-labelled precursors or intermediates (Llewellyn and Spencer, 2006), but a particular breakthrough was made in the demonstration of 2-DOS synthesis from D-glucose-6-phosphate in cell-free extracts of neomycin producer *Streptomyces fradiae* (Yamauchi and Kakinuma, 1992). Later, the key enzyme BtrC, which established the carbocyclic ring of 2-DOS, was purified from the butirosin producer (Kudo et al., 1999a), and its gene *btrC* was identified (Kudo et al., 1999b) This led to the cloning and sequencing of both the butirosin biosynthetic

gene cluster from *Bacillus circulans* (Ota et al., 2000, Kudo et al., 2005) and the neomycin gene cluster from *Streptomyces fradiae* (Huang et al., 2005).

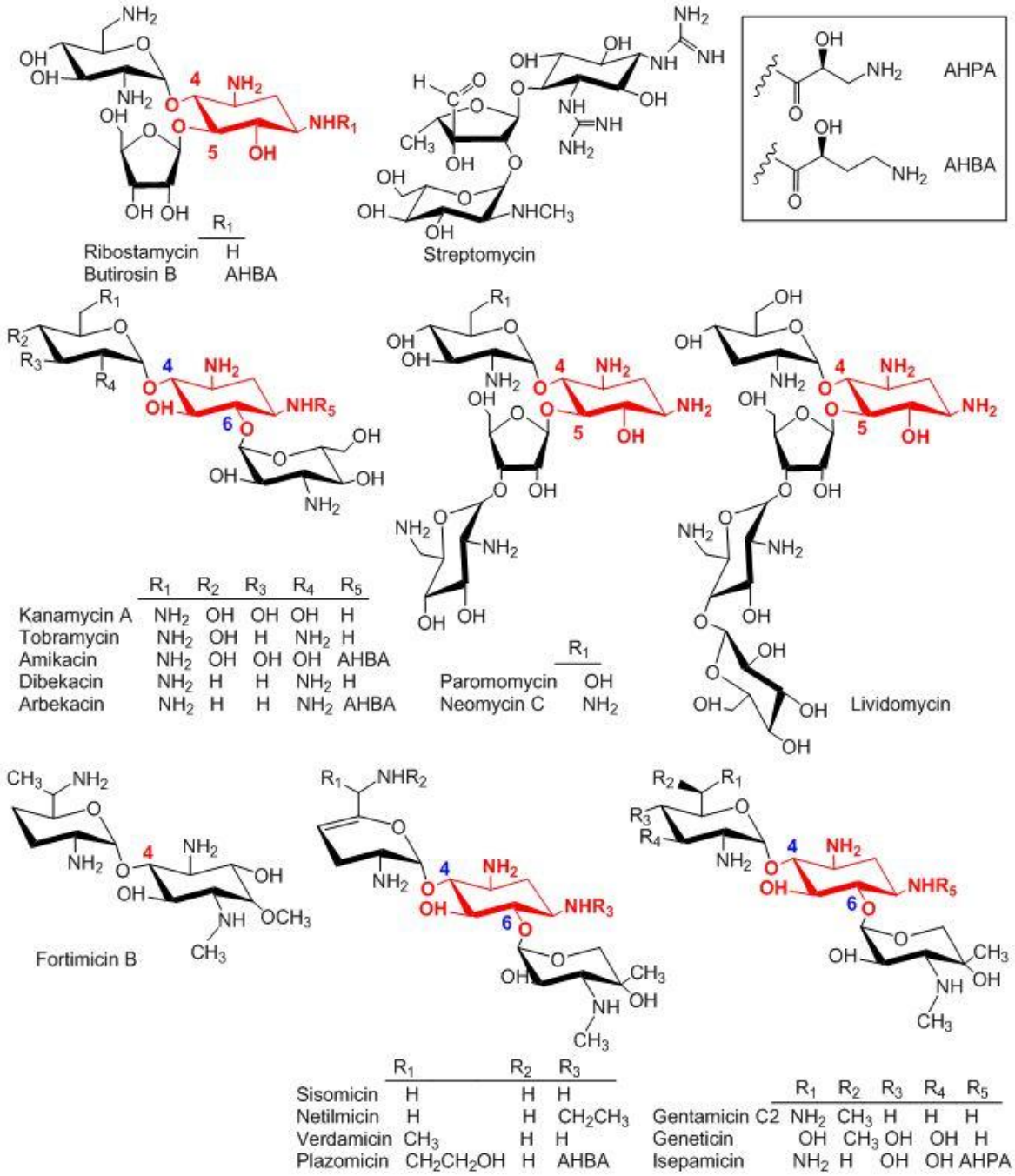

Figure 1.5 Examples of naturally occurring and semi-synthetic aminoglycoside antibiotics. Aminoglycosides are hydrophilic molecules consisting of a central aminocyclitol ring linked to one (e.g. fortimicin) or more amino sugars by pseudoglycosidic bond (s). 2-Deoxystreptamine (Ring I) is shown in red. In streptomycin the central ring is streptidine, and in fortimicin - fortamine. Ring II has primed numbers, and is attached at carbon 4; ring III (if present) is attached at carbon 5 or 6, and is doubly primed. AHBA: (*S*)-4-amino-2-hydroxybutyryl side chain; AHPA: (*S*)-3-amino-2-hydroxypropyl side chain; Figure adapted from Figure 1 in (Park et al., 2013).

Because these strains, unlike other aminoglycoside producers, proved genetically tractable at that time (Llewellyn and Spencer, 2006), work on these pathways proceeded quickly and provided valuable insights into the enzymology of the common early steps of aminoglycoside biosynthesis. The reaction sequence for 2-DOS production during butirosin biosynthesis is shown in Figure 1.6A. Apart from BtrC, it features a pyridoxal phosphate (PLP)-dependent aminotransferase BtrR (Huang et al., 2002), that is also known as BtrS (Tamegai et al., 2002), which catalyses both the conversion of 2-DOI to 2-DOIA and the later conversion of keto-2-DOIA into 2-DOS. This was the first example of a recurring theme in aminoglycoside biosynthetic pathways: a single enzyme catalyses the same type of reaction on different substrates at different points in the pathway. The remaining enzyme is a dehydrogenase, which in neomycin biosynthesis was shown to be NAD^+-dependent Neo5. The homologue of Neo5 in the butirosin cluster, BtrE, is inactive in this step. Later work has established that dehydrogenation of 2-DOIA is carried out by the radical-SAM dehydrogenase BtrN instead (Yokoyama et al., 2007). BtrE, on the other hand, is now known to catalyse the NAD^+-dependent oxidation at C-3" in the ribose ring of the late-stage pseudotrisaccharide intermediate ribostamycin (Figure 1.6B), as the first step in epimerisation at this position to give xylostasin, the precursor of butirosin A (Takeishi et al., 2015). These results highlight a second general theme in aminoglycoside pathways: the gene clusters typically contain multiple genes encoding similar enzymes (e.g. methyltransferases, dehydrogenases, aminotransferases) with potentially overlapping activities, whose contributions are only definitively resolved by *in vitro* experiments using purified recombinant enzymes and appropriate substrates.

The conversion of 2-DOS into the pseudodisaccharide paromamine, the most advanced common intermediate to 2-DOS-based aminoglycosides (Figure 1.6), is accomplished by attachment of an *N*-acetyl-D-glucosaminyl moiety to 4-O of 2-DOS (catalysed by BtrM and Neo15 respectively) followed by removal of the acetyl group by a deacetylase (Neo16 and BtrD respectively) (Figure 1.6A).

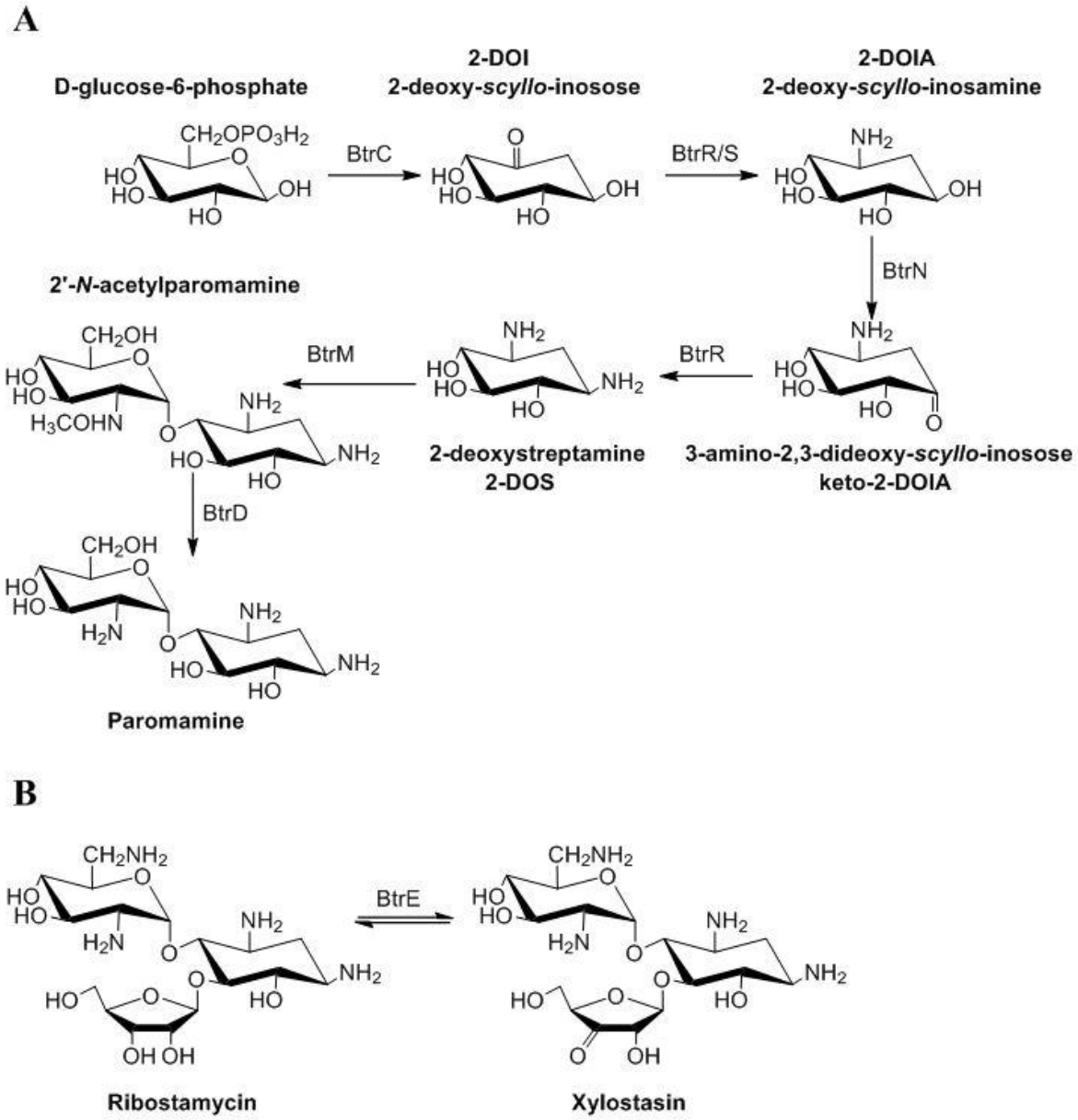

Figure 1.6 Biosynthesis of 2-deoxystreptamine and paromamine. (A) Glucose-6-phosphate is converted to 2-deoxy-*scyllo*-inosose (2-DOI) by a carbocyclization reaction catalysed by BtrC . BtrR (also known as BtrS) catalyses a transamination at C3 using L-glutamine as amino donor. BtrN acts as a dehydrogenase (SAM- and NAD (P)$^+$-dependent) on C1, and BtrR performs a transamination on C1. This produced 2-deoxystreptamine (2-DOS). The glycosyltransferase BtrM catalyses *N*-acetyl-D-glucosamine transfer from uridine diphosphate *N*-acetyl-D-glucosamine (UDP-GlcNac) to the hydroxy group at C4 of 2-DOS to form 2'-*N*-acetylparomamine. BtrD deacetylates it to give paromamine. (B) Dehydrogenase BtrE catalyses epimerisation at C-3" in butirosin biosynthesis.

Paromamine is the precursor of 4,5-disubstituted aminoglycosides like neomycin C, ribostamycin, and paromomycin (Figure 1.5) via ribosyltransfer to the hydroxyl group at C5 of the aminocyclitol ring. In the case of neomycin, the flavin-dependent dehydrogenase Neo18 and the aminotransferase Neo11 first

convert the 6'-hydroxy group to a 6'-amino group to form neamine. After attachment of the ribose moiety to neamine to give ribostamycin (Figure 1.5), catalysed by Btr equivalents (Kudo et al., 2005) (the neomycin equivalents are Neo13, Neo17 and Neo19 (Huang et al., 2007)). The glycosyltransferase Neo15 is used and deacetylase Neo16 is re-used to add a second GlcNac moiety and de-protect it to form 6'''-deamino-6'''-hydroxyneomycin (Fan et al., 2008). Finally, flavin-linked dehydrogenase Neo11 and aminotransferase Neo18 are also re-used to produce neomycin B and C (Huang et al., 2007).

Paromamine is also the precursor to 4,6-disubstituted aminoglycosides like kanamycin, tobramycin, apramycin, and gentamicin (Figure 1.5), through glycosyltransferase-catalysed transfer to paromamine of a D-xylohexose moiety from UDP-xylose to the hydroxy group at C6 of the 2-DOS ring. The introduction of the sugar group is followed in each case by a dehydrogenation-transamination sequence to introduce an amino group and specific methylation, as described in more detail in Section 1.3 for gentamicin. The final steps of tailoring offer fresh examples of novel enzymology. For example, kanamycin A is unique among 2-DOS-derived aminoglycosides in having a hydroxy group at C-2' instead of an amino group. It has been shown that KanJ is an FeII/2-oxoglutarate-dependent oxygenase that oxidises the amino group to a keto group, which is then specifically reduced by NADPH-dependent KanK to complete the deamination (Sucipto et al., 2012). It appears also that kanamycin biosynthesis does not follow a unique linear pathway, but rather can proceed by alternative routes to converge on kanamycin A (Figure 1.7) (Park et al., 2011, Yu et al., 2017).

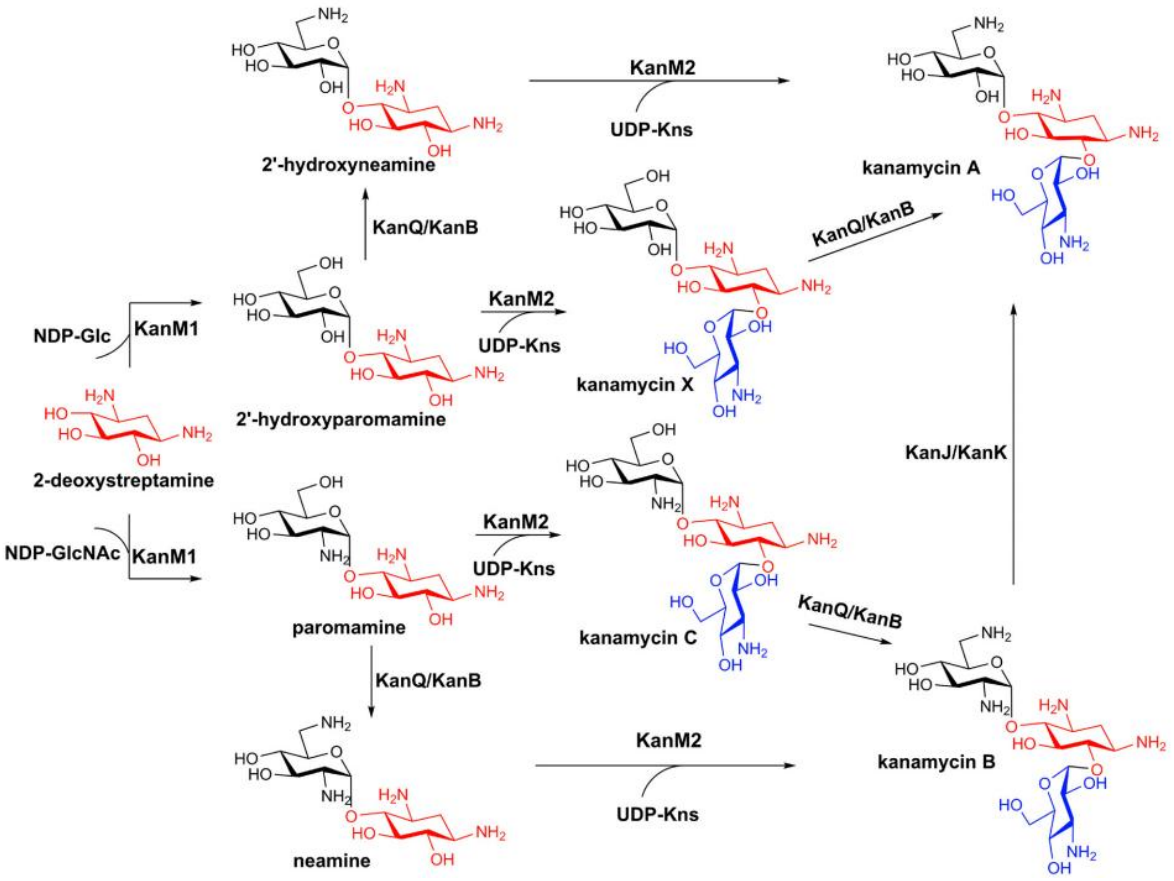

Figure 1.7 Biosynthetic network of kanamycin. The 2-deoxystreptamine (2-DOS) moiety is in red and kanosamine is in blue. Figure adapted from Figure 1 in (Yu et al., 2017)

This can be traced to the unusual substrate flexibility of some of the *kan* biosynthetic enzymes.

Similarly, apramycin biosynthesis has been shown to follow a branched pathway that means that oxyapramycin is not (as previously thought) the precursor of apramycin (Figure 1.8) (Kim et al., 2016, Lv et al., 2016). The *in vitro* study of the unusual 3-deoxygenation step, catalysed by a radical SAM-dependent dehydratase enzyme AprD3 and its partner, the NADPH-dependent reductase AprD4, has shown that it operates on paromamine. This again reflects the flexibility of certain of the biosynthetic enzymes in this pathway.

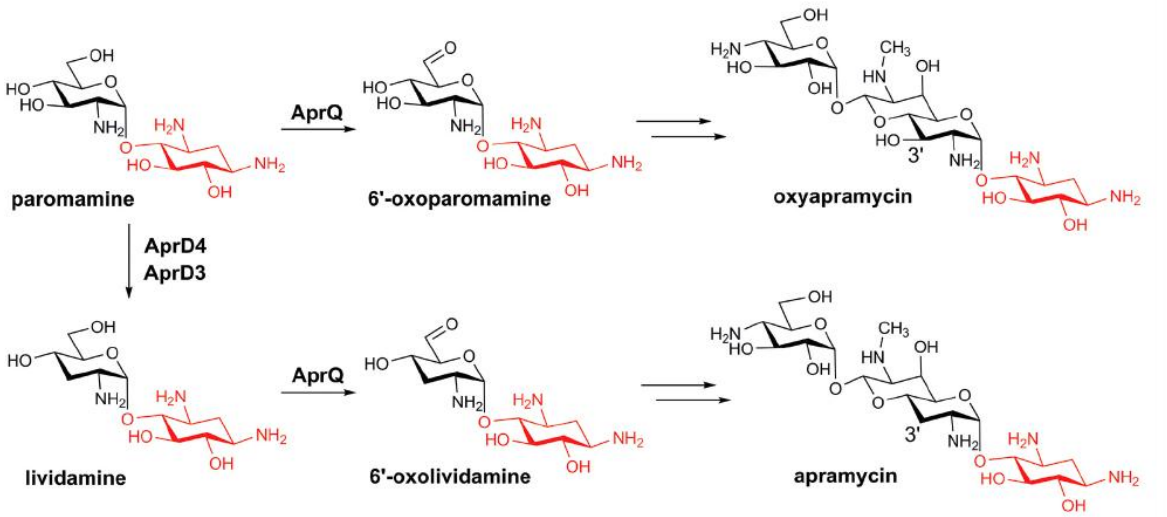

Figure 1.8 Biosynthetic branch point of apramycin. The narrow substrate specificity of AprD4 and the wide specificity of AprQ together create a branch point within the biosynthetic pathway of apramycin. The 2-deoxystreptamine (2-DOS) moiety is in red. Figure adapted from Figure 8 in (Lv et al., 2016)

1.2.3 Biosynthetic clusters for aminoglycosides

Genomes of most known actinomycetes have high G+C content (above 70%). The DNA is arranged in a single large chromosome and multiple plasmids. As discussed previously, genes encoding secondary metabolism proteins, like production gene clusters, are in areas generally associated with higher rates of horizontal gene transfer. The clustered biosynthetic genes are strain-specific and highly variable. Moreover, the regulation of these genes is dependent on the environmental conditions and may additionally be dependent on cell differentiation (Piepersberg et al., 2007b).

Most of the genes necessary for the biosynthesis of a chemical are grouped together in the genome, forming clusters (Figure 1.9). A typical gene cluster consists of catalytic genes, self-resistance and/or export genes, and regulator elements. The regulators are generally highly conserved, and are used to monitor the organism's vegetative state and environment (Liu et al., 2013). Entry into late phase of growth, change of pH and temperature, infection, presence of other organisms, and nutrient deprivation are known to trigger the onset of antibiotic production (Bibb, 2005). Pathway products and intermediates can also participate in feedback control.

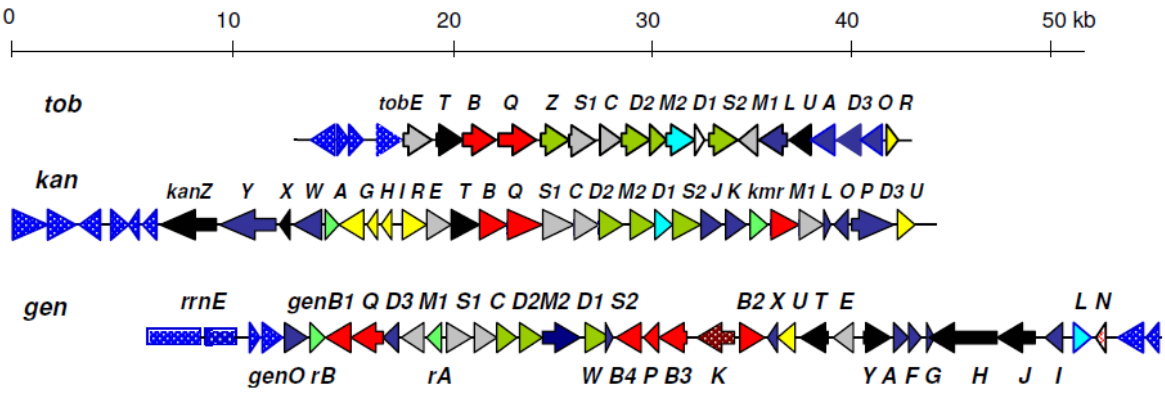

Fig. 3.5 Organization of ORFs for the gene clusters of the 4,6-glycosylated 2DOS-ACAGAs (KM group). The color codes for differentiating the genes encoding proteins putatively involved in:

- paromamine biosynthesis
- attachment of the first sugar unit at position 4 of the cyclitol ring and its modification
- attachment of the second sugar unit at position 6 of the cyclitol ring and its modification
- UDP-D-glucosamine synthase or amidase
- resistance
- ACAGAs biosynthesis
- represent genes outside the ACAGA gene clusters
- C-methyltransferase
- transport
- regulation
- N-methyltransferase

Figure 1.9 Tobramycin, kanamycin, and gentamicin biosynthetic gene clusters. The biosynthetic genes are often clustered together in one part of the genome, possibly for better regulation. Biosynthesis of an antibiotic requires regulators (yellow), exporters (black), self-resistance (green) genes, and biosynthetic genes (all other colours). Figure adapted from Figure 3.5 of (Aboshanab, 2005).

1.2.4 Modes of action of aminoglycosides

The target of aminoglycoside antibiotics was first revealed by showing that streptomycin interfered with incorporation of radioactive amino acids in cell-free extracts of *Mycobacterium tuberculosis* (Erdos and Ullmann, 1959). This inferred that protein synthesis was the primary target of aminoglycoside action (Davies, 1964).

More recent work has shown that aminoglycosides cause error-prone translation and impede protein synthesis by binding specific sites on the 30S ribosomal subunit (Carter et al., 2000). Aminoglycosides are the antibiotics targeting protein synthesis that are broadly bactericidal - via an unknown

mechanism (Fair and Tor, 2014, Kohanski et al., 2010), although antibiotics inhibiting translation have previously been shown to trigger an apoptotic pathway (Sat et al., 2001). Protein mistranslation, especially of membrane proteins, also leads to changes to the cell membrane ultra-structure, changing its permeability (Kohanski et al., 2010).

1.2.5 Aminoglycoside use and toxicity

Aminoglycosides are used widely in the clinic to treat serious - especially Gram-negative - infections. Aminoglycosides must be administered either intravenously, intramuscularly, or as a topical treatment. Aminoglycosides taken orally pass through the gut unabsorbed, making them useful for treating gut infections.

Unfortunately, aminoglycosides are amongst the most toxic clinically-used substances. Their use risks damage to the kidney (nephrotoxicity), which is often reversible, and mostly-irreversible hearing damage (ototoxicity). As such, any administration and effects of the drug must be closely monitored for every patient and the duration of treatment kept as short as possible.

1.2.6 Resistance to aminoglycosides

When used properly, bactericidal effects of aminoglycosides tend to prevent instances of resistance from occurring. About 60-80% of all pathogenic strains resistant to aminoglycosides possess conjugative R plasmids, which add to the spread of resistance of pathogens (Mitsuhashi, 1982). Prevention of conjugation would not be an effective strategy for all pathogens however, as *Pseudomonas aureginosa*, has resistance encoded almost exclusively by non-conjugative resistance (r) plasmids.

Resistance to aminoglycosides occurs via three distinct mechanisms: 1) acquisition of aminoglycoside-inactivating enzymes, 2) mutation of the 30S ribosomal subunit to prevent efficient aminoglycoside binding, and 3) prevention of aminoglycoside uptake by the cell by changing cell membrane permeability and disrupting active transport and diffusion through porin channels (Karpiuk and Tyski, 2015).

1.2.7 Strategies for development of new aminoglycosides

Emergence of difficult-to-treat Gram-negative infections, such as carbapenem-resistant *Klebsiella pneumoniae*, and the ability of aminoglycoside antibiotics to kill a broad spectrum of pathogens (thus reducing the chance of resistance) have prompted more interest into development and discovery of novel aminoglycoside antibiotics (Durante-Mangoni et al., 2009); work has also been done to reduce the toxicity of existing ones.

Some existing aminoglycosides possess a natural way of overcoming resistance (Park et al., 2017). Tobramycin and gentamicin lack a 3' hydroxyl group, enabling activity against APH (3')-containing pathogens. Butirosin is produced by *Bacillus circulans*, and uniquely contains an (*S*)-4-amino-2-hydroxybutyryl (AHBA) side chain at 1-*N*. The presence of this group protects butirosin against the action of an acetyltransferase resistance enzyme (AAC (3)), reduces the activity of other modifying enzymes, and improves its activity (Llewellyn and Spencer, 2006). To provide this protective ability to other aminoglycosides, chemo-enzymatic addition of an AHBA side chain using BtrH and BtrG, the enzymes responsible for the biosynthetic step, to kanamycin A or gentamicin C was attempted. However, this approach failed to provide good yields.

Semisynthesis or partial chemical synthesis, using an antibiotic as a starting material, has found many applications in the clinical development of novel aminoglycosides, or neoglycosides. Addition of the AHBA side chain to kanamycin A produced a clinically useful compound amikacin (BB-K8, Figure 1.5). Amikacin was effective in treating over 80% of infections of kanamycin-resistant bacteria (Price et al., 1974). Addition of the same side chain to kanamycin B created arbekacin, which was effective in treating methicillin-resistant *Staphylococcus aureus* (MRSA) (Hamilton-Miller and Shah, 1995). The same strategy created netilmicin from sisomicin, and isepamicin from gentamicin B (Figure 1.5). Another semisynthetic aminoglycoside dibekacin, 3',4'-dideoxykanamycin B, has recently been used as a substrate for further chemical modifications to generate novel antibiotics (Umemura et al., 2015). Such a modification has also been demonstrated using enzymes: the genes *btrH* and *btrG* were cloned into a kanamycin X-producing *S. venezuelae* strain, and

the mutant produced a novel antibiotic 1-*N*-AHBA-kanamycin X *in vivo* (Park et al., 2011).

More recently, plazomicin (ACHN-490) was created, with the AHBA side chain added to the 1-*N* position and a 2-hydroxyethyl chain added to the 6'-*N* position of sisomicin (Aggen et al., 2010). The minimal inhibitory concentration (MIC) values of plazomicin were significantly lower than those of gentamicin, tobramycin, and amikacin against a range of tested strains (Endimiani et al., 2009). Furthermore, all the multidrug-resistant (MDR) isolates of *Klebsiella pneumoniae* were susceptible to plazomicin treatment (Galani et al., 2012). Plazomicin passed Phase III clinical trials in December 2016, making it the newest clinically useful aminoglycoside.

A limiting factor in developing neoglycosides has been the availability of a pure starting material. A detailed understanding of the relevant biosynthetic pathway is necessary for access to intermediates and mono-components. The biosynthetic pathway to 4,6-disubstituted 2-DOS-containing aminoglycosides, such as gentamicin, has still not been fully elucidated (Park et al., 2013). Both *in vitro* (recombinant protein) and *in vivo* (mutant generation) strategies need to be employed to provide complete characterisation of the pathway. Furthermore, better purification strategies and generation of monocomponent-producing mutants would generate new substrates for medicinal chemistry.

1.3 Gentamicin

The gentamicin antibiotics were discovered in 1963 by Weinstein and co-workers (Weinstein et al., 1963). Gentamicin is a fermentation product of *M. echinospora* DSM 43816 (Figure 1.4A, formerly *M. purpurea*), which was the first non-*Streptomyces* aminoglycoside producer discovered. It is currently the most widely used aminoglycoside antibiotic and is useful against infections by *Enterococci, Streptococci,* and *P. aeruginosa* (Fair and Tor, 2014). The World Health Organization (WHO) lists gentamicin as a Key Access Antibiotic, i.e. one that should be widely available, affordable and quality-assured (WHO, 2017).

The structure of gentamicin was elucidated by researchers at Schering (Cooper et al., 1971a, Daniels, 1975, Daniels et al., 1975). It consists of a central pseudo-sugar moiety of 2-deoxystreptamine (2-DOS); a purpurosamine (2',6'-diamino-2',3',4',6'-tetradeoxy-D-erythro-hexose) ring is attached at the C4 position, and a garosamine (3''-methylamino-3''-deoxy-4''-*C*-methyl-β-L-arabinose) ring is attached at the C6 position.

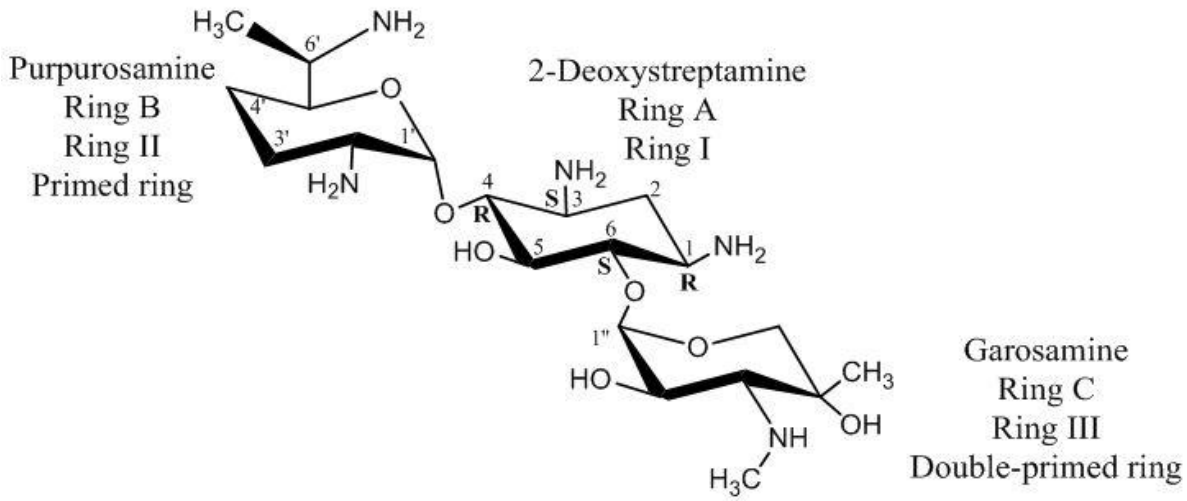

Figure 1.10 Gentamicin C2 structure. Gentamicins are closely-related tri-pseudosaccharide compounds, possessing a 2-deoxystreptamine centre (Ring A). Garosamine (Ring C) is attached to carbon 6, and purpurosamine (Ring B) is attached to carbon 4.

The numbering of ring atoms of gentamicin begins with the deoxystreptamine ring's *R*-carbon bound to nitrogen, and proceeds through an *S*-carbon bound to nitrogen. The sugar attached to 4-*R* carbon is annotated using

primed numbers, and the sugar attached to 6-*S* carbon is annotated using doubly primed numbers (Nagabhushan et al., 1982).

The gentamicin antibiotics are 2-DOS-based 4,6-disubstituted pseudosaccharides and are produced for clinical use as a mixture comprising gentamicins C1, C1a, C2a, C2, and C2b. Structurally, the compounds are very similar to each other, the only difference being the methylation pattern on the purpurosamine ring. All the members have similar bactericidal properties (Weinstein et al., 1967).

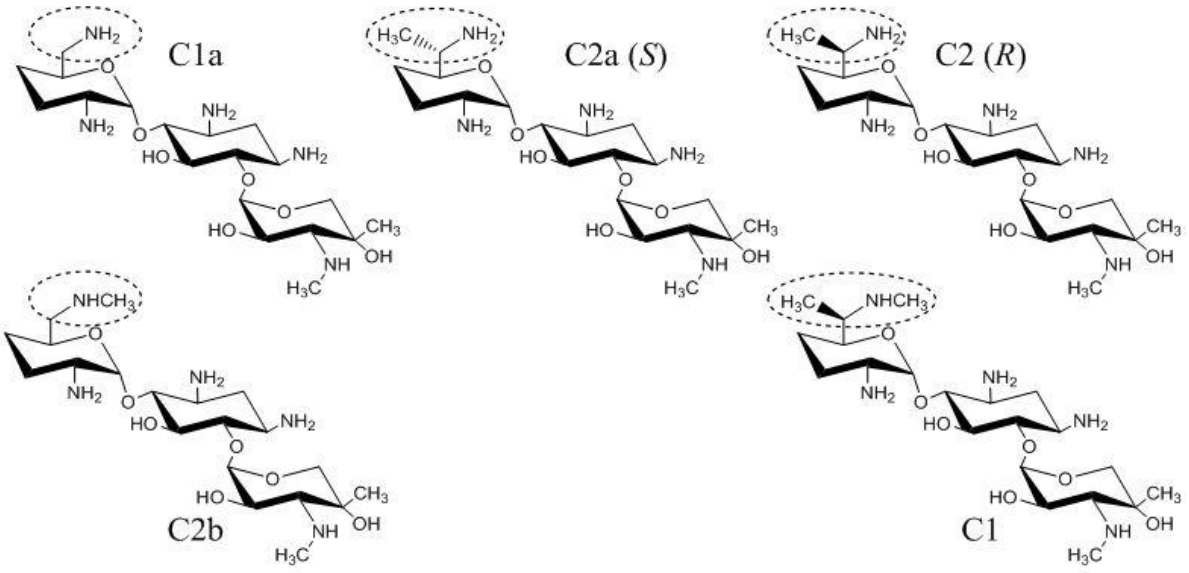

Figure 1.11 Gentamicin C complex. These five antibiotics differ only in their methylation pattern on the purpurosamine ring. Because of their close structural similarity, the individual components are notoriously hard to isolate, and gentamicin is clinically administered as a mixture of compounds instead.

Very similar compounds have been discovered as products in related *Micromonospora* species. *M. echinospora* sp. DSM 43816 (formerly *purpurea*), ssp. *ferruginea* DSM 43141, ssp. *pallida* DSM 43817, all produce gentamicin C complex; *M. sagamiensis* and mutant 2953 of *M. echinospora* both produce gentamicin C2b (sagamicin); *M. echinospora* (formerly *rhodorangea*) DSM 43822 produces gentamicin pathway intermediate G418 (geneticin™), and is probably a Δ*genQ* mutant (Ni et al., 2014); while mutant 2965 of *M. echinospora,* DSM

43036 produces intermediates JI-20A and JI-20B (named after their discoverer Jan Ilavsky (Ilavsky et al., 1975).

1.3.1 Sisomicin and verdamicin

A second group of *Micromonospora* compounds, called sisomicins (Figure 1.12), was discovered by Weinstein *et al* (Weinstein et al., 1970). Sisomicin is also a potent antibiotic and is the main product of *M. inyoensis*. When the structure of sisomicin (Figure 1.12) is compared to gentamicin C1a, it only differs in having a double bond between carbons 4' and 5' of the purpurosamine ring (ring II). *M. zionensis* also produces sisomicin, together with another antibiotic G-52, 6'-*N*-methylsisomicin or an 4'-unsaturated gentamicin C2b (Figure 1.12) (Marquez et al., 1976, Daniels et al., 1976). Verdamicins, 6'-methylated sisomicin (Figure 1.12), were discovered in 1975 as a product of another *Micromonospora* strain, *M. grisea* (Weinstein et al., 1975). Verdamicins also have a 4',5'-unsaturated ring II but are otherwise chemically identical to gentamicins C2 and C2a.

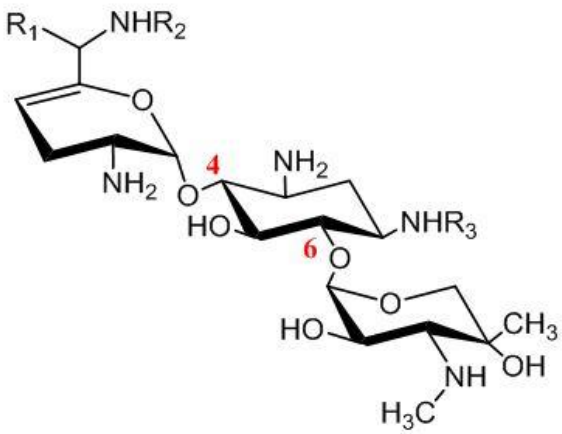

	R_1	R_2	R_3
Sisomicin	H	H	H
Netilmicin	H	H	CH_2CH_3
Verdamicin	CH_3	H	H
Plazomicin	CH_2CH_2OH	H	AHBA

Figure 1.12 Related compounds produced by other *Micromonospora* species. Both sisomicin and verdamicin possess a double bond between carbons 4' and 5'. The pattern of methylation of 6'-*C* and 6'-*N* is the difference between sisomicin, G-52, and verdamicin.

The close structural similarity of sisomicin and verdamicin to gentamicins has prompted speculation on their possible role as gentamicin pathway

intermediates, particularly during the loss of 3' and 4' hydroxyl groups from ring II during the biosynthesis of gentamicin.

The idea that sisomicin and verdamicin participate in gentamicin biosynthesis as intermediates was first proposed by Nakayama and colleagues (Kase et al., 1982a). Resting cells of mutant *M. echinospora*, *M. sagamiensis* (Kase et al., 1982c), or *M. rhodorangea* (Lee et al., 1977), which were blocked early in the gentamicin pathway, were fed sisomicin, which was reportedly converted into gentamicin C1a and C2b. Analogously, verdamicin C2a (4',5'-dehydro-gentamicin C2a), an antibiotic naturally produced by *M. grisea* (Weinstein et al., 1975), can be bioconverted by an (early stage) blocked mutant of *M. sagamiensis* (Kase et al., 1982c) into gentamicins C2a, C2, and C1. The proposal that verdamicin and sisomicin might be precociously exported intermediates or shunt products of the gentamicin pathway was later taken up and advocated by Wolfgang Piepersberg and his colleagues (Aboshanab, 2005, Piepersberg et al., 2007a). However, direct evidence for the identity of the enzymes and the exact mechanisms involved has remained elusive.

1.3.2 Mechanism of action of gentamicin

The mode of action of gentamicin is like that of other aminoglycosides: inhibition of protein synthesis. On exposure of bacteria to the drug, gentamicin is first attracted to the cell wall by electrostatic interactions, followed by an almost immediate uptake by the growing cells (Dubin et al., 1963) driven by respiration-dependent maintenance of the electrochemical potential across the membrane (Arrow and Taber, 1986). Because of this, gentamicin, like other aminoglycosides, is not effective against anaerobic bacteria. Gentamicin interferes with protein synthesis via an interaction with the 30S small ribosomal subunit (Bryan and Kwan, 1983). Specifically, it binds at the Aminoacyl site (A site): a conserved, asymmetric internal loop at the base of helix 44 of 16S component rRNA (Figure 1.13) (Bryan and Kwan, 1983, Feldman et al., 2010, Moazed and Noller, 1987). NMR spectroscopy of the complex of RNA and an aminoglycoside paromomycin has revealed that the binding of the antibiotic occurs in the major groove of the RNA, within a pocket created by an adenine base pair (A1408 and A1493) and a single adenine (A1492), where the antibiotic adopts an L-shaped conformation (Fourmy et al., 1996).

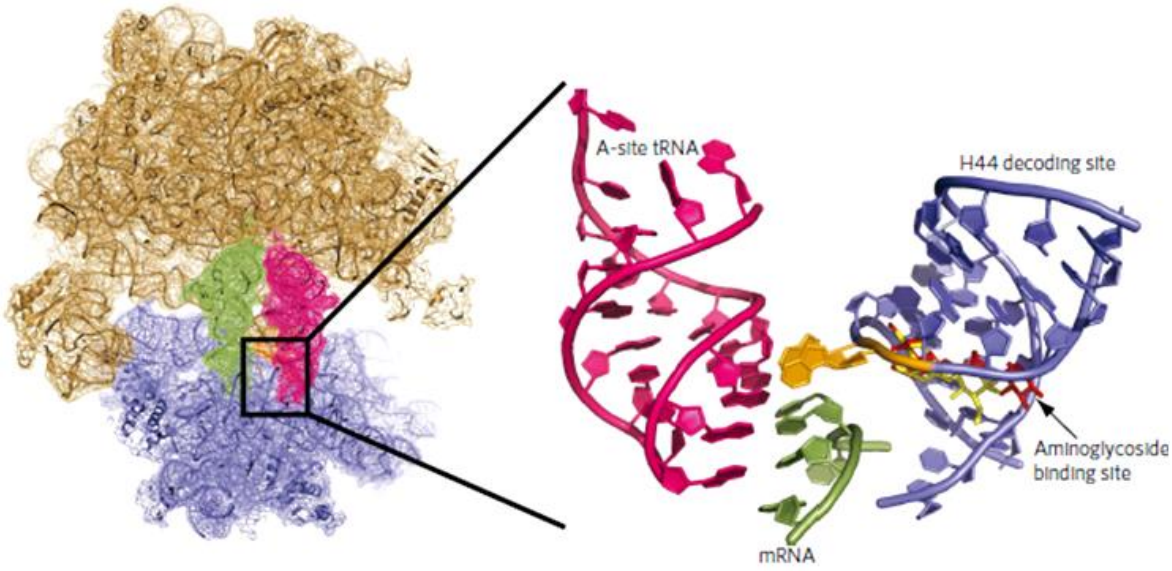

Figure 1.13 The site of aminoglycoside binding on the bacterial ribosome. Gentamicin, like other aminoglycosides, possesses several binding sites on the bacterial ribosome. The binding site that interferes with ribosomal function is the "decoding" site (in the black box). Binding of gentamicin to helix 44 of the 16S ribosomal subunit displaces the bases of A1492 and A1493 (yellow). This interferes with interactions between 16S rRNA (blue), tRNA (pink), and mRNA (green). Figure adapted from Figure 1 in (Feldman et al., 2010).

The central (Ring I) and purpurosamine (Ring II) rings of gentamicin make most of contacts with RNA (Figure 1.14). A bulge in the structure generated by the binding of the antibiotic interferes with the interactions between the codon of the mRNA and the anticodon of a charged tRNA. This causes protein mistranslation and truncation (Magnet and Blanchard, 2005). Although there is no complete biochemical explanation of the bactericidal effect of gentamicin, lethality is correlated with the increased concentration of mistranslated proteins.

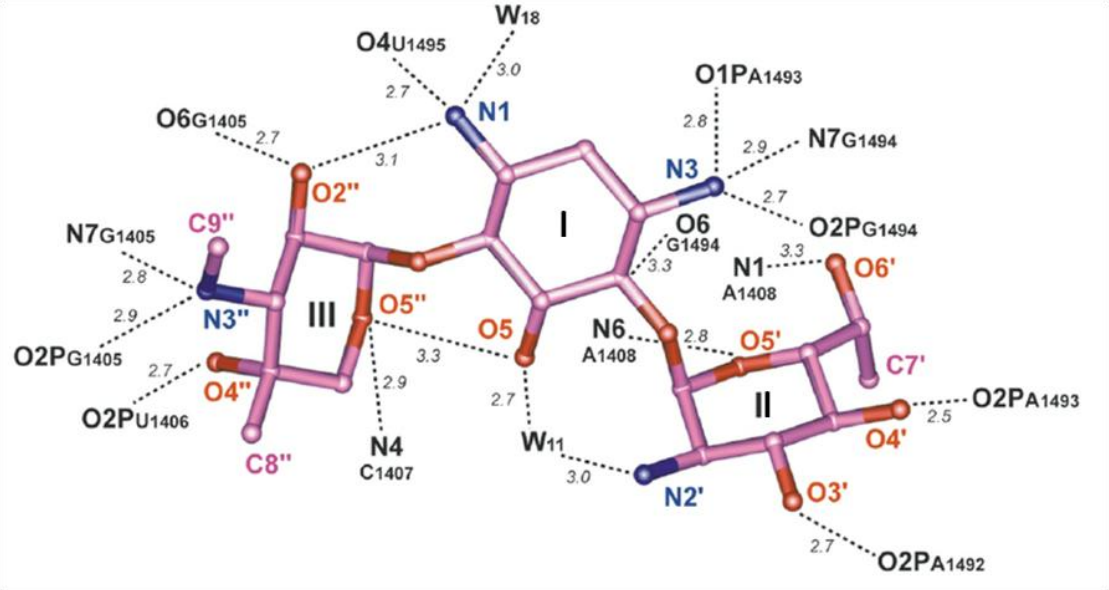

Figure 1.14 Points of interaction between geneticin™ or G418 and the ribosome A-site.
Hydrogen bonds between the gentamicin intermediate G418 and residues within the ribosomal A-site are shown as dotted lines. Figure adapter from Figure 5 from (Vicens and Westhof, 2003).

The sequences of both the prokaryotic and eukaryotic decoding regions exhibit elevated level of conservation and similarity. A point mutation A1408G in the prokaryotic A-site is known to reduce the efficacy of antibiotic therapy; G1408 distinguishes between prokaryotic and eukaryotic ribosomes (Lynch and Puglisi, 2001b). The presence of bacteria-like ribosomes, where residue 1408 is adenine, within human mitochondria is thought to contribute to the ototoxicity of gentamicin. The eukaryotic ribosome has a more shallow binding pocket for aminoglycosides, disrupting binding of the top ring of the antibiotic to the ribosome and causing displacement of A1492 (Figure 1.15) (Lynch and Puglisi, 2001a).

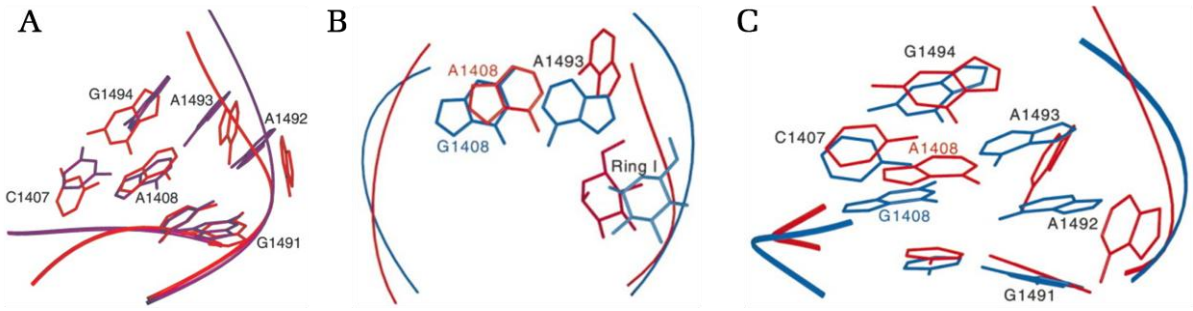

Figure 1.15 Comparison of prokaryotic and eukaryotic ribosomal A-site. (A) Free RNA (purple) undergoes a conformational change (red) on binding of an aminoglycoside paromomycin; (B) binding of paromomycin affects the structure of prokaryotic (red) RNA differently from eukaryotic (blue) RNA; (C) One of the key changes is in residue A1408 (red, prokaryotic) and G1408 (blue, eukaryotic) in the asymmetric internal loop. Adopted from Figures 1, 8 and 9 in (Lynch and Puglisi, 2001a).

In prokaryotic cells mistranslated membrane proteins change the structure and composition of the cell wall, affecting its permeability. Interestingly, this increases the irreversible accumulation of aminoglycoside molecules inside the cell (Magnet and Blanchard, 2005). In addition to causing mistranslation, gentamicin inhibits the formation of the 30S initiation complex and the release of fMet-tRNA$_F$ from the 70S initiation complex, reducing overall protein synthesis (Okuyama and Tanaka, 1972). Inhibition of protein synthesis is followed by impairment of respiration, inhibition of RNA and DNA synthesis, breakdown of RNA, and excretion of nucleotides from the cell, and, finally, loss of viability (Moellering, 1982).

In addition to binding bacterial ribosomes, gentamicin also interacts with tubulin, forming an insoluble complex *in vitro* (Akiyama et al., 1978). Insoluble complexes are also formed on contact with skeletal muscle actin (Someya and Tanaka, 1979).

1.3.3 Clinical use of gentamicin

Despite their side effects, aminoglycoside antibiotics firmly remain on the World Health Organization's List of Essential Medicine (WHO, 2017). Their discovery, starting with streptomycin, allowed tuberculosis to be cured for the first time, making it one of the major success stories of the 20th century. Their broad

spectrum of activity makes them ideal for use in emergencies and severe infections, with only rare cases of allergic reactions recorded. Aminoglycosides, gentamicin in particular, are amongst the few affordable medicines available in the developing world. Therefore, research into the biosynthetic pathway of gentamicin, which can and will lead to improved yields, safer and new antibiotics, as well as new pure starting materials for the semi-synthetic developments, is an important advancement of science.

Gentamicin is a water-soluble basic compound, that is stable over a wide range of pH and temperatures, which makes it widely applicable in the World. It is normally administered via an intravenous or intramuscular route. Pharmaceutical grade gentamicin varies in exact composition as it is a product of fermentation, but any sample has to conform to European Pharmacopoeia specifications: no less than 80% of the mixture is gentamicin C, the rest being gentamicin A, B, and X complexes (Vydrin et al., 2003). Gentamicin, like other aminoglycosides, exhibits concentration-dependent killing, with higher doses leading to greater effect, so a single dose is normally administered daily (Varley et al., 2009b). Curiously, the antimicrobial effect of gentamicin continues even after the serum level drops below the minimal inhibitory concentrations (MIC).

Clinical use of aminoglycosides tends to be limited to serious - but varied - infections. Severe forms of ear infection by *P. aeruginosa*, *Klebsiella*-caused pneumonitis (Hodges and Saslaw, 1972), complicated urinary tract infections (Chisholm, 1974), sepsis caused by any Gram-negative bacteria (*E. coli, Serratia, Proteus, P. aeruginosa*, *Klebsiella*) (Noone et al., 1974), skin and soft tissue infections with *Aeromonas, Acinetobacter,* and *Pseudomonas*, skin burns, bone and joint infections, as well as eye infections by *Serratia, Proteus,* or *P. aeruginosa* (Mathalone, 1974, Peyman and Herbst, 1974), have all found gentamicin treatment to be extremely useful.

There are other surprising applications for aminoglycosides in medicine. As aminoglycosides cause protein mistranslation, in disorders with nonsense mutations they can be used as an indirect gene therapy, often partially rescuing the affected protein's production. Cystic fibrosis has a long history of treatment with gentamicin, originally to protect against complications by infection

(Boxerbaum et al., 1971, Barton-Davis et al., 1999)). However, it was also shown to induce corrections of stop codons in the gene of cystic fibrosis transmembrane conductance regulator (*CFTR;* Figure 1.16) (Wilschanski et al., 2003).

Duchenne muscular dystrophy (DMD) is a debilitating disease of skeletal muscle caused by mutations in the dystrophin gene, many of which are premature stop codon mutations. Barton-Davies *et al* showed that gentamicin could be used *in vivo* to suppress stop codons and identified a treatment regimen that provided protection against muscular injury and could help 15% of patients with DMD (Barton-Davis et al., 1999). Gentamicin has also been used as a treatment for severe haemophilia and was successful in two out of five human patients (James et al., 2005).

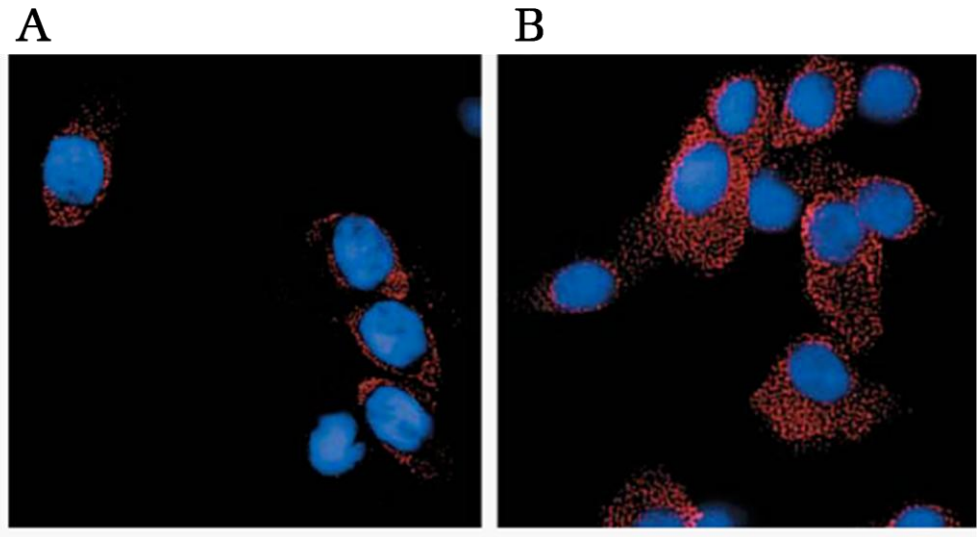

Figure 1.16 Full-length CFTR expression is improved by gentamicin. (A) Cystic fibrosis is caused by mutations in the Cystic Fibrosis Transmembrane conductance Regulator (CFTR) gene. Panel A shows full-length protein (red) in mice CFTR cells. (B) The quantity of protein is improved significantly on treatment with gentamicin. Figure adapted from Figure 4 in (Wilschanski et al., 2003).

Small molecules, such as aminoglycosides, can also be used to interfere with RNA-protein and RNA-RNA complex formation in viruses. Human immunodeficiency virus (HIV) is a global problem, with 40 million people living with HIV-caused auto-immune deficiency syndrome (AIDS) according to WHO. In 1993 Green *et al* showed that aminoglycosides can bind to the Rev response element and prevent the formation of a complex between this RNA and the HIV-

1 Rev protein (Zapp et al., 1993). Due to their promiscuity in binding many RNA targets, aminoglycosides will probably never become therapeutically used antiviral compounds, however, they provide a solid foundation for development of better anti-HIV drugs.

1.3.3.1 Synergistic use with other antibiotics

Partly to overcome the fast development of resistance by pathogens and partly to improve the targeted activity of the drugs, "mixing and matching" of antibiotics has become a recent trend in the clinical use of antimicrobials. A mixture of a β-lactam antibiotic, such as penicillin, and an aminoglycoside, such as gentamicin, exhibits synergistic behaviour, i.e. the combined antimicrobial effect of the two drugs mixed together is greater than the sum (Leekha et al., 2011). A variety of infections with Gram-positive or Gram-negative bacteria can be treated more effectively this way; for example, a combination of gentamicin and penicillin is used to treat endocarditis caused by *Enterococcus* bacteria (Drusano, 1990). When used individually, aminoglycosides have no effect and penicillins are bacteriostatic, but when used together a bactericidal effect is achieved (Varley et al., 2009b). Treatments with a combination of antibiotics tend to take less time to clear the infection, such as therapy with penicillin or ceftriaxone with gentamicin taking two weeks instead of four to treat endocarditis caused by *Streptococcus viridans* (Baddour et al., 2005).

1.3.4 Side-effects of gentamicin use

Clinical use of gentamicin, like most of the other aminoglycosides, is restricted by issues of nephrotoxicity (kidney damage) and ototoxicity (damage to the ear). Depending on the dose and duration of treatment, kidney damage occurs in 10-20% of cases (Swan, 1997). Aminoglycosides antibiotics damage the epithelial cells lining the proximal tubules, leading to tubular necrosis (Sairio et al., 1978). Gentamicin is not metabolised and therefore is eliminated from the body exclusively via glomerular filtration; due to this its kidney toxicity side-effects are closely related to the accumulation of the drug by the renal tubular cells.

Damage to the structure of nephrons is observed by scanning electron microscopy even on administration of low doses of gentamicin (Evans et al., 1979). The damage is slow in onset (five to seven days) and is normally

reversible in ten to thirty days after the cessation of treatment (Schentag, 1982). The level of gentamicin in the serum depends heavily on the state of renal function and the original health of the tissue. Both glomerular filtration and proximal tubule function (regulation of filtrate pH) are impaired because of aminoglycoside nephrotoxicity.

Other medications can often interact with gentamicin exacerbating its side-effects. For example, combination therapy with amphotericin can significantly increase the risk of nephrotoxicity (Leekha et al., 2011). It is also important to consider dehydration or the use of diuretic agents with gentamicin, as these are known to enhance renal toxicity (Chiu and Long, 1978).

Damage to the kidneys can be abated by close monitoring and proper use. It is also reversible. Other side effects from aminoglycoside treatment include damage to vestibular function, resulting in loss of balance, and damage to the cochlea, resulting in hearing loss (Forge and Schacht, 2000). Treatment can result in the permanent loss of inner ear function - hearing and balance - in approximately 5% of the patients on extended treatment (Brummett and Fox, 1982, Waguespack and Ricci, 2005). Ototoxicity of gentamicin is the major limiting factor of its clinical use, as a very narrow margin of safety exists between therapeutic and ototoxic doses of gentamicin; some people are also genetically predisposed to suffering greater damage from aminoglycoside therapy. Mutations affecting mitochondrial rRNA, such as the A1555G mutation in the 12S rRNA, predispose to hearing loss (Guan et al., 2000). Less than 1% of the human population carry this mutation, however, even a single dose of gentamicin can lead to permanent hearing loss (Prezant et al., 1992).

To visualise the damage, electron microscopy studies of the inner ear were performed on guinea pigs following aminoglycoside treatment (Brummett et al., 1972, Brummett and Fox, 1977, Brummett et al., 1978). Only sensory hair cells were affected; however, the cells were destroyed in successive rows from the innermost row of the outer hair cells to the inner hair cells (Figure 1.17). As the location of hair cells is linked to their ability to perceive specific frequencies of sound, the loss of hearing always progressed from high-frequency to low. Within a hair cell, an early target appears to be the 12S rRNA within the mitochondria

(Guan et al., 2000). Changes to protein synthesis caused by aminoglycosides reduce the translation level below critical, triggering progressive destruction of the cell, starting with mitochondrial compartments breaking into vesicles.

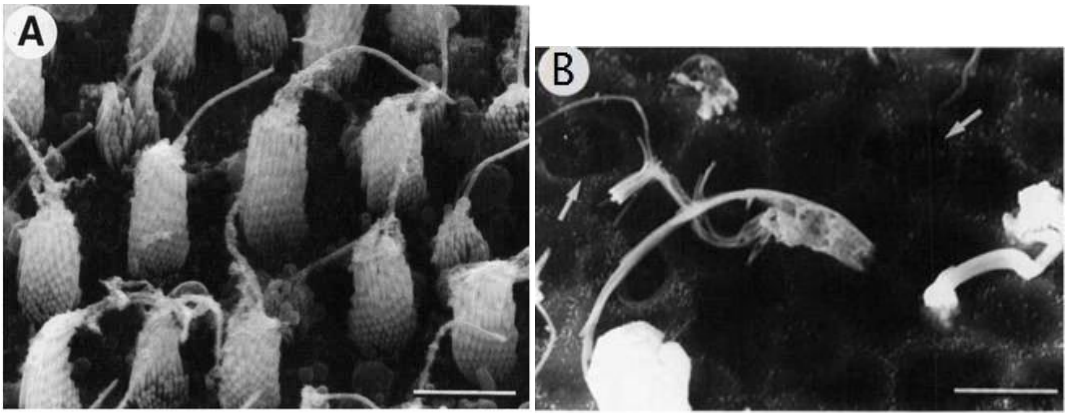

Figure 1.17 Effect of gentamicin treatment on the guinea pig inner ear. a) Scanning electron microscopy (SEM) image of the epithelium of inner ear of a control untreated guinea pig, showing healthy distribution of sensory hair cells. b) SEM image of the epithelium surface 2 days after gentamicin treatment. The darker areas and arrows indicate missing hair cells. Figures 1A and 2A from (Li et al., 1995). Scale bars = 5 μm.

On treatment with gentamicin two different modes of cell death are observed in the ear: cell degeneration within the epithelium and cell extrusion through the epithelial surfaces (Li et al., 1995). Neighbouring cells appear to expand to preserve the permeability barriers. No other cell type is affected by the treatment, and the overall tissue architecture is preserved. Within the cochlea the hair cells are unable to regenerate, leading to permanent damage and hearing loss.

The damage to the vestibular organ occurs through cell damage at the apex of the cristae, followed by damage to Type I vestibular hair cells, followed by damage to Type II cells. Severe loss of balance is observed after damage has occurred, however, regeneration of the vestibular hair cells has been observed in mammals (Forge et al., 1993).

Formation of reactive oxygen species (ROS) has long been suspected as being the underlying molecular mechanism of gentamicin toxicity (Walker and Shah, 1987). Gentamicin can form a 1:1 complex with iron (II) or iron (III)

(Figure 1.18) (Priuska et al., 1998). Gentamicin was able to accelerate the formation of free radicals by iron, leading to the hypothesis of redox-active complexes (Priuska and Schacht, 1995). Phosphatidyl inositol 4,5-bisphosphate can bind both iron and gentamicin, and facilitate aminoglycoside/iron-mediated superoxide formation as an electron donor (Lesniak et al., 2005). In addition to this non-enzymatic ROS formation, aminoglycosides enhance the activity of Rac-1 GTPase (involved in actin cytoskeleton dis/as-sembly control), leading to activation of the NADPH oxidase complex, and enzymatic ROS generation (Jiang et al., 2006). ROS readily oxidize many essential cellular components, triggering apoptotic pathways.

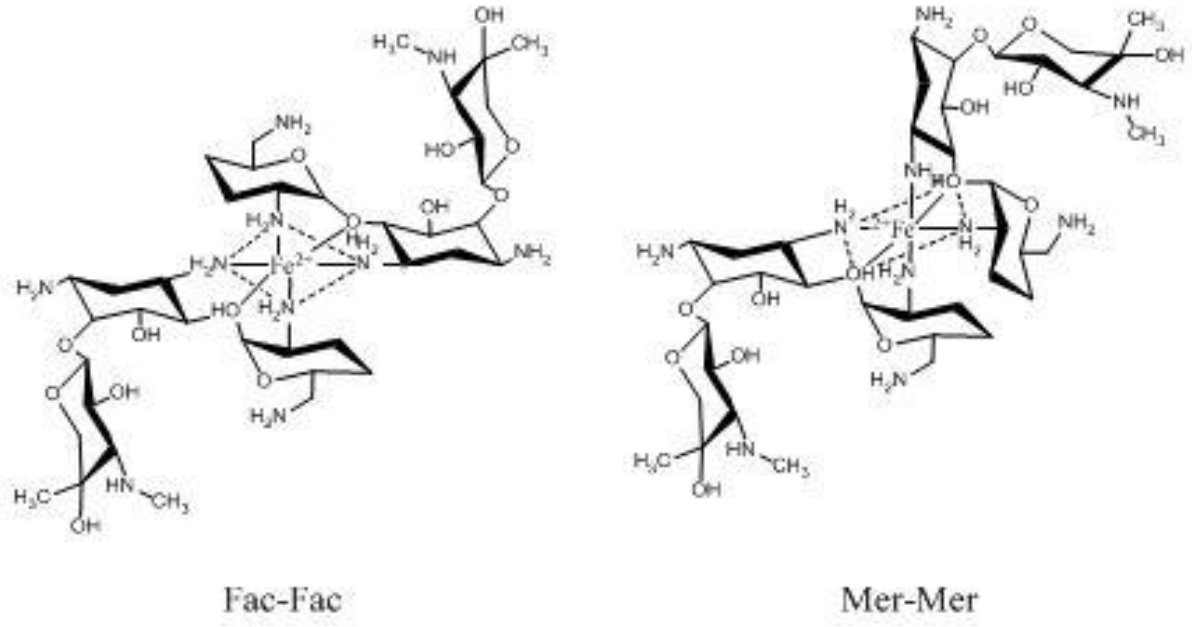

Figure 1.18 Gentamicin C1a:iron (II) complexes. Two gentamicin molecules form a complex with one iron (II) ion. Two possible coordination isomers were proposed by Evans *et al* based on two binding constants observed, Fac-Fac and Mer-Mer. Both require four ligating nitrogens (Priuska et al., 1998).

This ability of gentamicin to induce ROS damage to the cells can have surprising useful applications. Cuccarese *et al* reported that low doses of gentamicin could be used to improve anticancer therapy by sensitising NCI-H460 lung cancer cells to various anticancer agents, improving their efficacy (Cuccarese et al., 2013).

Other molecules can be used to minimise the toxic side-effects of gentamicin. Inhibition of protein synthesis with cycloheximide prevented hair

cell death in a chick model caused by aminoglycoside neomycin treatment, suggesting that *de novo* protein synthesis was required for activation of cell death pathways (Matsui et al., 2002). Antioxidant molecules, such as vitamin E or methionine, have a protective effect on the ear in guinea pig *in vivo*, presumably by removing the ROS from the cells (Song and Schacht, 1996); antioxidant therapy, therefore, could finally allow a wider use of aminoglycoside therapy (Sha et al., 2006). A more directed approach could be better for a successful clinical application, with local gene therapy e.g. introducing an antioxidant enzyme gene into the cochlea having been shown effective in guinea pigs (Kawamoto et al., 2004).

Appropriate control of the clinical regimen, use, and duration of treatment can prevent aminoglycoside toxicity. However, in addition to costs of production by fermentation, continuous and close monitoring of drug concentration in blood and urine increases the price of gentamicin treatment considerably. Extensive work has been done to create semi-synthetic derivatives of aminoglycosides designed to overcome pathogen resistance, but very little progress was achieved in reducing the toxic side-effects (Leitner and Price, 1982).

1.3.5 Resistance to gentamicin

Despite the broad spectrum and desirable bactericidal activity of aminoglycoside antibiotics, the interest in these compounds has rapidly decreased following the emergence of bacterial resistance and development of safer aminoglycosides.

Resistance to gentamicin occurs through three main methods: mutations of the ribosome (rare), alterations in membrane permeability, and enzymatic modification (Moellering, 1982). As it binds specifically to the 16S rRNA in the codon-decoding A-site, point mutations in the 16S rRNA can result in resistance to aminoglycosides, such as mutations of A1408 conferring high-level resistance. Other reported cases of resistance include methylation of the ribosomal A-site (N7 position of rRNA G1405 by Rmt and Arm methylases or N1 of A1408 by NpmA methylase) (Wachino et al., 2007, Wachino and Arakawa, 2012); increased efflux by MexXY and ABC transporters in *P. aeruginosa* (Bonomo and Szabo, 2006); and antibiotic-modifying enzymes (*N*-acetyltransferases (AAC), *O*-nucleotidyltransferases (ANT), and *O*-phosphotransferases (APH)). Out of the

three methods of resistance, aminoglycoside-modifying enzymes are the most common and clinically important type. Sites of enzymatic inactivation in gentamicin by resistant pathogens are shown in Figure 1.19.

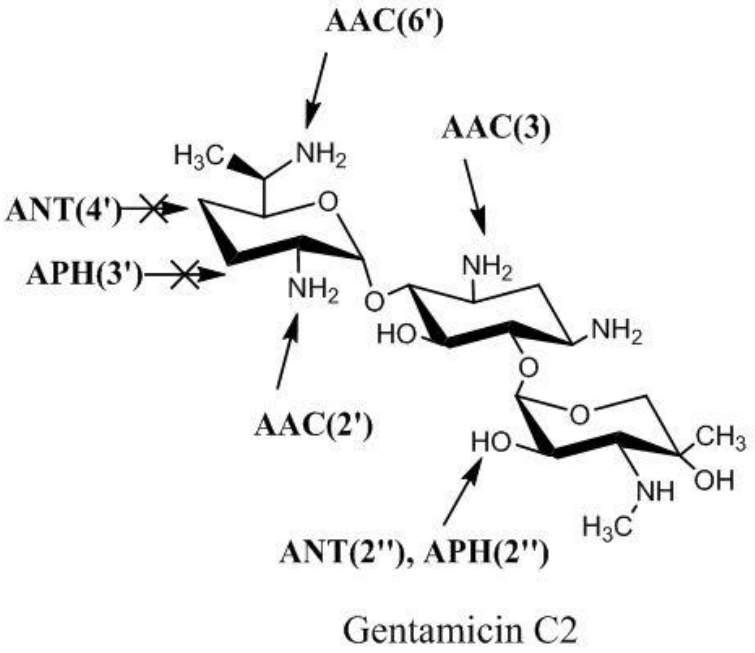

Figure 1.19 Gentamicin C2 enzymatic inactivation sites. Several positions of the gentamicin structure can be attacked by the antibiotic-modifying enzymes. AAC = sites of acetylation; ANT = site of adenylation; APH = site of phosphorylation.

Gentamicin was the treatment of choice for many Gram-negative infections before a new class of inactivation by aminoglycoside-modifying enzymes, 2' OH adenylation, started to appear in *Klebsiella* from 1971 onwards (Martin et al., 1971, Benveniste and Davies, 1971a, Benveniste and Davies, 1971b).

Gentamicin producer *M. echinospora* itself is a frequent donor of ribosomal methyltransferase resistance genes, with self-resistance gene *gmrA* responsible for G1405 methylation (Galimand et al., 2003).

1.3.6 The gentamicin (*gen*) biosynthetic gene cluster

The genome of *M. echinospora* consists of a circular 7.4 Mbp long chromosome. The DNA is 72% GC rich. Like most other antibiotics, gentamicin biosynthetic genes are clustered together in one portion of the genome. To date, no successful

heterologous expression of the entire cluster has been achieved, with several *Streptomyces* hosts failing to produce any gentamicin C complex. Therefore, the exact borders of the cluster and the identity of the minimal cluster required for a complete synthesis remained undefined.

The gentamicin cluster is estimated to contain 32 open reading frames within a 42 kbp region of DNA (ORFs, Figure 1.20). Based on the homology, predictions of function can be made for most of the encoded proteins (Table 1.3). In this work, nomenclature used by the Piepersberg group (Aboshanab, 2005), with "*gen*" for genes and "Gen" for proteins, is used, however, Table 1.3 lists alternative names used by other groups: "*gnt*" by Kwon and Kudo labs (Kim et al., 2008, Kudo and Eguchi, 2009, Li et al., 2013); and "*gac/gtm*" by Li, Kharel and Flatt (Li et al., 2013, Kharel et al., 2004, Flatt and Mahmud, 2007).

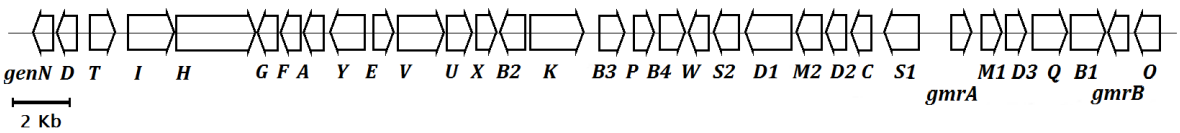

Figure 1.20 The *gen* cluster. Gentamicin biosynthetic genes (32) are clustered together in a 42 Kbp DNA segment.

Table 1.3 Gentamicin ORFs and predicted functions; adapted from (Flatt and Mahmud, 2007, Kudo and Eguchi, 2009).

gen Name	*gnt* Name	*gac/gtm* Name	Function	Product of catalysis
genN	-	-	*N*-methyltransferase	Gentamicin A
genD	-	*gtmM*	deacylase	paromamine
genT	-	-	*N*-methyltransferase	?
genI	-	-	exporter	-
genH	-	-	exporter	-
genG	-	-	6-pyruvoyl tetrahydropterin synthase	?
genF	*gntS*	-	production protein	?
genA	*gntR*	-	regulator	-
genY	*gntQ*	*gacI*	cation antiporter	
genE	*gntP*	*gacH*	dehydrogenase	3-amino-2,3-dideoxy-*scyllo*-inosose
genV	*gntO*	*gtmK*	efflux protein	-
genU	*gntN*	*gacG*	regulator	-
genX	*gntM*	*gacF*	hypothetical protein	?
genB2	*gntL*	*gacE*	aminotransferase	Gentamicin C2

genK	*gntK*	*gacD*	*C*-methyltransferase	G418
genB3	*gntW*	*gacC*	aminotransferase	?
genP	*gntI*	*gtmJ*	phosphotransferase, resistance	?
genB4	*gntL*	*gacB*	aminotransferase	?
genW	*gntG*	*gacA*	GTP cyclohydrolase I	?
genS2	*gntF*	*gtmD*	aminotransferase	3''-dehydro-3''-amino-gentamicin A2
genD1	*gntE*	*gtmI*	*C*-methyltransferase	Gentamicin X2
genM2	*gntD*	*gtmE*	glycosyltransferase	Gentamicin A2
genD2	*gntC*	*gtmC*	NAD-dependent dehydrogenase	3''-dehydro-3''-oxo-gentamicin A2
genC	*gntB*	*gtmA*	2-deoxy-*scyllo*-inosose synthase	2-deoxy-*scyllo*-inosose
genS1	*gntA*	*gtmB*	2-deoxy-*scyllo*-inosose aminotransferase	2-deoxy-*scyllo*-inososamine, 2-deoxystreptamine
gmrA	*grmA*	*gtmF*	ribosomal RNA-methyltransferase, resistance	-
genM1	*gntZ*	*gtmG*	glycosyltransferase	2'-*N*-acetylparomamine
genD3	*gntY*	*gtmH*	dehydrogenase	
genQ	*gntX*	*gacJ*	dehydrogenase	6'-dehydro-6'-oxo-gentamicin X2, 6'-dehydro-6'-oxo-gentamicin G418
genB1	*gntW*	*gacK*	aminotransferase	JI-20A, JI-20B
gmrB	*grmO*	*gtmL*	ribosomal RNA-methyltransferase, resistance	-
genO	*gntV*	*gacL*	tRNA ribosyltransferase	-

Gentamicin shares structural motifs and modification patterns of two other aminoglycosides, fortimicin and kanamycin (Piepersberg et al., 2007a). The gentamicin gene cluster is predicted to have arisen from a fusion of kanamycin (*kan*) and fortimicin (*for*) clusters due to high similarity of gentamicin genes to one or the other (Figure 1.21). Gentamicin cluster also contains fragments of *for* genes, probably from evolutionarily recent events of recombination and deletion. The DNA of *kan* and *for* clusters was analysed by sequence alignment and showed no similarity to each other. Portions of *gen* cluster, on the other hand, showed significant similarity to one or the other cluster. The two ends of the cluster appear to be more like *for* cluster, with the inside part homologous to *kan* cluster genes, apart from an interruption by another *for* stretch. Many DNA

rearrangements, including deletions, inversions, and insertions, are present within the cluster.

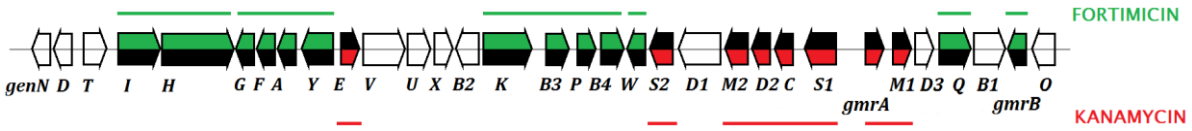

Figure 1.21 The probable origin of *gen* genes. Most of the gentamicin biosynthetic genes are highly similar to either fortimicin or kanamycin biosynthetic genes. The *gen* cluster in this Figure highlights sections probably inherited from either *for* (green) or *kan* (red) clusters.

The regions of conservation between the *gen* and *kan* clusters are *genM2-genD2-genC-genS1* and *kanM2-kanD2-kanC-kanS1, kanE* and *genE, kanS2* and *genS2, gmrA-genM1* and *kmr-kanM1*. The regions of conservation between *gen* and *for* clusters are *genH-genI* and *forH-forI-forJ*, *genQ* and *forD2*, *genK-genB3-genP-genB4* and *forP-forB-forK*, *genI* and *forT*, *genY-genA-genF-genG* and *fosD-fosE-fosF-fosG*, *genW* and *fosC*, *gmrB-genP* and *fmrB-fosA*.

1.3.7 Biosynthesis of gentamicin

The biosynthesis of gentamicin C was first outlined by Testa and Tilley (Testa and Tilley, 1976). Using feeding studies of a blocked mutant of *M. echinospora* (Paro 346), they showed that gentamicin C1a could be converted to gentamicin C2b, and gentamicin C2 was converted to gentamicin C1, suggesting a branched pathway. Feeding various minor components of wild-type or other blocked mutant fermentations, they further established the order of some intermediates in the pathway, later confirmed by other experimental work (Figure 1.22).

The proposed biosynthesis starts by converting paromamine to gentamicin X2 via gentamicin A2. The pathway then branches into two parallel routes: from gentamicin X2 to gentamicin C2b, and from 6'-*C*-methylated gentamicin X2, G418, to gentamicin C1. In contrast to kanamycin, the branches are truly separate, and intermediates from one branch cannot be *in vivo* converted to the other (Yu et al., 2017).

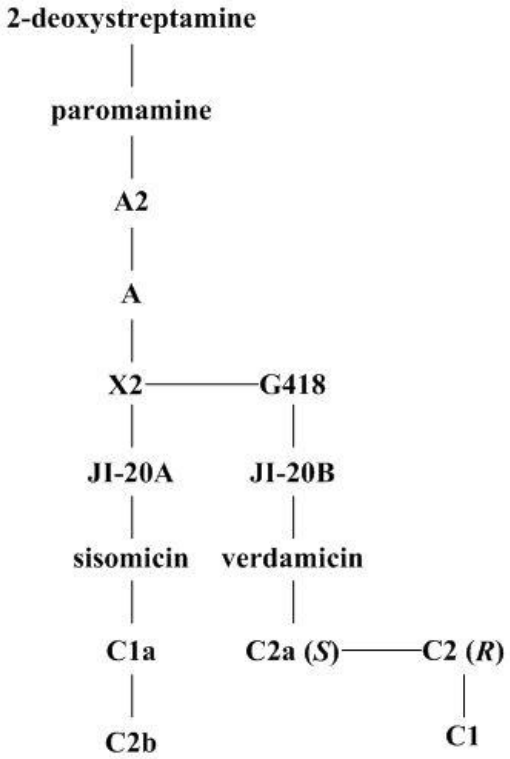

Figure 1.22 Biosynthetic pathway proposed for gentamicin or sisomicin (Adapted from Fig 8 of (Testa and Tilley, 1976)). Gentamicin and sisomicin are generated via identical routes. Compared to *M. inyoensis* and *M. grisea,* extra genes present in the *gen* cluster convert sisomicin and 6'-methylated sisomicin, verdamicin, into gentamicin C complex components.

The sisomicin biosynthetic pathway was also proposed by Testa and Tilley (Testa and Tilley, 1975). All the intermediates were the same between the gentamicin and the sisomicin pathway, and when sisomicin was fed to a *M. echinospora* mutant (*M. rhodorangea* NRRL 5326) production of gentamicin C2b was detected (Lee et al., 1977). Minor quantities of sisomicin can also be detected in the fermentation mixture of gentamicins, suggesting it might be an intermediate of the gentamicin pathway.

The sequence of gentamicin biosynthesis begins with generation of the three rings, their condensation together, and modifications. The synthesis of the central ring, 2-deoxystreptamine (2-DOS), was postulated by Rinehart and Stroshane and confirmed experimentally by Daum *et al*; using feeding studies the latter demonstrated that 2-DOS was formed from 2-deoxy-*scyllo*-inosose via 2-deoxy-*scyllo*-inosamine (Figure 1.23) (Rinehart and Stroshane, 1976, Daum et al., 1977). Grisebach then suggested that the garosamine ring was formed from D-

glucose, later shown to be glucose-6-phosphate (Grisebach, 1978). The purpurosamine ring is generated from D-xylose.

Heterologous expression performed by Park *et al* was then used to identify the minimal set of genes necessary for generation of the first tricyclic gentamicin intermediate, gentamicin A2 (Figure 1.23). *Streptomyces venezuelae* was transformed with six *Micromonospora* genes (Park et al., 2008a); 2-DOS was generated when a plasmid with a *genS1-genC-genE* gene cassette was present. GenM2 and GenD converted 2-DOS to paromamine via a reaction with upper D-*N*-acetyl-α-D-glucosamine, and GenM1 converted paromamine to gentamicin A2.

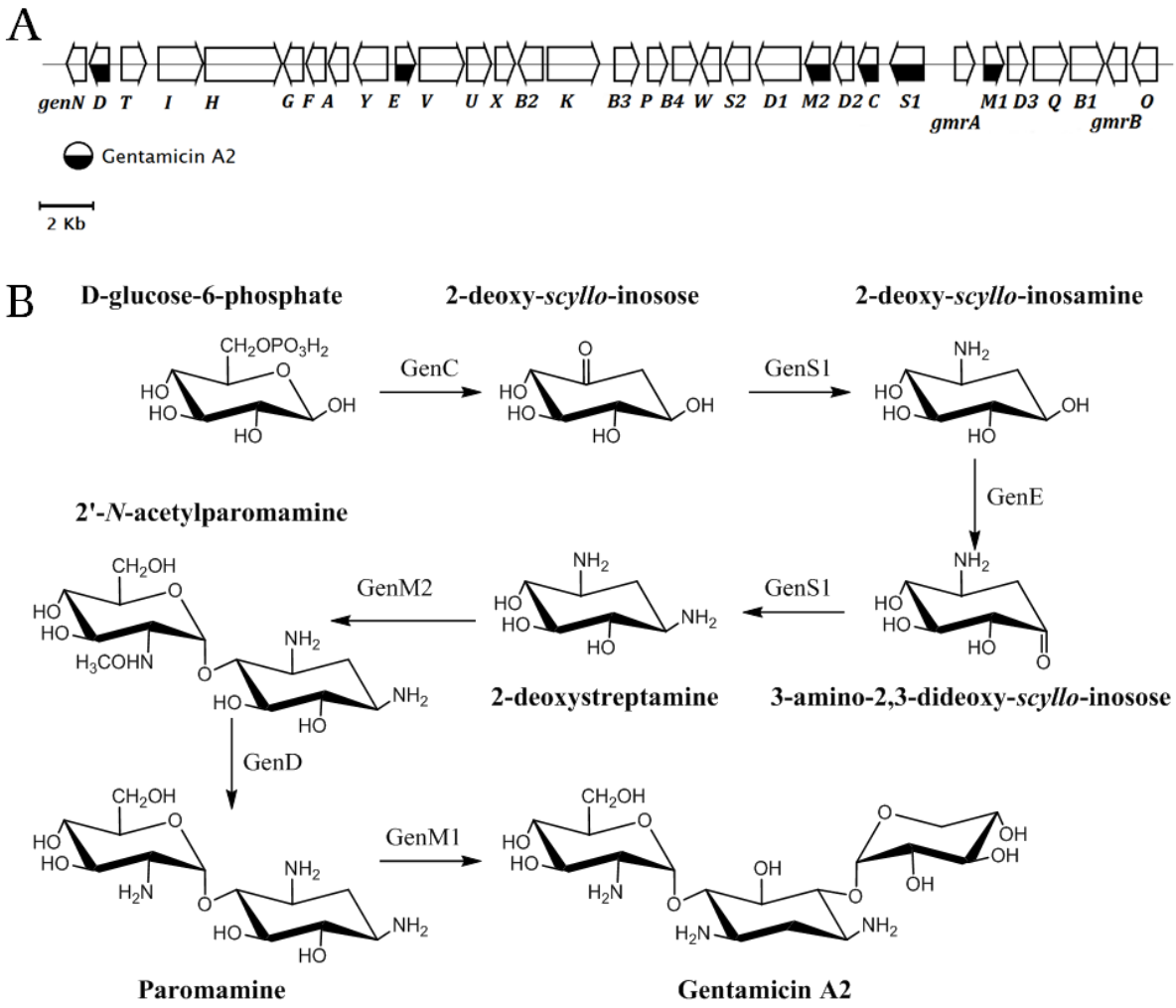

Figure 1.23 Early gentamicin biosynthesis. (A) The *gen* cluster with highlighted genes used for gentamicin A2 biosynthesis. (B) The biosynthesis begins with glucose-6-phosphate converted to 2-deoxy-*scyllo*-inosose by a carbocyclization reaction of GenC (Kharel et al., 2004). GenS1 performs a transamination on C3 using L-glutamine as a cofactor, GenE acts as a dehydrogenase (SAM- and NAD $(P)^{+}$-dependent) on C5, and GenS1 performs a transamination on C1. This produced 2-deoxystreptamine (2-DOS). GenM2 is a glycosyltransferase which catalyses addition of uridine diphosphate *N*-acetyl-D-glucosamine to 2-DOS to form a disaccharide precursor. GenD deacetylates it to give paromamine. Finally, GenM1 is another glycosyltransferase that adds uridine diphosphate D-xylose to paromamine generating the first tricyclic gentamicin intermediate, gentamicin A2 (Park et al., 2008a).

Two papers published by our group and a paper by Kim *et al* then dealt with conversion of gentamicin A2 to the JI-20 complex. In biosynthetic order, a paper published by Huang *et al* in 2015 showed how gentamicin A2 was converted to gentamicin X2, the last common precursor for all the gentamicin C complex components (Huang et al., 2015). Four proteins were necessary for the conversion: GenD2 and GenS2 performed a transamination reaction; GenN acted

as a 3''-*N*-methyltransferase to form gentamicin A, and GenD1 added a methyl group to 4'' carbon to form gentamicin X2 (Figure 1.24).

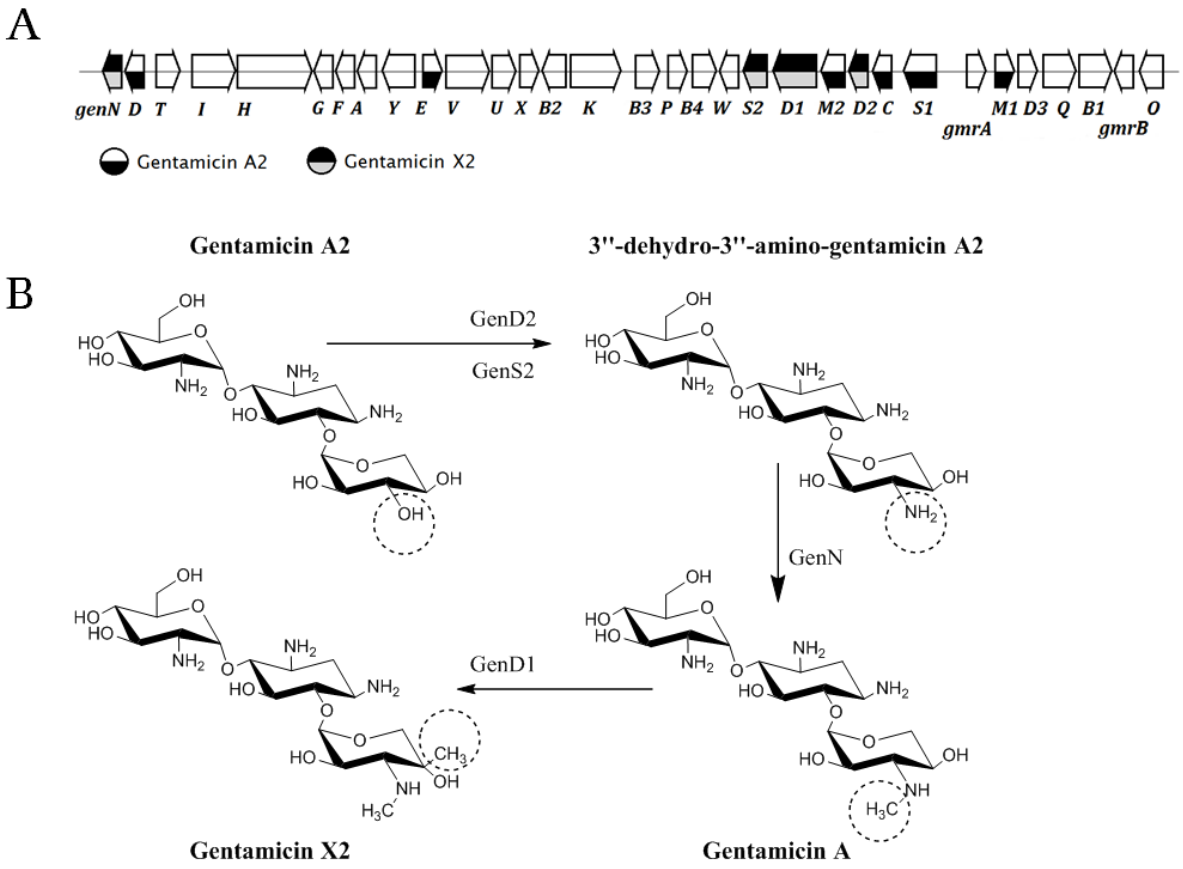

Figure 1.24 Early-middle gentamicin biosynthesis. (A) The *gen* cluster highlighting the genes used for gentamicins A2 and X2 biosynthesis. (B) Oxidoreductase GenD2 and pyridoxal phosphate-dependent aminotransferase GenS2 catalyse transamination of 3'' hydroxyl of gentamicin A2 in a reversible manner. SAM-dependent GenN methylates the newly-formed 3''-amino group to form gentamicin A. Finally, radical SAM- and cobalamine-dependent GenD1 adds a methyl group to C2'', forming gentamicin X2, the last common precursor for all the components of the gentamicin C complex (Huang et al., 2015).

Kim *et al* showed that GenK was the cobalamine-dependent 6'-*C*-methyltransferase that generated two parallel branches of the gentamicin biosynthetic pathway (Figure 1.25) (Kim et al., 2013). Guo *et al* then showed GenQ and GenB1 to be responsible for JI-20 synthesis via a transamination reaction (Guo et al., 2014). The paper also suggested GenB2 enzyme acting as an epimerase, inter-converting gentamicins C2 and C2a. Gu *et al* proposed an alternative pathway, with GenQ and GenB1 creating JI-20Ba, an *S* isomer, and GenQ and GenB2 creating JI-20B, an *R* isomer (Gu et al., 2015).

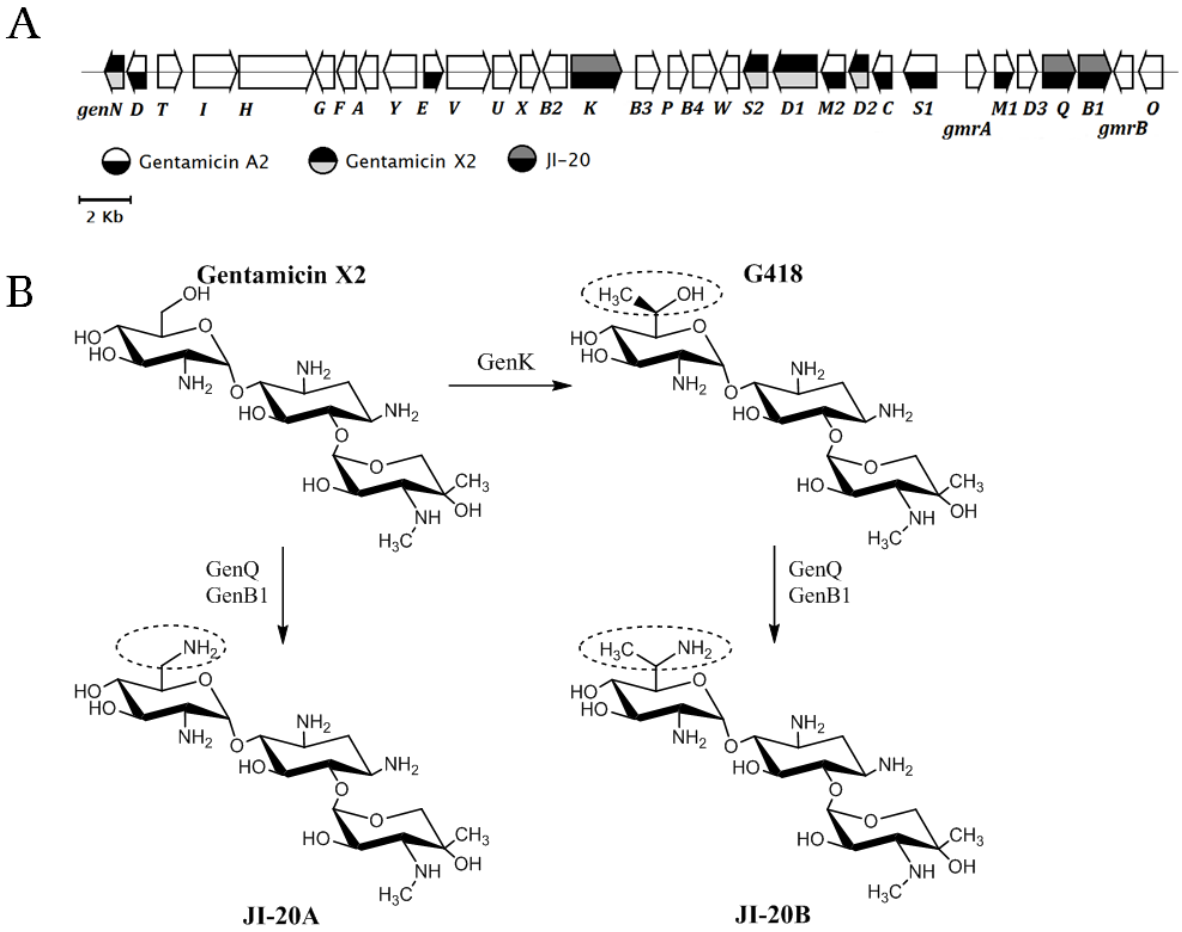

Figure 1.25 Late-middle gentamicin biosynthesis. (A) The *gen* cluster highlighting the genes used for JI-20 biosynthesis. (B) Cobalamine- and radical SAM-dependent methyltransferase GenK converts a portion of gentamicin X2 to G418 via a 6'-carbon methylation (Kim et al., 2013). Dehydrogenase GenQ catalyses both of the created branches to form keto intermediates. Work done in our lab showed that aminotransferase GenB1 completed the transamination reaction using L-methionine as the amino group donor, although other GenB enzymes could substitute for GenB1 to an extent (Guo et al., 2014). JI-20A (non-6'-*C*-methylated) and JI-20B (6'-*C*-methylated) are thus formed.

Therefore, most of the steps of gentamicin biosynthesis have enzymes from the cluster assigned to them already (Figure 1.26). The two branches of biosynthesis have a largely parallel sequence of enzyme-catalysed conversions, with only one step missing from the non-6'-*C*-methylated or JI-20a branch. The late steps of gentamicin biosynthesis involve di-dehydroxylation of JI-20, change of stereochemistry of gentamicin C2a, and terminal *N*-methylation of gentamicins C1a and C2. Enzyme GenB2 was found to be the gentamicin C2a epimerase (Guo et al., 2014). The other two steps will be discussed in more detail in the later chapters.

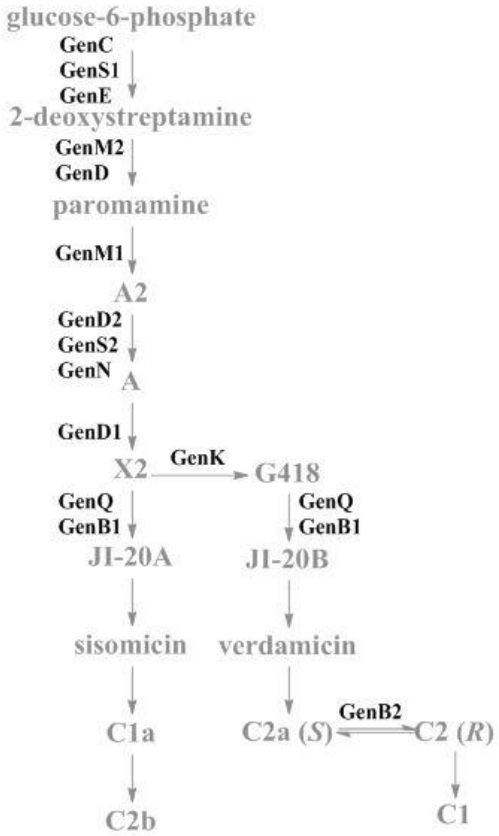

Figure 1.26 Gentamicin biosynthetic pathway. Prior to this work the identity and mechanism of the late steps of gentamicin biosynthesis remains unexplained.

1.3.8 Biological properties of individual components of the gentamicin C complex

Out of all the components of *M. echinospora* fermentation, the gentamicin C complex (Figure 1.11) possesses the highest bioactivity. Gentamicin C complex is comprised of five compounds: gentamicins C1a, C2b, C2a, C2, and C1. Structurally, the components are very similar to each other, with only the methylation extent and pattern on the purpurosamine ring varying between components. Gentamicin C2a, C2, and C1 have a 6'-*C*-methyl group; gentamicins C2b and C1 have a 6'-*N*-methyl group. Bioactivity tests of individual components of the C complex separated by HPLC shows that all the members have similar bactericidal properties (Weinstein et al., 1967).

It is also worth mentioning that if all three non-6'-*N*-methylated components of the C complex - gentamicins C1a, C2a, and C2 - were substrates for the final methylation step, the complex would have consisted of six

components, rather than five. The missing compound is the 6'-*N*-methylated gentamicin C2a, with *S* stereochemistry at the C-6'.

Small structural changes such as presence of a methyl, hydroxyl, or amino group, can have diverse effects on the antibiotic activity, changing the potency or broadening the spectrum. Removal of hydroxyl groups is known to make an antibiotic active against a previously-resistant pathogen, as phosphorylation is one of the main aminoglycoside inactivation strategies. An example of this is a higher-activity tobramycin produced by *Streptomyces tenebrarius*, which lacks a 3' hydroxyl group when compared to kanamycin B (Stark et al., 1967). All gentamicin C complex components lack 3' and 4' hydroxyl groups, reducing the incidence of resistance.

Most aminoglycosides are separated for clinical use. However, gentamicin, the largest selling aminoglycoside, is sold as a mixture of similar compounds. By international standards, no less than 80% of clinically used gentamicin has to be made up of gentamicin C complex (Vydrin et al., 2003). The other 20% is made of minor pathway intermediates, such as G418, JI-20a and JI-20b, all of which possess 3' and 4' hydroxyl groups (Wagman et al., 1972). Compared to kanamycin, gentamicin C's lack of a 3' hydroxyl group prevents inactivation by 3' phosphotransferase enzymes; gentamicins C1 and C2b, with a modified 6' amino group, also kill resistant strains possessing 6' acetyltransferase genes. A combination of related congeners in the gentamicin C mixture may thus reduce the occurrence of resistance.

Due to the difficulty of isolating gentamicin C mono-components, few extensive studies of individual components have been undertaken. The limited data, however, showed that despite nearly-identical bioactivity, the toxicity properties varied between the congeners. Gentamicin C2 was shown to be less nephrotoxic in an *in vivo* pig model, despite possessing bactericidal properties similar to the others (Figure 1.27) (Sandoval et al., 2006).

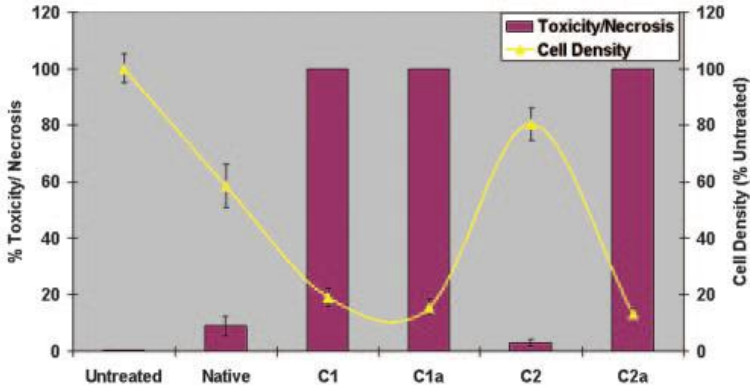

Figure 1.27 Nephrotoxicity of gentamicin mono-components. The toxicity of individual components of gentamicin C complex separated by HPLC was tested *in vivo* on porcine proximal tubule (kidney) cells. For gentamicins C1, C1a, and C2a, the cell density dropped below 20% of control value, while the values for gentamicin C2 were significantly higher (80.3%). Figure 2B in (Sandoval et al., 2006).

Slow clearance of gentamicin from the body and its subsequent accumulation in renal tubular cells can lead to severe damage to the kidneys. Faster clearance from the kidneys was observed for gentamicin C1a in horses, while gentamicin C1 was eliminated faster in dogs (Isoherranen et al., 2000, Steinman et al., 2010). If a single component of gentamicin C complex could be proven to be eliminated faster in humans, it could be offered to patients with a history of a kidney condition.

Gentamicin C1 was also shown to cause less damage to the hair cells (located in the inner ear) (Fox et al., 1980). There is no known correlation between the effects on the ear and on the kidney of a given antibiotic. Clinical application of gentamicins could be greatly enhanced if the properties of all the mono-components are studied in greater detail. Another example of a non-ototoxic aminoglycoside is netilmicin, or 1-N-ethyl-substituted sisomicin (McCormick et al., 1985).

If specific components possess reduced toxicity profiles in humans, at least the purification strategy of gentamicins will need to be re-thought. Further genetic work can also lead to *Micromonospora* mutants producing mono-component gentamicin or a mixture enriched in the desired compound. Availability of online medical history of the patient on demand, as well as faster

genotyping, can accurately establish if a patient would be at a higher risk of losing renal function or hearing because of gentamicin therapy, and a safer gentamicin could be used in that case. Gentamicin therapy could become one of many that is tailored to the patient in the 21st century.

1.4 The aims of the project

The central aim of the work in this thesis was to uncover the intriguing enzymology of the final steps of gentamicin biosynthesis in *M. echinospora*, which have remained enigmatic for over 50 years. The deoxygenation of sugar rings in the formation of specialised metabolites is not chemically straightforward, and the enzymology of this part of the gentamicin pathway was expected to be novel. It was aimed to identify key intermediates and to obtain evidence to formulate a detailed mechanistic proposal.

The main approach used was to attempt to reconstitute these steps *in vitro* using recombinant purified candidate enzymes from the gentamicin gene cluster. To do this, it would be necessary to obtain the successive intermediates to use them as substrates, by taking advantage of specific blocked mutants that accumulate such intermediates. For all this work, a major technical challenge would be the identification and separation of closely structurally similar gentamicins and gentamicin-related metabolites. Ideally, it might even be possible to reconstitute major parts of the late pathway in a single *in vitro* incubation.

A further aim was to identify and characterise the selectivity of one or more SAM-dependent methyltransferases that catalyse the terminal steps in gentamicin C complex formation. If the full set of biosynthetic enzymes could be defined, it would allow proof of concept for the idea of engineering the pathway to enrich in specific single components, which in the longer term could be properly tested for their potential therapeutic benefit.

2

Materials, media, and methods

2.1 Materials

2.1.1 Chemical reagents

All chemicals were purchased from the following companies:

- ACROS Organics: imidazole, Dowex® 50WX8-200 cation exchange resin, Dowex®1X2 anion exchange resin;
- Bio-Rad: Gel Filtration standard, Precision Plus Protein™ Dual Color standards;
- Cayman Chemical: *S*-adenosyl-L-homocysteine (SAH);
- GE Healthcare: *N*-hydroxysuccinimidyl (NHS) - activated sepharose;
- Generon: isopropyl β-D-1-thiogalactopyranoside (IPTG);
- Honeywell: acetonitrile (high-performance liquid chromatography (HPLC) grade);
- Melford Laboratories Ltd: guanidine hydrochloride, glycine, agarose, Tris, MOPS;
- Merck Millipore: acetonitrile (gradient grade);
- Nippon Genetics: MIDORI green DNA stain;
- Riedel-de Haën®: glacial acetic acid (99% v/v, 17.4 M), NaOH pellets;
- Severn Biotech: 30% (w/v) acrylamide;
- Sigma-Aldrich®: ammonium hydroxide solution (28-30% v/v, 14.8 M), Brilliant Blue G, $CaCl_2$, $CoCl_2$, ethanol, K_2HPO_4, $MgCl_2x6H_2O$, sodium dodecyl sulphate (SDS), $(NH_4)_2SO_4$, $NiCl_2$, reduced disodium salt hydrate of β-nicotinadmide adenine dinucleotide (NADH), His-select resin, phoshoenol-puruvate, SIGMAFAST™ protease inhibitor ethylenediaminetetraacetic acid (EDTA) - free cocktail, pyruvate kinase/lactic dehydrogenase enzymes, trifluoroacetic acid (TFA);
- Thermo Fisher Scientific: 1 kb Plus DNA Ladder, EDTA, conc. HCl (32% v/v, 10.2 M), conc. H_2SO_4 (98% v/v, 18.4 M), KH_2PO_4, NaCl.

and were analytical or HPLC grade (unless otherwise stated).

For mass spectrometry, gradient-grade solvents were used. Otherwise, HPLC-grade solvents were used. High-purity MQ water was generated by a Millipore Synergy® Milli-Q® (MQ H_2O) water purification system (filter pore size: 0.18 µm).

2.1.1.1 Buffers and solutions

Table 2.1 Buffers and solutions

Buffer	Application	Chemical composition
Binding buffer	Metal affinity chromatography	20 mM Tris-HCl, pH 7.8, 0.5 M NaCl, 10 mM imidazole
Binding buffer 2	Metal affinity chromatography	50 mM K_2HPO_4/KH_2PO_4, pH 8 (i.e. 94% 1 M K_2HPO_4, 6% 1 M KH_2PO_4), 0.1 M NaCl, 10% (v/v) glycerol, 10 mM imidazole, 0.5% (v/v) Tween® 20
CCC Solvent system I, lower phase	CCC, gentamicin C complex	Lower phase of solvent system I, consisting of 1 part water, 1 part ammonium hydroxide solution, 4 parts chloroform, and 2 parts methanol
CCC Solvent system I, upper phase	CCC, gentamicin C complex	Upper phase of solvent system I, consisting of 1 part water, 1 part ammonium hydroxide solution, 4 parts chloroform, and 2 parts methanol
CCC Solvent system VII, lower phase	CCC, gentamicin C intermediates	Lower phase of solvent system VII, consisting of 1 part 5 mM ammonium sulfate solution, 1 part ammonium hydroxide solution, 4 parts chloroform, and 3 parts methanol
CCC Solvent system VII, upper phase	CCC, gentamicin intermediates	Upper phase of solvent system VII, consisting of 1 part 5 mM ammonium sulfate solution, 1 part ammonium hydroxide solution, 4 parts chloroform, and 3 parts methanol
CD buffer	Circular dichroism of GenL	10 mM K_2HPO_4/KH_2PO_4 pH 8.0, 10% (v/v) glycerol, 0.5% (v/v) Tween® 20
Cobalt chloride	Metal affinity column regeneration	50mM cobalt chloride
Denaturation buffer	Refolding experiments	6 M guanidine-HCl
Elution buffer	Metal affinity chromatography	20 mM Tris-HCl, pH 7.8, 0.5 M NaCl, various high concentrations of imidazole, refer to Section 2.4.3.1.1

Elution buffer 2	Metal affinity chromatography	50 mM K_2HPO_4/KH_2PO_4, pH 8, 0.1 M NaCl, 10% (v/v) glycerol, 500 mM imidazole, 0.5% (v/v) Tween® 20
Exchange buffer	Metal affinity chromatography	20 mM Tris-HCl, pH 7.8, 0.5 M NaCl
Exchange buffer 2	Metal affinity chromatography	50 mM K_2HPO_4/KH_2PO_4, pH 8, 0.1 M NaCl, 10% (v/v) glycerol, 0.5% (v/v) Tween® 20
Inclusion body wash	Refolding experiments	1 M guanidine-HCl
IEX low-salt buffer	Ion exchange chromatography	20 mM Tris-HCl, pH 7.8
IEX high-salt buffer	Ion exchange chromatography	20 mM Tris-HCl, pH 7.8, 1 M NaCl
4x Laemmli buffer	SDS-PAGE	277.8 mM Tris-HCl, pH 6.8, 44.4% (v/v) glycerol, 4.4% (w/v) SDS, 0.02% (v/v) bromophenol blue Addition of 10% (v/v) DTT is required immediately prior to use.
Lysis buffer	Refolding experiments	20 mM Tris-HCl, pH 7.8, 0.5 M NaCl, 1 mM DTT, 1% (w/v) SDS
Nickel chloride	Metal affinity column regeneration	50 mM nickel chloride
Ninhydrin stain	CCC sample blotting	0.1 g ninhydrin, 0.5 mL glacial acetic acid, 100 mL acetone
10% (v/v) polyethyleneimine (PEI)	Protein encapsulation	200 µL of 50% PEI stock, 500 µL of conc. HCl (32% v/v), 300 µL of MQ H_2O
Reagent A1	Pre-crystallization test	0.1 M Tris-HCl, pH 8.5, 2.0 M $(NH_4)_2SO_4$
Reagent B1	Pre-crystallization test	0.1 M Tris-HCl, pH 8.5, 1.0 M $(NH_4)_2SO_4$
Reagent A2	Pre-crystallization test	0.1 M Tris-HCl, pH 8.5, 0.2 M $MgCl_2x6$ H_2O, 30% (w/v) polyethylene glycol 4000
Reagent B2	Pre-crystallization test	0.1 M Tris-HCl, pH 8.5, 0.2 M $MgCl_2x6$ H_2O, 15% (w/v) polyethylene glycol 4000
Refolding buffer A	Refolding experiments	2 M guanidine-HCl, 20 mM Tris-HCl, pH 7.8, 0.5 M NaCl, 10% (v/v) glycerol, 0.1 M EDTA
Refolding buffers B	Refolding experiments	20 mM Tris-HCl, pH 7.8, 0.5 M NaCl
Safe Coomassie Blue stain	SDS-PAGE	100 mL ethanol, 10 mL 1% (w/v) Brilliant Blue G, 3 mL concentrated HCl (32%), water to 1 L
SET buffer	Genomic DNA	20 mM Tris-HCl, pH 7.5, 75 mM NaCl,

	isolation	25 mM EDTA
Strip buffer	Metal affinity column regeneration	20 mM Tris-HCl, pH 7.8, 0.5 M NaCl, 100 mM imidazole, 100 mM EDTA
50x TAE buffer	DNA gel electrophoresis	242 g Tris, 18.6 g EDTA, 90 mL glacial acetic acid, water to 1 L
TE buffer	Genomic DNA isolation	25 mM Tris-HCl, pH 7.5, 25 mM EDTA
1M TMOS solution	Protein encapsulation	This solution was made immediately prior to immobilization experiments. 147.5 µL of 100% TMOS solution, 852.5 µL of 1 mM HCl
Tris-glycine buffer	SDS-PAGE	3.2 g Tris, 18.8 g glycine, 10 mL of 10% (w/v) SDS, water to 1 L
Wash buffer	Metal affinity chromatography	20 mM Tris-HCl, pH 7.8, 0.5 M NaCl, various medium concentrations of imidazole, refer to Section 2.4.3.1.1
Wash buffer 2	Metal affinity chromatography	50 mM K_2HPO_4/KH_2PO_4, pH 8, 0.1 M NaCl, 10% (v/v) glycerol, 40 mM imidazole, 0.5% (v/v) Tween® 20

2.1.2 Biological reagents

2.1.2.1 Gentamicin and intermediates

Gentamicins C2 and C2a were obtained as pure sulphate salts from TOKU-E. Other intermediates were generated from a culture of WT or mutant *Micromonospora* sp. Gentamicin C complex solution (10 mg/mL; by PAA The Cell Culture Company) was used for separation by dynamic counter-current chromatography.

2.1.2.2 Oligonucleotides

All DNA primers were purchased from Eurofins UK before May 2016 and from Sigma Aldrich after. All tubes containing lyophilized primers were spun at 13'000 RPM for 2 minutes prior to resuspension with Ambion™ Nuclease-free water. In all cases the final concentration of the primer solution used in PCR was 10 pmol. The stock solutions were stored at -20˚C.

Table 2.2 Primers

Primer name	Sequence 5' – 3’	Application
GenL GF	GCCGCGCGGCAGCCATATGATGCGGG	sGenL construct Gibson

	ACTCCACGCTCA	PCR
GenL GR	TGTCGACGGAGCTCGAATTCTCAGGC CGACTCGCCGACGG	sGenL construct Gibson PCR
GenL KO F	TACGTCTTCCACCCCGACCA	pYH7-*genL* sequencing
GenL KO F	TACGTCTTCCACCCCGACCA	pYH7-*genL* sequencing
GenL KO R	ACAGCATCGTCAAGGCGTA	pYH7-*genL* sequencing
GenL KO R	ACAGCATCGTCAAGGCGTA	pYH7-*genL* sequencing
GenP trans F	CGCGCGAATTCCATATGGTTGCAGCA	*genP* to pEX-A2 cloning for mutagenesis
GenP trans R	GGAGCGCGGCCGCGGATCCAGTCAGA GAAA	*genP* to pEX-A2 cloning for mutagenesis
GenP (D189A) F	GTCTGCCACGGTGCCTTCTGCCTCGAC	*genP* site-directed mutagenesis
GenP (D189A) R	GTCGAGGCAGAAGGCACCGTGGCAGA C	*genP* site-directed mutagenesis
GenP (D189L) F	GTCTGCCACGGTCTCTTCTGCCTCGAC	*genP* site-directed mutagenesis
GenP (D189L) R	GTCGAGGCAGAAGAGACCGTGGCAGA C	*genP* site-directed mutagenesis
GenP (D189N) F	GTCTGCCACGGTAACTTCTGCCTCGAC	*genP* site-directed mutagenesis
GenP (D189N) R	GTCGAGGCAGAAGTTACCGTGGCAGA C	*genP* site-directed mutagenesis
lGenL_ncoi	AGGCCATGGTGCTGAGCATCTCCGAT	lGenL construct PCR
lGenL_xhoi	CCTCGAGTGCGGCCGACTCGCCGAC	lGenL construct PCR
M13 F	GTAAAACGACGGCCAGT	pUC19 vector sequencing
M13 R	GTCATAGCTGTTTCCTG	pUC19 vector sequencing
pB2	TGGTACCCGCAGCTCGCGAT	His tag-less genB2 sequencing
pB2-bamhi	CGGCCCCTGCCGGATCCGTCAGAGCTG AGC	His tag-less genB2 PCR
pB2-ncoi	CGGAGGTTTCGCATATGATTATTGCC AACG	His tag-less genB2 PCR
pB3	CCAACTCCACCCGCGGAA	His tag-less genB3 sequencing
pB3-ecori	CCGGCCCTGGAATTCCTACGCC	His tag-less genB3 PCR
pB3-ncoi	GGGGACCATGGATGGCAGTCGCCGAC CA	His tag-less genB3 PCR
pB3-ndei	CGGCAGCCATATGGCAGT	*genB3* cloning to pGP9
pB3-xbai	AATTTCTAGACCAGGGTCCGGGT	*genB3* cloning to pGP9
pB4	GACCCGTCGCCGCTCGCG	His tag-less genB4 sequencing
pB4-ecori-2	GGGAATTCACCGCACCCCCCC	His tag-less genB4 PCR
pB4-ncoi-2	TGGTCCATGGATGAACTACCGTGAGT TG	His tag-less genB4 PCR
pCJ F	AGCCATATGCTGAGCATCT	pCJW93 sequencing

pCJ R	TAGATCTGGGGAATTCACGAG	pCJW93 sequencing
pEX F	GGAGCAGACAAGCCCGTCAGG	pEX-A2 vector sequencing
pEX R	AGGCTTTACACTTTATGCTTCCGGC	PEX-A2 vector sequencing
pWHU77-F	ACTCTAGTATGCATGCGAGTGT	pWHU77 vector sequencing
pWHU77-Rev	TGTGAGCGGATAACAATTTCACACA	pWHU77 vector sequencing
RBS1 F	TGCCCATGGTATAACGTCGTAGTAAA GTTAAACAA	pAR1 RBS mutagenesis
RBS1 R	TTGTTTAACTTTACTACGACGTTATA CCATGGGC	pAR1 RBS mutagenesis
RBS2 F	GCCCATGGTATAGTCCTTAATTAAAG TTAAAC	pAR2 RBS mutagenesis
RBS2 R	GTTTAACTTTAATTAAGGACTATACC ATGGGC	pAR2 RBS mutagenesis
RBS3 F	TGCCCATGGTATATGTGCCTCCTAAA GTTAAACA	pAR3 RBS mutagenesis
RBS3 R	TGTTTAACTTTAGGAGGCACATATAC CATGGGC	pAR3 RBS mutagenesis
T7	TAATACGACTCACTATAGGG	pET-28a (+) and pAR1-3 vector sequencing
T7t	CTAGTTATTGCTCAGCGGTG	pET-28a (+) and pAR1-3 vector sequencing
VM GenL F	CATATGCTGAGCATCTCCGAT	GenL construct PCR
VM GenL R	GAATTCTCAGGCCGACTCGCC	GenL construct PCR

2.1.2.3 Plasmids

Table 2.3 Plasmids

Plasmid	Description	Application	Source
pET-28 (+)	*Kan*^{R}, N-terminal or C-terminal His_6 tag, T7 expression, *lacI*	Protein expression	PFL plasmid collection
pEX-A2	*lacI, Amp*^{R}	*genP* site-directed mutagenesis	LP plasmid collection
pUC19	*lacI, Amp*^{R}	RBS mutagenesis for pAR vector generation	LP plasmid collection
pWHU77	*Thio*^{R}, phage ϕC31 insertion, PermE* promoter	Insertion vector for *Micromonospora*	PFL plasmid collection
pYH7	*Apr*^{R}	Deletion vector for *Micromonospora*	PFL plasmid collection
pGP9	*Apr*^{R}, λ insertion	Insertion vector for *Micromonospora*	PFL plasmid collection
pCJW93	*Apr*^{R}, N-terminal His_6	Expression of GenL	PFL plasmid

	tag, *tipA* promoter (thiostrepton-inducible)	in *Streptomyces coelicolor*CH999	collection
pAR1	pET-28 (+) with weak RBS	Protein expression	This study
pAR2	pET-28 (+) with weak RBS	Protein expression	This study
pAR3	pET-28 (+) with super-strong RBS	Protein expression	This study

2.1.2.4 Bacterial strains

Table 2.4 Bacterial strains

Species	Strain	Genotype	Source
E. coli	NovaBlue (DE3)	*Tet*^{R}, *recA1, relA1*	PFL strain collection
E. coli	BLR (DE3)	*Tet*^{R},*recA*$^-$BL21	PFL strain collection
E. coli	BL21 (DE3)	Deficient in lon and omp-t proteases	PFL strain collection
E. coli	Rosetta2™ (DE3)	*Chlor*^{R}, codon-optimised	LP strain collection
E. coli	ET12567/pUZ8002	Methylation-deficient, *dam, dcm, hsdM, hsdS, hsdR,* *Tet*^{R},*Chlor*^{R} (Kieser et al., 2000). RK2/RP4 derivative, non-transmissible, *Kan*^{R} (MacNeil, 1988).	PFL strain collection
S. coelicolor	CH999	*act*$^-$ cluster	PFL strain collection

2.1.2.5 Antibiotic solutions

The antibiotic solutions were used as selective markers at a one in a thousand dilution.

Table 2.5 Antibiotic solutions

Antibiotic	Company	Solvent	Concentration/ mg per mL
Ampicillin	Melford	MQ H_2O	100
Apramycin	Sigma Aldrich	MQ H_2O	25
Chloramphenicol	Duchefa Biochemie	Ethanol	25
Gentamicin	PAA The Cell Culture Company	MQ H_2O	10
Kanamycin	Melford	MQ H_2O	50
Nalidixic acid	Sigma Aldrich	0.15M NaOH	25
Thiostrepton	TOKU-E	DMSO	10
Tetracycline	Sigma Aldrich	MQ H_2O	10

2.1.2.6 DNA purification kits

Table 2.6 DNA purification kits

DNA purification kit	Company
DNA Clean & Concentrator™	Zymo Research
E.Z.N.A.® Plasmid Mini Kit	Omega Biotek
FastGene® Gel/PCR extraction kit	NIPPON Genetics
PureYield™ Plasmid Miniprep System	Promega

2.1.2.7 Enzymes and reagents

Table 2.7 Enzymes

Enzyme	Company	Restriction site
Quick ligase™	New England BioLabs®	-
Phusion High-Fidelity MM w/GC buffer	New England BioLabs®	-
Shrimp Antarctic Phosphatase	New England BioLabs®	-
*Sph*I/*Pae*I-HF®	New England BioLabs®	GCATG'C
T4 ligase	New England BioLabs®	-
T4 polymerase	New England BioLabs®	-
*Bam*HI FastDigest®	Thermo Fisher Scientific	G'GATCC
*Bsp*1407i FastDigest®	Thermo Fisher Scientific	T'GTACA
*Dpn*I FastDigest®	Thermo Fisher Scientific	GA'TC
*Eco*RI FastDigest®	Thermo Fisher Scientific	G'AATTC
*Nco*I FastDigest®	Thermo Fisher Scientific	C'CATGG
*Nde*I FastDigest®	Thermo Fisher Scientific	CA'TATG
*Nhe*I FastDigest®	Thermo Fisher Scientific	G'CTAGC
*Not*I FastDigest®	Thermo Fisher Scientific	GC'GGCCGC
*Sal*I FastDigest®	Thermo Fisher Scientific	G'TCGAC
*Sma*I FastDigest®	Thermo Fisher Scientific	CCC'GGG
*Xba*I FastDigest®	Thermo Fisher Scientific	T'CTAGA
*Xho*I FastDigest®	Thermo Fisher Scientific	C'TCGAG

2.2 Culture Media

The components of the media were purchased from -

- ACROS organics: glycerol;
- ArkaSoy: soya flour;
- Bacto™: soytone;
- BDH: $ZnSO_4$ x 7 H_2O;
- Thermo Fisher Scientific: BD Bacto™ tryptic soy broth (TSB), K_2HPO_4, sucrose;
- Formedium™: tryptone, yeast extract, agar, peptone;
- Sigma Aldrich: beef extract, $CaCO_3$, corn steep powder, $FeSO_4$ x 7 H_2O, glucose, KNO_3, L-aspartate, L-arginine, L-cysteine, L-histidine, KNO_3, K_2HPO_4, malt extract, $MgCl_2$ x 6H_2O, $MnCl_2$ x 4 H_2O, *N-Z* amine® type A, soluble starch, thiamine, uracil.

For all the media, the components were combined in the order stated.

2.2.1 *Escherichia coli* media

Table 2.8 *E. coli* media

Media	Components
LB	Tryptone - 10 g, yeast extract - 5 g, NaCl - 10 g, agar (if needed) - 15 g, distilled water - to 1 L. Adjust pH to 7.5 with NaOH.
Low-salt LB	Tryptone - 10 g, yeast extract - 5 g, NaCl - 5 g, agar (if needed) - 15 g, distilled water - to 1 L. Adjust pH to 7.5 with NaOH.
SOC	Tryptone - 20 g, yeast extract - 5 g, NaCl - 2 mL of 5 M solution, KCl - 2.5 mL of 1 M solution, $MgCl_2$ - 10 mL of 1 M solution, $MgSO_4$ - 10 mL of 1 M solution, glucose - 20 mL of 1 M solution, distilled water - to 1 L.
TB	Autoclave separately: a) tryptone - 15 g, yeast extract - 24 g, glycerol - 4 mL, distilled water - to 900 mL; and b) K_2HPO_4 - 12.54 g, KH_2PO_4 - 2.31 g, distilled water - to 100 mL. Combine in a ratio of 9 to 1.
TB:AIM	Tryptone - 12 g, yeast extract - 24 g, $(NH_4)_2SO_4$ - 3.3 g, KH_2PO_4 - 6.8 g, Na_2HPO_4 - 7.1 g, glucose - 0.5 g, α-lactose - 2 g, $MgSO_4$ - 0.15 g, trace elements - 0.03 g, distilled water - to 1 L. No IPTG was added to the cells grown on this medium.
2x YT	Tryptone - 16 g, yeast extract - 10 g, NaCl - 5 g, distilled water - to 1 L.

2.2.2 *Micromonospora* media

Table 2.9 *Micromonospora* media

Media	Components
5006	Sucrose - 3 g, dextrin - 15 g, beef extract - 1 g, yeast extract - 2 g, tryptone soy broth - 5 g, NaCl - 0.5 g, K_2HPO_4 - 0.5 g, $MgSO_4$ x 7 H_2O - 0.5 g, $FeSO_4$ x 7 H_2O - 0.01 g, agar - 20 g, distilled water - to 1 L.
A	Soluble starch - 10 g, corn steep powder - 2.5 g, yeast extract - 3 g, $CaCO_3$ - 3 g, $FeSO_4$ - 120 µL of 100 mg/mL stock, $MgCl_2$ x 6 H_2O - 100 mL of 100 mM stock, agar - 30 g, distilled water - to 1 L. Adjust pH to 7.0 with KOH.
ABB	Soytone - 5 g, soluble starch - 5 g, $CaCO_3$ - 3 g, MOPS - 2.1 g, thiamine-HCl - 100 µL of 100 mg/mL stock, $FeSO_4$ - 120 µL of 100 mg/mL stock, $MgCl_2$ x 6 H_2O - 100 mL of 100 mM stock, agar - 30 g, distilled water - to 1 L.
ATCC ® 172	Glucose - 10 g, soluble starch - 20 g, yeast extract - 5 g, *N-Z* amine® type A - 5 g, $CaCO_3$ - 1 g, agar (if needed) - 15 g, distilled water - to 1 L.
Bennet's (spores)	Glucose - 10 g, yeast extract - 1 g, beef extract - 1 g, *N-Z* amine® type A - 2 g, agar - 15 g, distilled water - to 1 L. Adjust pH to 7.3.
DSMZ 127	Glucose - 10 g, soluble starch - 20 g, yeast extract - 5 g, *N-Z* amine type A - 5 g, $CaCO_3$ - 1 g, agar - 15 g, distilled water - to 1 L.
F50	Soya flour - 20 g, soluble starch - 30 g, peptone - 1 g, glucose - 3 g, $(NH_4)_2SO_4$ - 0.3 g, KNO_3 - 0.3, $CaCO_3$ - 3 g, $CoCl_2$ - 5 µL of 50 mM stock per 50 mL, distilled water - to 1 L.
GYM	Glucose - 4 g, yeast extract - 4 g, malt extract - 10 g, $CaCO_3$ - 2 g, agar (if needed) - 12 g, distilled water - to 1 L.
ISP2/ Yeast malt (Shirling and Gottlieb, 1966)	Malt extract - 10 g, yeast extract - 4 g, glucose - 4 g, agar - 15 g, distilled water - to 1 L.
ISP3/ Oatmeal (Shirling and Gottlieb, 1966)	Oat flakes - 10 g, oatmeal - 10 g, agar - 15 g, distilled water - to 1 L. Adjust pH to 7.0.
ISP5 (Shirling and Gottlieb, 1966)	L-Asparagine - 1 g, glycerol - 10 mL, K_2HPO_4 - 1 g, salt solution - 1 mL, agar - 20 g, distilled water - to 1 L. Salt solution: 1g of $FeSO_4 \cdot 7H_2O$, 1g of $MnCl_2 \cdot 4H_2O$, 1g of $ZnSO_4$ x 7 H_2O in 100mL of distilled water.
Wagman (Wagman et al., 1974)	Soya flour - 30 g, dextrin - 50 g, dextrose - 5 g, $CoCl_2$ - 0.00024 g, $CaCO_3$ - 7 g, distilled water - to 1 L.
Xia (Gu et al., 2015)	Soluble starch - 50 g, soya flour - 35 g, glucose - 15 g, peptone - 2 g, KNO_3 - 0.5 g, $(NH_4)_2SO_4$ - 0.5 g, NH_4Cl - 1 g, corn powder - 15 g, $CoCl_2$ - 0.1 g, $CaCO_3$ - 6 g, distilled water - to 1 L.

2.2.3 *Streptomyces coelicolor* media

Table 2.10 *Streptomyces coelicolor* media

Media	Components
TSBY	BD Bacto™ TSB - 30 g, sucrose - 103 g, yeast extract - 5 g, distilled water - to 1 L.
TWM	Sucrose - 10 g, glucose - 5 g, tryptone - 5 g, yeast extract - 2.5 g, EDTA - 0.036 g, tap water - to 1 L.
Super-YEME	Yeast extract - 3 g, peptone - 5 g, glucose - 10 g, malt extract - 3 g, sucrose - 340 g, glycine - 5 g, $MgCl_2$ x 6 H_2O - 2.35 g, L-proline - 0.075 g, L-arginine - 0.075 g, L-cysteine - 0.075 g, L-histidine - 0.1 g, uracil - 0.015 g, distilled water - to 1 L.

2.3 Machines and Programs

2.3.1 Machines

Table 2.11 Machines

Machine	Company	Used for
Emulsiflex C5	AVESTIN	Mechanical lysis of *E. coli* cells
AVANTI™ J-20 XP centrifuge	Beckman Coulter™	High-speed centrifuge
Microflow Laminar flow cabinet	BioQuell	Antiseptic work
PowerPAC™ 300	BioRad	Power supply for gel tank
PHERAstar FS	BMG Labtech	Spectrophotometer for kinetic studies
Clasixx Fridge-freezer	Bosch	Storage of samples at 4˚C and -20˚C
OmniPage Mini Vertical	Cleaver Scientific Ltd	Protein gel electrophoresis
Modulyo® Freeze drier	EC	Sample lyophilisation
RV5 pump	Edwards Vacuum	Freeze dryer pump
Centrifuge 5424	Eppendorf Ltd	Small tube centrifuge
Centrifuge 5810	Eppendorf Ltd	50 mL tube centrifuge
Centrifuge 5804 R	Eppendorf Ltd	Protein concentration
Thermomixer Compact	Eppendorf Ltd	Growing of transformed *E. coli* cells
Concentrator Plus	Eppendorf Ltd	DNA or fermentation product drying
LCQ™	Finnigan™	Mass spectrometry
Äkta Purifier	GE	Gel filtration and ion exchange
Flowgen tank	Geneflow	Agarose gel running
Heat Block	Grant Instruments Ltd	Restriction digest, gel

		melting
Water bath SUB14	Grant Instruments Ltd	Heat-shock
LCQ LC-MS 1100	Hewlett Packard	HPLC for mass spectrometry
Ret Basic	IKA®	Magnetic stirring
Multitron shaker	Infors	Shaking incubator
ISF-4-W incubator	Kuhner Switzerland	30˚C shaking incubator
Model 250 EX	Life Technologies™	Power supply for gel tank
Scales AG385	Mettler Toledo Ltd	High-precision mass measurement
Scales PR2003	Mettler Toledo Ltd	Mass measurement
pH meter 340	Mettler Toledo Ltd	pH measurement
ND-1000 Spectrophotometer	NanoDrop®	DNA and protein concentration measurements
Innova™ 4330	New Brunswick Scientific	37˚C shaking incubator
Inverter NN-SD446W microwave	Panasonic	Agarose and agar melting
VIP Series MDF-U33V-PE freezer	Panasonic	Storage of samples at -80˚C
Ultrospec 3000 UV-Vis	Pharmacia Biotech	Absorbance measurement
Classic autoclave	Prestige Medical	Media sterilization
Labo Autoclave MLS-3750	Sanyo	Media sterilization
CERTOMAT® BS-1	Sartorius Stedim Biotech	18˚C incubator for protein expression
Vibra-cell™ sonicator	Sonics and Materials Inc	Lysis of small cell cultures
Incubator	Stuart Scientific	Plates incubator
GeneAmp® PCR System 9700	Thermo Fisher Scientific	Cloning and colony PCR

UVIdoc HD5	Uvitec	Gel imaging
Whirlimixer	Whirlimixer™	Vortex-mixing
Microscope	Zeiss West Germany	Magnification pictures

Analytical Ultra centrifugation was performed on a Beckman Optima XL-1 centrifuge, circular dichroism measurements and thermal melt were performed on Circular Dichroism Spectrometer Model 410, AVIV Biomedical, Inc., under the supervision of Dr Katherine Stott.

Sanger DNA sequencing for confirmation of cloning, transformation, gene insertion, or gene deletion, was carried out in the DNA sequencing facility on an Applied Biosystems 373xl DNA Analyser.

Protein identification by MALDI fingerprinting was performed by Dr Len Packman of the Proteomics facility using a Bruker ultrafleXtreme MALDI mass spectrometer. Biochrom 30 Ion-exchange Analyser© was used to perform amino acid analysis (for exact protein concentration calculation) by Mr Peter Sharratt.

Mosquito crystallisation robot (TTPLabtechTld) was used to set up GenL crystal trays with help from Dr Dimitry Chirgadze.

Structural determination of compounds was performed using NMR data obtained from the NMR facility of the Department of Chemistry under the supervision of Dr Peter Grice. Dr Finian Leeper aided with NMR data analysis and molecular modelling of compounds.

2.3.2 Software and Online Tools

2.3.2.1 Software

The following programs were used in this study:

Table 2.12 Software

Program	Description	Company
ChemBioDraw Ultra 14.0	Chemical reactions' drawing	PerkinElmer®
CLC Main Workbench 6	Generating and viewing DNA sequences	QIAGEN® Bioinformatics

EndNote™	Bibliography referencing	Thomson Reuters
SnapGene®	Generating and viewing DNA sequences; primer design	SnapGene
TopSpin 3.5pl6	Processing data from nuclear magnetic resonance	Bruker
Xcalibur™	Processing data from mass spectrometry	Thermo Fisher Scientific

2.3.2.2 Online Tools

The following online programs were used in this study:

Table 2.13 Online programs

Program	Description	Link
Ammonium sulphate calculator	Ammonium sulphate calculator	http://encorbio.com/protocols/AM-SO4.htm
BLAST®	Homology analysis of protein sequences	https://blast.ncbi.nlm.nih.gov/
BRENDA	Enzyme reaction database	http://www.brenda-enzymes.org/index.php4
CFSSP	Protein secondary structure prediction	http://www.biogem.org/tool/chou-fasman/
ChemDoodle	2D to 3D chemical structure prediction	https://web.chemdoodle.com/demos/2d-to-3d-coordinates/
ExPASyProtParam	Protein parameters	http://web.expasy.org/protparam/
ExPASy Translate	DNA translation to protein	http://web.expasy.org/translate/
ExPASY PROSITE	Database of protein domains, families and functional sites	http://prosite.expasy.org/
I-TASSER	Protein function prediction	http://zhanglab.ccmb.med.umich.edu/I-TASSER/

MolBiol DNA calculator	Conversion of DNA concentrations	http://molbiol.edu.ru/eng/scripts/01_07.html
MolBiol protein calculator	Conversion of protein concentrations	http://molbiol.edu.ru/eng/scripts/01_04.html
NEBcutterV2.0	Restriction site maps of DNA	http://nc2.neb.com/NEBcutter2/
PDBsum	Protein database	http://www.ebi.ac.uk/thornton-srv/databases/cgi-bin/pdbsum/GetPage.pl?pdbcode=index.html
PHYRE[2]	Protein 3D structure prediction	http://www.sbg.bio.ic.ac.uk/phyre2/html/page.cgi?id=index
Predict 1H NMR	NMR spectrum prediction	http://www.nmrdb.org/new_predictor/index.shtml?v=v2.66.0
Promega Biomath	Conversion of DNA concentrations	http://www.promega.com/a/apps/biomath/
PSIPRED	Protein sequence analysis	http://bioinf.cs.ucl.ac.uk/psipred/
RBS calculator	RBS strength calculator	https://salislab.net/software/forward
Reverse Compliment	DNA reverse complementation	http://www.bioinformatics.org/sms/rev_comp.html
Rock Maker[web]	Crystallography plate imager	http://metis.bioc.cam.ac.uk/RockMakerWeb
SciFinder®	Chemical reaction database	http://www.shef.ac.uk/library/cdfiles/scifinderweb

2.4 Methods

2.4.1 *Escherichia coli* cell culture

2.4.1.1 Competent cell preparation

Heat-shock competent *E. coli* cells (Bergmans et al., 1981, Oishi and Cosloy, 1972) were used for all transformations. Competent cells were grown from glycerol stocks on LB plates containing the appropriate antibiotic at 37˚C overnight. The plates were scraped and the cells put into 200 mL of LB medium with the appropriate antibiotic until the A_{600}= 0.3. The cells were collected into 50 mL tubes and placed on ice for 15 minutes, then spun at 3600 RCF for 10 minutes at 4˚C. The cells were resuspended with 30 mL of 0.1 M $CaCl_2$ and kept on ice for 30 minutes. The cells were spun at 3600 RCF for 10 minutes at 4˚C, then resuspended in 1 mL of 0.1 M $CaCl_2$, 15% glycerol. Aliquots of 50 µL each were put into 0.5 mL tubes (previously cooled down to -80˚C) and kept in the -80˚C freezer for a maximum 3 months or until used.

2.4.1.2 Protein expression in E. coli

E. coli BLR (or other protein-expression) cells transformed with the recombinant plasmid encoding the gene of interest along with kanamycin resistance, were grown in LB broth containing kanamycin (50 µg/mL) at 37˚C, until A_{600} reached 0.7. The cells were then cooled down to 18˚C, and protein expression was induced with IPTG (0.5 mM), unless AIM medium was used. The cells were left shaking at 18˚C overnight.

For GenL expression, the cells were grown in TB medium instead.

2.4.2 DNA methods

2.4.2.1 Vector generation in silico

Snapgene™ was used to generate all cloning vectors. It was also used to align DNA sequencing reads with the query and generate primer sequences.

2.4.2.2 Transformation of competent E. coli cells

An aliquot of competent *E. coli* cells was taken out of the -80˚C and kept on ice for 5 minutes. DNA (typically 1 µL) was pipetted on top of the cells and gently stirred in. The cells were left on ice for 30 minutes, then heat-shocked at 42˚C for 45 seconds. The cells were again kept on ice for 5 minutes. A 100 µL of SOC medium was added to the cells, and the tubes were kept in the 37˚C shaker for at least an hour. The cells were plated out on appropriate antibiotic-containing agar plates and grown overnight at 37˚C.

2.4.2.3 DNA purification

DNA quality in all cases was assessed by measuring the absorbance at 230, 260, and 280 nm with Nanodrop® spectrophotometer.

2.4.2.3.1 Plasmid DNA isolation from *E. coli*

Plasmid DNA would typically be isolated from a 10 mL culture of *E. coli* cells. The protocol of a plasmid-isolation kit was followed. Briefly, the cells were spun down at 3800 RCF for 4 minutes. The medium was removed with the last of it removed with a pipette. The cell pellet was resuspended in 250 µL of Solution I (50 mM Tris-HCl, pH 8.0, 10 mM EDTA, 100 µg/mL RNase) and moved into a 1.5 mL Eppendorf tube, then 250 µL of Solution II (200 mM NaOH, 1% (w/v) SDS) was added and the tubes were left at room temperature for 3 minutes. Solution III (350 µL; 3.0 M CH_3CO_2K, pH 5.5) was added and the tubes' contents were mixed by inversion. Cell debris were removed by centrifugation at 20000 RCF for 10 minutes. The plasmid DNA was then bound to the supplied column, washed with 70% (v/v) ethanol, and dried by centrifugation for 2 minutes. Hot (80˚C) Nuclease-free water was put on the filter membrane of the column, and the tubes were left for 1 minute. The plasmid DNA was eluted by centrifuging at maximum speed for 2 minutes.

2.4.2.3.2 Enzymatic isolation of DNA from *Micromonospora* sp.

The cell pellet from 50 mL of culture was resuspended in 10 mL SET buffer with 500 µL of lysozyme solution (50 mg/mL stock), 300 µL of 0.5 M EDTA, and left at 37˚C for 1 hour. Proteinase K (500 µL of 20 mg/mL stock) and 5 mL of 10% (w/v)

SDS were added. The tube was incubated at 55˚C for 1 hour. A solution of NaCl (5 mL of 5 M) was added, and the tube was left at room temperature for 15 minutes.

To precipitate the proteins, 30 mL of chloroform was added, mixed by inversion, and spun at 5000 RCF for 5 minutes. The upper phase was transferred to 2 mL tubes, spun at 2000 RCF at room temperature for 15 minutes. The supernatant from all tubes was transferred to a clean 50 mL tube. Equal-to-supernatant volume of isopropanol was added to the tube; the tube was gently inverted until DNA was visible.

The DNA was transferred to a clean tube using a pipette tip, washed with 70% (v/v) ethanol, dried, and resuspended in Nuclease-free water.

2.4.2.3.3 Non-enzymatic isolation of DNA from *Micromonospora* sp.

The cell pellet from a 10 mL culture of *Micromonospora* was resuspended in 500 µL TE buffer and mixed well. The cells were spun down and resuspended in 450 µL of TE buffer with lysozyme (4 mg/mL). The tubes were incubated at 37˚C for 30 minutes, mixing every 5 minutes. A solution of NaCl (50 µL of 5 M stock) and 120 µL of 10% (w/v) SDS were added and mixed in; the tubes were incubated at 65˚C for 30 minutes.

The tubes were cooled down to room temperature. Potassium acetate (240 µL of 5 M stock) was mixed in. The tubes were kept at -20˚C for 10 minutes. The tubes were spun at 20000 RCF at 4˚C for 20 minutes.

Isopropanol was added to the tubes and mixed in by inversion. The DNA was centrifuged down, washed with 70% (v/v) ethanol, dried, and resuspended in Nuclease-free water.

2.4.2.3.4 PCR product purification

PCR reaction was mixed with DNA binding buffer, passed through a DNA binding column, washed with 70% (v/v) ethanol, dried, and eluted with hot Nuclease-free water.

2.4.2.3.5 Gel-band DNA purification

A gel band was excised and melted with DNA binding buffer at 60˚C for 10 minutes, passed through a DNA binding column, washed with 70% (v/v) ethanol, dried, and eluted with hot Nuclease-free water.

2.4.2.3.6 DNA purification for DNA sequencing

DNA requiring further purification was mixed with DNA binding buffer, passed through a DNA binding column, washed with 70% (v/v) ethanol, dried, and eluted with hot Nuclease-free water.

2.4.2.4 Polymerase chain reaction

2.4.2.4.1 Phusion polymerase for cloning

A DNA template (100 ng), primers (10 pmol each), DMSO (5% (v/v)), MQ H_2O, and Phusion Mastermix were mixed to a total volume of 50 µL in a 125 µL PCR tube. A typical program was comprised of an initial denaturation at 98˚C for 2 minutes, then 30 cycles of denaturation (15 seconds at 98˚C), annealing (15 seconds at primer-annealing temperature), and extension (72˚C, time depended on the length of the product, 30 seconds/kb of DNA), then a final elongation step (72˚C for 5 minutes).

2.4.2.4.2 *Taq* polymerase for colony PCR

Primers (10 pmol each), DMSO (5% (v/v)), MQ H_2O, 5X T4 Red Buffer and T4 polymerase were mixed to a total volume of 11 µL in a 125 µL PCR tube. A sharp toothpick was used to pick up an *E. coli* colony and put it into the PCR tube. A typical program was comprised of an initial denaturation at 95˚C for 5 minutes, then 25 cycles of denaturation (15 seconds at 95˚C), annealing (15 seconds at primer-annealing temperature), and extension (72˚C, time depended on the length of the product, 30 seconds/kb of DNA), then a final elongation step (72˚C for 5 minutes).

2.4.2.5 Agarose gel electrophoresis

A 1% (w/v) agarose gel was prepared by mixing 0.4 g of agarose with 40 mL of TAE buffer. The agarose was melted for 50 seconds in a microwave set on high power. The agarose was cooled down and 0.5% (v/v) (2 µL) of Midori Green DNA stain was added. The agarose was poured into the mould, the comb was inserted, and the gel was left to solidify at room temperature.

The gel was submerged under 1X TAE buffer, and the samples were loaded into the wells. 1 kb Plus DNA ladder (5 µL) was used as a standard. The gel was run at 180 V for 25 minutes, then imaged using a UV camera.

2.4.2.6 Restriction digest cloning

Substrate DNA was mixed with 10X Restriction digest buffer and 1 µL of Restriction endonuclease. The reaction was incubated at 37˚C for an hour. For plasmid DNA, removal of 5' phosphate would then be carried out using shrimp alkaline phosphatase (15 minutes at 37˚C) without purification. The DNA was then purified either by agarose gel electrophoresis and gel extraction (for inserts) or by a DNA Clean and Concentrator kit (for vector). The following vectors were used in this study:

Table 2.14 Vectors

Insert gene	Size/bp	Plasmid	Restriction sites	Source	Features
genB1	1250	pET-28 a (+)	*Nde*I, *Bam*HI	Dr F Huang	
genB2	1248	pET-28 a (+)	*Nde*I, *Bam*HI	Dr F Huang	
genB2	1252	pET-28 a (+)	*Nco*I, *Bam*HI	This study	No His-tag
genB2 (C9A)	1248	pET-28 a (+)	*Nco*I, *Bam*HI	Dr F Huang	Inactive mutant
genB3	1470	pET-28 a (+)	*Nde*I, *Eco*RI	Dr F Huang	
genB3	1496	pET-28 a (+)	*Nco*I, *Eco*RI	This study	No His-tag
genB3	1492	pWHU77	*Nde*I, *Eco*RI	Wuhan	*Micromonospora* expression
genB4	1386	pET-28 a (+)	*Nde*I, *Eco*RI	Dr F Huang	
genB4	1386	pWHU77	*Nde*I, *Eco*RI	Wuhan	*Micromonospora*

					expression
genB3-genB4	2878	pWHU77	*Nde*I, *Eco*RI	Wuhan	*Micromonospora* expression
genG	350	pET-28 a (+)	*Nde*I, *Eco*RI	Dr F Huang	
genF	645	pET-28 a (+)	*Nde*I, *Eco*RI	Dr F Huang	
genK	1990	pWHU77	*Nde*I, *Eco*RI	This study	Gene insertion
Δ*genL*	4176	pYH7	*Nde*I, *Hind*III	Dr F Huang	Gene deletion
genL	812	pET-28 a (+)	*Nde*I, *Eco*RI	Dr F Huang	
genL	812	pAR1	*Nde*I, *Eco*RI	This study	Weak RBS1
genL	812	pAR2	*Nde*I, *Eco*RI	This study	Weak RBS2
genL	812	pAR3	*Nde*I, *Eco*RI	This study	Super-strong RBS3
sgenL	673	pET-28 a (+)	*Nde*I, *Eco*RI	This study	Cloned by Gibson Assembly®
lgenL	725	pET-28 a (+)	*Nco*I, *Xho*I	This study	C-terminal His-tag
genL	812	pCJW93	*Nde*I, *Eco*RI	This study	*Streptomyces* expression
VM-genQ	1521	pET-28 a (+)	*Nde*I, *Eco*RI	Dr F Huang	
genP	811	pET-28 a (+)	*Nde*I, *Bam*HI	Dr F Huang	
genP (D189A)	811	pET-28 a (+)	*Nde*I, *Bam*HI	This study	
genP (D189A)	811	pEX-A2	*Nde*I, *Bam*HI	This study	SDM vector
genP (D189L)	811	pET-28 a (+)	*Nde*I, *Bam*HI	This study	
genP (D189L)	811	pEX-A2	*Nde*I, *Bam*HI	This study	SDM vector
genP (D189N)	811	pET-28 a (+)	*Nde*I, *Bam*HI	This study	
genP (D189N)	811	pEX-A2	*Nde*I, *Bam*HI	This study	SDM vector
genD2	1023	pET-28 a (+)	*Nde*I, *Eco*RI	Dr F Huang	
genD3	807	pET-28 a (+)	*Nde*I, *Eco*RI	Dr F Huang	
gmrA	825	pET-28 a (+)	*Nde*I, *Eco*RI	Dr F Huang	
IstU	839	pEX-A2	*Nde*I, *Eco*RI	This	Synthetic gene

				study	
IstU	839	pET-28 a (+)	*Nde*I, *Eco*RI	This study	
Orf82	749	pET-28 a (+)	*Nde*I, *Eco*RI	Dr F Huang	
Orf1566	773	pET-28 a (+)	*Nde*I, *Not*I	Dr F Huang	
Orf2195	894	pET-28 a (+)	*Nde*I, *Bam*HI	Dr F Huang	
Orf2_904	861	pET-28 a (+)	*Nde*I, *Eco*RI	This study	
RBS1	419	pUC19	*Sal*I, *Pae*I	This study	
RBS1	419	pET-28 a (+)	*Sal*I, *Pae*I	This study	pAR1
RBS2	419	pUC19	*Sal*I, *Pae*I	This study	
RBS2	419	pET-28 a (+)	*Sal*I, *Pae*I	This study	pAR2
RBS3	419	pUC19	*Sal*I, *Pae*I	This study	
RBS3	419	pET-28 a (+)	*Sal*I, *Pae*I	This study	pAR3
genX1/ whu5560	1198	pET-28 a (+)	*Nde*I, *Eco*RI	Dr F Huang	
genX2/ whu1520	801	pET-28 a (+)	*Nde*I, *Eco*RI	Dr F Huang	
genX3/ whu5344	795	pET-28 a (+)	*Nde*I, *Eco*RI	Dr F Huang	
genX4/ whu475	1449	pET-28 a (+)	*Nde*I, *Eco*RI	Dr F Huang	
genX5/ whu5373	748	pET-28 a (+)	*Nde*I, *Bam*HI	Dr F Huang	
genX6/ whu6656	1585	pET-28 a (+)	*Nde*I, *Bam*HI	Dr F Huang	
genX7/ whu0283	901	pET-28 a (+)	*Nde*I, *Eco*RI	Dr F Huang	
genX8/ whu5598	817	pET-28 a (+)	*Nde*I, *Eco*RI	Dr F Huang	
genX9/ whu5664	787	pET-28 a (+)	*Nde*I, *Eco*RI	Dr F Huang	
genX10/ whu4864	1495	pET-28 a (+)	*Nde*I, *Eco*RI	Dr F Huang	
genX11/ whu0088	805	pET-28 a (+)	*Nde*I, *Eco*RI	Dr F Huang	
genX12/ whu2148	673	pET-28 a (+)	*Nde*I, *Eco*RI	Dr F Huang	
genX13/ whu639	661	pET-28 a (+)	*Nde*I, *Eco*RI	Dr F Huang	

genX14/ whu2298	619	pET-28 a (+)	*Nde*I, *Eco*RI	Dr F Huang	
genX15/ whu5907	637	pET-28 a (+)	*Nde*I, *Eco*RI	Dr F Huang	
genX16/ whu2746	766	pET-28 a (+)	*Nde*I, *Eco*RI	Dr F Huang	
genX17/ whu3388	1057	pET-28 a (+)	*Nde*I, *Eco*RI	Dr F Huang	
genX18/ whu4521	994	pET-28 a (+)	*Nde*I, *Eco*RI	Dr F Huang	

The insert and vector fragments were mixed in a molar ratio of 3 to 1 respectively, ligation buffer and ligase were added in. In case of Quick ligase™, the reaction was incubated at room temperature for 15 minutes, then an aliquot of competent cells was transformed with the DNA. For T4 ligase, the reaction was left at 16˚C overnight.

2.4.2.7 Gibson assembly®

A Phusion-polymerase PCR was carried out with Gibson primers. Gibson assembly® (Gibson, 2011) was used to generate *sgenL*-pET-28a (+) vector. The fragments were mixed in a 5 to 1 ratio of insert to vector (cut with restriction enzymes), Gibson assembly® Master Mix (PFL-made, 2X, containing exonuclease, polymerase, an DNA ligase) was added and the reaction kept at 50˚C for 1 hour. The cells were transformed with the DNA.

2.4.3 Protein methods

2.4.3.1 Protein purification

2.4.3.1.1 Protein purification by metal affinity chromatography from *E. coli*

Protein purification for GenL is explained in Section 6.4.5. For all other proteins, the cells were collected by centrifugation at 3600 RCF for 10 minutes. The cell pellet was resuspended in Binding buffer. Emulsiflex homogenizer was used to lyse the cells. Supernatant was separated from cell debris by centrifugation at 48000 RCF for 1 hour at 4˚C and filtering through a 5µm membrane. The supernatant was then passed through a 1mL Co^{2+} (Ni^{2+} for GenP and GenG) His-Select resin (see Table 2.15 for resin preparation) column.

Table 2.15 Resin preparation for affinity chromatography

Resin	Application	Preparation
Co^{2+} resin	Metal affinity chromatography	1mL of Sigma His-Select resin would initially be striped with 0.5 M EDTA, washed with 5 mL MQ H_2O, then charged with 2 mL cobalt chloride solution, washed once with 5 mL MQ H_2O, and stored in 30% ethanol solution. Each column would be reused an average of 10 times. The column would be cleaned with Strip buffer and recharged after every purification.
Ni^{2+} resin	Metal affinity chromatography	Each column would be reused an average of 10 times. The column would be cleaned with Strip buffer, recharged after every purification, and stored in 30% ethanol solution.

After washing the column with 10 mL of Binding and Wash buffers each, the protein was eluted off the column with Elution buffer (see Table 2.17 for imidazole concentrations of the wash and elution buffers for different proteins). A CentriPure P25 desalting column was used to buffer-exchange the protein into Exchange buffer. The protein was then concentrated using a VivaSpin PES concentrator of appropriate pore size. The protein solution was stored in 10% glycerol at -20˚C.

Table 2.16 Imidazole concentration of buffers for recombinant protein purification

Enzyme	Size/kDa	Resin metal	Wash Buffer's [imidazole] / mM	Elution Buffer's [imidazole] / mM
GenB1	47	Cobalt	25	250
GenB2	47	Cobalt	25	200
GenB3	56	Cobalt	40	400
GenB4	51	Cobalt	40	600
GenG	13	Zinc	50	750
GenL	29	Cobalt	40	500
GenQ	53	Cobalt	50	600
GenP	30	Nickel	50	1000
GenD2	37	Cobalt	25	200
GenD3	28	Cobalt	40	400
gmrA	31	Cobalt	40	500
GenL (from *Streptomyces)*	42	Cobalt	40	500

2.4.3.1.3 Protein purification by size-exclusion chromatography

An ÄKTA Purifier system with a HiLoad 16/60 column packed with Superdex200 resin was used to perform gel filtration chromatography of samples at 4˚C - to isolate proteins by size (in the same oligomeric state and/or predict the molecular mass of complexes).

Individual protein samples were concentrated to ≤1 mL and loaded into a 2-mL sample loop. The column was equilibrated into Exchange buffer, with the contents of the loop injected onto the column. Protein was tracked with a upperC-900 monitor (A_{280}) with 2 mL fractionations collected into a 96-well plate. The column was then washed with 125 mL (1 column volume) of Exchange buffer, followed by 125 mL of MQ H_2O. Weekly cleaning with 0.1 M NaOH was also performed.

Peak fractions were confirmed by SDS-PAGE gel, pooled, and concentrated using a VivaSpin PES concentrator.

2.4.3.1.4 Protein purification by ion-exchange chromatography

An ÄKTA Purifier system with a Q sepharose High Performance column was used to perform ion-exchange chromatography of samples at 4˚C - to isolate proteins based on their surface charge.

Individual protein samples were concentrated to ≤1 mL and loaded into a 2-mL sample loop. ÄKTA pump A contained IEX low-salt buffer with pump B containing IEX high-salt buffer. The column was equilibrated into 20 mM Tris-HCl, pH 7.8, 0.1 M NaCl (90% A, 10% B), the contents of the loop were injected onto the column, and the column was washed with the same buffer for 30 mL. A salt gradient from 10% to 100% IEX high-salt buffer was established to elute the protein while collecting 2 mL fractionations into a 96-well plate. The column was then washed with 30 mL IEX high-salt buffer, followed by 30 mL of MQ H_2O.

Protein was tracked with a upperC-900 monitor (A_{280}). Fractions containing the protein of interest were confirmed by SDS-Page, pooled, and concentrated using a VivaSpin PES concentrator.

2.4.3.2 Protein quantification

2.4.3.2.1 Protein concentration estimate by Bradford assay

The purified protein to be measured (1 µL) was mixed with 99 µL of MQ H_2O and 900 µL of the Bradford reagent. The spectrophotometer was blanked at 595 nm using a standard (100 µL of MQ H_2O and 900 µL Bradford reagent) before the absorbance of sample was read.

A standard curve was created using BSA as a protein standard, to obtain an equation used to determine the protein concentration:

$$c_{protein} = \frac{A_{595} - 0.0242}{0.4356} \times 20$$

2.4.3.2.2 Protein concentration estimate by absorbance measurement

Protein concentration was determined by an absorbance reading at 280 nm using a NanoDrop™ spectrophotometer with extinction coefficient and molecular mass input.

2.4.3.2.3 Protein size estimation by gel filtration standard curve

A standard curve could be used to estimate the molecular mass of a protein complex. BioRad Gel Filtration Standards were run on the S200 column. A straight-line plot was generated by plotting volume of retention (x-axis) versus Log_{10} (Molecular Mass) (y-axis), and the following equation was obtained (R^2=0.991):

$$MM = 10^{-0.039 \times V_{retention}} + 4.414$$

2.4.3.2.4 Protein identification by mass spectrometry

A sample of pure recombinant protein (20 pmol) was denatured by heating to 98˚C and run on a C4 column. Biomass deconvolution was then used to determine the accurate mass of the protein loaded. The first methionine would normally be destroyed by the analysis.

2.4.3.3 Acrylamide gel electrophoresis

2.4.3.3.1 Gel preparation, running, and staining

Acrylamide gels (12% (v/v); for smaller proteins a 15% (v/v) gel was made) were prepared in house. For the resolving part of a single gel, 1.6 mL of MQ H_2O, 2 mL of 30% (v/v) acrylamide, 1.3 mL of 1.5 M Tris-HCl, pH 8.8, 50 µL of 10% (w/v) SDS, 50 µL of 10% (w/v) APS, 2 µL of TEMED were mixed and pipetted in-between a glass and a silica plate. Isopropanol (70%) was pipetted on top to prevent gel crystallization. After the gel had set, the isopropanol was carefully poured off. For the stacking part of a single gel, 0.68 mL of MQ H_2O, 0.17 mL of 30% (v/v) acrylamide, 0.13 mL of 1.0 M Tris-HCl, pH 6.8, 10 µL of 10% (w/v) SDS, 10 µL of 10% (w/v) APS, 2 µL of Bromophenol Blue, and 2 µL of TEMED were mixed and pipetted in-between a glass and a silica plate. A comb was inserted and left until the gel had solidified and the wells were made. The gels were stored in the fridge, wrapped in Tris-glycine buffer-soaked tissue.

The protein samples were mixed with 4X Laemmli buffer with 10% (v/v) 1 M DTT and denatured at 98˚C for 2 minutes. The gels were run at constant voltage of 200 V for 1 hour or until the protein dye reached the bottom.

The gels were washed with MQ H_2O and microwaved in it for 30 seconds on high power, twice. The gel was covered with safe Brilliant Blue stain and microwaved on high power for 30 seconds. The gel was left in the dye for 15 minutes. It was then washed with MQ H_2O and left in it to de-stain.

2.4.3.3.2 MALDI-analysis

The gel was submitted to Protein Fingerprinting Facility for analysis. Briefly, the gel band of interest was excised, digested with trypsin protease, and fragments were separated by mass spectrometry. The fragments were analysed and compared to the probe sequence.

2.4.4 Mass spectrometry

2.4.4.1 In vitro assay

In vitro assays were set up in a total volume of 50 µL. A typical *in vitro* reaction contained 50 mM Tris-HCl, pH 7.8, 0.2 mM aminoglycoside substrate, 1 mM any cofactors required, 20 µM protein, and MQ H_2O. Reactions were typically incubated at 30˚C for 1 hour or overnight. The protein was extracted using chloroform precipitation, three times. The upper, aqueous phase was then transferred into an HPLC vial with an insert.

2.4.4.2 LC–MS running program

The following solvent system was used to run all *in vitro* and fermentation samples on a C18 column: pump C with acetonitrile, pump D with MQ H_2O + 0.2% (v/v) trifluoroacetic acid (TFA).

The following program was used to run the samples (5 µL):

Table 2.17 HPLC-MS running program

Time/ minutes	Percentage of MQ H_2O + 0.2% (v/v) TFA in total	Percentage of acetonitrile in total
0	98	2
14	94	6
16	92	8
25	75	25
26	10	90
34	10	90
35	98	2
45	98	2

2.4.4.3 Data analysis

Xcalibur™ software was used to analyse the data obtained from the mass spectrometer. Retention time, m/z (mass over charge) of molecular ion, and fragmentation pattern were used to define a compound.

3

Generation of gentamicin intermediates

The difference in toxicity between the gentamicin C complex components, as well as the need for purer substrates for semi-synthesis, creates a desire for pure mono-component gentamicins. Any strategy enriching the component mixture towards a desired component, e.g. by creating a *Micromonospora* mutant, is a welcome advance in clinical production of gentamicin.

3.1 Introduction

Current methods of gentamicin production and isolation involve batch fermentation and purification by chromatography. Commercially-available gentamicin and pathway intermediates are obtained by fermentation of *M. echinospora* and related strains. The complicated structure and stereochemistry of gentamicins makes chemical synthesis of these clinical antibiotics unfeasible. Fermentation mixture produced by *M. echinospora* consists of five major (gentamicin C complex) and up to seventeen minor components (Grahek and Zupancic-Kralj, 2009). The composition of the clinical gentamicin varies depending on the growing and purification conditions.

3.1.1 *Micromonospora* cell culture

M. echinospora cells were typically grown from glycerol stocks on agar plates with #172 medium at 30˚C. Plates with actively-growing cells were kept at room temperature and re-plated every two weeks. For gentamicin production, actively-growing cells were grown for 2 days in 10 mL of liquid #172 medium in a 25-mL flask with a spring, then for 5 days at 30˚C in 50mL of F50 medium in 250 mL flasks with springs and foam bungs. The growth and the production of gentamicins was accompanied by a colour change, from orange to purple.

M. inyoensis (sisomicin producer) and *M. olivasterospora* (fortimicin producer) cells were grown on GYM medium. *M. grisea* (verdamicin producer) cells were grown on 127 medium. The rest of the protocol was the same.

3.1.1.1 Export of produced aminoglycosides

Most of the produced antibiotic is exported to the outside of the cell. In the *gen* cluster there are four genes encoding aminoglycoside transporters, *genV, genY, genH,* and *genI.* GenV is an efflux pump, GenY is a transmembrane antiporter, and GenH and GenI are exporter proteins (Kudo and Eguchi, 2009, Unwin et al., 2004).

GenH and GenI proteins together belong to the drug resistance transporter EmrB/QacA subfamily of drug efflux proteins. In most cases, members of this family have two components. However, the transporters from aminoglycoside clusters, conserved between gentamicin, fortimicin, and istamycin, contain three

components, and are predicted to be structurally new. In the *gen* cluster, *genH* is a fusion of two of the components ("H" and "J"). The protein is also predicted to contain a 300-amino acid extracellular domain, with an unknown catalytic or binding function (Piepersberg et al., 2007a).

Most of the exported gentamicins remain bound to the cell wall and require acid hydrolysis to be released (Reiblein et al., 1973).

3.1.2 Component purification

The cells and media were pooled into a glass beaker and acidified to pH 2 with 6 M H_2SO_4, and left stirring overnight. The supernatant was collected by centrifugation at 3600 RCF for 20 minutes, and further clarified by passing through a Whatman#1 filter paper. The filtrate was passed through Dowex® 50WX8-200 cation exchange resin (H^+ form, 1.5 g per 50 mL of culture; see Table 3.1 for resin preparationand Figure 3.1 for resin structure) column, the bound gentamicin was washed with MQ water. Gentamicins were eluted off with 15 mL of 1 M NH_4OH.

The eluted material was passed through Dowex® 1X2 anion exchange resin (OH^- form; see Table 3.1 for resin preparation and Figure 3.1 for resin structure) to remove impurities. The collected flow-through was left in a fume hood to allow ammonia to evaporate. It was then subjected to lyophilization. Lyophilised powders were weighed and resuspended in water to a final concentration of approximately 20 mM for *in vitro* reactions. Alternatively, the compounds were separated using dynamic Counter-current chromatography (CCC) or HPLC.

Table 3.1 Resin preparation for gentamicins purification

Resin	Application	Preparation
Dowex® 50WX8-200 cation exchange resin (H^+ form)	Gentamicins purification	Prepare the resin by washing it with 50 mL of acetonitrile, followed by washing 3 times with 50 mL MQ H_2O
Dowex® 1X2 anion exchange resin (OH^- form)	Gentamicins purification	Prepare the resin by washing it with MQ H_2O. Soak in 2 volumes of 4% (w/v) NaOH for 4 hours, wash with MQ H_2O until the pH becomes neutral. Soak in 2 volumes of 4% (v/v) HCl for 4 hours, wash with MQ

		H_2O until the pH becomes neutral. Soak in 2 volumes of 4% (w/v) NaOH for 4 hours, wash with MQ H_2O until the pH becomes neutral.

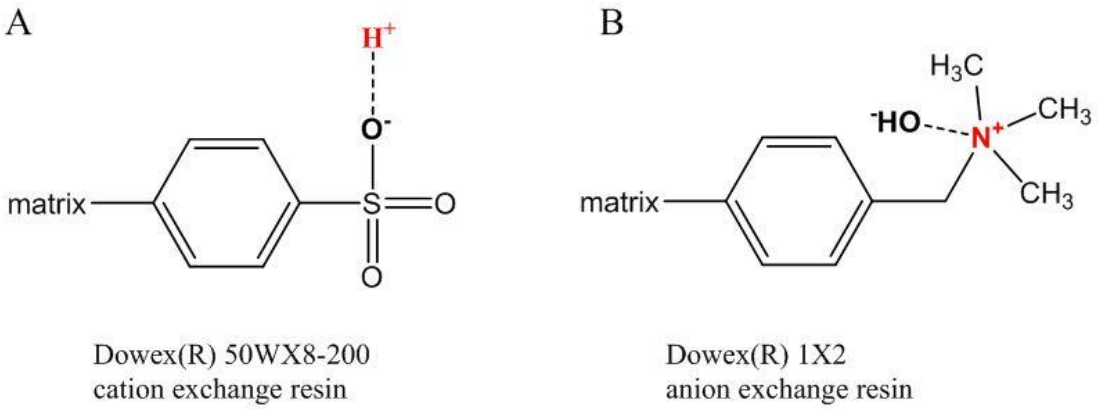

Figure 3.1 Dowex® ion exchange resin structures. (A) Dowex® 50WX8-200 cation exchange resin (H^+ form) with sulfonic acid functional group; (B) Dowex® 1X2 anion exchange resin (OH^- form) with trimethylbenzylammonium functional group.

Gentamicin molecules do not possess a UV absorbing chromophore. Several High-Performance Liquid Chromatography (HPLC) techniques have been developed to detect and identify gentamicin compounds. In our lab mass spectrometry is used to reveal the products of fermentations and *in vitro* assays.

3.1.3 Improving production yields

Gentamicin is the main product of *M. echinospora*. Due to its high value as a medicine, several studies have been undertaken to elucidate strategies for improved gentamicin production.

Historically, to generate an overproducer strain, classical mutagenetic and screening approaches were used to isolate new strains of *M. echinospora* (Himabindu et al., 2007). A mutant with an enhanced production (1.26-fold) of gentamicin was isolated in this way. Starch as a sole carbon source and soybean meal as a nitrogen source further improved gentamicin yields (Himabindu and Jetty, 2006). The medium used in our lab for gentamicin production, F50, is used

to produce gentamicin at industrial scale, and contains both soya flour and soluble starch.

Other strategies can be used to improve the yields further. Gentamicin, like other aminoglycosides, readily binds to the mycelium of the producer, and can be released with strong acid or alkali (Reiblein et al., 1973). Up to 90% of produced gentamicin can be bound to *M. echinospora* peptidoglycan cell wall. Cations, such as Mg^{2+} ions, compete with gentamicin for the binding sites on peptidoglycan, and alleviate negative feedback. Thus, addition of $MgSO_4$ to the fermentation medium improves the yield of gentamicin (Chu et al., 2004). Ultrasound can also be used to dissociate gentamicin from the cell wall (Chu et al., 2000). It can be used during growth of culture to induce greater production of the antibiotic via inhibiting negative feedback of cell wall-bound gentamicin.

3.1.3.1 Genetic control

As discussed previously, aminoglycosides are predicted to act as signalling and transcription regulating molecules in nature (Yim et al., 2007, Bibb, 2013). To test if gentamicin participated in regulation of its own biosynthesis, induction of antibiotic production was tested on *M. echinospora* grown on #172 agar plates. A small filter paper disk, saturated with either the purified antibiotic or culture supernatant, was put near a cell colony of wild-type *M. echinospora* (Figure 3.2). Colour change (orange to brown/purple) was considered as an indication of entry into late stages of cell growth and antibiotic production.

Gentamicin C complex and G418 (geneticin™) both induced faster entry into the late stages of the growth cycle. Both substances are used as antibiotics. JI-20b did not result in a notable change. JI-20b is a worse antibiotic than the others, which might explain why it did not elicit the same response. Water was used as a negative control and had no effect, *M. echinospora* DSM1040 total extract was used as a positive control and induced the colour change.

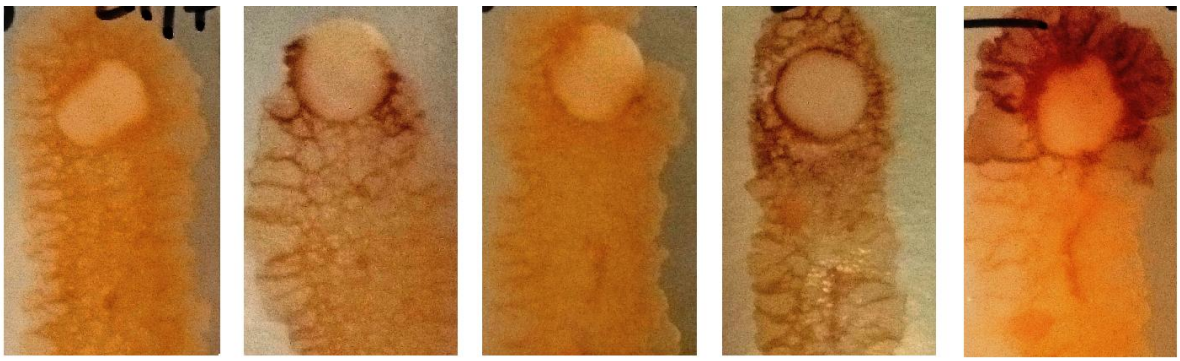

Figure 3.2 Induction of gentamicin production. Parts of the *Micromonospora echinospora* mycelium closest to the saturated filter paper disks turned brown or purple earlier. Gentamicin C complex and intermediate G418, which are both bactericidal, are both able to induce earlier production of gentamicins.

3.1.4 Genetic manipulation for access to novel molecules

3.1.4.1 Mutant generation by conjugation of Micromonospora sp.

Knock-out mutants of key biosynthetic genes provide an access point to intermediates and gentamicin mono-components. *Micromonospora* species can be genetically modified using conjugation vectors in *E. coli*.

3.1.4.1.1 Gene deletion

Gene deletion was used to create a Δ*genK* Δ*genL M. echinospora* mutant for mono-component gentamicin C1a biosynthesis. The *Micromonospora* cells were re-plated on #172 medium at 30˚C until an actively-growing culture was obtained. The cells were then inoculated into 30 mL of ABB medium with 10 mM $MgCl_2$ and grown at 30˚C for 2-3 days.

Separately, competent *E. coli* ET12567/pUZ8002 cells were prepared. These were transformed with the pYH7 (*Apr*^{R}) plasmid containing the *genL*-flanking regions of DNA and grown on antibiotic-selective agar (Figure 3.3). The cells were grown in 5 mL of 2x TY medium with apramycin until the A_{600} reached 0.3. The *E. coli* cells were spun down at 4˚C, 3000 RCF, for 3 minutes. Leftover antibiotics were removed by re-suspending the *E. coli* cells in antibiotic-free medium and spinning them down again, twice. The cells were resuspended in 200 µL of 2xTY medium.

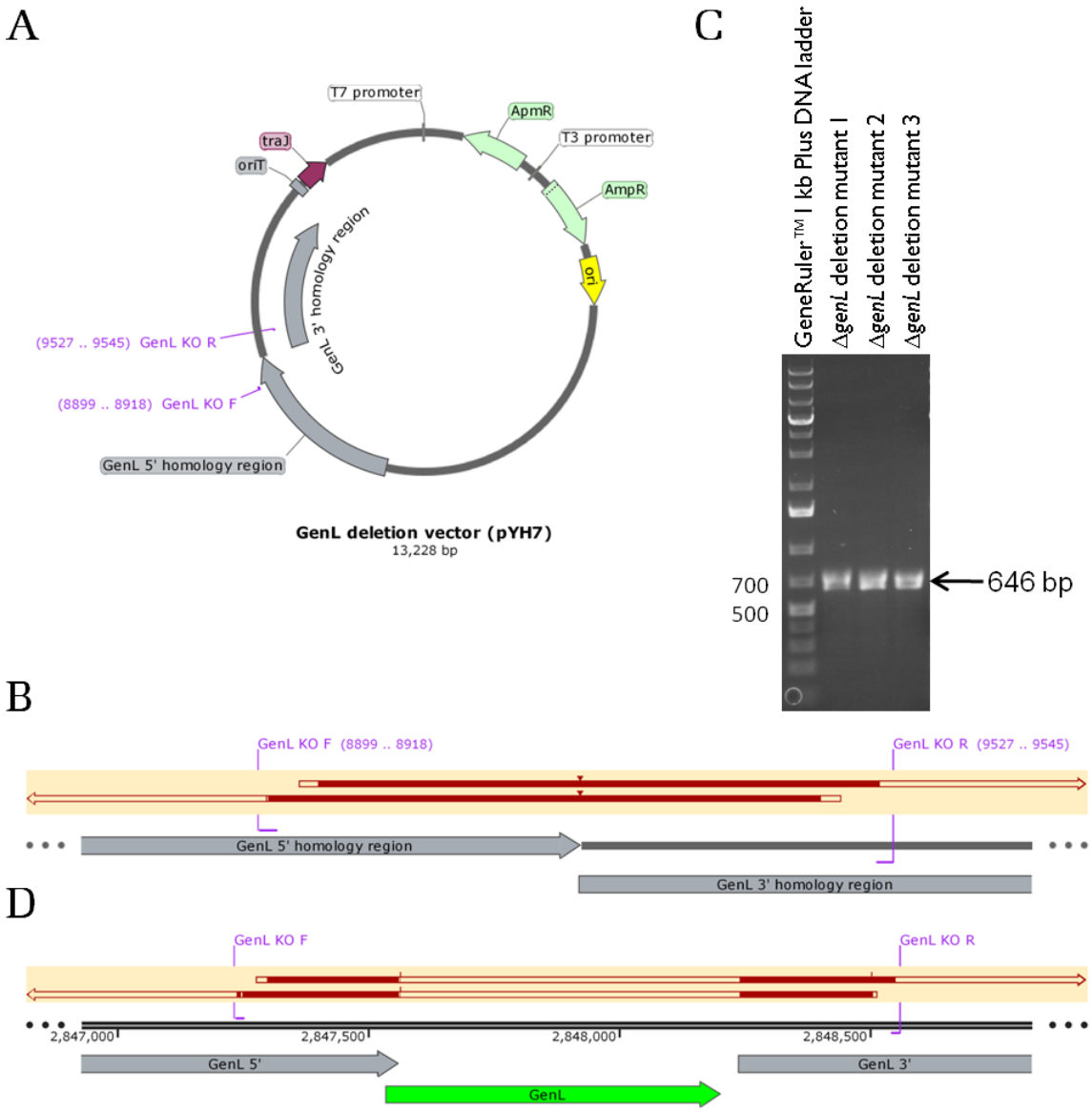

Figure 3.3 *genL* Gene deletion in *M. echinospora* Δ*genK*. (A) Gene deletion vector was constructed on the basis of pYH7 plasmid. (B) The Δ*genL*-pYH7 vector sequence was confirmed through DNA sequencing. (C) Following relaxation, PCR suggested deletion of *genL* from *M. echinospora* Δ*genK*. (D) DNA sequencing confirmed generation of *M. echinospora* Δ*genK* Δ*genL*.

M. echinospora cells were spun down and washed twice with 30 mL of 2xTY medium. *M. echinospora* cells (100 µL) were carefully mixed with 100 µL of *E. coli* cells. The mixture was plated out on ABB medium with 10 mM $MgCl_2$ and dried before incubating at 30˚C for 10 hours.

The plate was overlaid with 1 mL of MQ H_2O containing nalidixic acid (12.5 µg/mL) and apramycin (25 µg/mL) per mL of agar, i.e. a 30-mL agar plate required 375 µg of nalidixic acid and 750 µg of apramycin. The plates were

incubated at 30˚C for 4-5 days until the exconjugant *M. echinospora* colonies could be observed.

The exconjugants were re-plated twice on ABB plates with nalidixic acid (25 µg/mL) and apramycin (25 µg/mL). Twenty-five colonies were obtained this way (Figure 3.4). The presence of vector was checked by PCR and DNA sequencing.

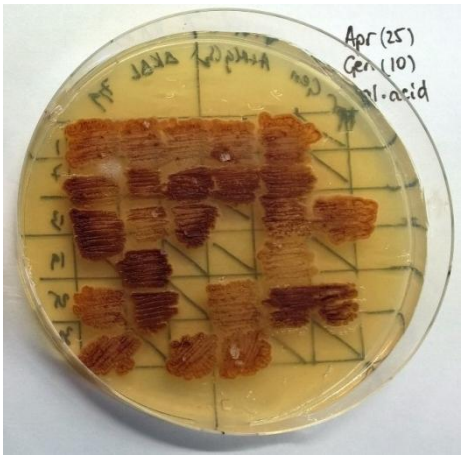

Figure 3.4 *M. echinospora* Δ*genK* Δ*genL*. Successful exconjugants of *M. echinospora* were selected by growing on apramycin-containing medium.

The exconjugants were then plated on ABB plates without antibiotics to induce a second crossover event. The exconjugants that no longer exhibited resistance to apramycin were tested using PCR and DNA sequencing. Deletion of *genL* was thus confirmed in three colonies.

Fermentation of *M. echinospora* Δ*genK* Δ*genL* in F50 production medium was followed by extraction and purification of total gentamicins. Presence of mono-component gentamicin C1a was confirmed by HPLC-MS (Figure 3.5).

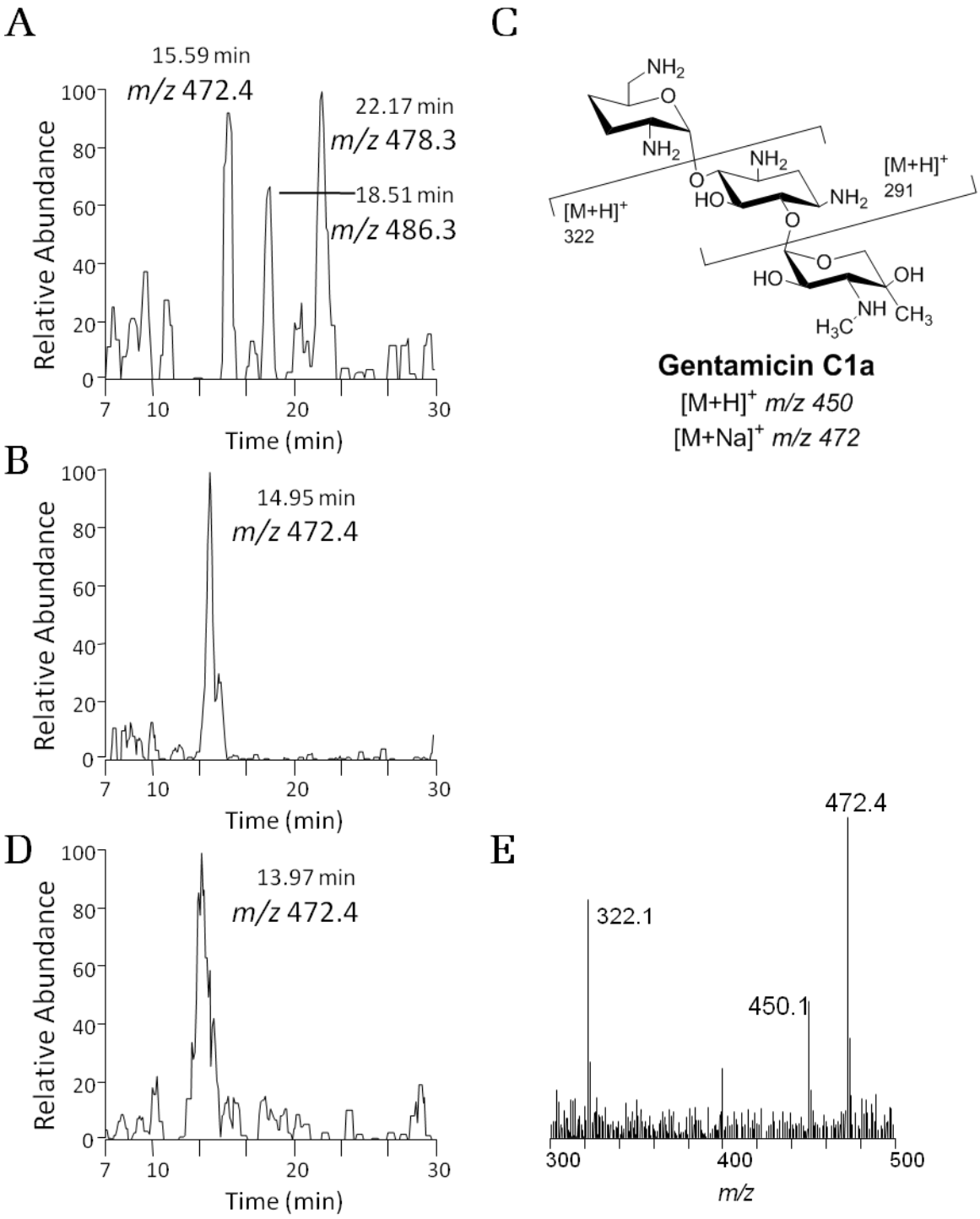

Figure 3.5 *M. echinospora* Δ*genK* Δ*genL* produces gentamicin C1a. (A) *M. echinospora* WT produces gentamicin C complex (gentamicin C1a - *m/z* 472,gentamicins C2, C2a, and C2b - *m/z* 486, gentamicin C1 - *m/z* 478). (B) HPLC chromatogram of gentamicin C1a standard. (C) Gentamicin C1a fragmentation map. (D) HPLC chromatogram of fermentation product of *M. echinospora* Δ*genK* Δ*genL* (selective ion monitoring for the gentamicin C complex) showing presence of only gentamicin C1a ions. (E) Fragmentation of the major peak of (D).

3.1.4.1.2 Gene insertion

Gene insertion was used to clone *genK* gene into *M. inyoensis* (Figure 3.6), and to clone *genB4* gene into *M. inyoensis* and *M. grisea* (Figure 3.7). The former should produce verdamicin instead of sisomicin, and the latter should confirm the findings of Chapter 6, although the experiments remain to be performed later. Gene insertion was performed following the gene deletion protocol up to the relaxation stage; insertion vector pWHU77 (*Thio*^{R}) was used instead of pYH7 (*Apr*^{R}).

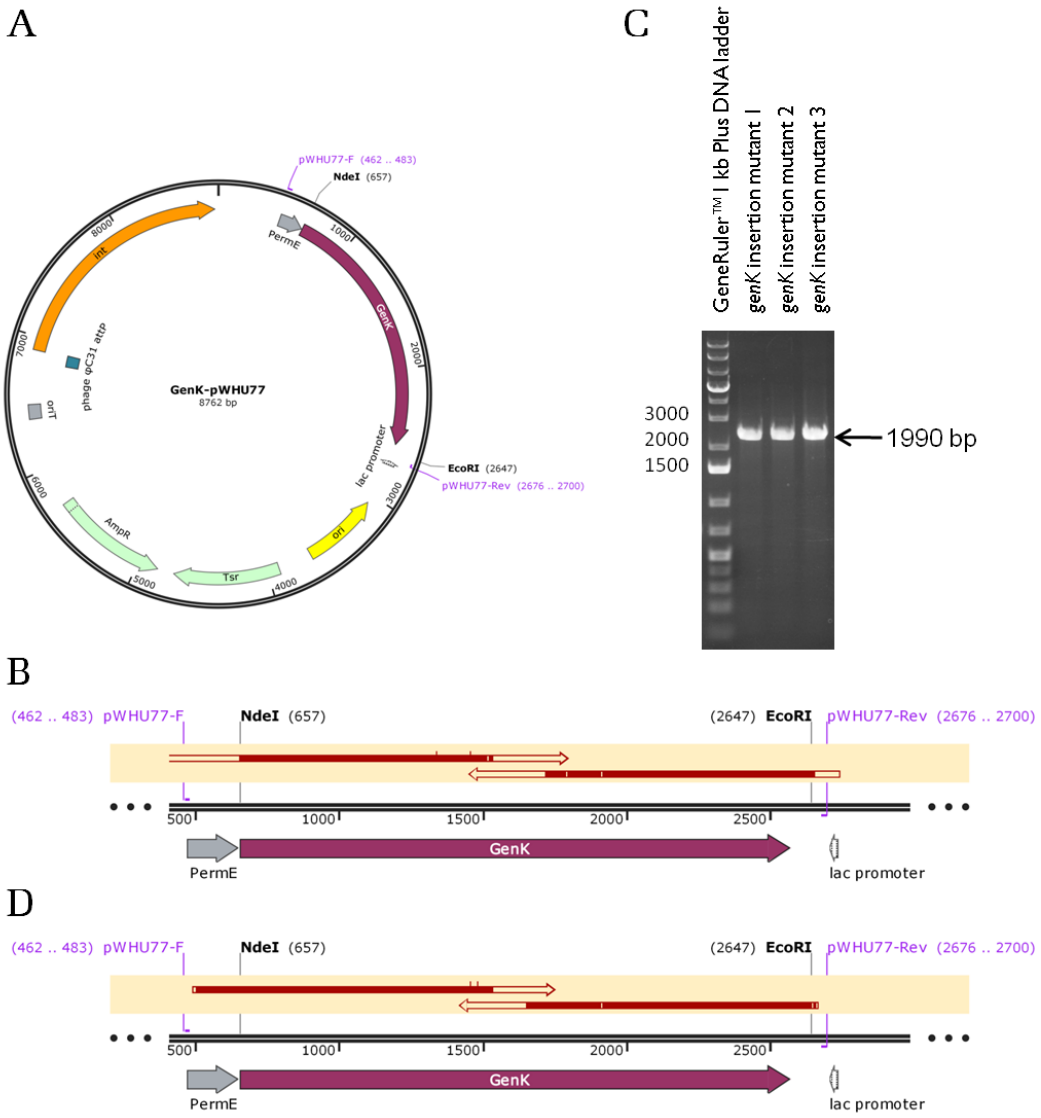

Figure 3.6 Insertion of *genK* gene into *M. inyoensis*. (A) Gene insertion vector was constructed on the basis of pWHU77 plasmid. (B) The *genK*-pWHU77 vector sequence was confirmed through DNA sequencing. (C) Following relaxation, PCR suggested insertion of *genK* from *M. inyoensis*. (D) DNA sequencing confirmed generation of *M. inyoensis::genK.*

Following conjugation, the cells were grown on ABB medium containing thiostrepton (10 µg/mL). No relaxation was required. Twenty-four exconjugants were obtained for *M. inyoensis.* The presence of the vector was confirmed by PCR and DNA sequencing.

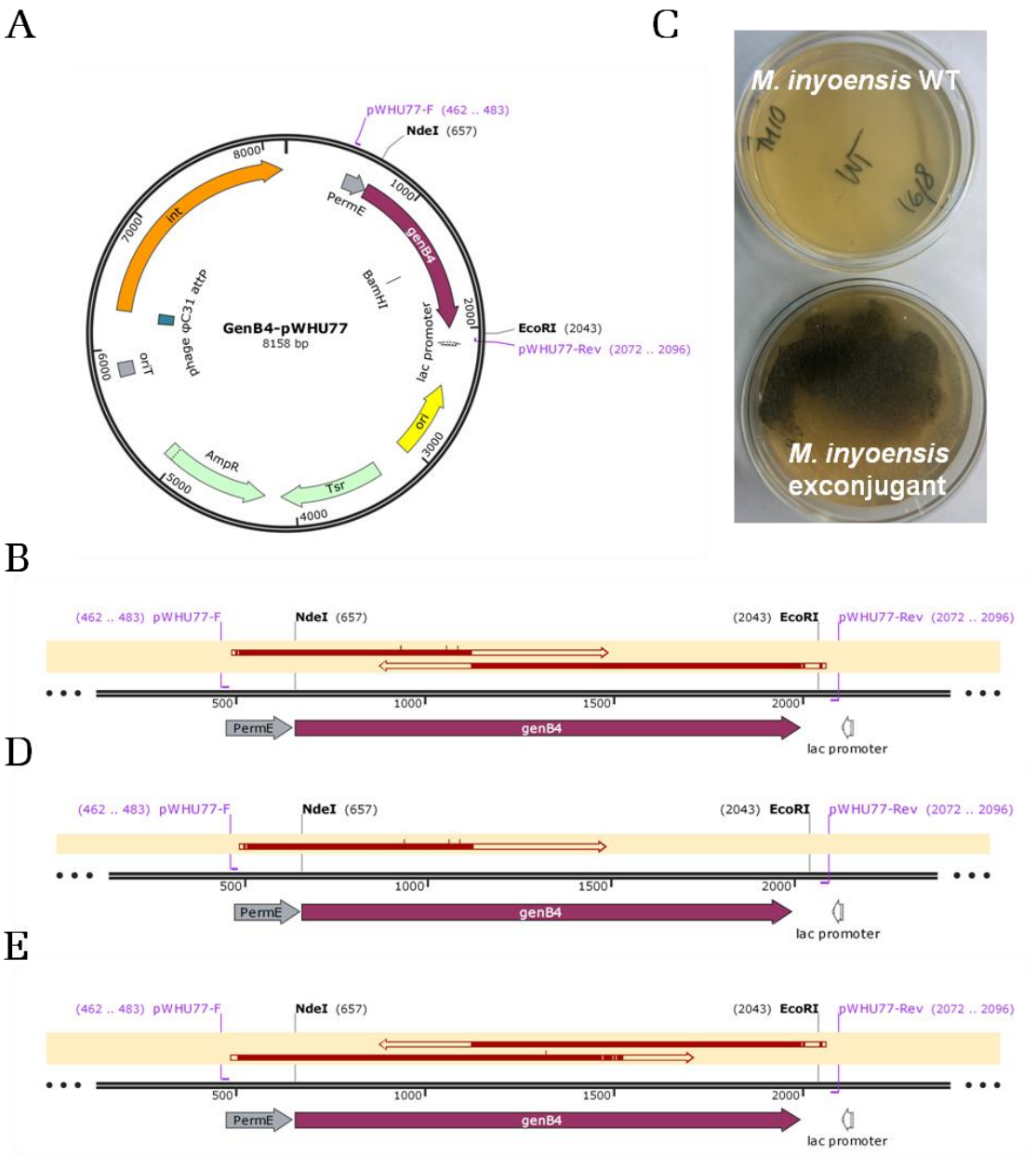

Figure 3.7 Insertion of *genB4* gene into *M. inyoensis* and *M. grisea*. (A) Gene insertion vector was constructed on the basis of pWHU77 plasmid. (B) The *genB4*-pWHU77 vector sequence was confirmed through DNA sequencing. (C) Following relaxation, PCR could not distinguish between WT and successful exconjugant. Antibiotic selection on thiostrepton suggested presence of *genB4*-pWHU77 suggested insertion of *genB4* from *M. inyoensis*. (D) DNA sequencing confirmed generation of *M. inyoensis::genB4.* (E) DNA sequencing confirmed generation of *M. grisea::genB4.*

Table 3.2 summarises the main fermentation products of a few of *Micromonospora* mutants.

Table 3.2*Micromonospora* strains and mutants

Species	Mutant strain	Products	Origin
M. echinospora	WT, ATCC ® 15835	Gentamicin C complex (C1a, C2b, C2a, C2a, C1)	PFL strain collection
	Δ*genQ*	Gentamicin X2, G418	PFL strain collection
	DSM 1040	JI-20B, JI-20A	PFL strain collection
	Δ*genP*	JI-20B, JI-20Ba	PFL strain collection
	Δ*genB2*	Gentamicins C1a, C2b, and C2a	PFL strain collection
	Δ*genB3*	JI-20B, JI-20A	PFL strain collection
	Δ*genB4*	Verdamicin, keto-verdamicin	PFL strain collection
	Δ*genB2* Δ*genB3*	JI-20B, JI-20A	PFL strain collection
	Δ*genK*	Gentamicin C1a, C2b	PFL strain collection
	Δ*genK* Δ*genQ*	Gentamicin X2	PFL strain collection
	Δ*genK* Δ*genP*	JI-20a	Wuhan
	Δ*genK* Δ*genL*	Gentamicin C1a	This study
M. inyoensis	WT, ATCC ® 27600	Sisomicin	PFL strain collection
	::*genK*	Unknown (m/z 486)	This study
	::*genB4*	Currently unknown	This study
M. grisea	WT, DSM 1043	Verdamicin	PFL strain collection
	::*genB4*	Currently unknown	This study

3.1.5 Large-scale substrate generation *in vitro*

Generation of milligram quantities of pathway intermediates was necessary for structural studies by NMR. Specifically, phosphorylated JI-20 complex was analysed for the position of the phosphate group. To generate pure Pi-JI-20b and Pi-JI-20a, the substrates JI-20b and JI-20a were first purified from cultures of Δ*genB3* (in Cambridge) and Δ*genK* Δ*genP* (by our collaborators in Wuhan) *M. echinospora* respectively. Compounds were isolated using ion exchange chromatography and HPLC purification.

3.1.5.1 Incubation with biosynthesis enzymes

Purified compounds JI-20a and JI-20b were mixed with pure recombinant GenP enzyme (see Section 2.4.3.1 for details on protein purification), $MgCl_2$ and a 100-fold excess of ATP, and incubated at 30˚C for a minimum of 1 hour. Chloroform precipitation was then used to remove all protein, followed by anion exchange chromatography with Dowex® 1X2 resin (OH^- form).

3.1.5.2 Protein immobilization to improve stability and substrate yield

Protein adsorption onto silica-based nano-particles is an efficient method of improving protein thermo- and mechanical stability. To provide a reusable and stable platform for gentamicin intermediate generation, specifically Pi-JI-20b, GenP was encapsulated in silica.

A previously established protocol (Betancor, 2009, Betancor et al., 2003, Betancor and Luckarift, 2008, Betancor et al., 2008) for protein immobilization was carried out. Recombinant protein in Exchange buffer (200 µL) was mixed with a 100 µL of a 10% (v/v) solution of polyethyleneimine (PEI), pH 8.0, and 100 µL of 1 M solution of hydrolysed tetramethylorthosilica (TMOS). Please refer to Section 2.1.1.1 for details on buffer preparation. The mixture was agitated at room temperature for 2 minutes using a Vortex. The silica particles with encapsulated protein were collected by gentle centrifugation and washed with Exchange buffer to remove any unreacted protein. Particles were then stored in buffer at 4˚C.

For substrate generation, the beads were carefully moved into a 1.5 mL Eppendorf tube containing an insert. JI-20b and excess ATP were added, the mixture mixed with a pipette tip and kept at 30˚C for 1 hour. The tubes were spun at maximum speed to collect Pi-JI-20b.

3.2 Method development: Dynamic counter-current chromatography

Gentamicins are a globally-used antibiotic medicine that is due for a 21st century upgrade. Access to mono-component gentamicin and its intermediates would improve the toxicity profile of this aminoglycoside substance and provide novel starting material for semi-synthetic development of new antibiotics (Sandoval et

al., 2006, Fox et al., 1980, Karpiuk and Tyski, 2015). Separation of gentamicins has always presented a problem for its research, as the small structural differences between the components prevent efficient and scalable isolation by various chromatography techniques.

The two parallel branches of gentamicin biosynthesis are separated by 6'-*C*-methylation by GenK. The last step in either branch is a 6'-*N*-methylation, whereby gentamicin C2b is made from gentamicin C1a, and gentamicin C1, the major product of *M. echinospora* fermentation, is produced from gentamicin C2a.

Gentamicin C2, a component of the gentamicin C complex, is non-nephrotoxic. It has been shown to be generated in a reversible reaction from gentamicin C2a by epimerase GenB2 (Guo et al., 2014, Sandoval et al., 2006). Creating a *Micromonospora* mutant that produces mono-component gentamicin C2 will probably require an in-depth study into the active site of GenB2, as well as an extra copy of GenK to push the biosynthesis towards the 6'-*C*-methylated branch of the pathway.

Non-ototoxic gentamicin C1 is the 6'-*C*- and 6'-*N*-methylated component of the gentamicin C complex and requires 6'-*C*-methylation by GenK, epimerisation by GenB2, and 6'-*N*-methylation by the terminal methyltransferase GenL (Fox et al., 1980). Production of gentamicin C1 by a mutant *Micromonospora* strain as a mono-component is unlikely.

Therefore, an improved separation technique is necessary to create an industrially-viable way of producing mono-component gentamicin. Separately, purification advances are also required for generating the intermediates of the pathway in pure form to provide substrates for *in vitro* assays and confirm the mechanism of one of the last steps of the biosynthesis, 3',4'-didehydroxylation.

Counter-current chromatography (CCC) is a technique that was developed in the mid-20th century and has recently become more powerful because of technological and material advances, as well as a better understanding of the process. Application of counter-current chromatography to the isolation of

gentamicin promises to finally enable easy access to mono-components of this important antibiotic.

3.2.1 Principles of dynamic counter-current chromatography

Counter-current chromatography (CCC), or liquid-liquid chromatography (LLC), uses two immiscible liquids to form a stationary phase and a mobile phase. The separation of compounds depends on their partition coefficient or K_D (also known as "distribution ratio" or "distribution constant", (D): the equilibrium constant for the distribution of a compound in two solvents, or the ratio of the total analytical concentration of a solute in the stationary phase to its total analytical concentration in the mobile phase (Rice et al., 1993). For most chromatographic techniques, K_D represents the ratio of concentration of compound within an organic phase to the concentration of compound within an aqueous phase:

$$K_D = \frac{[Organic\ phase]}{[Aqueous\ phase]}$$

and D represents the ratio of concentration of a compound between two separate phases:

$$D = \frac{[Organic\ phase]}{[Aqueous\ phase]}\ or\ \frac{[Aqueous\ phase]}{[Organic\ phase]}$$

and are thus not interchangeable, however, in the case of CCC, either one can be used to describe the distribution of a given compound between the stationary and mobile phase:

$$K_D = D = \frac{[Stationary\ phase]}{[Mobile\ phase]}$$

A distribution coefficient close to 1 is the most desired for a compound and a given solvent system. In practical terms, it means that only one volume of mobile phase equivalent to the stationary phase's volume is needed to elute a compound. As the pump pushes new mobile phase through the existing stationary phase, more and more of the compound is passed into the mobile phase to retain the equilibrium. Therefore, compounds with a lower K_D for a

given system are eluted first, while compounds with higher K_D (and better solubility in the stationary phase) are retained for a longer period and eluted later.

3.2.2 Development of modern CCC

The first CCC machine was developed in the late 1940s by Craig and Post, and was nothing more than a series of interconnected glass "separating funnels" filled with solvents (Craig and Golumbic, 1945). The Earth's gravity was used to form a stationary phase, which was always the denser solvent. Although the machine was slow and required a lot of solvent, very complex mixtures, such as natural extracts, could be separated to high resolution without the loss of product. It became a technique of choice for the separation of natural products of high value, such as Chinese medicine.

In the 1970s Ito *et al* developed a similar system with a pump connected to it, a Droplet Counter-current chromatograph. The machine offered a choice as to which of the phases was used as a stationary phase, but was still extremely slow and had poor phase mixing. As both systems use gravity to stabilise and retain the stationary phase, they are known as "1g".

Ito *et al* realised that centrifugal force could also be used to retain the stationary phase, and to a much better extent (Ito et al., 1966). This would enable the use of higher flow rates and would cut down the experimental times. In this "high g" instrument, developed in the late 1970s, Teflon or stainless-steel tubing was wound helically in layers on a bore. When the coil was filled with one liquid (stationary phase), and then the other immiscible liquid (mobile phase) was introduced, within every turn of the helical coil, there was a pocket of each solvent phase (Figure 3.8A). Pushing more of the mobile phase through the coil with the help of the pump slowly created a separation of the injected sample. However, introduction of rotation around the bore's own axis created a much more complex hydrodynamic equilibrium system, where in addition to two separate-liquid sections there is also an interchange phase, created by the centrifugal force (Figure 3.8B and C). The ratio of the phases remains the same between all the coil units as soon as the equilibrium is established (Ito, 1981).

Pumping more mobile phase through after this equilibrium has been reached displaces only the mobile phase, allowing for efficient compound partitioning.

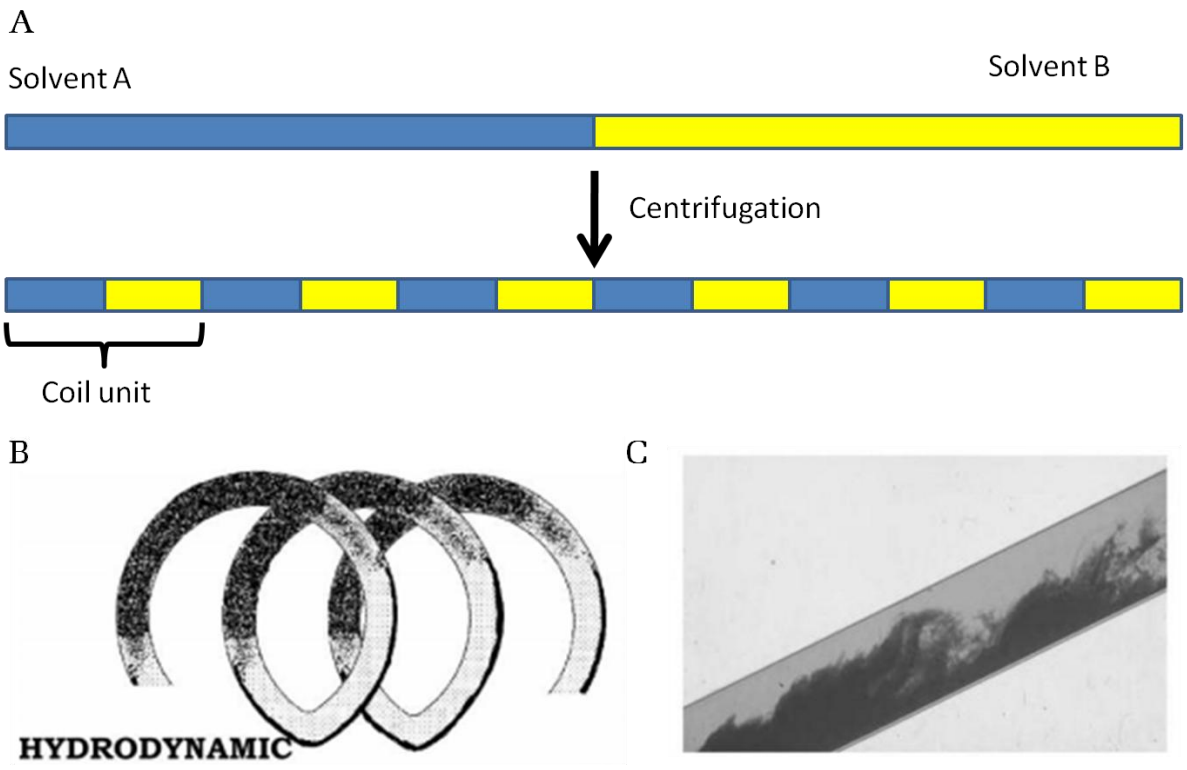

Figure 3.8 Separation of two phases inside the coil. (A) Following centrifugation, the distribution of two immiscible solvents within a single helical coil creates zones of each phases and an interchange phase. Solvent A is represented by blue, and solvent B by yellow. Diagram adopted from Figure 3-III in (Ito et al., 1966). (B) Within each of the coil units a hydrodynamic equilibrium system is created; (C) Rotation around a sun axis created turbulence which facilitates the mixing of two phases and improves matter transfer.

The bore is rotated around its own axis to create a centrifugal force of 80g that holds the stationary phase within. It is also spun around a sun axis to facilitate mixing of the two phases and maximise the contact surface area between them (Figure 3.9a and b). Every molecule or point of the column follows a cardioid trajectory (Figure 3.9c).

For a particle suspended within a rotating water-filled coil, regardless of its weight and density, the Archimedes screw action of the liquid will move it from the start of the coil - tail - to the end - head. In normal-phase CCC, the mobile phase is pumped head to tail, i.e. in the direction it is pushed to go. In reverse-phase CCC, the mobile phase is pumped from tail to head. The identity

of the stationary and the mobile phases can be switched if the coil is rotated in the opposite direction - or if the pump is connected the other end of the tube.

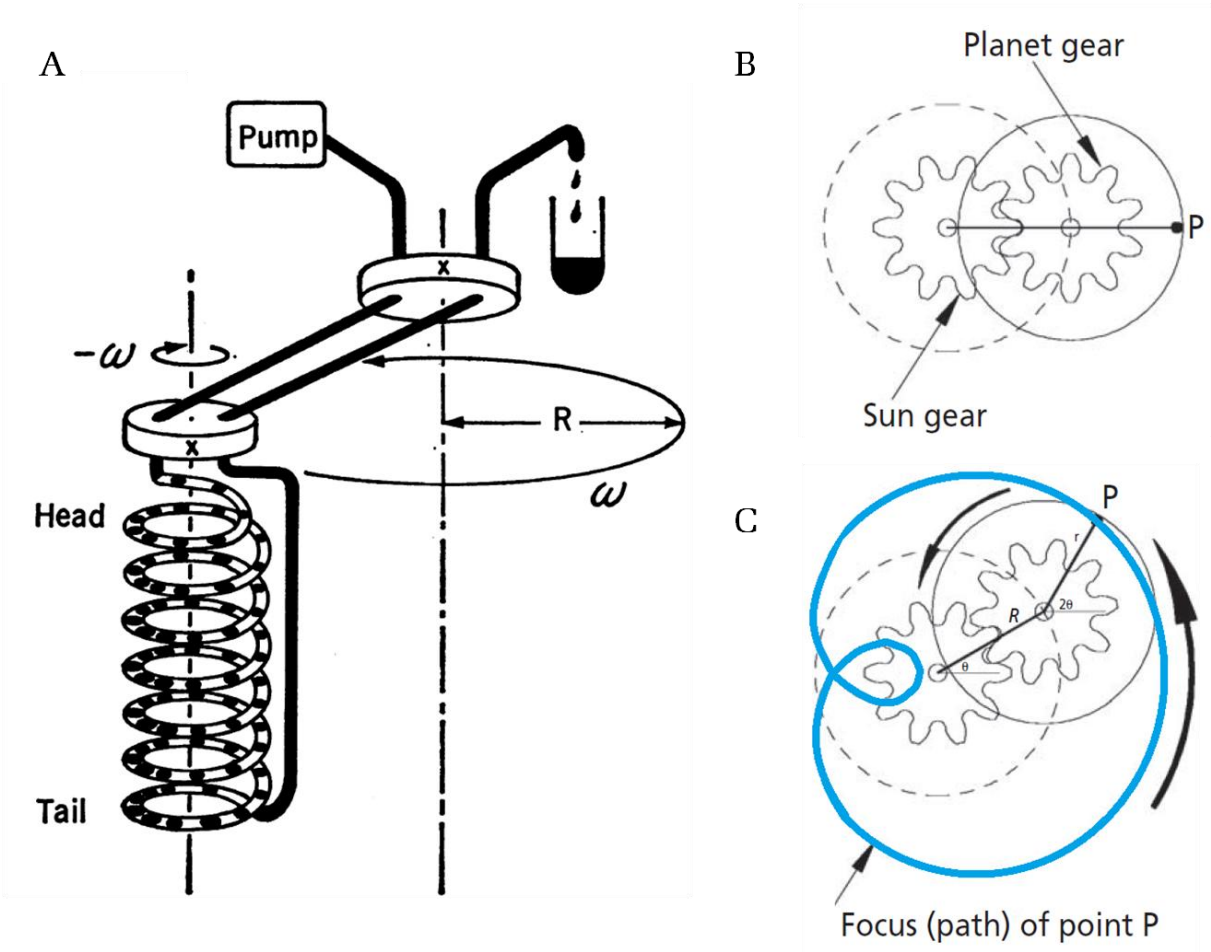

Figure 3.9 A coil planet centrifuge. (A) A helical tube is wound around a bore and filled with sample. The bore is then spun with centrifugal field applied perpendicularly to the axis. (B) It is also rotated around a sun axis, generating (C) a cardioid trajectory (blue) for any molecule suspended within the solvent. The mobile phase is continuously pumped through the coil, with fractions collected from the other end of the tube. Figure adopted from Figure 1A in (Ito and Bowman, 1971) and Figure 1 in (Garrard et al., 2008).

The heat generated by the fast rotation was the limiting factor overcome next by Dynamic Extractions Ltd in early 2000s. A High Performance CCC, HPCCC, capable of running at 240 g was developed. Modern machines, CCC centrifuges, are essentially the same, apart from using a long narrow-bore plastic tubing wound around a central bore. Columns of several thousand turns can be made if the narrow-bore tubing of less than 0.5 mm in inner diameter is wound tightly around the central bore. The sample re-dissolved in a small volume is

injected into the tube; its components are distributed according to their K_D. The total volume of solvents used is minor compared to HPLC techniques.

Compared to a traditional solid-liquid chromatography technique, such as HPLC, the ability to push out the stationary phase in CCC means that all the analysed compound can be recovered. There is no interaction with the solid support of a column that may cause denaturation or compound loss. The relative active mobile phase is essentially the same between HPLC and CCC, but (A) an HPLC system also contains a stagnant mobile phase as well as solid silica support, and (B) the relative active stationary phase in CCC is proportionately much greater than in HPLC, enabling larger samples to be analysed. Furthermore, in CCC both phases can be changed at will to improve efficiency and selectivity. In HPLC, the changes can only be made to the mobile phase.

3.2.3 Separation of aminoglycosides

In the original paper describing the discovery of gentamicin, only two components of the gentamicin C complex were separated by chromatography, gentamicins C1 and C2 (Weinstein et al., 1963). Chromatographic separation of three components of the gentamicin C complex, gentamicins C1a, C1, and C2, was achieved by TLC and column chromatography with a system made of chloroform, methanol, and 17% (v/v) ammonium hydroxide in a 2:1:1 ratio (Wagman et al., 1968). The same technique coupled with eluting from a TLC plate with 0.1 M potassium phosphate, pH 8.0, was used to separate and assess the bioactivity of the three components (Kantor and Selzer, 1968). A silica column with a chloroform, ammonia, and isopropyl alcohol system was used to obtain enough pure gentamicins C1a, C1, and C2 for mass spectrometry and NMR analysis, and their structures and the purpurosamine class of antibiotics were discovered (Cooper et al., 1971b, Cooper et al., 1971a). The gentamicins appeared as pale-yellow syrups or amorphous hygroscopic solids.

By varying the ratio of chloroform, methanol, 28% (v/v) ammonium hydroxide, and water up to 16 components of a *Micromonospora* fermentation were isolated (Maehr and Schaffner, 1967). Complete separation of gentamicins C1 and C2 was obtained using a 10:5:3:2 (v/v) ratio of the above. A cellulose

phosphate column could also be used with increasing concentrations of sodium chloride (from 2.0 to 2.2 M) to separate seven gentamicin components (Thomas and Tappin, 1974). A second component with a mass identical to gentamicin C2, gentamicin C2b, was isolated by this method.

Finally, Byrne *et al* isolated all five components of the C complex, including gentamicin C2a by using a Craig apparatus (Figure 3.10), the first counter-current chromatography machine (Byrne et al., 1977, Craig and Golumbic, 1945). The same solvent system of a 2:1:1 ratio of chloroform, methanol, and 17% (v/v) ammonium hydroxide was used, and gentamicin C complex could be separated from the co-produced polar intermediates. Additionally, counter-current chromatography with the same solvent system was used as a purification strategy for gentamicin C2a. Its identity as a 6'-*C* epimer of gentamicin C2 was confirmed in 1976 (Daniels and Marquez, 1976).

.

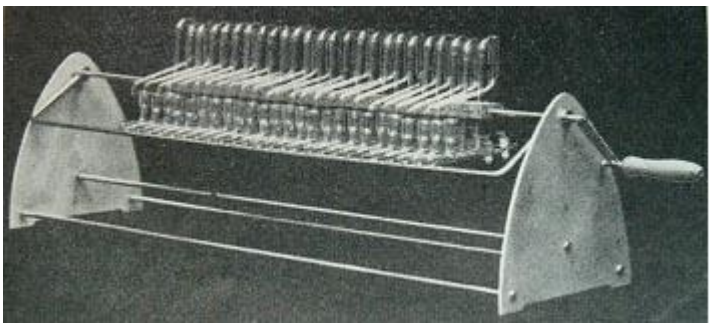

Figure 3.10 A Craig apparatus. A series of interconnected tubes on a rotating platform were used to mix two solvent phases. Natural compounds could be separated from a complex mixture based on their relative solubility in the two phases (Craig and Golumbic, 1945).

Counter-current chromatography has been used to separate antibiotics since their discovery. A counter-current system of solvents was used to purify the first true antibiotic, penicillin, by extracting it into amyl acetate and then back into water (Aldridge, 1999). As noted above, CCC was even used to separate gentamicins. Modern advances have made dynamic CCC into a fast and powerful technique for separation of difficult substances, such as gentamicin. To our

knowledge, the modern apparatus with a planetary centrifuge had not been used for gentamicin isolation prior to the work described here.

3.2.4 Dynamic counter-current chromatography for gentamicins

There are many advantages to using CCC for separation of compounds. As previously stated, this technique is particularly applicable to fragile and complex natural product mixtures, providing gentle and complete separation of components. The ability to change both the mobile and the stationary phases, as well as the pH, temperature, flow-rate, direction of flow, and applied g force, creates a versatile platform for a chromatography technique. Efficiency of the process can be improved by reducing the flow rate, decreasing the bore diameter, and increasing the tube length (Ito and Bowman, 1970). The risk of cross-contamination is very low as long as appropriate precautions are taken to maintain the system. Sample preparation is simple, as the compound just needs to be dissolved in the stationary phase. All the sample is recovered. As no expensive solid support is present, the sample may be dirty, viscous, or contain particulates. The experiments are easily upscaled, with relatively little solvent required for efficient separation of large quantities of sample (Sutherland et al., 2009). CCC can be used to compliment other chromatography techniques and, if a detector is linked to a fraction collector, the eluted fractions can be collected and analysed concurently for the presence of the desired compound.

3.2.4.1 Method

A DE Mini System with an 18.4 mL coil on a 0.8 mm bore was used for separation and purification of up to 400 mg of gentamicin compounds. The coil was placed for a head-to-tail (centre to periphery) run. To prepare the system, the chiller was turned on and the system was washed with 60 mL methanol at a flow rate of 10 mL/min. The sample loop (0.43 mL) and injection port were also washed with methanol. Temperature was set at 20˚C.

The coil is filled with the stationary phase. At the chosen flow rate, mobile phase is pumped through, at the expense of some - called displaced - stationary phase. The percentage of retained stationary phase at high g, and a specific flow rate and temperature, is another important parameter for the

success of the separation. The sample, dissolved in less than 5-10% of the stationary phase, is then injected into the coil, and eluted fractions of the mobile phase are collected and analysed.

Extrusion, or stationary phase, fractions can also be collected if the stationary phase is pumped through. These fractions normally contain compounds or contaminants with K_D approaching infinity.

3.2.4.2 Solvent system development

A CCC experiment begins with the development of a suitable solvent system. A small quantity of the desired compound is dissolved in equal volumes of the future stationary and mobile phases and the ratio of its concentrations provides an estimate of a K_D. A system with K_D of approximately 0.2 - 2.5 is ideal. The K_D of the contaminant or other substance of interest is equally important, as the greater the difference between the two, the better the separation of the compounds.

A successful CCC experiment depends largely on the difference between K_D values of the compounds to be separated. The K_D in turn depends on the two-phase solvent system, which is equivalent to choosing both the solid support and the solvent in HPLC. Development of a solvent system can occupy up to 90% of the total CCC operation time (Liu et al., 2015b).

Separation of compounds, for example components of the gentamicin C complex, rather than purification of a singular compound is the most complicated of the CCC methods, as it requires all the individual components to have K_D values near the sweet spot (0.5 - 5). Empirical solvent system selection is an iterative process, whereby systems are tested and adjusted until a desired K_D value is reached (Figure 3.11). There are many ways of developing a solvent system for a given compound.

Recent advances in generating novel ways of screening solvent systems involve a fully automated process, whereby the separation of compounds by different solvent systems in a classic HEAMWat (heptane, ethyl acetate, methanol, water) series is tested one after the other (Bradow et al., 2015). This

enabled a solvent system for all tested compounds to be found in under two hours.

Industrial preparation of gentamicin mono-components would benefit from this automated approach. However, initial testing was done to see if modern dynamic CCC could be used for small-to-medium scale separation.

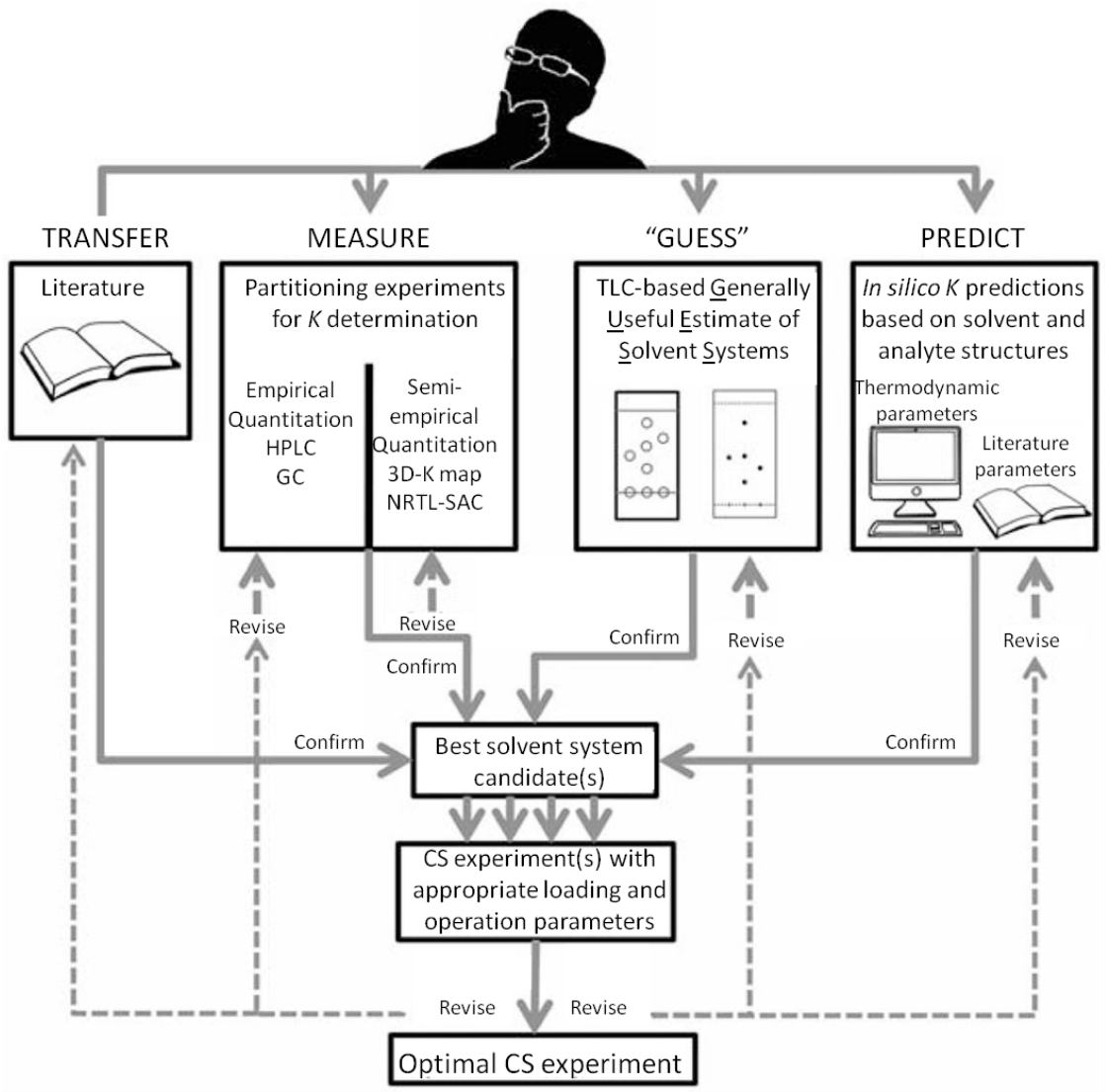

Figure 3.11 CCC solvent system development process. There are four main methods employed in the solvent system development for CCC. A previously-developed CCC solvent system can be transferred directly from the literature. Similarly, literature on similar compounds can be used to predict the solvent system. The solvent system can be tested on small scale by partitioning experiments, with various analytical methods used to analyse the data. Thin-layer chromatography (TLC) is another useful starting point, with single-phase TLC solvent system having to be converted to two-phase CCC system. Figure adapted from (Liu et al., 2015a, Liu et al., 2015b).

3.2.4.2.1 Solvent system for gentamicin C complex separation

Historically, thin-layer chromatography (TLC) was used for separation and identification of *Micromonospora* fermentation components. A solvent system for TLC, while normally consisting of both organic and inorganic solvents, is a single-phase system. The solvent system for CCC must consist of two immiscible phases, one of which will serve as the stationary phase, while the other acts as the mobile phase. Methanol can mix with both organic and inorganic solvents, and reducing the percentage of methanol in the system can allow it to go from a single phase to two phases.

For TLC, two main categories of solvent systems exist in literature. In the first category water is mixed with acetic acid, alcohol and either methanol or pyridine (Taniyama et al., 1972, Wagman and Weinstein, 1973, Ito et al., 1964). In the second category, water is mixed with ammonium hydroxide, methanol, and chloroform.

For separation of gentamicin C complex components, a solvent system from the literature was used (named "CCC Solvent system I"). The ratio of water, ammonium hydroxide, methanol, and chloroform was 1:1:2:4 respectively. The solvent system was prepared by mixing DI H_2O with chloroform, ammonia, and methanol (in this order) in a large separating funnel. The funnel was stoppered, shaken, and the air was released, 3 times. The solvent system was left to settle for a minimum of 10 minutes (or until the 2 phases were fully separate). The lower (CCC Solvent system I, lower phase: organic, chloroform-based, mobile phase) layer was collected into a 1 L glass bottle; the upper (CCC Solvent system I, upper phase: aqueous, water-based, stationary phase) layer was collected into a separate 1 L glass bottle.

The system was purged with CCC Solvent system I, upper phase at 10 mL/min for 5 minutes. The flow rate was reduced to 1 mL/min and the spinner was started (21000 RPM). Ten minutes later, the pump was stopped and the solvent was changed to CCC Solvent system I, lower phase. The exit tube was transferred to a 10-mL glass measuring cylinder. The pump was started at 1 mL/min. The volume of displaced stationary phase was measured and recorded.

The following equations were used to calculate the percentage of stationary and mobile phases in the system:

$$V_M = V_D - V_{ECV}$$

where V_M is volume of the mobile phase, V_D is displaced volume, and V_{ECV} is extra-column volume (= 1.5 mL);

$$\%S_f = \frac{V_M}{V_T} \times 100$$

where $\%S_f$ is the percentage of total volume that is stationary phase, V_M is volume of the mobile phase, V_T is total volume (= 18.4 mL);

$$\%M_f = 100 - \%S_f$$

where $\%M_f$ is the percentage of total volume that is mobile phase.

Commercially available gentamicin C complex solution (10 mg/mL; by PAA The Cell Culture Company) was lyophilised to 400 mg. The sample was dissolved in 400 µL of CCC Solvent system I, upper phase before it was slowly injected into the sample loop until a bubble could be observed in the tube just before. The injection valve was turned to load the sample. Fractions were collected using a fraction collector into glass HPLC vials. Seventy-two fractions of 2 mL each (144 mL in total) were collected at a flow rate of 2 mL/min. Extrusion fractions (twenty, 2 mL each) were also kept and contained other intermediates, such as G418 and JI-20B.

The system worked in isolating all five gentamicin C complex components in the main fractions, and more polar intermediates within the extrusion fractions. Analysis of fractions using HPLC-MS revealed that an ion with m/z = 500, corresponding to gentamicin C1 was present in fractions 21 to 31, four ions with m/z = 486 but different retention times, corresponding to gentamicins C2a, C2b, and C2, were present in fractions 35-39, 41-43, and 45-60 respectively. An ion with m/z = 472, corresponding to C1a, was present in fractions 73 to 81 (Figure 3.12). The order of gentamicin appearance in the fractions was the mirror image of an HPLC purification: gentamicin C1, C2a, C2b, C2, and C1a.

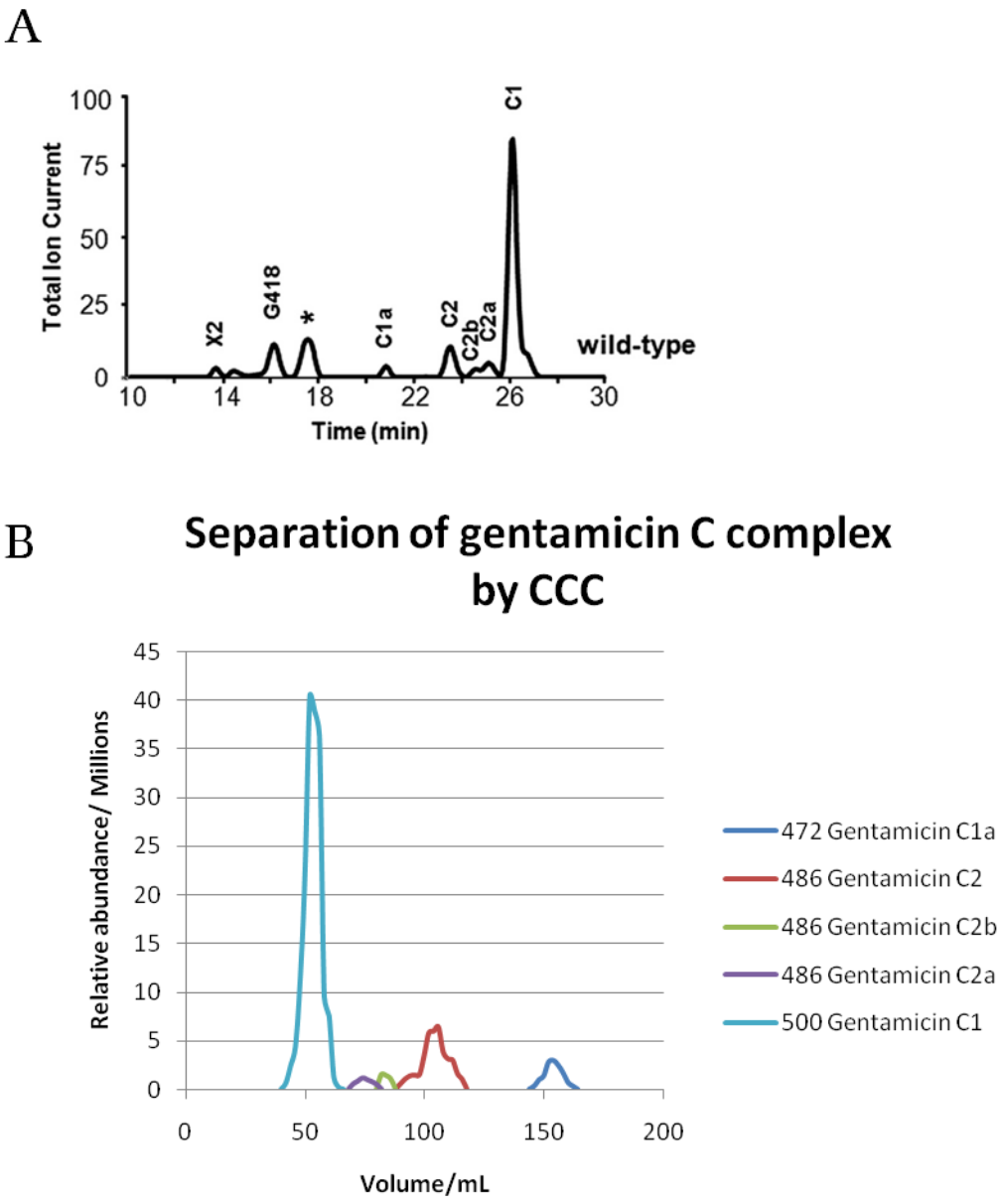

Figure 3.12 Separation of gentamicin C complex components. (A) HPLC can be used to resolve a gentamicin C complex mixture into individual components; (B) Fractions containing gentamicins separated by CCC were analysed for presence of C complex components using a HPLC-MS. Gentamicin C complex components were present in separate fractions.

3.2.4.2.2 Solvent system for JI-20b's and Pi-JI-20b separation

CCC was also used to separate Pi-JI-20b from JI-20b generated by incubating Δ*genB3 M. echinospora* extract with recombinant GenP phosphotransferase, and verdamicin and keto-verdamicin from the compounds isolated from Δ*genB4 M. echinospora*. For any gentamicin intermediate purification, the selection of the

solvent system was based on the K_D value of JI-20b. As this compound is more polar than the components of the gentamicin C complex due to the presence of two extra hydroxyl groups, more polar systems with a higher percentage of methanol were tested first.

Partitioning experiments, or shake flask experiments, were used to calculate the K_D values for a compound in each system. They rely on the fact that the distribution of the compound in the static equilibrium between two systems will be the same as that in the hydrodynamic equilibrium within the coil. Only compounds with different K_D values can be separated by a system.

To calculate the K_D, a range of different solvent systems (10 mL each) was prepared. The phase ratio and settling time of each system were measured after thorough mixing by vortexing. To the tube containing the target compound (1 mg), 1 mL of equilibrated upper and lower phases were added, and vortex mixed. A sample of each phase (6.44 µL) was taken out with a pipette and dried in a new tube. MQ H_2O (50 µL) was added to give a 200 µL solution. After 5 µL of each sample was analysed by mass spectrometry, the peak area of a compound in the upper phase was divided by a peak area of the same compound in the lower phase to obtain the distribution ratio, K_D. A distribution ratio of 1 would indicate that the compound was equally distributed between two phases, and only solvent systems which gave K_D of target compound between 0.4 and 2.5 were tested further.

The proportion of methanol to other components of the system (chloroform, ammonia, and water) was gradually increased (Table 3.3).

Table 3.3 Various solvent systems tested for intermediate purification

Solvent	System				
	I	II	III	IV	V
Methanol	2	3	7	15	5
Chloroform	4	4	8	16	4
Ammonia	1	1	2	4	1
Water	1	1	2	4	1
Calculated K_D of JI-20b	**0**	**56.4**	**4.6**	**1.4**	**∞**

System IV was initially used to separate JI-20b from Pi-JI-20b. However, most of the stationary phase was displaced, with only 15.8% of the total coil

volume remaining. This amount of the stationary phase was not enough for efficient separation. The high-methanol system was not retained within the coil under high gravitational force conditions.

System III was used next. More of the stationary phase was retained (5.9 mL, 32.1% of total volume). Sample (10 mg of Δ*genB3 M. echinospora* extract) was dissolved in 400 μL of upper (aqueous) phase. A 100-minute run, at 1mL/min, was started, 67 fractions of 1.5 mL each were collected. Extrusion fractions were also collected (21 in total).

Blotting of samples, and staining with ninhydrin revealed amino group-containing compounds in 49 fractions (fractions 17 to 65). By mass spectrometry all were confirmed to be JI-20b. Therefore, the peak of the compound is present in 73% of fractions. No JI-20b was detected in extrusion fractions.

After the K_D of a compound was found out, the retention time could be calculated by the following equation:

$$t_A = \frac{V_M + K_D V_S}{F} + \frac{V_{ECV}}{F}$$

where t_A is retention time, V_M is volume of the mobile phase, K_D is distribution ratio, V_S is volume of the stationary phase, F is flow rate, and V_{ECV} is extra-column volume (= 1.5 mL).

The calculated K_D for JI-20b (=4.6) was used to calculate the predicted retention time:

$$t_A = \frac{12.5 + 4.6 \times 5.9}{1} + \frac{1.5}{1} = 41.14\ min$$

which was the exact middle fraction containing JI-20b. However, the presence of it in most of the fractions made System III not viable for large scale purifications.

A reason for a wide peak could be the hydrogen bonding between methanol and JI-20b. To counteract this effect nine new solvent systems (solvent systems VI - XIV) were tested. Specifically, acetonitrile was used instead of methanol or water was substituted for a weak salt (ammonium sulphate and ammonium acetate) solution. The systems were tested for their settling time,

percentage of upper and lower phases, and K_D of JI-20b. Three systems - VII, VIII, and XI - were selected for further testing.

Table 3.4 Various solvent systems tested for intermediate purification

Solvent	System		
	VII	VIII	XI
5 mM Ammonium acetate	1	2	
Methanol	1	2	1
Chloroform	4	8	4
Ammonia	3	7	3
5 mM Ammonium sulphate			1
Average settling time/ s	**28**	**39**	**29**
Percentage of lower phase	**58.9**	**60.6**	**58.4**
Calculated K_D of JI-20b	**1.98**	**2.04**	**2.11**

System VII was tested first. Stationary phase was retained well (5.3 mL, 28.8% of total volume). Sample (26.2 mg of JI-20b and Pi-JI-20b) was dissolved in 400 µL of upper (aqueous) phase. A 100-minute run, at 1 mL/min, was started, 30 fractions of 1.5 mL each were collected. Extrusion fractions were also collected (20 in total, 2 mL each). Analysis of fractions revealed that JI-20b was present in collected fractions, whereas Pi-JI-20b, being more polar of the two due to its phospho group, was in the extrusion fractions (Figure 3.13). Therefore, System VII is a viable system for separation of JI-20b and Pi-JI-20b.

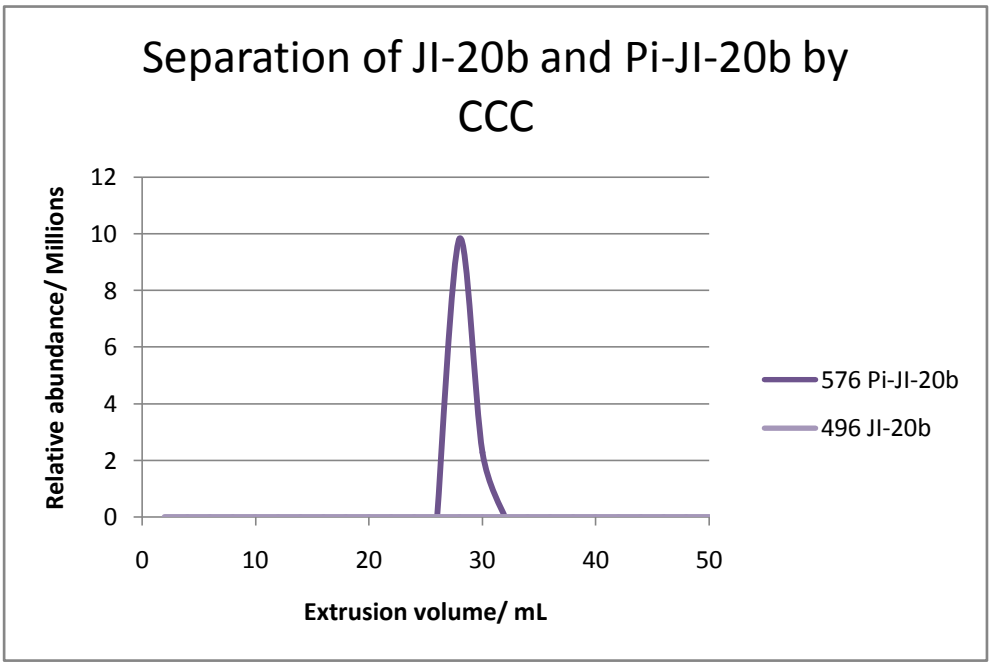

Figure 3.13 Separation of JI-20b and Pi-JI-20b by CCC. Pi-JI-20bwas only found in extrusion fractions as analysed by HPLC-MS, while all the JI-20b was found in elution fractions. The two compounds are completely separated by CCC with a solvent system containing 5 mM ammonium acetate.

Another sample consisting of a dried Δ*genB4 M. echinospora* extract (50 mg of verdamicin and keto-verdamicin) was dissolved in 400 μL of upper (aqueous) phase. A 100-minute run, at 1mL/min, was started, 40 fractions of 1.5 mL each were collected. Extrusion fractions were also collected (20 in total, 2 mL each). Analysis of fractions revealed that keto-verdamicin and verdamicin were not separated fully, although enriched fractions existed (Figure 3.14). Therefore, System VII needs further work to be a viable system for separation of verdamicin and keto-verdamicin. Interestingly, a small amount of a verdamicin with a different retention time, possibly a 6' epimer of verdamicin, was also detected.

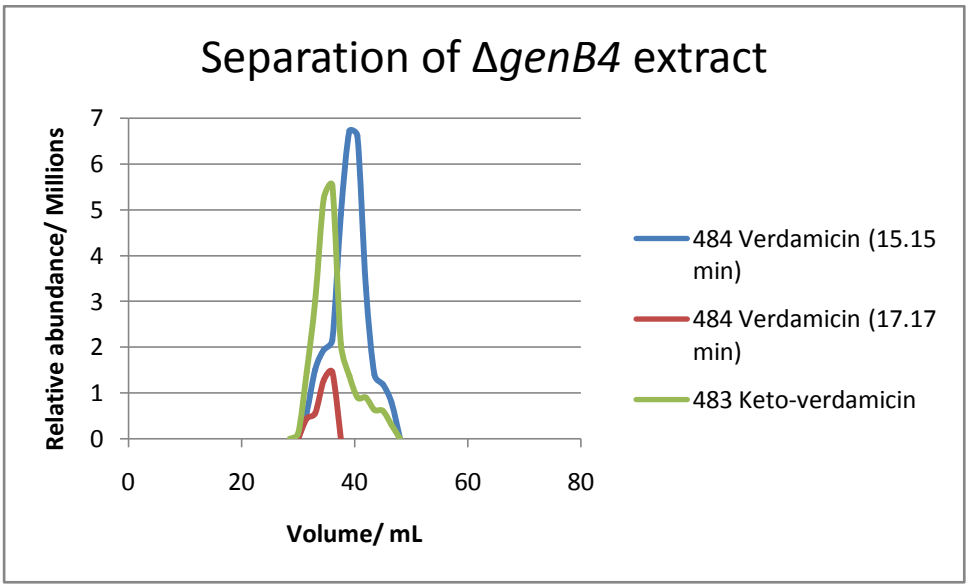

Figure 3.14 Separation of Δ*genB4 M. echinospora* extract components. Fraction were created by CCC and analysed by HPLC-MS. Three verdamicin components were identified by their retention time and *m/z* but not separated by the Solvent System VII.

3.2.4.3 Summary of CCC conditions and outcomes

The systems for separating gentamicin C complex components or for separating JI-20b are described in Table 3.5.

Table 3.5 CCC Buffer systems

Buffer	Application	Chemical Composition
CCC Solvent system I, lower phase	CCC, gentamicin C complex	Lower phase of solvent system I, consisting of 1 part water, 1 part ammonia, 4 parts chloroform, and 2 parts methanol
CCC Solvent system I, upper phase	CCC, gentamicin C complex	Upper phase of solvent system I, consisting of 1 part water, 1 part ammonia, 4 parts chloroform, and 2 parts methanol
CCC Solvent system VII, lower phase	CCC, gentamicin C intermediates	Lower phase of solvent system VII, consisting of 1 part 5 mM ammonium sulfate solution, 1 part ammonia, 4 parts chloroform, and 3 parts methanol
CCC Solvent system VII, upper phase	CCC, gentamicin intermediates	Upper phase of solvent system VII, consisting of 1 part 5 mM ammonium sulfate solution, 1 part ammonia, 4 parts chloroform, and 3 parts methanol

3.2.4.4 Fraction analysis

3.2.4.4.1 Fraction analysis by blotting and staining with ninhydrin

The fractions were kept in the fume-hood to allow ammonia, chloroform, and methanol evaporation. The dried samples were resuspended in 50 or 100 µL of MQ H_2O. Each fraction (5 µL) was pipetted and dried on Whatman #1 filter paper. The filter paper was dipped into ninhydrin solution and dried in the fume hood (Moore, 1968). A heat gun was then used to heat the paper to develop colour in samples with primary amines via the following reaction:

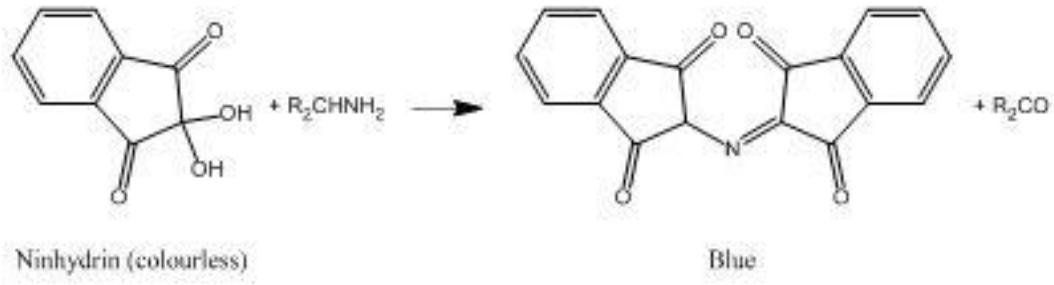

Figure 3.15 Reaction of ninhydrin stain with primary amino groups. On heating of ninhydrin chemical with a compound containing a primary amino group, a dimerization of ninhydrin molecule occurs and leads to a colour change.

3.2.4.4.2 Fraction analysis by mass spectrometry

Fractions exhibiting a strong colour after ninhydrin staining were analysed by mass spectrometry. The dried sample was re-dissolved in MQ H_2O. The sample (5-10 µL of 0.2 mM solution in MQ H_2O) was run on a C18 column as previously described in Section 2.4.4.2.

3.2.4.4.3 Analysis by Nuclear Magnetic Resonance

For gentamicins C2 and C2a, all 10 mg of commercial sample was dissolved in 200 µL of MQ H_2O. A portion (40 µL, 2 mg) was transferred to a new tube and dried. The compounds were then re-dissolved in 650 µL of D_2O, moved to an NMR tube, and submitted to the Department of Chemistry's Nuclear Magnetic Resonance (NMR) service for analysis. An 800 MHz spectrometer was used to

perform ^{1}H, ^{13}C, COSY, NOESY, and HSQC analyses. For the Pi-JI-20b sample, ^{1}H, COSY, ^{31}P, ^{1}H-^{31}P analyses were performed.

TopSpin software was used to visualize and analyse the data. Molecular mechanics minimizations to determine the absolute conformation of gentamicins was performed by Dr Finian Leeper using ChemDraw software. The stereochemistry of gentamicins C2a and C2 was confirmed, which is consistent with the literature (Byrne et al., 1977, Gu et al., 2015). The NMR results of Pi-JI-20b are discussed in Chapter 4.

4

Di-dehydroxylation: Phosphorylation by GenP

4.1 Dehydroxylation in aminoglycoside antibiotics

Clinical application of antibiotics is undermined by the fast emergence of resistance in pathogens (Davies and Davies, 2010). Resistance to aminoglycosides most often happens through an emergence of an antibiotic inactivating enzyme: acetylating (AAC), nucleotidylating (ANT), and phosphorylating (APH) enzymes. These enzymes attack specific sites on the aminoglycoside molecule, adding chemical groups to prevent efficient binding of the antibiotic to the ribosome (Figure 4.1).

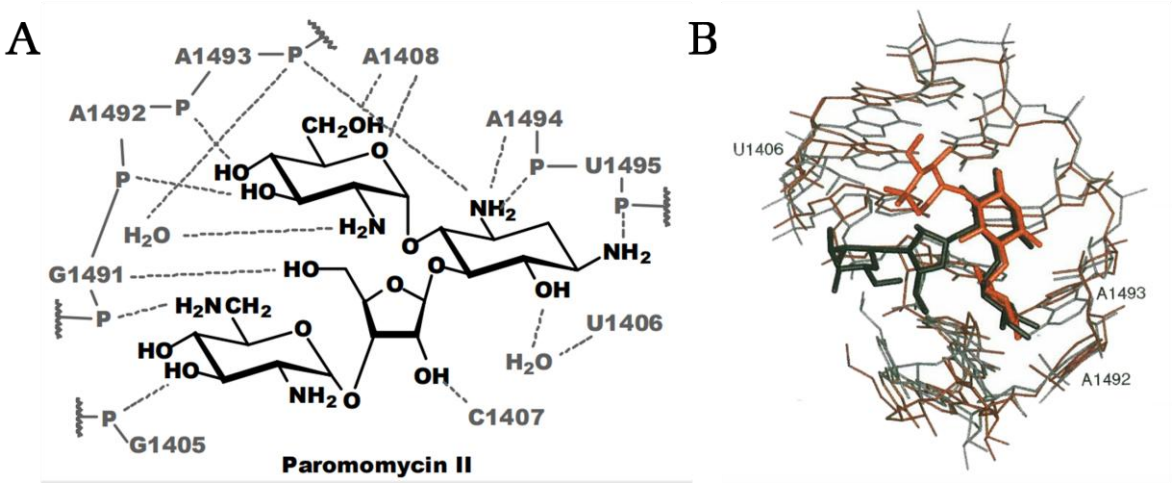

Figure 4.1 Interactions of aminoglycoside and the A-site of the ribosome. (A) The two hydroxyl groups on the top ring of paromomycin form bonds to the peptide bonds before residues A1492 and A1493 within helix 44 of 16S rRNA. Phosphorylation of the 3' hydroxyl and adenylation of the 4' hydroxyl group lead to inactivation of the antibiotic. Figure adapted from Figure 1.7 of (Mandt, 2008); (B) NMR spectroscopy was used to create this model of the binding of paromomycin (black) and gentamicin C1a (red) to A-site of ribosome. The top two rings bind in nearly identical manner and induce the same conformation change in the RNA. Figure adapted from Figure 5 in (Lynch et al., 2000).

Two of these modification sites are 3' and 4' hydroxyl groups, which are phosphorylated and adenylated respectively. Based on the susceptibility of an aminoglycoside to these two methods of inactivation, the antibiotics can be divided into three classes: fully susceptible, where both hydroxyl groups are present, aminoglycosides susceptible to adenylation of the 4' hydroxyl group only, and resistant, where both of the hydroxyl groups are removed (Figure 4.2). Kanamycin, butirosin, and neomycin have both 3' and 4' hydroxyl groups. Apramycin, lividomycin, and tobramycin lack the 3' hydroxyl group. And fortimicin, sisomicin, verdamicin, and gentamicin lack both hydroxyl groups.

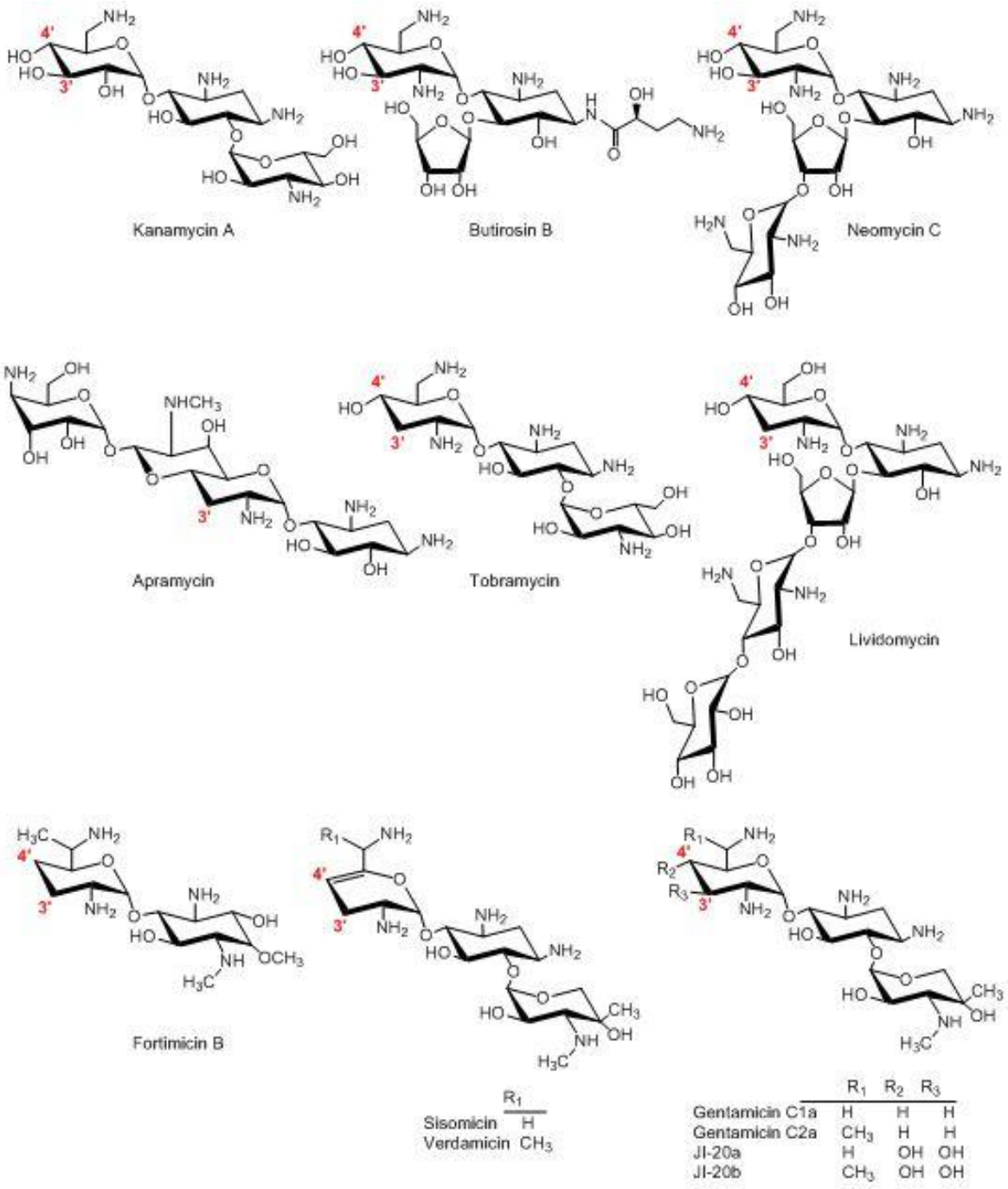

Figure 4.2 Aminoglycoside antibiotics. Presence or absence of hydroxyl groups at 3' and 4' positions (in red) can be used to divide the aminoglycoside antibiotics.

Dehydroxylation as a replacement of a hydroxyl group with a hydrogen is a common strategy for aminoglycoside antibiotic modification during biosynthesis. As such, the dehydroxylation reaction often happens during the late steps of an antibiotic's biosynthesis. Understanding the mechanism of dehydroxylation reactions can lead to a greater variety of aminoglycoside antibiotics, with in-built protection against two of the more common resistance

mechanisms. To date, only apramycin biosynthesis possesses a detailed explanation of the dehydroxylation reaction. This and the following two chapters describe the di-dehydroxylation reaction in the gentamicin biosynthetic pathway.

4.1.1 Apramycin, tobramycin, and lividomycin

Apramycin and tobramycin are both produced by *Streptomyces tenebrarius*, and both lack the 3' hydroxyl group. Recently the mechanism of dehydroxylation in the apramycin biosynthetic pathway has been described in detail (Kim et al., 2016, Lv et al., 2016). The biochemistry of the deoxygenation at the 3' position was novel and unusual (Figure 4.3). AprD4 was described as a radical SAM-dependent dehydratase, possessing an unusual CX_3CX_3C motif for binding of a [4Fe-4S] cluster; AprD3 was shown to be a NADPH-dependent reductase acting on a 4'-oxo intermediate, 3'-deoxy-4'-oxoparomamine.

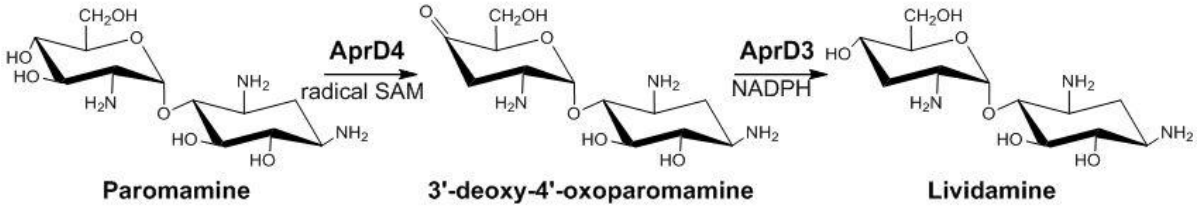

Figure 4.3 Deoxygenation in apramycin biosynthesis. AprD4 (a Fe-S oxidoreductase) and AprD3 (dehydrogenase) catalyse the removal of a hydroxyl group at 3' of paromamine.

AprD3 and AprD4 were identified as the possible catalysts of the deoxygenation reaction by a bioinformatics analysis of the *apr* cluster (Kudo and Eguchi, 2009). Deletion of *aprD3* and *aprD4* in *S. tenebrarius* resulted in loss of both deoxygenated apramycin and tobramycin (Ni et al., 2011). Their cloning into a kanamycin-producing strain resulted in production of 3'-deoxykanamycins, confirming their roles (Park et al., 2011).

Tobramycin is also produced by *Streptomyces tenebrarius*, alongside apramycin. The *tob* cluster possesses no *aprD3* and *aprD4* homologous. However, disruption of these genes in the apramycin cluster stops production of tobramycin, too, leading to the conclusion that AprD4 and AprD3 also catalyse deoxygenation of tobramycin (Ni et al., 2011). The lividomycin cluster of

Streptomyces lincolnensis contains *aprD3* and *aprD4* homologues, *livW* and *livY* respectively (Kudo and Eguchi, 2009). Although no work could be found that confirmed this, the deoxygenation of lividomycin probably happens via the same mechanism as apramycin, using LivW and LivY.

4.1.2 Fortimicin, sisomicin, and gentamicin

Both of the hydroxyl groups from 3' and 4' positions are removed in the fortimicin, sisomicin, verdamicin, and gentamicin biosynthetic pathways. Homologous enzymes often catalyse similar reactions in different biosynthetic pathways. As dehydroxylation is well defined in the apramycin pathway, homologues of the proteins involved were searched for. The search for *aprD4* and *aprD3* homologues within the available clusters (*for, sis,* and *gen*) revealed that only the *sis* and *gen* clusters possess an *aprD3* homologue (Kudo and Eguchi, 2009). Both of these homologues were 60% identical to *aprD3* by PSI-BLAST (Sequence ID: SCL15227.1 and AGB13917.1). The *aprD3*-homologous reductase gene in the *gen* cluster was *genD3.* The lack of an *aprD4* orthologue in the *gen* cluster suggests that either an enzyme is present elsewhere in the genome or a different mechanism of deoxygenation is used. The latter would also explain why both hydroxyl groups are removed. A Δ*genD3 M. echinospora* mutant prepared by Dr Chuan Huang in Wuhan still produced all the gentamicin C complex components, proving that a different mechanism was in use.

The first suggestions for the mechanism of di-dehydroxylation reaction *in vivo* came from a paper describing fortimicin (Dairi et al., 1992). Fortimicin is produced by *M. olivasterospora*, and at least a part of the *gen* cluster has evolved from the *for* cluster, and shares high gene sequence similarity with it. The purpurosamine rings of gentamicin C2a and fortimicin are identical, both lacking 3' and 4' hydroxyl groups. The genes encoding the enzymatic machinery for the di-dehydroxylation reaction should be highly similar between the two clusters.

An Δ*fms8* mutant of *M. olivasterospora*, AN38-1, produces compounds with 3' and 4' hydroxyl groups only, proving that the encoded protein, ForP, is involved in the di-dehydroxylation step (Hasegawa, 1991). In their paper, Dairi *et al* show that the mutant can be complemented by the neomycin phosphotransferase (APH (3')II type) gene, *nmrA*. They further show that the di-

hydroxylated fortimicin substrate of ForP, fortimicin KK1, is depleted *in vitro* in an ATP-dependent manner (Dairi et al., 1992). This shows that di-dehydroxylation in fortimicin happens through an initial ATP-dependent activation by phosphorylation of a hydroxyl group (Dairi et al., 1992). An *fms8* gene encoding an ATP-dependent phosphotransferase ForP was located in the *for* cluster (Figure 4.4).

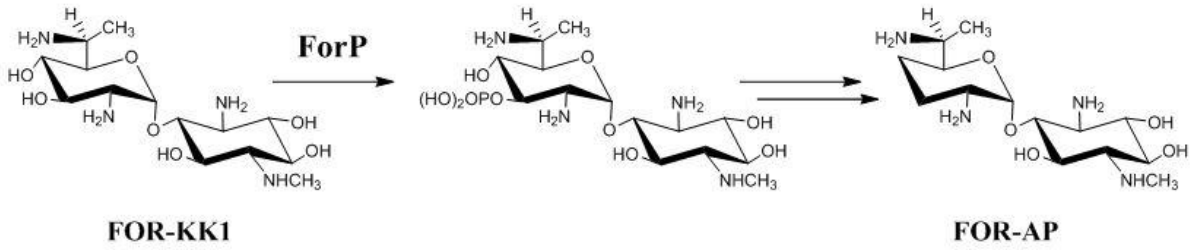

Figure 4.4 Reaction catalysed by ForP phosphotransferase. A deletion mutant of ForP gene, *fms8*, does not produce di-dehydroxylated compounds, showing that the action of ForP is essential for this step.

4.2 Phosphorylation in gentamicin

A search for *fms8* homologues in *gen* and *sis* clusters revealed *genP/gntI* and *sis17/gtc17* respectively (Figure 4.5, Table 4.1). Both were predicted to be ATP-dependent phosphotransferases. The search also showed a great number of highly similar genes present in resistant pathogens. However, alignment of the sequences of various 3' phosphotransferase enzymes by Shao *et al* predicted that GenP, Sis17, and ForP belong to a novel group of their own, which is specific for aminoglycoside biosynthesis pathways (Shao et al., 2013).

A

```
ForP       MFPPSRPPAALAGRLRLDGAWTHVASRSYGTVIHRVDGRRHAFYVKTTPPRRDNDLRFHP 60
GenP       ---MVAAPIPVAGWGDKDDPWECLGERSSGATVYRV-GEVPSFYVKTTPPRHPDDHRFNP 56
Sis17      ---MVAAPIPVAGWGDKDDPWECLGERSSGATVYRV-GEGPSFYVKTTPPRHPDDHRFNP 56
                  *  :**    *. *  :..** *:.::** *.  :*********: :* **:*

ForP       GSEAERLQWLAARGFPVAEVVDVGGDDELMWLVTTAVEGRSAAGPWATHERPVVLDVVAD 120
GenP       TKEAERLRWLAAQGLPVPEVVALDANDELAWVVTRALPGRPAARHWKPEERWRVIDVVAD 116
Sis17      TKEAERLRWLAAQGLPVPEVVALDANDELAWVVTRALPGRPAARHWKPEERWRVIDVVAD 116
            .*****:****:*:** *** :..:*** *:** *: ** **  *  .**  *:*****

ForP       VVRALHELPLTDCPFDRTLAVTLPLARLAAEMGWIDLDDLDPQHRGWSARQLLDELTATP 180
GenP       VARTLHALPVAECPFERRLADLIHQASSSMALGALDLDDVDPSHEGWTAQQLWDELSKMT 176
Sis17      VARTLHALPVAECPFERRLADLIHQASSSMALGALDLDDVDPSHEGWTAQQLWDELSKMT 176
           *.*:** **:::***:* **  :  *  :  :* :****:**.*.**:*:** ***:

ForP       PPAVEDLVVCHGDPCLDNFLVAPDTLALTGILDVGRLGAADRWKDLAIAVRDVTEQCADE 240
GenP       PPAEDDLVVCHGDFCLDNVLVDPETLTLAGILDVDRAGVSDRWMDLALALYNIGQD--DV 234
Sis17      PPAEDDLVVCHGDFCLDNVLVDPETLTLAGVLDVDRAGVSDRWMDLALALYNIGQD--DV 234
           *** :******** ****.** *:**:*:*:***.* *.:*** ***:*: :: ::  *

ForP       GDEGQAAAARFLARYGARPDAGKDRFYRLLDEFV   274
GenP       WGYGPPHAEHFLRRYGITVDQHKLTYIQLLDEFL   268
Sis17      WGYGPPHAEHFLRRYGISVNQHKLTYIQLLDEFL   268
            . *   * :** ***   :  *  : :*****:
```

B

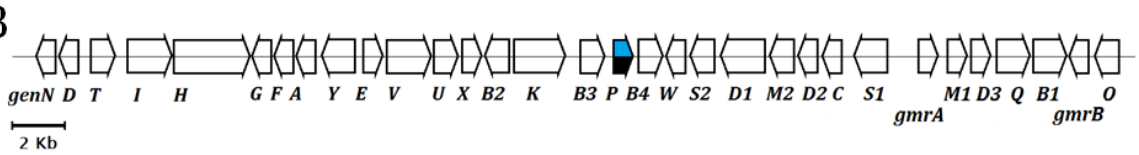

Figure 4.5 Homologues of *fms8:sis17* and *genP.* (A) Homologues of ForP protein were identified using BLAST. Their sequences were aligned using Clustal Omega program. High identity was observed. The purple box shows a conserved VCHgDFCLDNVLV active-site motif of a kinase protein (tyrosine class) in all the sequences.
An * (asterisk) indicates a fully conserved residue, a : (colon) indicates groups with similar properties, a . (period) indicates weakly similar groups.
(B) Only one candidate for an *fms8* equivalent was found within each cluster. For the *gen* cluster, it was *genP* (blue).

Using PSI-BLAST to analyse the gentamicin genes, *genP* gene was 52% identical to *fms8* (Table 4.1).

Table 4.1 Phosphotransferases in the *for*, *gen*, and *sis* clusters.

Protein	Organism	Antibiotic product	Accession number	Identity to GenP protein sequence
Fms8	*M. olivasterospora*	Fortimicin	CAF31545.1	52%
GenP	*M. echinospora*	Gentamicin	AAR98555.1	100%
Gtc17	*M. inyoensis*	Sisomicin	ACJ046351	99%

4.2.1 Δ*genP M. echinospora*

Deletion of *genP* resulted in accumulation of JI-20a and JI-20b, 3',4'-dihydroxy-gentamicin C1a and C2 respectively (Figure 4.6). This confirmed the role of GenP in the di-dehydroxylation of gentamicin. GenP is highly similar to aminoglycoside antibiotic resistance genes and may be involved in self-resistance of *M. echinospora*, as indicated by the large drop in the total yield of gentamicins from *M. echinospora* Δ*genP*. More of JI-20b was produced, accounting for about 80% of the total antibiotics purified from a Δ*genP* mutant of *M. echinospora*.

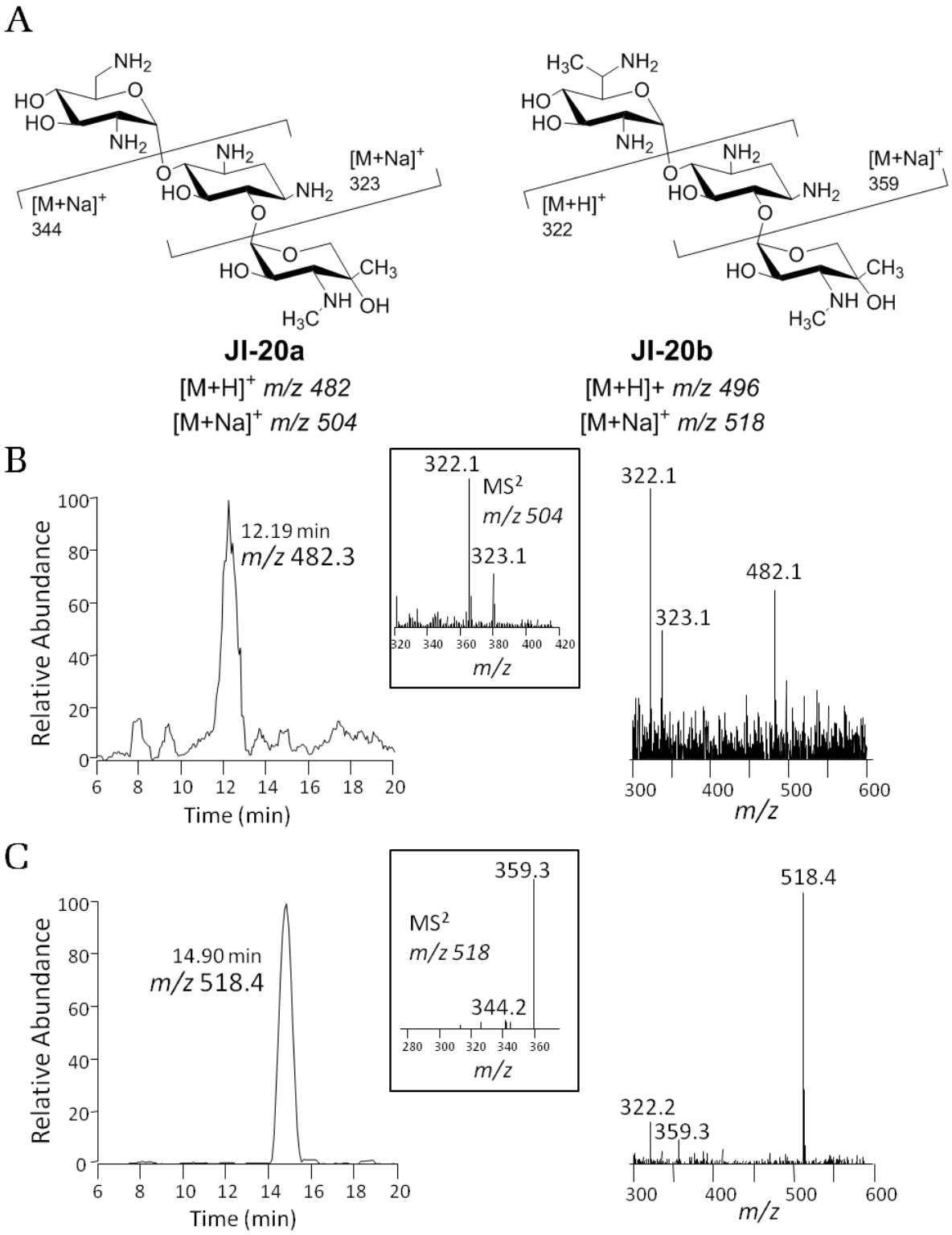

Figure 4.6 Products of Δ*genP* mutant of *M. echinospora*. *M. echinospora* Δ*genP* primarily produces JI-20a and JI-20b, gentamicin intermediates with 3' and 4' hydroxyl groups. No dehydroxylated products were detected. (A) Fragmentation patterns of JI-20a and JI-20b; (B) LC-MS chromatogram showing selected ion monitoring of JI-20a (left), MS:MS ion fragments of the JI-20a peak (middle, *m/z* 320 to 420), and ion spectrum [*m/z* 300 to 600] of the selected peak. (C) Data for JI-20b.

4.2.2 Phosphorylation by GenP as a resistance mechanism

In addition to being the catalyst for the first step of di-dehydroxylation of JI-20a and JI-20b, GenP may act as another method of self-resistance for *M. echinospora*. In *in vitro* assays GenP was shown to be able to phosphorylate a variety of gentamicin intermediates and other aminoglycoside substrates with 3' hydroxyl groups: G418, gentamicin X2, and kanamycins A and B. Interestingly, tobramycin which only has a 4' hydroxyl group was not accepted as a substrate. Introduction of a *genP*-containing plasmid into *E. coli* cells gave the cells the ability to grow on agar containing either kanamycin or the gentamicin intermediate G418, which have both 3' and4' hydroxyl groups.

In another experiment, recombinant GenP was incubated with G418 or JI-20b in the presence of ATP and $MgCl_2$ at 30˚C overnight. Filter paper disks were soaked with 10 µL of the substrate (G418 or JI-20b) or 10 µL of product (Pi-G418 or Pi-JI-20b) of the GenP reaction. The concentrations of antibiotics were the same (0.2 mM). *Bacillus subtilis* culture (100 µL of actively growing cells) was spread on the LB plate, and the disks were placed on top. The cells were grown overnight at 37˚C (Figure 4.7). Phosphorylated aminoglycosides could not inhibit the growth of *B. subtilis,* whereas G418 and JI-20b created a clear cell-free halo around the disks. GenP had no activity-inhibiting effect on the gentamicin C complex, which does not possess the hydroxyl group.

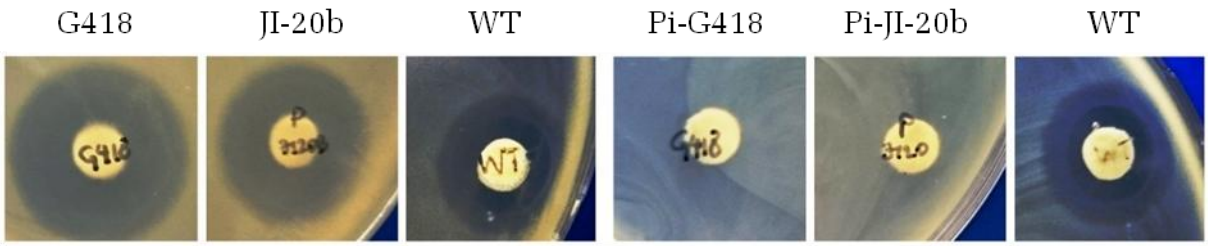

Figure 4.7 Inhibition assay with GenP. Left: growth of *Bacillus subtilis* on LB plates is inhibited by gentamicin precursors G418 and JI-20b, and gentamicin C complex (WT). Right: *B. subtilis* cells are capable of growing on areas containing phosphorylated (*in vitro* by GenP) gentamicin intermediates, Pi-G418 and Pi-JI-20b. GenP has no effect on antibacterial properties of gentamicin C complex (WT). The paper disks contain 10 µL of 0.2 mM solution of antibiotics.

4.2.3 Phosphorylation by GenP as a catalytic activation mechanism

A paper characterising GenP was published in 2013 by Shao *et al.* Due to the difficulty in obtaining pure gentamicin intermediates, the group used closely-related aminoglycosides, kanamycin, neomycin, and amikacin, as substrates (Shao et al., 2013). They further used these substrates to interrogate the kinetic parameters, finding K_M to be around 14 μM and k_{cat} to be around 0.12 s^{-1}. NMR analyses of the obtained phosphorylated aminoglycosides showed that a single phospho group was present at the 3' position. The ability of GenP to accept a wide range of substrates also showed its function as a broad-spectrum aminoglycoside phospho-transferase.

As the Δ*genP* mutant accumulates primarily JI-20 complex, consisting of JI-20a and its 6'-*C*-methylated counterpart from the other branch, JI-20b, and both are direct 3',4'-dihydroxylated precursors of gentamicin C1a and C2a respectively, they are presumed to be the native substrates of GenP. To determine the activity of GenP on JI-20a and JI-20b the gene was cloned into pET-28a (+), transformed into BLR *E. coli*, and over-expressed and purified as described in Chapter 2 (Figure 4.8).

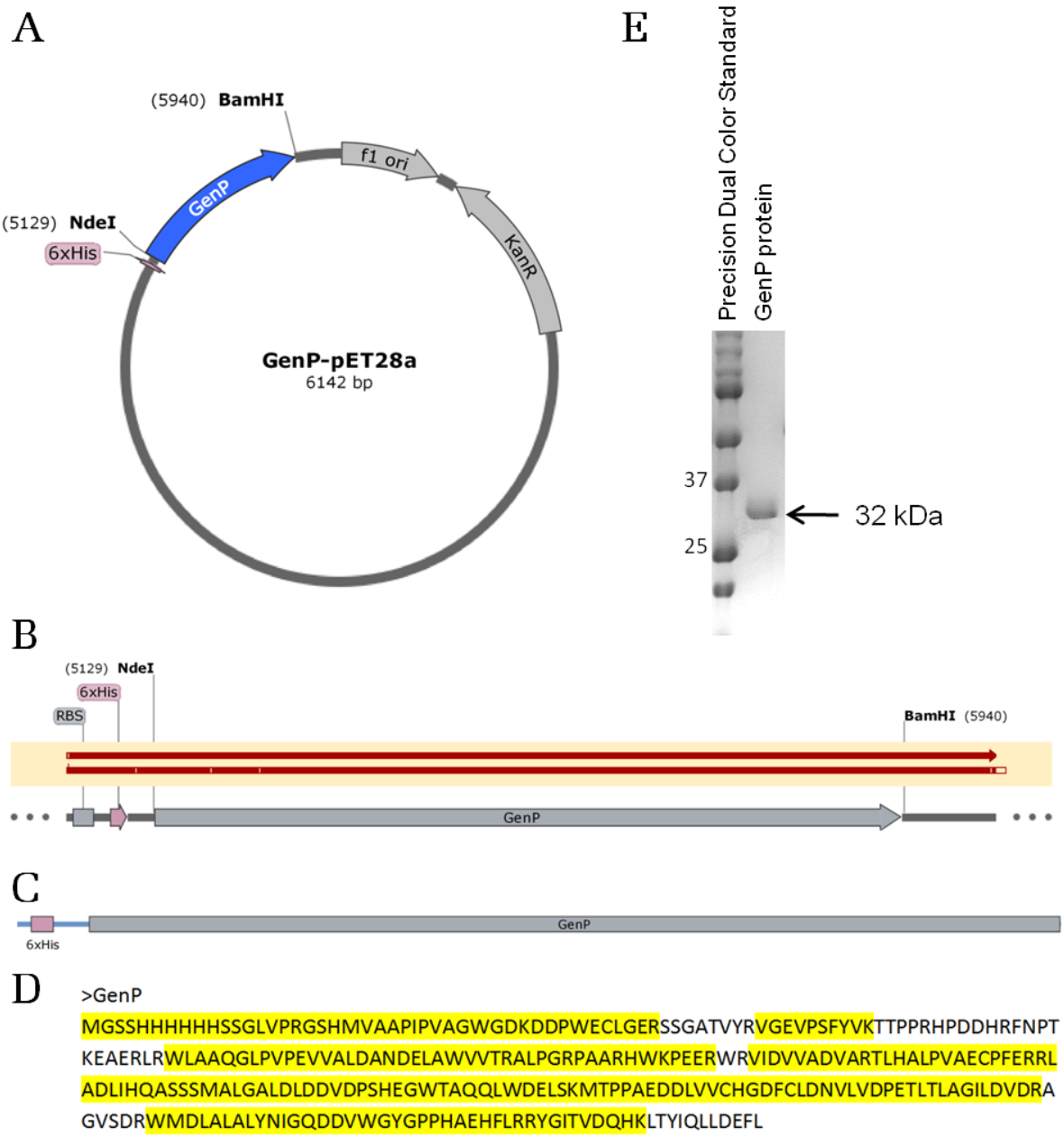

Figure 4.8 GenP protein profile. (A) *genP*-pET-28a (+) vector map; (B) confirmation of *genP* sequence by DNA sequencing with T7 and T7t primers; (C) GenP protein map; (D) MALDI fingerprinting analysis showing detected protein fragments in yellow; (E) SDS-PAGE gel of recombinant GenP purified by Ni^{2+} affinity chromatography.

Both JI-20a and JI-20b were successfully phosphorylated by GenP in the presence of ATP and magnesium ions (Figures 4.10 and 4.11). The average conversion was above 80%.

A larger scale reaction produced enough Pi-JI-20b compound for NMR analysis. The phosphorylated and un-phosphorylated JI-20b were separated using CCC as previously described. NMR (^{1}H, COSY, ^{31}P, ^{1}H-^{31}P) was performed.

A single phosphorus signal (chemical shift = δ = 4.48 ppm) was detected, and this signal was coupled to a proton at δ = 4.07 ppm. Analysis of the COSY spectrum using TopSpin software showed that the proton at 4.07 ppm coupled to two other protons at 2.875 ppm and 3.5 ppm (Figure 4.9).

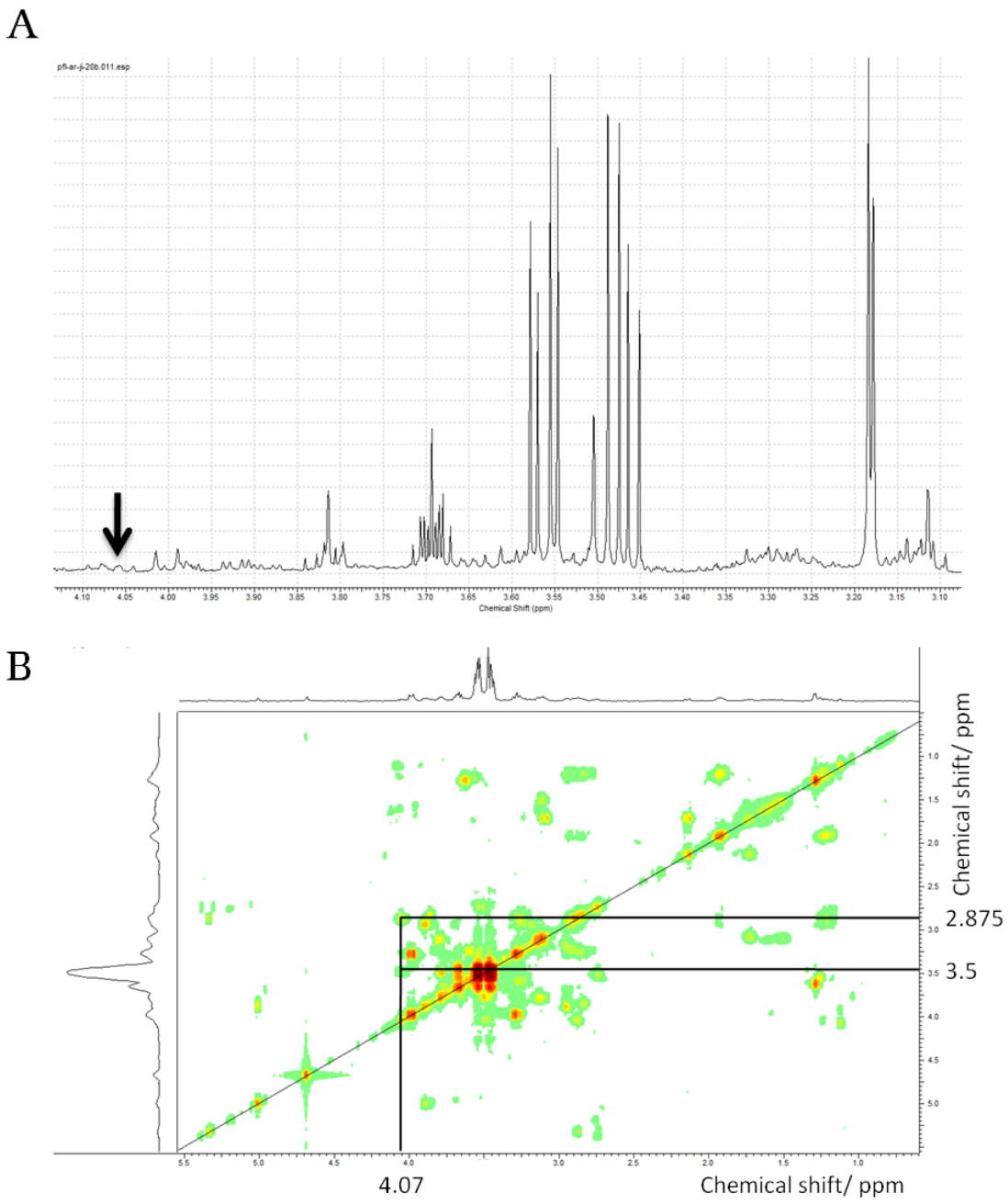

Figure 4.9 NMR spectra of Pi-JI-20b. (A) ^{1}H and (B) COSY spectra of Pi-JI-20b define the position of the phospho group to the 3'. (A) Black arrow indicates the signal (4.07 ppm) of the only proton linked to the phosphorus signal (not shown). (B) COSY identifies two coupled protons at 2.875 ppm and 3.5 ppm. As the chemical shifts of these protons are not the same, a 3' position is proposed for the phospho group.

Figure 4.10 shows the proposed structure of Pi-JI-20b. If the phospho group was at the 4' position, the proton coupled to phosphorus would in turn be coupled to protons at the 3' and 5' positions, both of which are next to oxygens. The expected chemical shift would be around 3.5 ppm. If the phospho group was at the 3' position, the proton coupled to the phosphorus would in turn be coupled to protons at the 2' and 4' protons. The proton at the 4' would still be next to oxygen and have a chemical shift of 3.5. The proton at 2' position, however, would be next to an amine. The expected chemical shift for it would be 3.0.

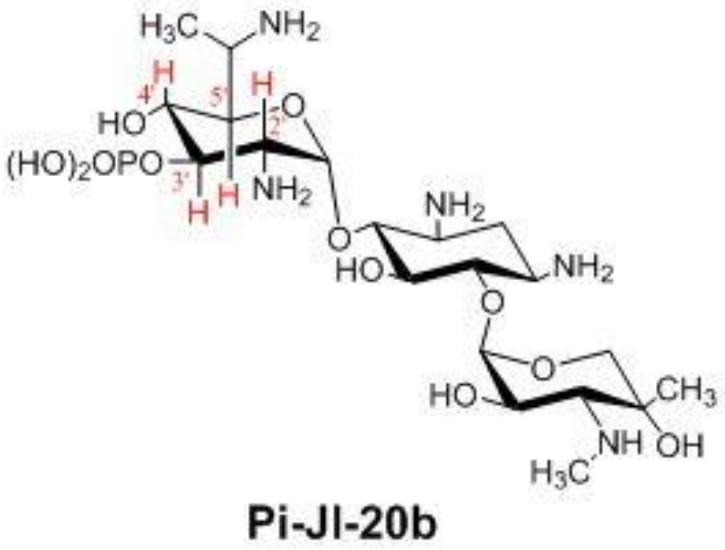

Figure 4.10 Pi-JI-20b structure. The phosphate group was determined to be at the 3' position.

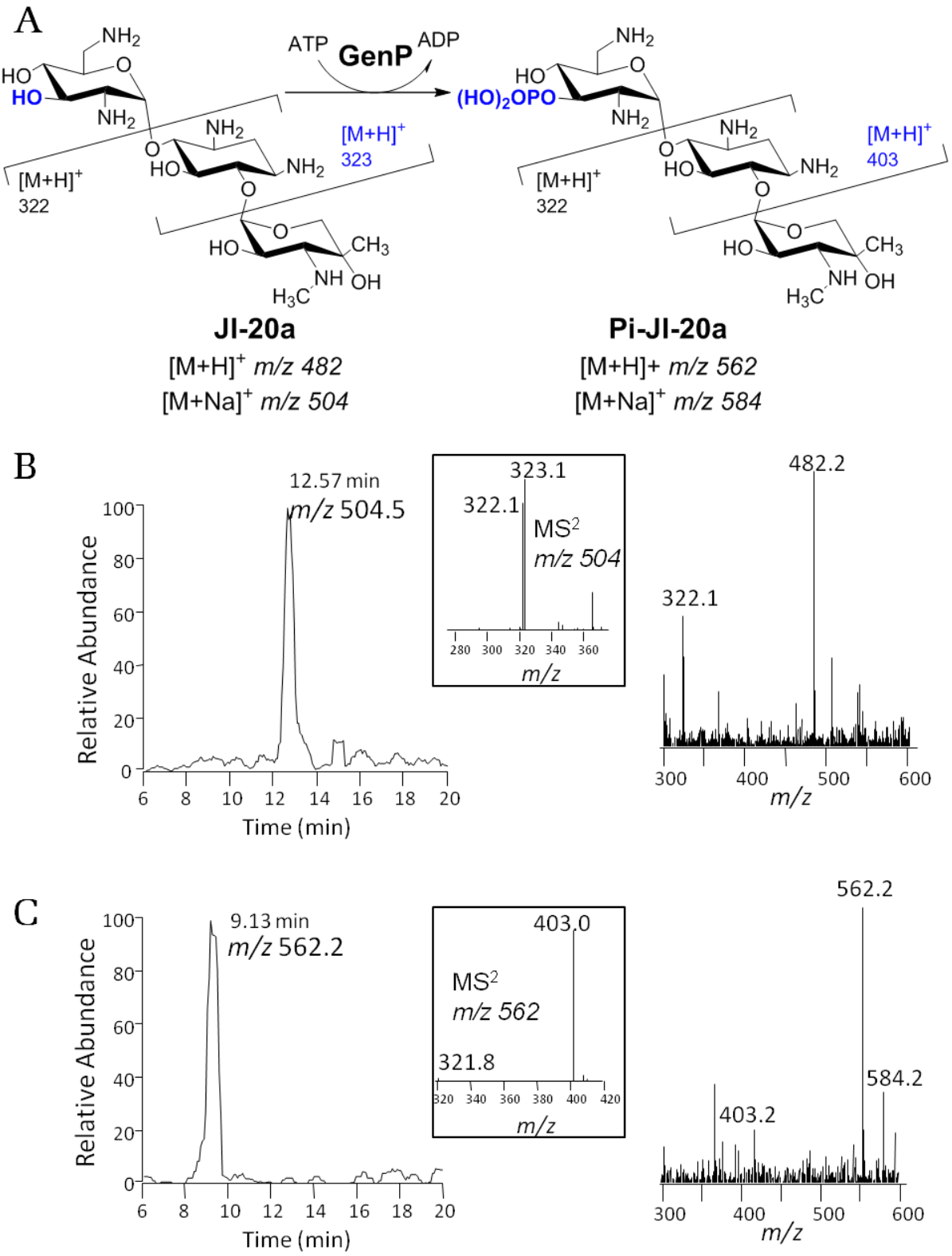

Figure 4.11 Phosphorylation of JI-20a by recombinant GenP. (A) Fragmentation patterns of JI-20a and Pi-JI-20a, a product of ATP-dependent phosphorylation by GenP; (B) LC-MS chromatogram showing selected ion monitoring of substrate, JI-20a (left), MS:MS ion fragments of the JI-20a peak (middle, *m/z* 320 to 420), and ion spectrum [*m/z* 300 to 600] of the selected peak. (C) Data for product, Pi-JI-20a.

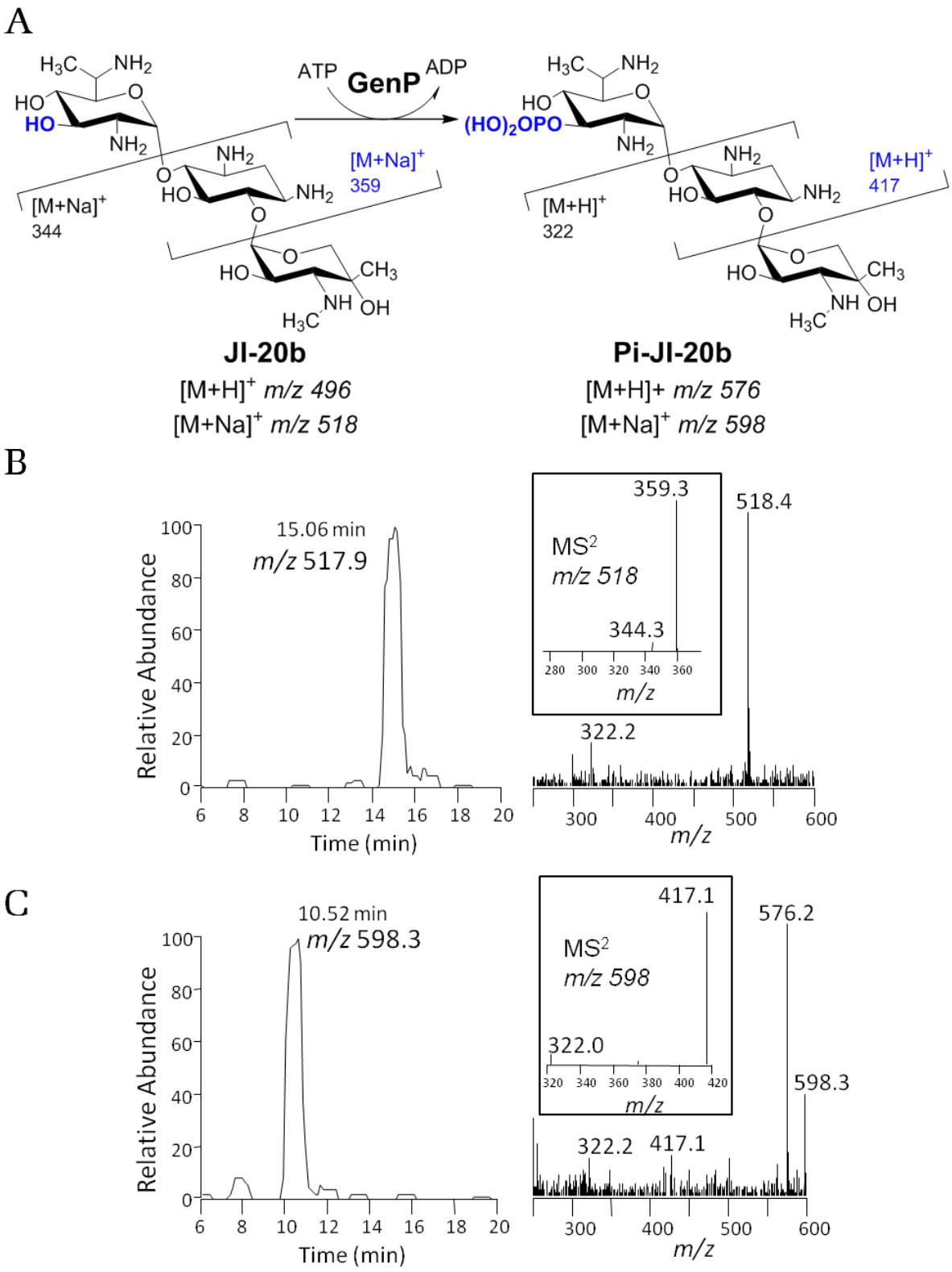

Figure 4.12 Phosphorylation of JI-20b by recombinant GenP. (A) Fragmentation patterns of JI-20b and Pi-JI-20b, a product of ATP-dependent phosphorylation by GenP; (B) LC-MS chromatogram showing selected ion monitoring of substrate, JI-20b (left), MS:MS ion fragments of the JI-20a peak (middle, *m/z* 320 to 420), and ion spectrum [*m/z* 250 to 600] of the selected peak. (C) Data for product, Pi-JI-20b.

4.2.4 GenP kinetics

Kinetic assessment of GenP was performed by coupling its reaction to a pyruvate kinase/lactate dehydrogenase assay (Figure 4.13) (Jenkins, 1991). By following the steady decrease of absorbance at 340 nm, the rate of ATP consumption and thus Pi-JI-20a generation was studied.

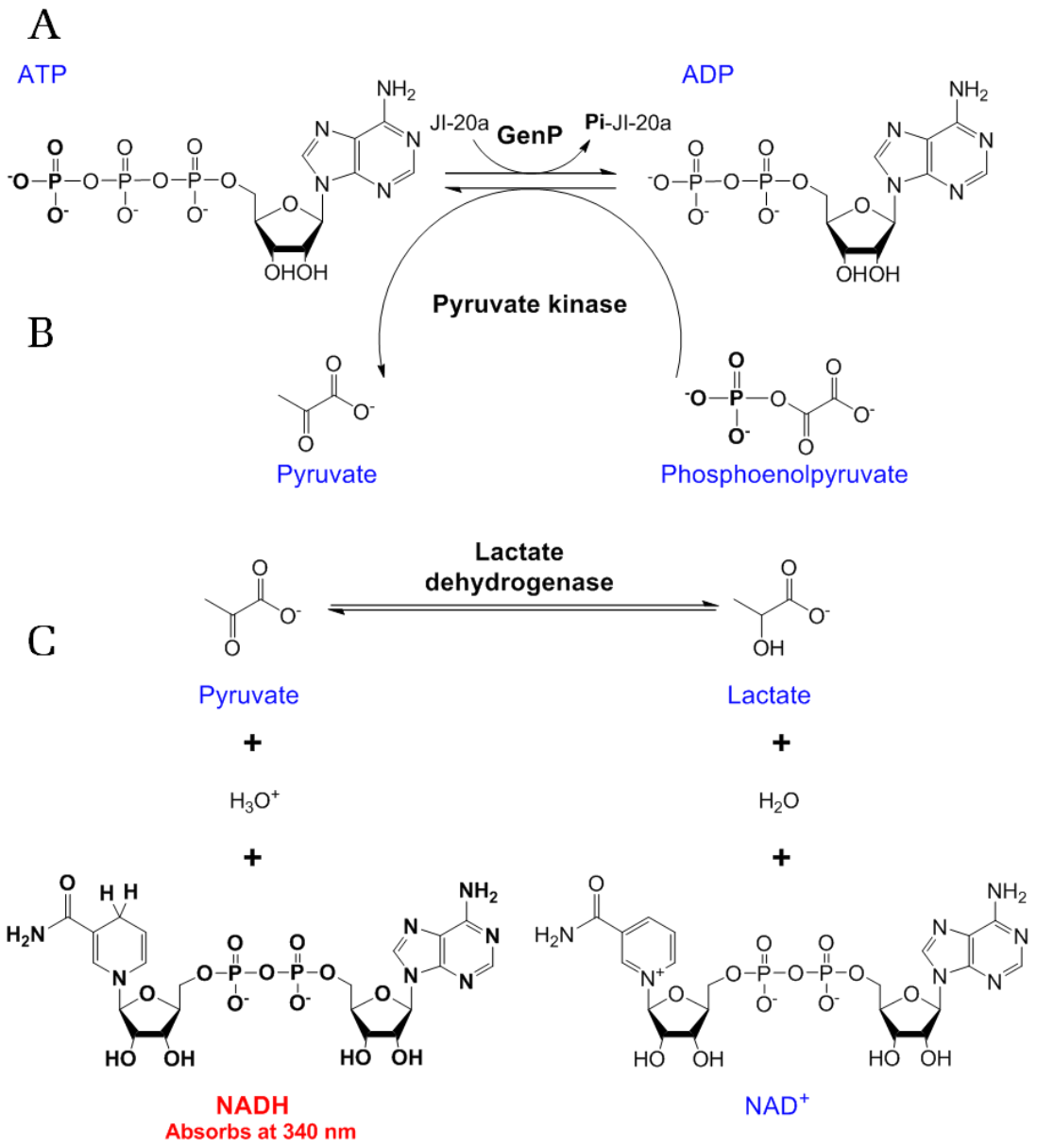

Figure 4.13 ATP/NADH coupled assay for GenP phosphotransferase. (A) GenP reaction with ATP and JI-20a producing ADP and Pi-JI-20a; (B) pyruvate kinase regenerates ATP by transferring a phosphate group from phosphoenolpyruvate to ADP. A molecule of pyruvate is produced; (C) lactate dehydrogenase uses pyruvate and NADH (which absorbs at 340 nm) to form lactate and NAD^+. Decrease in absorbance at 340 nm can thus be linked to formation of Pi-JI-20a in a GenP-catalysed reaction.

Individual wells of a 96-well plate were filled with 50 µL of 20 mM Tris-HCl, pH 8.0 containing 2.5 µM GenP and 150-1200 µM of various aminoglycoside substrates. To this a MasterMix (kept on ice in a dark tube to prevent NADH degradation) was added. The final concentration of components in a typical reaction of 150 µL was 0.25 mM ATP, 0.6 mM NADH, 5 mM $MgCl_2$, 0.6 mM PEP, 3 µL of the PK/LDH mixture (stock solution x50), 0.1 mg/mL BSA, and 1 mM DTT. The plate (half-area, flat-bottom wells) was shaken for 10 seconds, and absorbance at 340 nm was recorded every minute over 1 hour using a BMG Pherastar spectrophotometer. These reactions were performed at 30˚C, in triplicate. A negative control with no GenP protein was used to generate the background signal.

Eight compounds were tested as substrates for GenP. Gentamicin intermediates (gentamicin X2, G418, JI-20a, JI-20b, and gentamicin C2a) were used alongside related aminoglycosides, kanamycins A and B, and tobramycin (Figure 4.13). The data were analysed using GraphPad Prism 7. Absorbance at 340 nm was plotted against time in minutes. True substrates of the gentamicin biosynthetic pathway, JI-20a and JI-20b, were converted fastest, alongside kanamycin B, whose 6-deoxo-6-amino-glucosamine ring is identical to that of JI-20a. GenP also accepted gentamicin X2, kanamycin A, and G418 as substrates, although reaction was slower. Gentamicin C2a and tobramycin, both of which lack a 3' hydroxyl group, were not acted upon at all.

To calculate the maximum rate, V_{max} (µM s^{-1}) and the Michaelis constant, K_m apparent (µM; at 0.25 mM concentration of ATP), of GenP-catalysed phosphorylation of the substrates, the linear part of the curve was used to determine the rate of change of absorbance per minute, ΔA/t (min^{-1}). The background signal was subtracted before the data was converted to reaction rate, v (µM s^{-1}), by the following equation:

$$v = \Delta c = \frac{\Delta A}{\epsilon \times l} \times \frac{1000}{60} = \frac{\Delta A \times 1000}{6.22 \times 0.166 \times 60} = \Delta A \times 16.1$$

where v is reaction rate (µM s^{-1}), Δc is change in substrate concentration (µM s^{-1}), ΔA is change of absorbance at 340 nm of the linear portion of the curve (min^{-1}), ε is the extinction coefficient of NADH (mM^{-1} cm^{-1}), l is path length (= 0.166 cm),

1000 is the factor for converting mM to μM, and 1/60 is the factor for converting second to minutes.

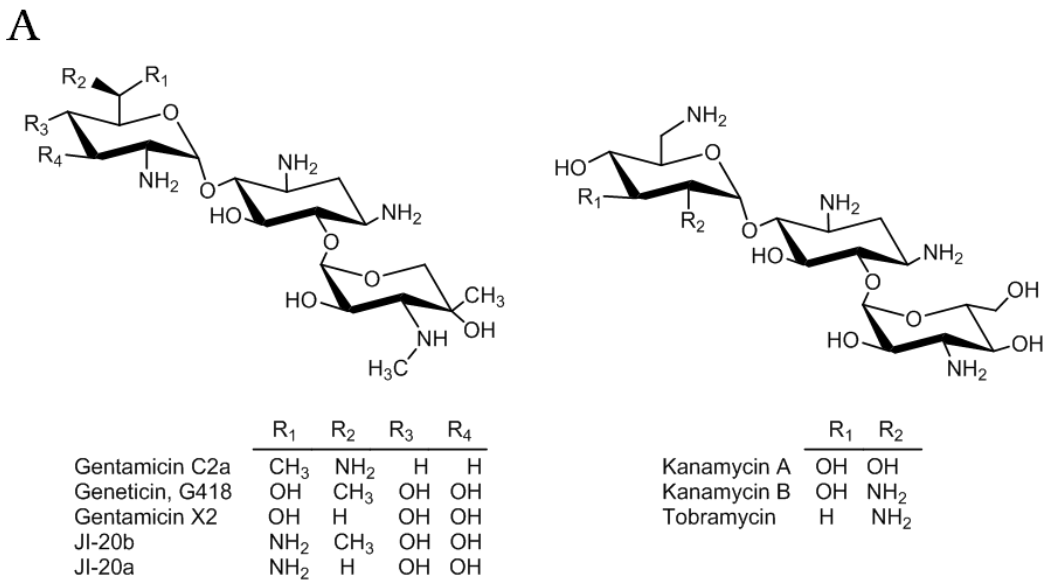

	R_1	R_2	R_3	R_4
Gentamicin C2a	CH_3	NH_2	H	H
Geneticin, G418	OH	CH_3	OH	OH
Gentamicin X2	OH	H	OH	OH
JI-20b	NH_2	CH_3	OH	OH
JI-20a	NH_2	H	OH	OH

	R_1	R_2
Kanamycin A	OH	OH
Kanamycin B	OH	NH_2
Tobramycin	H	NH_2

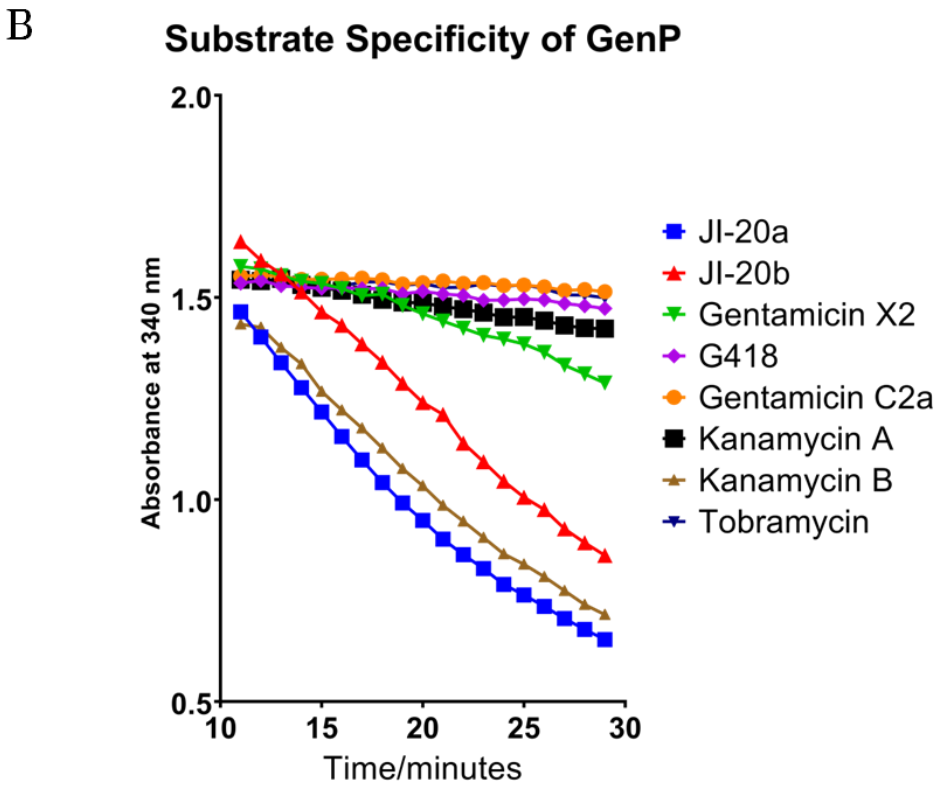

Figure 4.14 Substrate specificity of GenP. (A) Gentamicin pathway intermediates (JI-20a, JI-20b, G418, gentamicins X2 and C2a) and related aminoglycosides (kanamycins A and B, tobramycin) were tested for conversion by GenP. (B) The concentration of all aminoglycoside substrates was kept the same, and true substrates, JI-20a and JI-20b, and kanamycin B were converted well; gentamicin X2, G418, and kanamycin A were accepted as substrates. Gentamicin C2a and tobramycin, both of which lack a 3' OH group, were not converted.

The reaction rate (μM s^{-1}) was plotted against the substrate concentration (μM), and fitted to the Michaelis-Menten equation (Figures 4.15 and 4.16). The parameters for the maximum rate, V_{max} (μM s^{-1}) and the Michaelis constant, K_m apparent (μM), were obtained. The following equation was used to calculate k_{cat}:

$$k_{cat} = \frac{V_{max}}{[E]},$$

where [E] is enzyme concentration (μM) in the reaction.

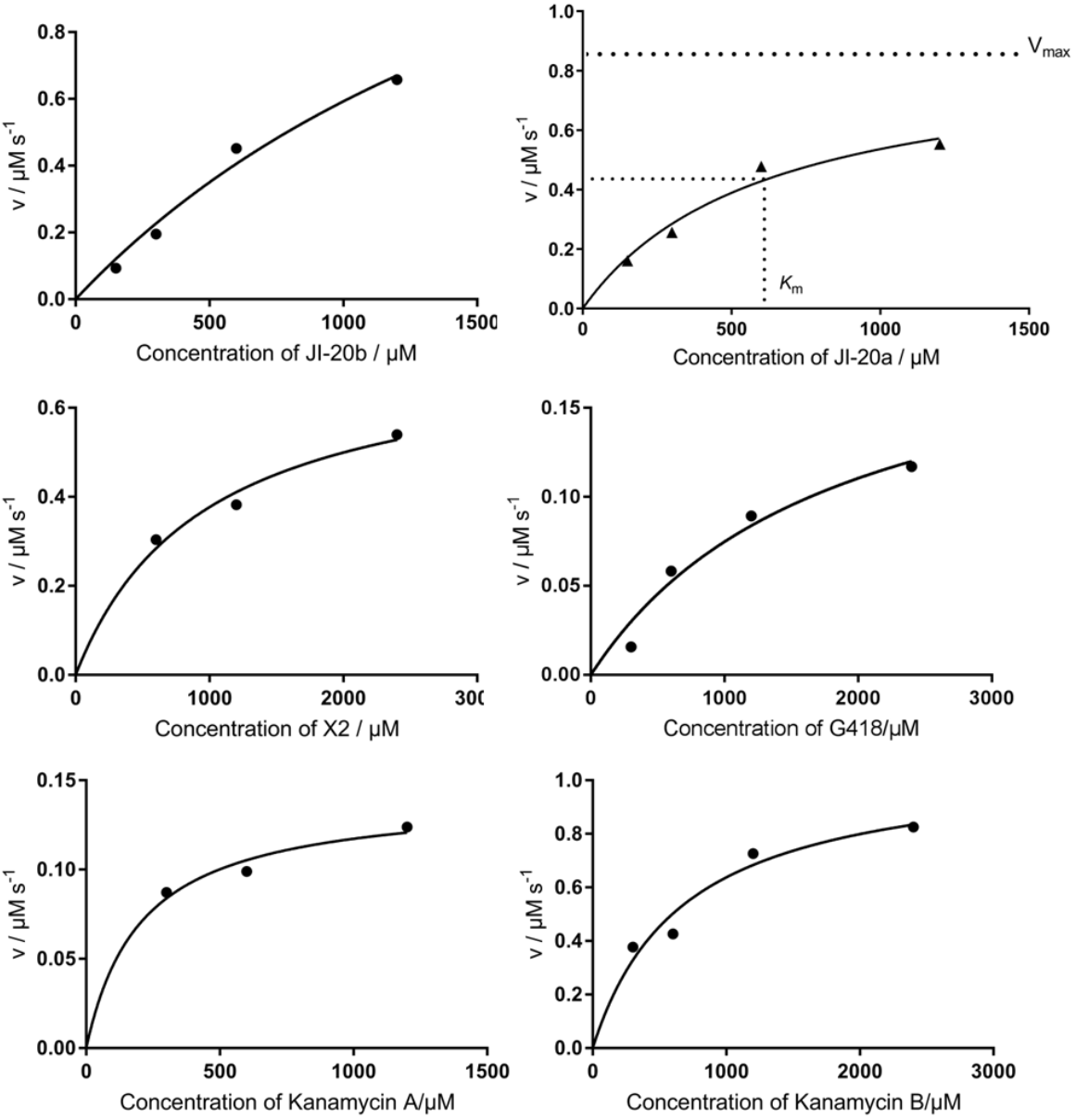

Figure 4.15 Kinetic curves of GenP. GenP is a wide-specificity enzyme that is able to catalyse phosphorylation of various substrates in the presence of ATP.

The kinetic parameters of K_M apparent and k_{cat} for the various substrates are shown in Table 4.2. The catalytic rate constant is much higher for the native substrates than for the previously reported substrate analogues (Shao et al., 2013). The high value of K_M apparent is consistent with previous reports. Specificity constant is highest for the true substrates JI-20a and JI-20b, but also kanamycin B.

Table 4.2 Kinetic parameters of GenP

Substrate	K_M/ µM	k_{cat}/ s^{-1}	Specificity constant (k_{cat}/K_M) / $s^{-1}mM^{-1}$
JI-20a	609± 238	0.35 ± 0.06	0.57
JI-20b	2252 ± 1461	0.77 ± 0.36	0.34
Gentamicin X2	965±402	0.30 ± 0.05	0.31
Geneticin, G418	1822±1062	0.08 ± 0.03	0.06
Kanamycin A	206±89.2	0.06 ± 0.01	0.29
Kanamycin B	680±266.9	0.43 ± 0.06	0.63

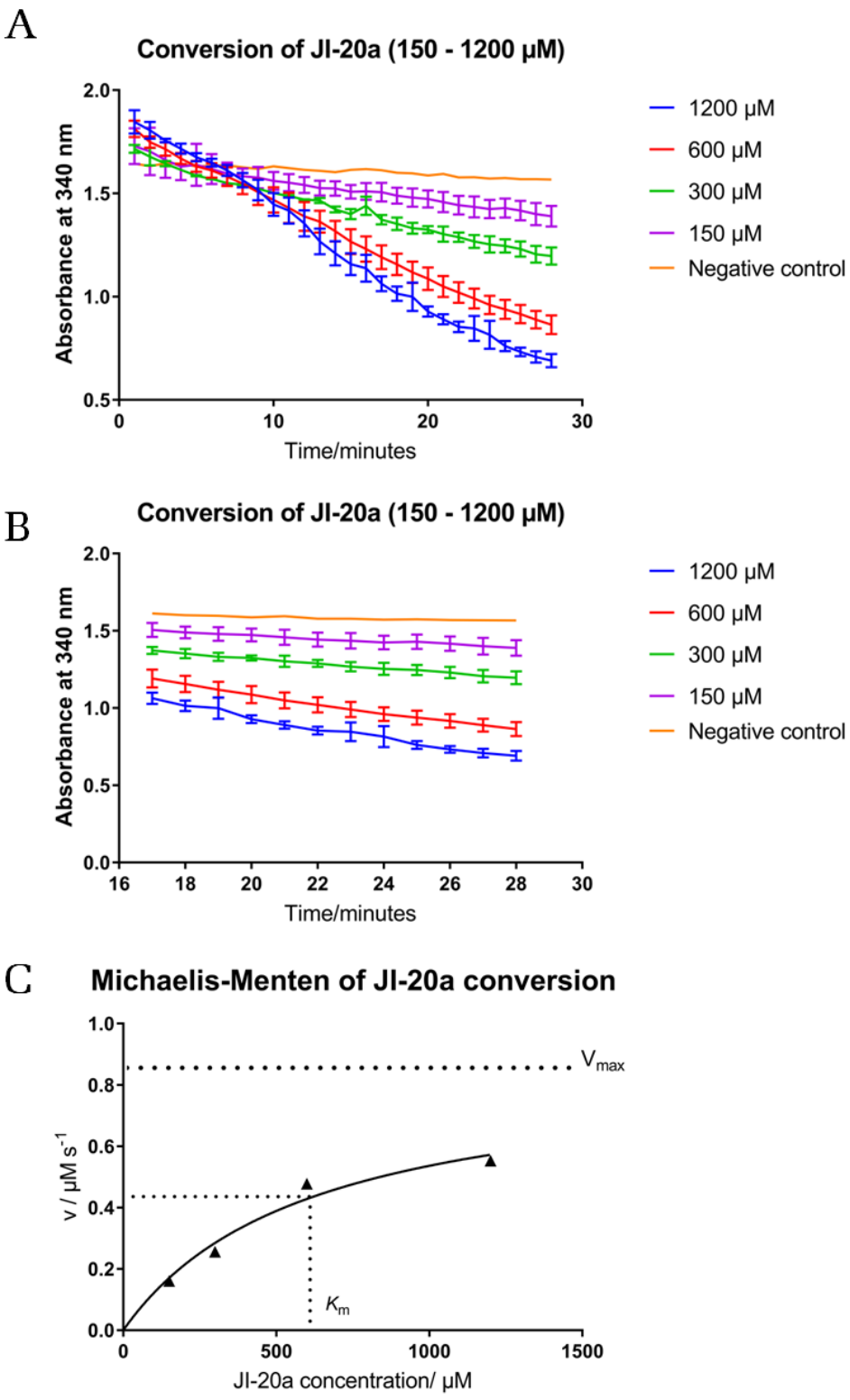

Figure 4.16 Conversion of JI-20a by GenP phosphotransferase. (A) JI-20a conversion can be followed by a continuous PK/LDH-linked assay; (B) the linear portion of the graph was used to calculate change of absorbance per minute (slope) values; (C) calculated *v* values fitted to Michaelis-Menten equation.

4.2.5 Side-directed mutagenesis of *genP*

Analysis of the GenP sequence by Prosite Expasy predicted aspartic acid 189 to be the active site residue (Figure 4.17). This hypothesis was further strengthened by creating a GenP structure model using PHYRE2, with Asp189 in a clear proximity to the aminoglycoside in the active site. Mutagenesis of equivalent Asp in Fms8 completely inactivated the enzyme.

A

>AAR98555.1 GntI [Micromonospora echinospora]
MVAAPIPVAGWGDKDDPWECLGERSSGATVYRVGEVPSFYVKTTPPRHPDDHRFNPTKEAERLRWLAAQG
LPVPEVVALDANDELAWVVTRALPGRPAARHWKPEERWRVIDVVADVARTLHALPVAECPFERRLADLIH
QASSSMALGALDLDDVDPSHEGWTAQQLWDELSKMTPPAEDDLVVCHGDFCLDNVLVDPETLTLAGILDV
DRAGVSDRWMDLALALYNIGQDDVWGYGPPHAEHFLRRYGITVDQHKLTYIQLLDEFL

B

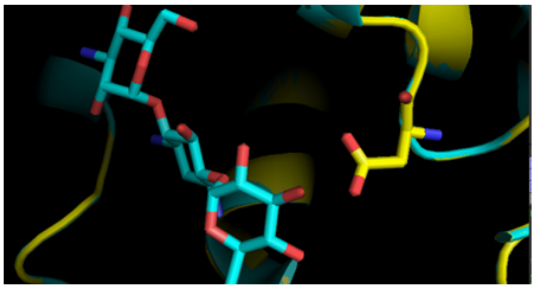

C

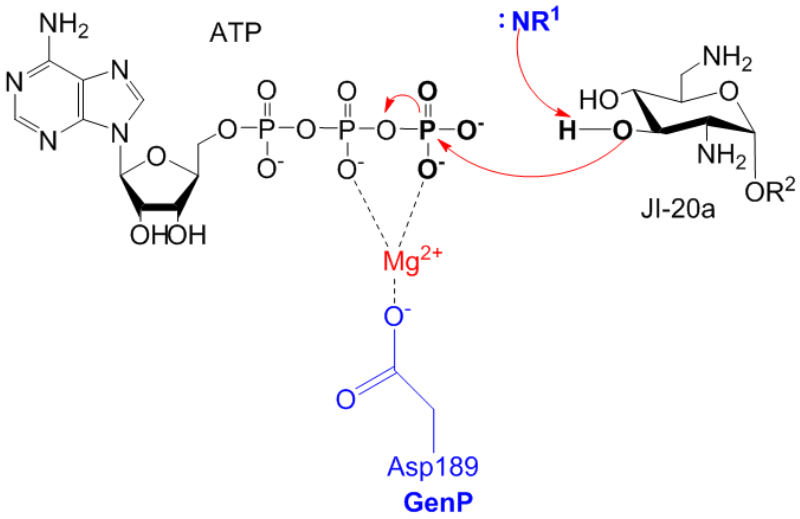

Figure 4.17 GenP catalytic site. (A) GenP (GntI) protein sequence with the purple box showing a conserved VCHgDFCLDNVLV active-site motif of a kinase protein (tyrosine class), identified by Expasy Prosite. Highlighted aspartic acid 189 is predicted to be the catalytic proton acceptor (by Prosite Expasy); (B) PHYRE2 model of D189 of GenP (yellow) near an aminoglycoside substrate; (C) possible mechanism of phosphate transfer by GenP.

Single amino acid mutations - aspartic acid-289 to alanine, asparagine, or leucine - were generated in GenP to confirm the mechanism of catalysis involving residue 189. Gene *genP* was first cloned into a smaller vector, pEX-A2, by PCR with "GenP trans" primers and Phusion polymerase, and a restriction digest of PCR product and pEXA2 vector with *Not*I and *Eco*RI FastDigest® endonucleases. T4 ligase was then used to generate the *genP*-pEX-A2 vector. NovaBlue cells were transformed with the ligation product and selected using ampicillin resistance as a marker. Plasmid DNA was isolated and the DNA was sequenced. The double primer method (Zheng et al., 2004) was used to generate DNA mutations. A PCR reaction with GenP-pEX-A2 and mutagenic primers was set up using Phusion High-Fidelity MasterMix with GC buffer. A restriction digest was performed on PCR product with *Dpn*I FastDigest® endonuclease for 3 hours at 37˚C. A DNA Clean & Concentrator™ kit was used to purify the DNA. NovaBlue *E. coli* competent cells were transformed with the DNA and plated on ampicillin-containing LB agar plates. Following DNA sequencing of isolated plasmids, a restriction digest of *genP (D189*)*-pEX-A2 and pET-28a (+) with *Nde*I and *Eco*RI FastDigest® endonucleases was performed. T4 ligase was used to generate *genP (D189A)*-pET-28a, *genP (D189L)*-pET-28a, and *genP (D189N)*-pET-28a vectors. NovaBlue *E. coli* cells were transformed with the ligation product and grown on kanamycin-containing LB agar plates. The inserts were confirmed by DNA sequencing and transformed into protein-expressing BLR *E. coli* cells.

The proteins were expressed and were all soluble. Their identity was confirmed by MALDI-ToF. To test for the activity of the residue 189 mutants, *in vitro* assays with JI-20b and ATP were performed in triplicate (Figure 4.18). Surprisingly, although the activity of GenP (D189A) and GenP (D189L) was reduced to 61 and 52% respectively, all proteins were still active.

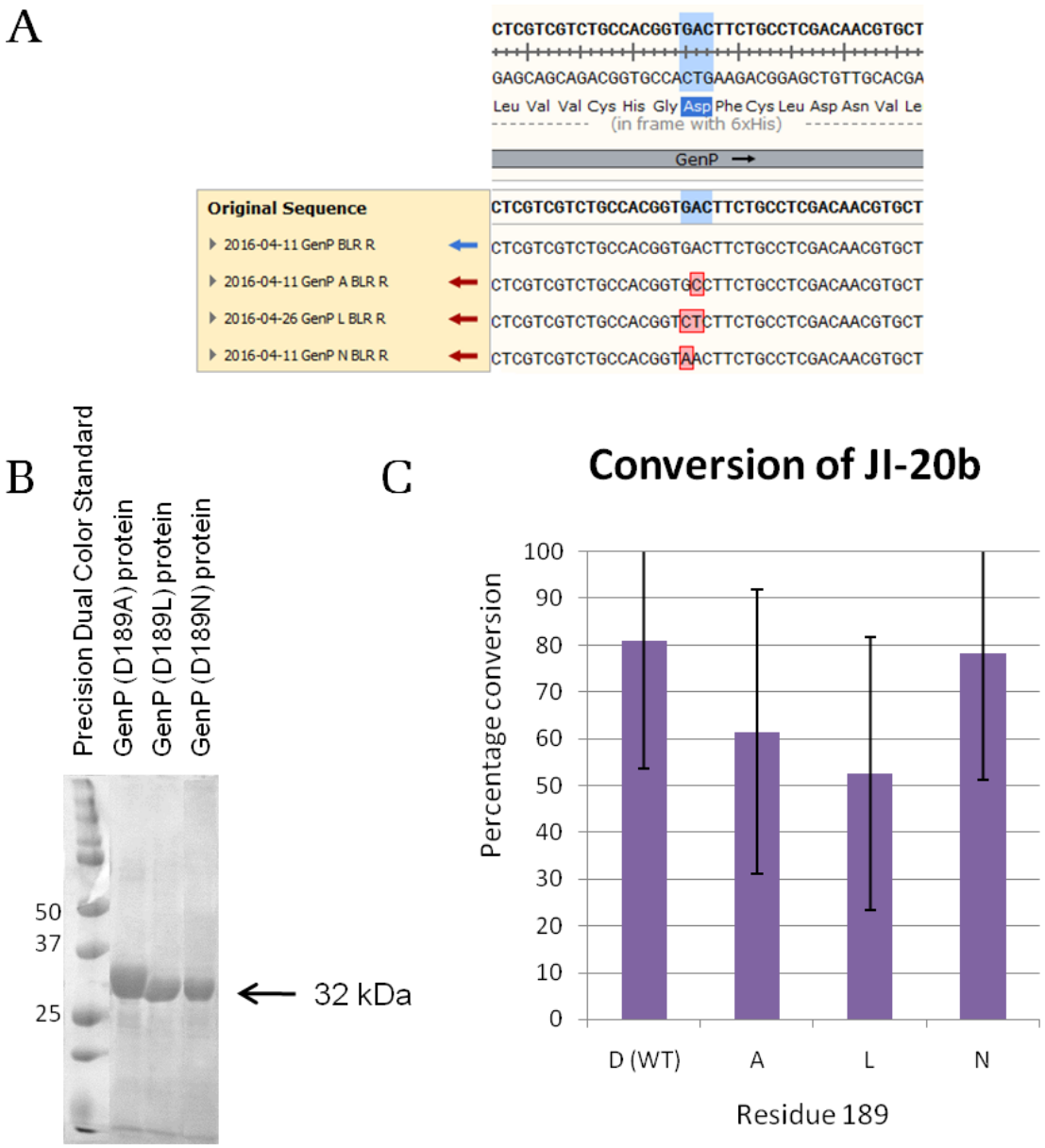

Figure 4.18 Site-directed mutagenesis of GenP. (A) DNA sequencing confirmed mutation of Residue 189 (aspartic acid) to alanine, leucine, and asparagine; (B) SDS-PAGE gel showing all three proteins purified using Ni^{2+} affinity chromatography; (C) average percentage of JI-20b converted by GenP proteins with different Residue 189.

4.3 Discussion

The absence of 3' and 4' hydroxyl groups on the purpurosamine ring of gentamicin C complex components improved their antibiotic activity and increases their stability (Vydrin et al., 2003). GenP has been shown here to be the enzyme catalysing the first step of the di-dehydroxylation, phosphorylation. Shao *et al* have previously used related aminoglycosides kanamycin and

neomycin with GenP to show that the hydroxyl group phosphorylated was at the 3' position. They further characterised GenP by its kinetic parameters, K_M apparent and k_{cat}, on these substrates. Here, for the first time its native substrates JI-20a and JI-20b have been shown to be phosphorylated by GenP at the 3' position. Various alternative substrates were tested and found to be accepted by GenP (gentamicin intermediates, G418 and gentamicin X2, and kanamycins A and B).

The mechanism of the di-dehydroxylation reaction is thus different from the previously-described apramycin 3' dehydroxylation. In both gentamicin and fortimicin, the reaction mechanism of di-dehydroxylation is predicted to occur through five key steps: 3'-phosphorylation, 3',4'-phospholysis, 3',4'-reduction, 4',5'-dehydratation, and 4',5'-reduction (Piepersberg et al., 2007a). It is important to note that such a mechanism would have sisomicin and verdamicin as true intermediates of the pathway, and both *sis* and *ver* clusters should lack the final reductase gene. Phosphorylation at the 3' position is catalysed by GenP. The identity of the genes involved in catalysis of the other steps is proposed in the following chapters.

5

Di-dehydroxylation by GenB3

5.1 Dehydroxylation reactions of Pi-JI-20a and Pi-JI-20b

The mechanism of di-dehydroxylation of gentamicin differs significantly from the dehydroxylation in the apramycin pathway. As previously discussed, the removal of the hydroxyl group from the 3' position of apramycin involves a radical SAM-dependent dehydratase AprD4 and NADPH-dependent reductase AprD3 (Lv et al., 2016, Kim et al., 2016). This mechanism does not involve a phosphorylated intermediate.

The previous chapter showed the essential nature of an ATP-dependent phosphotransferase GenP in gentamicin biosynthesis. A deletion mutant constructed in Wuhan by Dr Chuan Huang showed that phosphorylation was an essential first step of the di-dehydroxylation reaction. Therefore, an enzyme catalysing the next part of di-dehydroxylation must accept Pi-JI-20a and Pi-JI-20b as substrates. There is no information concerning the ability of AprD4 to catalyse phosphorylated substrates, and the *gen* cluster does not contain an *aprD4* homologue (Kudo and Eguchi, 2009).

Piepersberg *et al* postulated that GenG phospholyase and a reductase enzyme, such as GenW or GenD3 could catalyse the reaction converting phosphorylated JI-20's via a 4',5'-unsaturated intermediate, sisomicin or

verdamicin (Piepersberg et al., 2007a). After the initial 3'-phosphorylation, four more steps would result in the removal of the 3' phospho and 4' hydroxyl groups: 3',4'-phospholysis, 3',4'-reduction, 4',5'-dehydratation, and 4',5'-reduction. To investigate this possibility GenG was expressed and GenW was cloned and expressed. The recombinant enzymes could not catalyse the conversion of Pi-JI-20b (data not shown). Another mechanism had to be used during the biosynthesis of gentamicin to achieve di-dehydroxylation at 3' and 4' positions.

5.1.1 Removal of hydroxyl groups from sugar moieties

In contrast to most sugars being used in the cell for metabolic purposes, deoxysugars - with one or more hydroxyl groups substituted for hydrogen - are used for execution of roles that require stability and specific binding affinity (Agnihotri and Liu, 2001). Gentamicin as a pseudotrisaccharide has two sugar rings with various degrees of deoxygenation. Depending on the position of the hydroxyl group to be removed, different strategies and mechanisms are employed. For example, removal of a 4' hydroxyl group requires a radical SAM-dependent enzyme (Lv et al., 2016, Kim et al., 2016). Dehydroxylation at 2' or 6' positions proceed through an α-anion β-dehydration mechanism (Romo and Liu, 2011).

5.1.2 Enzymes with pyridoxal phosphate cofactors

Dehydroxylation at the 3' position of a deoxysugar happens through several different routes. Another class of enzymes capable of catalysing a diverse range of reactions, including dehydroxylation, are vitamin B_6-dependent aminotransferases and are often used to catalyse removal of the 3' hydroxyl group from sugars. The vitamin B_6 group of cofactors consists of pyridoxal 5'-phosphate (PLP) and pyridoxamine 5'-phosphate (PMP) and these are common in nature (Figure 5.1). Presence of a pyridinium moiety allows enzymes with PLP cofactors to stabilise high-energy anionic intermediates during various reactions (Agnihotri and Liu, 2001).

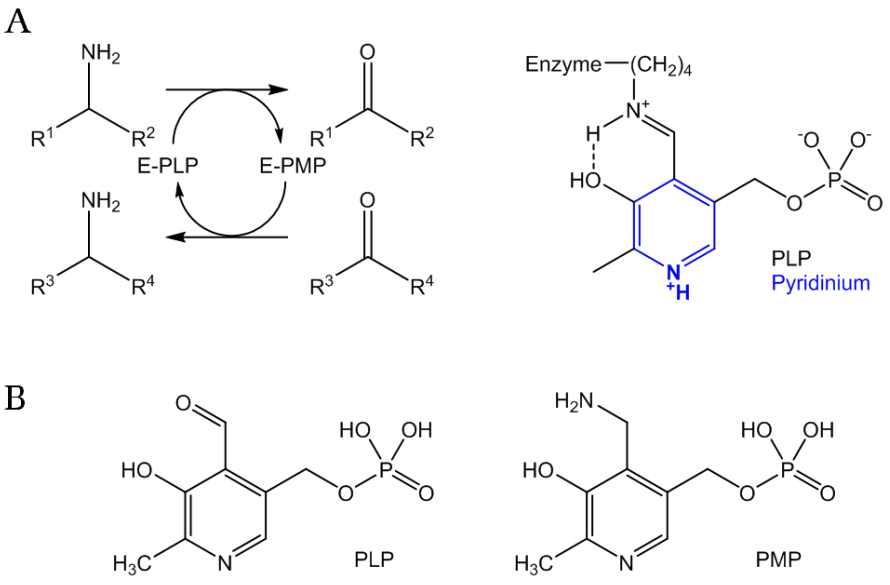

Figure 5.1 PLP and PMP cofactors. (A) PLP and PMP molecules are used as cofactors during a number of reactions, including transaminations. Pyridium moiety (blue) stabilises high-energy anionic intermediates; (B) PLP- and PMP-containing enzymes often possess unusual catalysis mechanisms.

Dehydroxylation at the 3' position during ascarylose biosynthesis proceeds through a 4'-keto intermediate and is reversible (Figure 5.2). The first stage is catalysed by a PMP-dependent aspartate aminotransferase (Agnihotri and Liu, 2001, Romo and Liu, 2011). In contrast to PLP-dependent enzymes, the dehydratase enzyme involved has a [2Fe-2S] cluster and is a dark-red protein. In contrast to PLP-binding proteins, this protein has a histidine residue instead of a conserved lysine at position 220. Mutation of this histidine to lysine and use of PLP instead of PMP can turn this enzyme into an aminotransferase; further mutations of the active site transformed the enzyme into a transaminase (Wu et al., 2007, Smith et al., 2008).

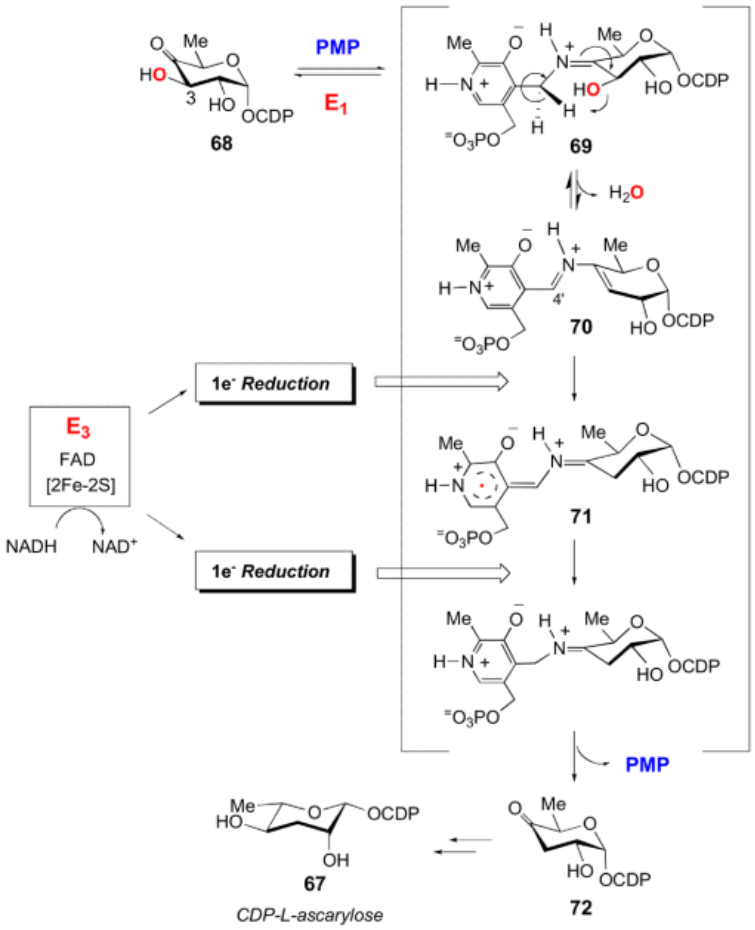

Figure 5.2 3'-Dehydroxylation mechanism of ascarylose. A PMP-dependent aspartate aminotransferase catalyses the removal of a hydroxyl group during the biosynthesis of ascarylose. The reaction proceeds through a 4'-keto intermediate. Figure 9 of (Romo and Liu, 2011).

Synthesis of similar sugars also relies on a 3'-dehydroxylation step using PMP-dependent proteins. In colitose biosynthesis a single enzyme - ColD - is responsible for 3'-dehydroxylation and reduction (Beyer et al., 2003). Like the ascarylose dehydratase, this enzyme uses PMP and has a conserved histidine. However, it lacks a [2Fe-2S] cluster and the cofactor must be regenerated in a separate reaction.

In forosamine biosynthesis, SpnQ dehydratase is responsible for the removal of a hydroxyl group from the 3' position (Hong et al., 2006). SpnQ has a [2Fe-2S] cluster, uses PMP, but the reductase necessary for the last step of the dehydroxylation is borrowed from general cellular metabolism. Therefore, PMP-dependent enzymes can catalyse a 3' hydroxyl group removal.

5.2 GenB enzymes: a group of aminotransferases

Within the *gen* cluster there are four related aminotransferase genes: *genB1, genB2, genB3,* and *genB4.* Assessment of their similarity by homology scores predicts that *genB1* was the original precursor gene, as it is the most similar class III ("B"-type) 6'-aminotranferase enzyme to a highly-conserved group from other producers of the neomycin-family of aminoglycosides (Figure 5.3). Gene *genB2* is predicted to have arisen from a duplication event, and through genetic drift has acquired the ability to catalyse a similar reaction on a different substrate. The ancestor of the *genB3* and *genB4* genes, which are highly similar to each other, but not to the other two aminotransferases, is predicted to have come later via horizontal gene transfer from a fortimicin producer (Piepersberg et al., 2007a). The essential nature and the functions of GenB1 and GenB2 have been discussed previously (Guo et al., 2014).

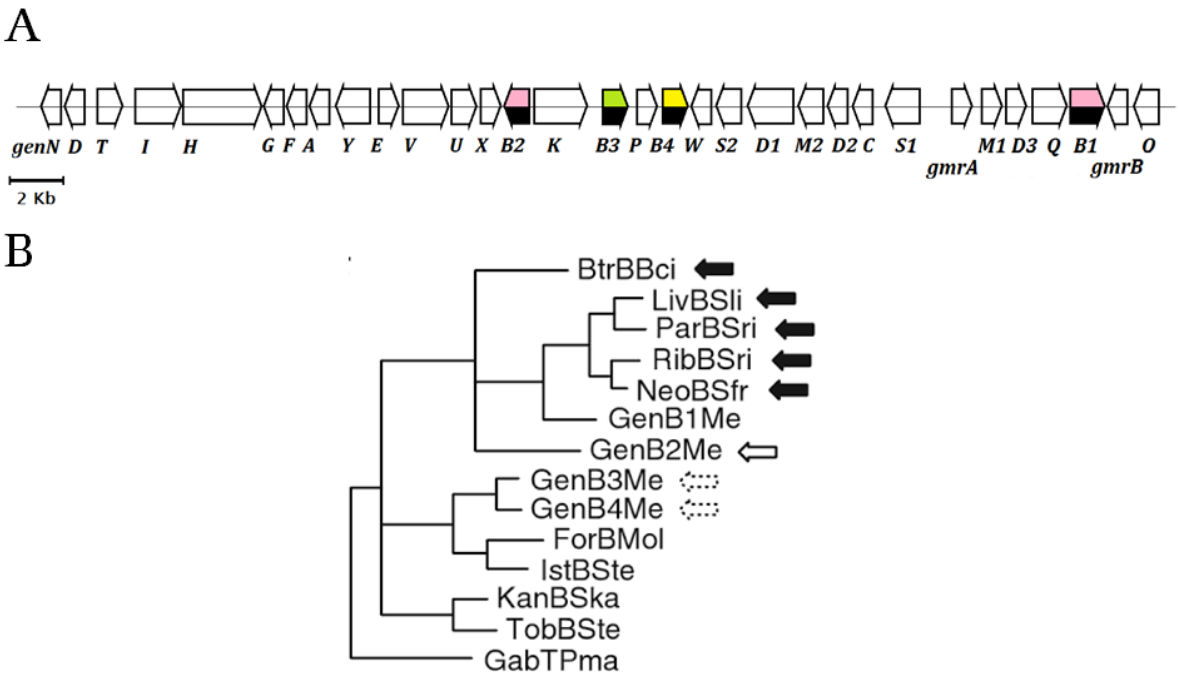

Figure 5.3 Phylogram of the class III 6'-aminotransferases. (A) The *gen* cluster with highlighted GenB aminotransferases. Colour is related to the colour of the expressed protein; (B) PAUP3.1.1 program was used to generate the phylogenetic tree, with 500-times bootstrapping and above-50% threshold for matches. The tree was rooted by including an outgroup, aminotransferase GabT of cyanobacterium *Prochlorococcus marinus* MIT 9313 (accession code NP893836.1) in this case.

The filled arrows indicate highly-conserved aminotransferases from the neomycin-family of aminoglycoside producers. The open arrow indicates *genB2*, probably evolved by duplication. Dotted arrows indicate a pair of *genB3* and *genB4,* which has evolved from horizontal recruitment and subsequent duplication events. Figure adapted from Figure 2.29B-f of (Piepersberg et al., 2007a).

Both GenB3 and GenB4 are predicted to belong to the family of pyridoxal phosphate-dependent aminotransferases. Analysis by Expasy PROSITE shows that GenB3 possesses a PLP-binding motif at residues 253-288 (with Lysine 283 serving as the PLP attachment site); the PLP-binding motif of GenB4 is formed by residues 208-243, with Lysine 238 serving as the PLP attachment site. One of these proteins could be responsible for removal of the 3' phospho group and the 4' hydroxyl group from Pi-JI-20a and Pi-JI-20b.

5.2.1 Δ*genB3 Micromonospora echinospora*

The work described in a paper published by our group in 2014 showed the fermentation products of Δ*genB1* and Δ*genB2 M. echinospora* (Guo et al., 2014). The former produced a drastically reduced amount of gentamicin C complex, while the later "lost" gentamicins C2 and C1. *In vitro* experiments showed that GenB1 aminotransferase was a JI-20a and JI-20b synthase (with other GenB enzymes capable of replacing it to some extent), while GenB2 acted as an essential epimerase for gentamicin C2 synthesis. Although *M. echinospora* mutants of the other GenB proteins - GenB3 and GenB4 - were not discussed in detail, their deletion mutants were also prepared by Dr Chuan Huang in Wuhan (Table S1 in (Guo et al., 2014)). Surprisingly, predominant products of the fermentation of Δ*genB3 M. echinospora* were JI-20b, Pi-JI-20b, JI-20a, and Pi-JI-20a (Figure 5.4). The yield of gentamicin intermediates of Δ*genB3 M. echinospora* was about five times greater than Δ*genP M. echinospora*, so Δ*genB3 M. echinospora* was used to generate substrates for in vitro assays.

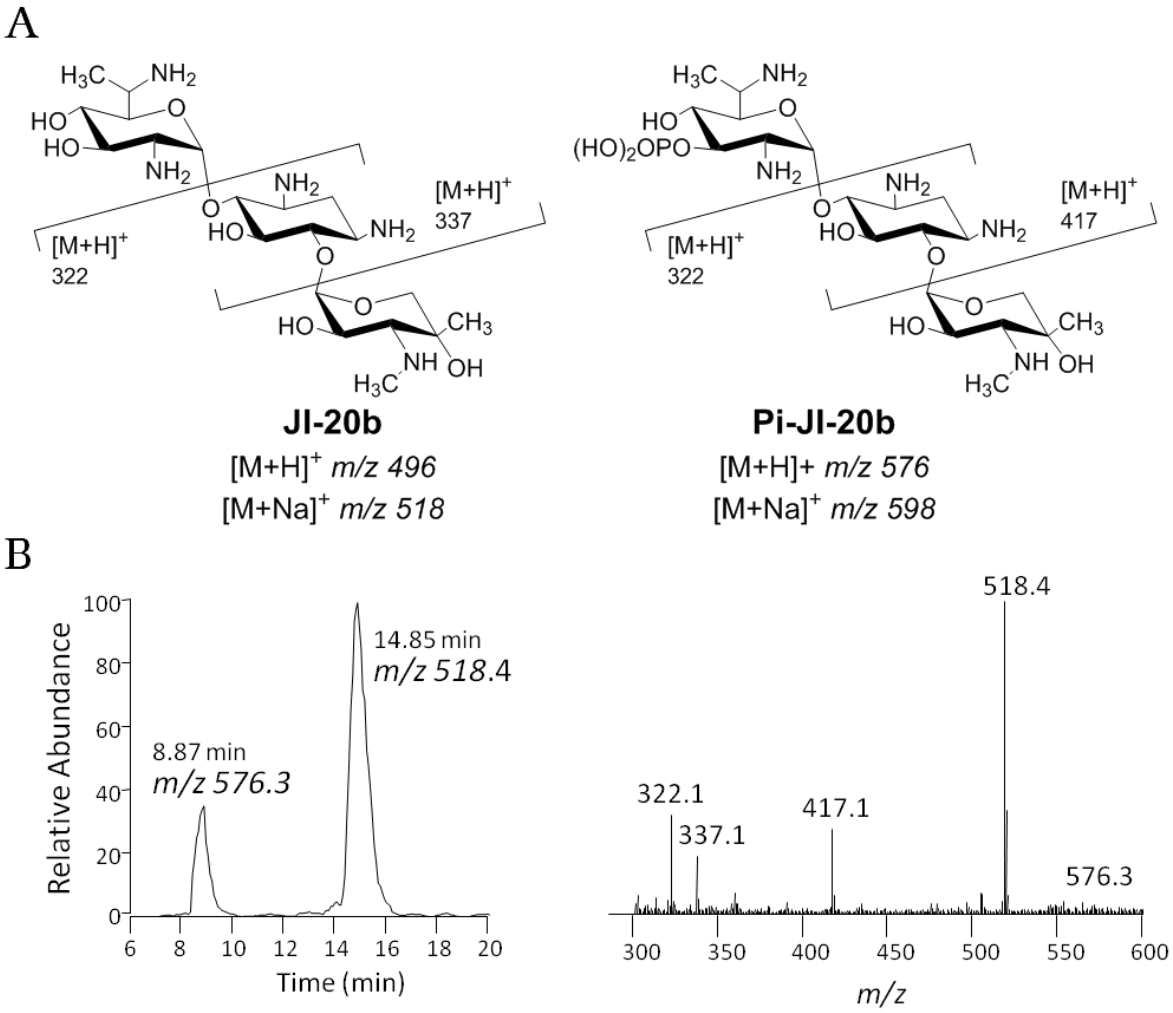

Figure 5.4 Products of Δ*genB3* mutant of *M. echinospora*. Like Δ*genP,* Δ*genB3 M. echinospora* produces JI-20b and JI-20b, gentamicin intermediates with 3' and 4' hydroxyl groups. Pi-JI-20b and Pi-JI-20a are also present in small amounts. No dehydroxylated products were detected. (A) Fragmentation patterns of more abundant products: JI-20b and Pi-JI-20b; (B) LC-MS chromatogram showing selected ion monitoring of JI-20b and Pi-JI-20b (left) and total ion spectrum [*m/z* 300 to 600] (right).

5.3 GenB3

To study the activity of GenB3 on Pi-JI-20a and Pi-JI-20b *in vitro* the gene was cloned into pET-28a (+), transformed into BLR *E. coli*, and over-expressed and purified as described in Chapter 2 (Figure 5.5). Recombinant GenB3 was a pale yellow-green colour.

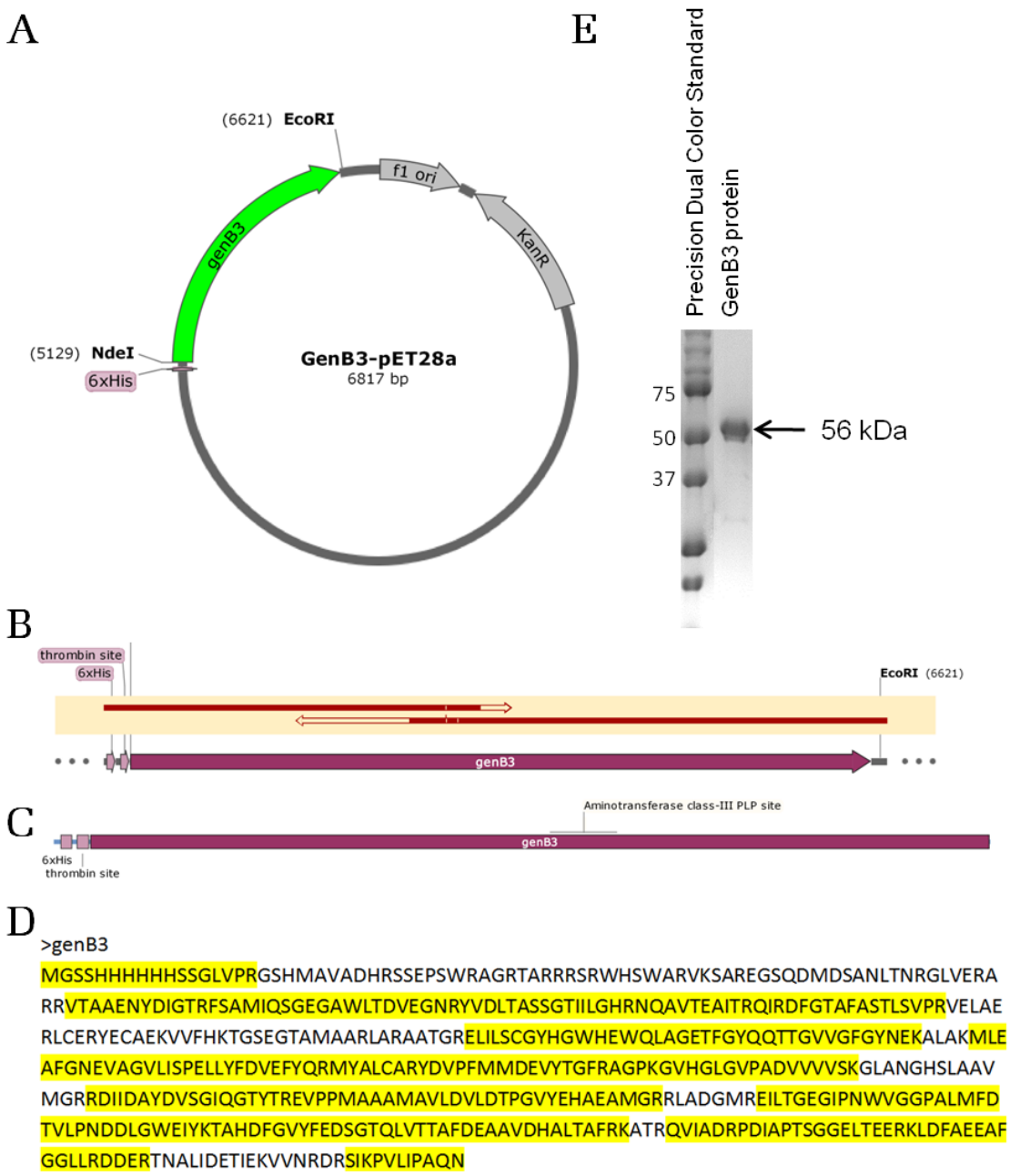

Figure 5.5 Recombinant GenB3 protein profile. (A) *genB3*-pET-28a (+) vector map; (B) confirmation of *genB3* sequence by DNA sequencing with T7 and T7t primers; (C) GenB3 protein map; (D) MALDI fingerprinting analysis showing detected protein fragments in yellow; (e) SDS-PAGE gel of recombinant GenB3 purified by Co^{2+} affinity chromatography.

5.3.1 *In vitro* assays with JI-20b and Pi-JI-20b

Gentamicin intermediates for *in vitro* assays are obtained from fermentation of Δ*gen M. echinospora* mutants. Although Δ*genB3 M. echinospora* produced some phosphorylated JI-20b, the quantities we had access to initially were not sufficient for testing. As more JI-20b was available from the Δ*genB3* mutant of *M.*

echinospora, a same-pot reaction with GenB3 and GenP (in the presence of ATP and magnesium) was used to test GenB3 activity (Figure 5.6).

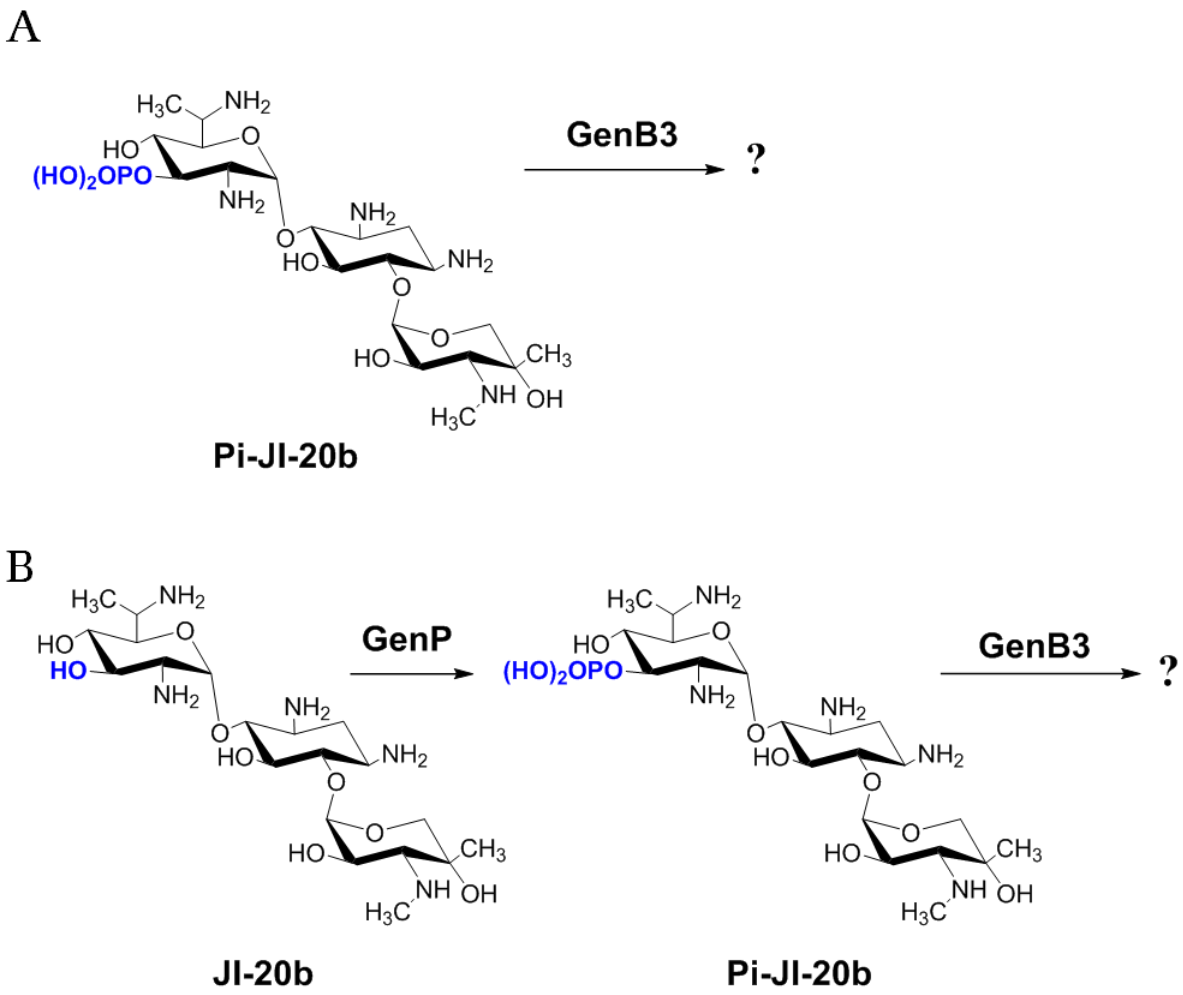

Figure 5.6 Reaction of 6'-methylated substrates with recombinant GenB3 protein. (A) One of the substrates for GenB3 is Pi-JI-20b; (B) Due to initial unavailability of Pi-JI-20b, the GenB3 reaction was linked to GenP catalysis of JI-20b.

Recombinant GenB3 enzyme could convert Pi-JI-20b (Figure 5.7). Two new peaks were observed on addition of GenB3 to the GenP with JI-20b reaction: *m/z* 462 and *m/z* 461. The former had the fragmentation pattern and elution time of verdamicin. The fragmentation pattern and the NMR (performed by Mr Sicong Li in Wuhan) of compound *m/z* 461 showed it to be 6'-keto-verdamicin (Figure 5.8). The ratio of keto-verdamicin to verdamicin was 3 to 1. Complete conversion from phosphorylated compounds could be achieved if PLP was added to the resuspended cells prior to cell lysis before purification of the recombinant protein (Figure 5.9).

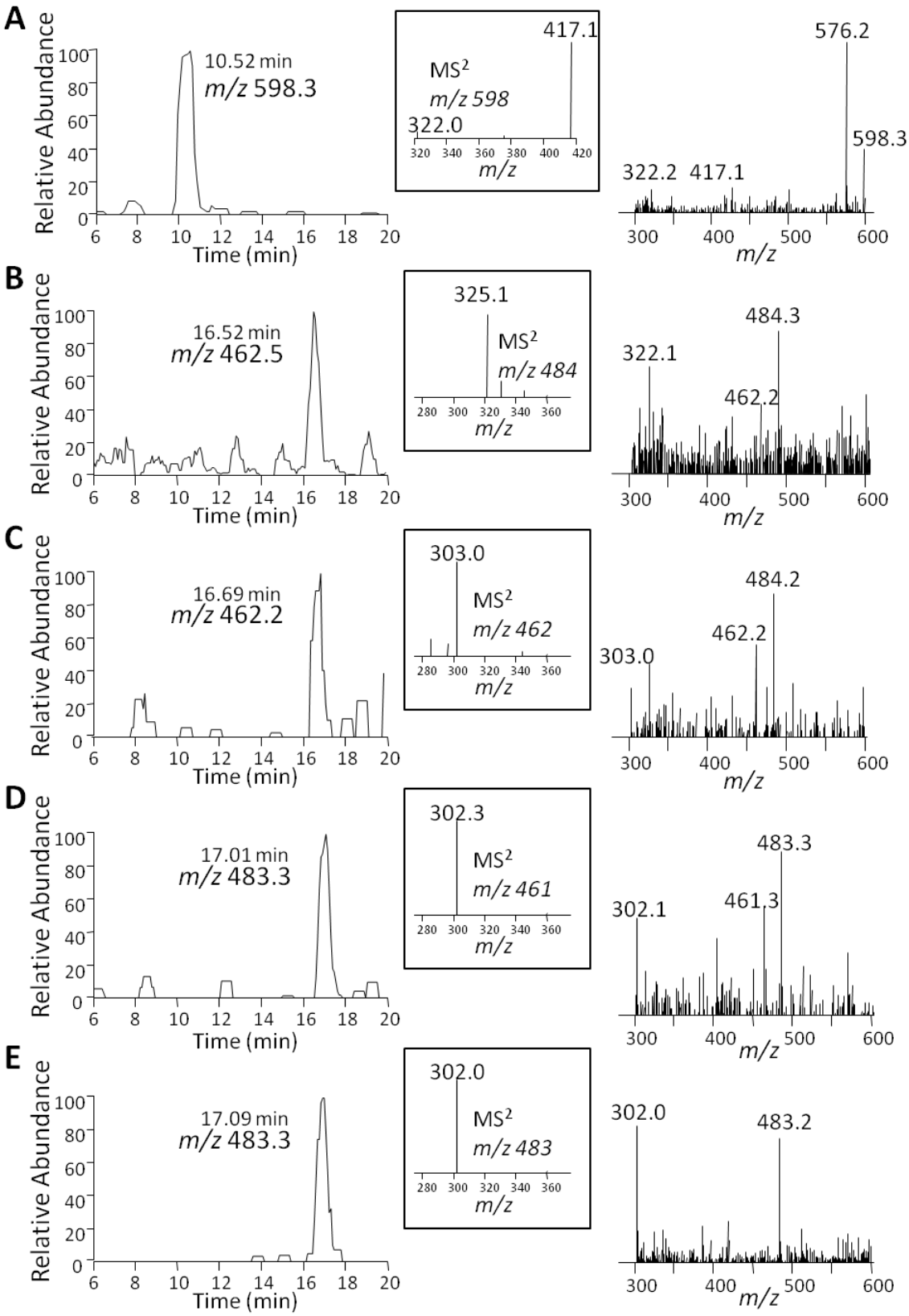

Figure 5.7 HPLC-MS of *in* vitro reactions of Pi-JI-20b with recombinant GenB3 protein. (A) GenB3 accepts Pi-JI-20b as a substrate. LC-MS chromatogram showing selected ion monitoring of the compound (left), MS:MS ion fragments of the peak (middle, *m/z* 320 to 420), and ion spectrum [*m/z* 300 to 600] of the selected peak. Two products are observed (B and D); (C) verdamicin stantard; (E) keto-verdamicin standard.

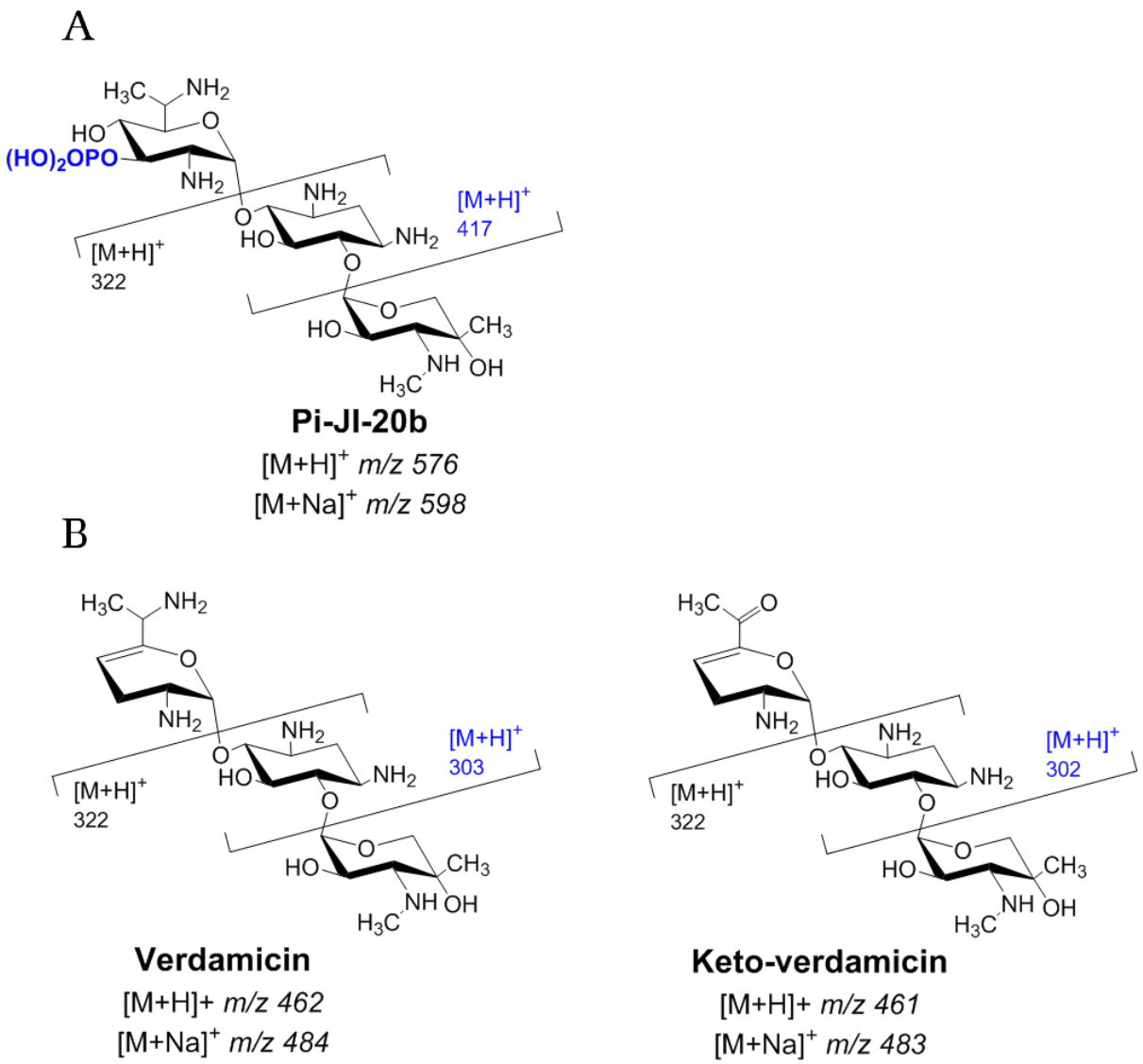

Figure 5.8 Substrate and possible products of reaction catalysed by GenB3. (A) GenB3 accepts Pi-JI-20b as a substrate; (B) two products are observed, verdamicin and keto-verdamicin, in a 1 to 3 ratio.

Pi-JI-20b was finally obtained by several methods: a large-scale incubation of JI-20b with GenP in the presence of ATP and magnesium was used to generate Pi-JI-20b for NMR analysis, while GenP immobilization and subsequent large-scale reaction with JI-20b were used for generating Pi-JI-20b as substrate for subsequent reactions. Both techniques are discussed in Chapter 3. Incubation of purified Pi-JI-20b with GenB3 produced the same two products, verdamicin and keto-verdamicin, with an excess of keto-verdamicin. In a few *in vitro* assays a small amount of 6'-keto-gentamicin C2a could also be observed.

GenB3 could therefore remove both the 3' phospho and the 4' hydroxyl group in a single step without addition of any cofactor other than PLP. The ability of GenB3 to catalyse reaction of a single phospho-group JI-20b means that GenP acts once and only on the 3' hydroxyl group.

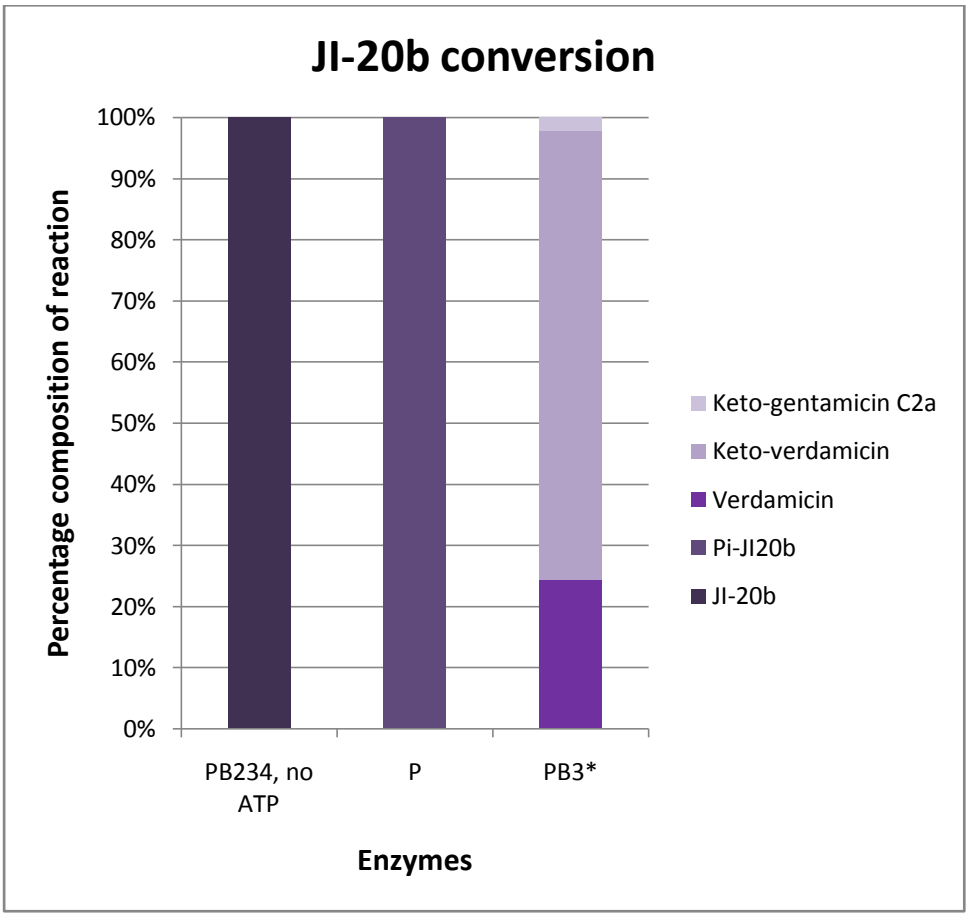

Enzymes	JI-20b	Pi-JI20b	Verdamicin	Keto-verdamicin	Keto-gentamicin C2a
GenP, GenB2, GenB3, no ATP	100.0	0.0	0.0	0.0	0.0
GenP	0.0	100.0	0.0	0.0	0.0
GenP, GenB3*	0.0	0.0	24.4±4.7	73.3±3.9	2.3±3.1

*an average of five experiments

Figure 5.9 Percentage conversion of Pi-JI-20b by GenB3. *In vitro* reactions were set up containing described mixtures of enzymes and JI-20b incubated at 37˚C for 1 hour. Five replicates were performed. GenP fully phosphorylates JI-20b in the presence of ATP. GenB3 produces keto-verdamicin and verdamicin in a 3 to 1 ratio.

5.3.2 *In vitro* assays with JI-20a and Pi-JI-20a

The two parallel branches of gentamicin biosynthesis, separated by a 6'-*C* methylation by GenK, are expected to be further catalysed by the same enzymes.

GenQ and GenB1, for example, catalyse dehydrogenation and transamination, respectively, of gentamicin X2 and the 6'-*C*-methylated compound G418. GenP can catalyse a wide variety of substrates with 3' hydroxyl groups, such as gentamicin intermediates and kanamycins A and B.

Obtaining JI-20a was essential to test if GenB3 could also catalyse the conversion of Pi-JI-20a. This was possible through generation of a Δ*genK* Δ*genB3* double mutant of *M. echinospora* by Mr Sicong Li in Wuhan. This enabled access to JI-20a for the first time. JI-20a was then incubated with GenP in the presence of ATP and magnesium. Recombinant GenB3 enzyme was added to the generated Pi-JI-20a (Figure 5.10).

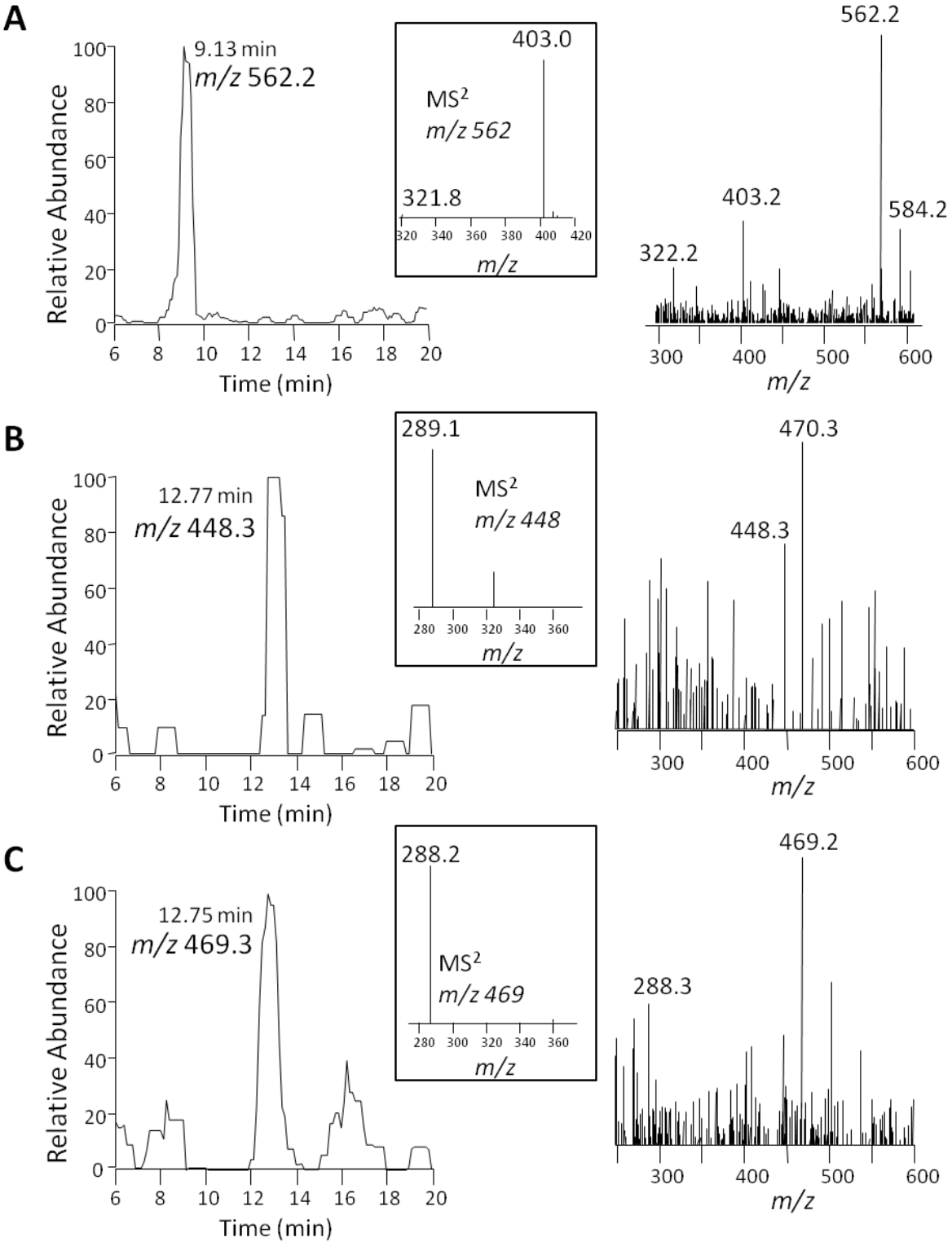

Figure 5.10 HPLC-MS of *in vitro* reaction of Pi-JI-20a with recombinant GenB3 protein. (A) GenB3 accepts Pi-JI-20a as a substrate. LC-MS chromatogram showing selected ion monitoring of the compound (left), MS:MS ion fragments of the peak (middle, *m/z* 320 to 420), and ion spectrum [*m/z* 300 to 600] of the selected peak. (B and C) two products are observed, sisomicin and keto-sisomicin, in a 1 to 3 ratio.

The two predicted products of this reaction, sisomicin and keto-sisomicin, were observed (Figure 5.11). The structure of keto-verdamicin was confirmed by an NMR analysis, however, insufficient yield prevented a similar analysis of the products of reaction of Pi-JI-20a with GenB3. The identity of *m/z* 447 ([M+Na] *m/z* 469) is presumed to be keto-sisomicin due to the fragmentation pattern of the compound during mass spectrometry.

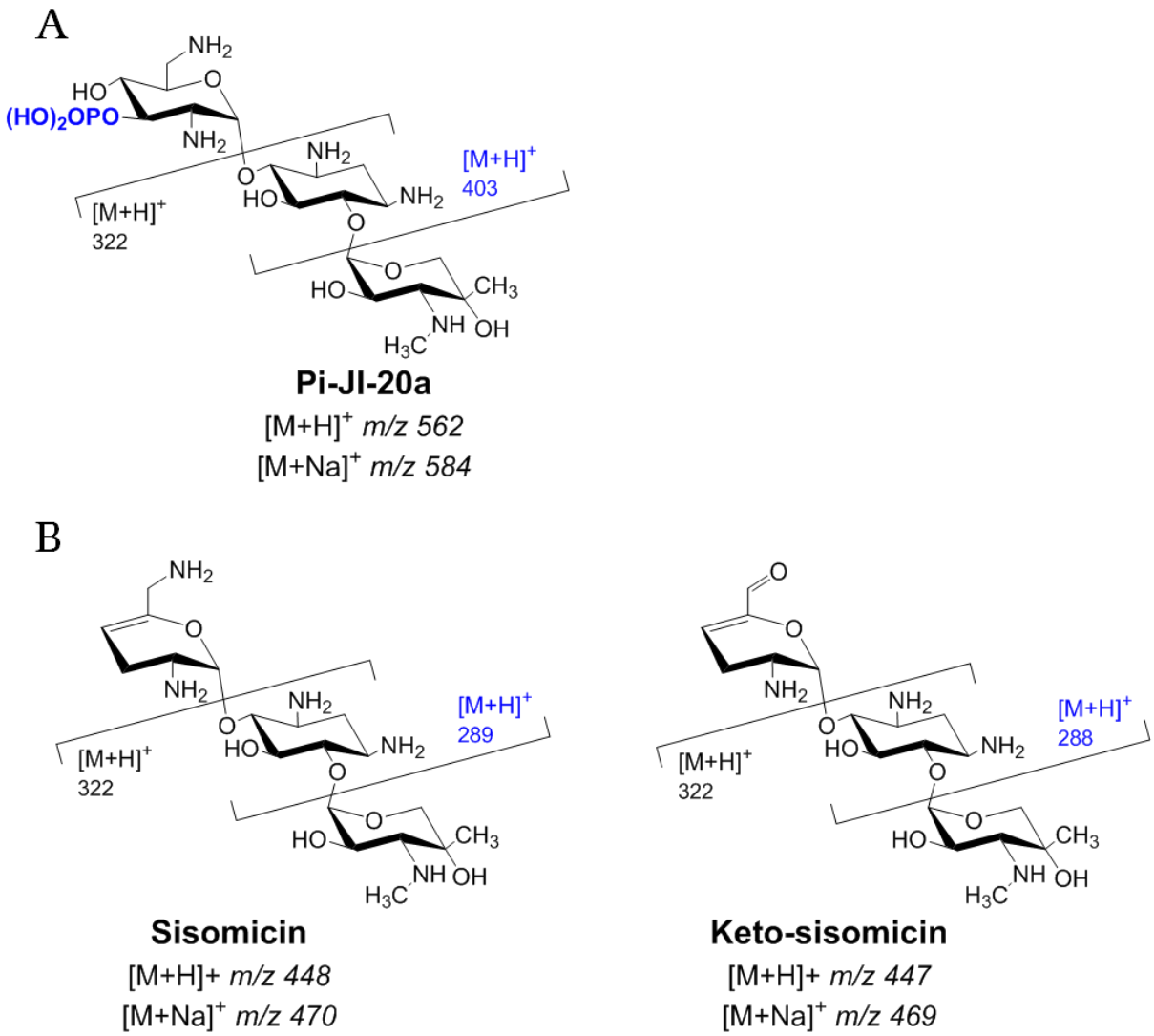

Figure 5.11 Substrate and possible products of reaction catalysed by GenB3. (A) GenB3 accepts Pi-JI-20a as a substrate; (B) two products are observed, sisomicin and keto-sisomicin, in a 1 to 3 ratio.

Therefore, GenB3 can catalyse the removal of a 3' phospho and 4' hydroxyl group from both branches of the gentamicin biosynthetic pathway. It accepts Pi-JI-20a and Pi-JI-20b as substrates, and produces sisomicin and keto-sisomicin, and verdamicin and keto-verdamicin, respectively.

5.4 A possible mechanism of GenB3 catalysis

Based on the observations from *in vitro* assays and the fact that GenB3 is a PLP-dependent enzyme, Dr Finian Leeper from the Department of Chemistry proposed a mechanism of catalysis (Figure 5.12).

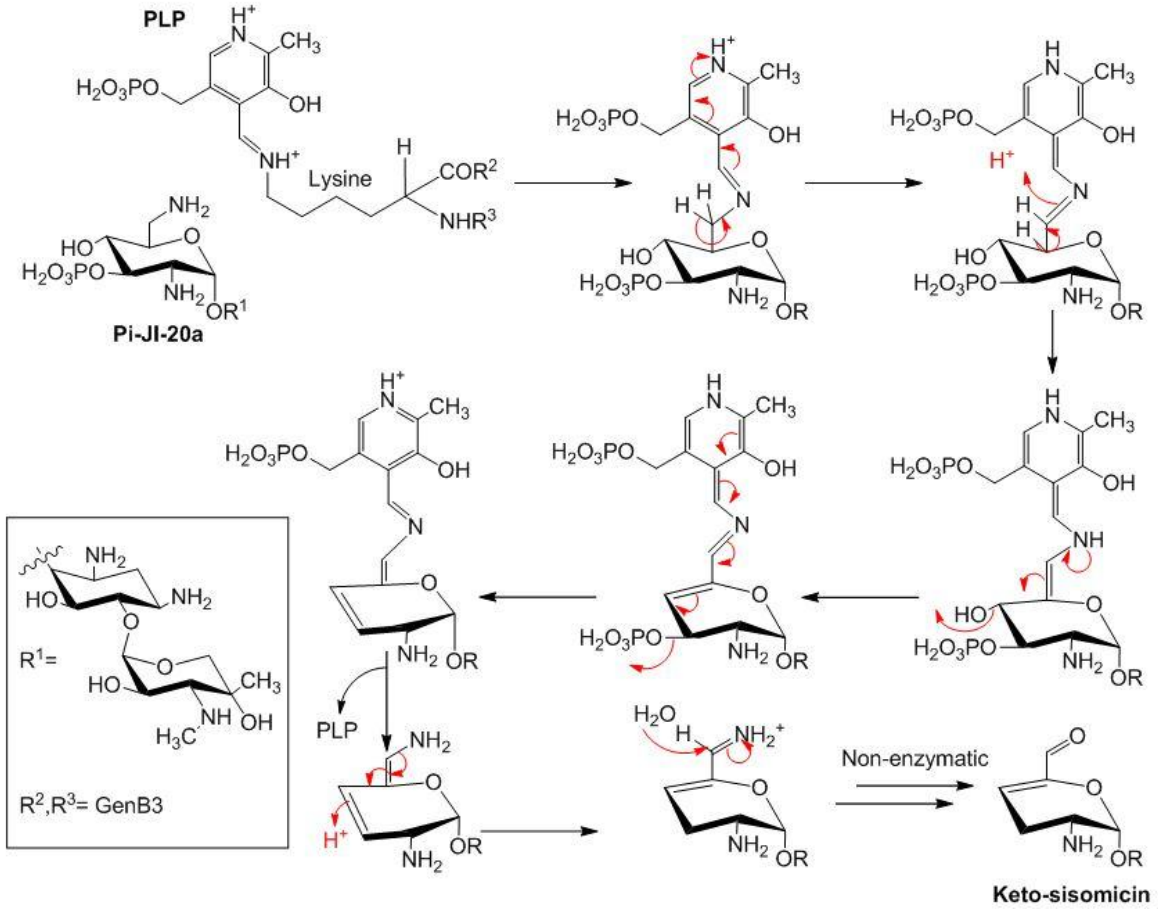

Figure 5.12 Possible mechanism of reaction catalysed by GenB3. Based on the observed products, a mechanism of phosphate and hydroxyl groups elimination can be drawn out. Here Pi-JI-20a is used as the substrate.

Most of the catalysis steps happen to a PLP-bound substrate inside the GenB3 active site and are hard to study. However, a proton is incorporated at the 3' position. *In vitro* reaction of GenB3 in heavy water resulted in incorporation of a deuterium ion, increasing the mass of the product by 1 (Figure 5.13).

5.4.1 Reaction of GenB3 in D_2O

The proposed mechanism was tested by adding recombinant GenB3 to Pi-JI-20b in D_2O. Keto products are more abundant following catalysis by GenB3 and the *m/z* of keto-verdamicin is 461. A +1 mass of keto-verdamicin, should the

deuterium ion be incorporated, would be 462, which is identical to verdamicin without the deuterium (Figure 5.13). The fragmentation patterns of the two compounds would also be the same. Therefore, only an increase in abundance of *m/z* 462 as well as presence of *m/z* 463 ([M+Na] *m/z* 485), the +1 ion of verdamicin could be used to check for deuterium incorporation during the GenB3 reaction.

Reaction of Pi-JI-20b with recombinant GenB3 enzyme yielded a +1 mass increase (Figures 5.13 and 5.14) for both verdamicin (new [M+D] *m/z* 463, [M+D+Na] *m/z* 485) and keto-verdamicin (new [M+D] *m/z* 462, [M+D+Na] *m/z* 484). For a control experiment the products of reaction of GenB3 with Pi-JI-20b were dried, resuspended in D_2O, then dried and resuspended several times in water. No incorporation of deuterium was observed. It was not possible to obtain sufficient quantities of deuterium-labelled compounds for NMR analysis.

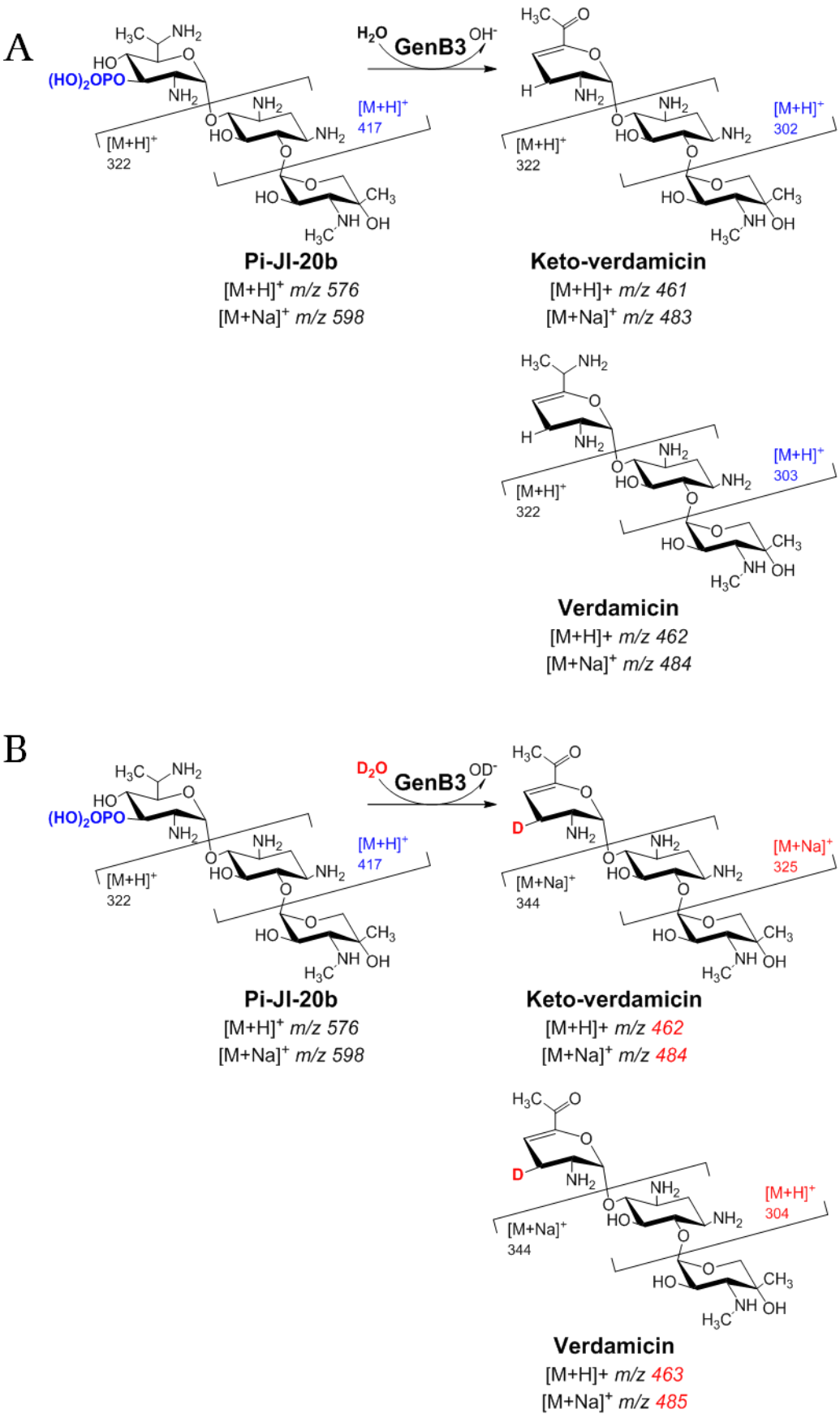

Figure 5.13 Incorporation of H^+ or D^+ during GenB3 reaction. (A) A proton from water is incorporated at 3' position; (B) deuterium ion incorporated at 3' position increases the mass by 1.

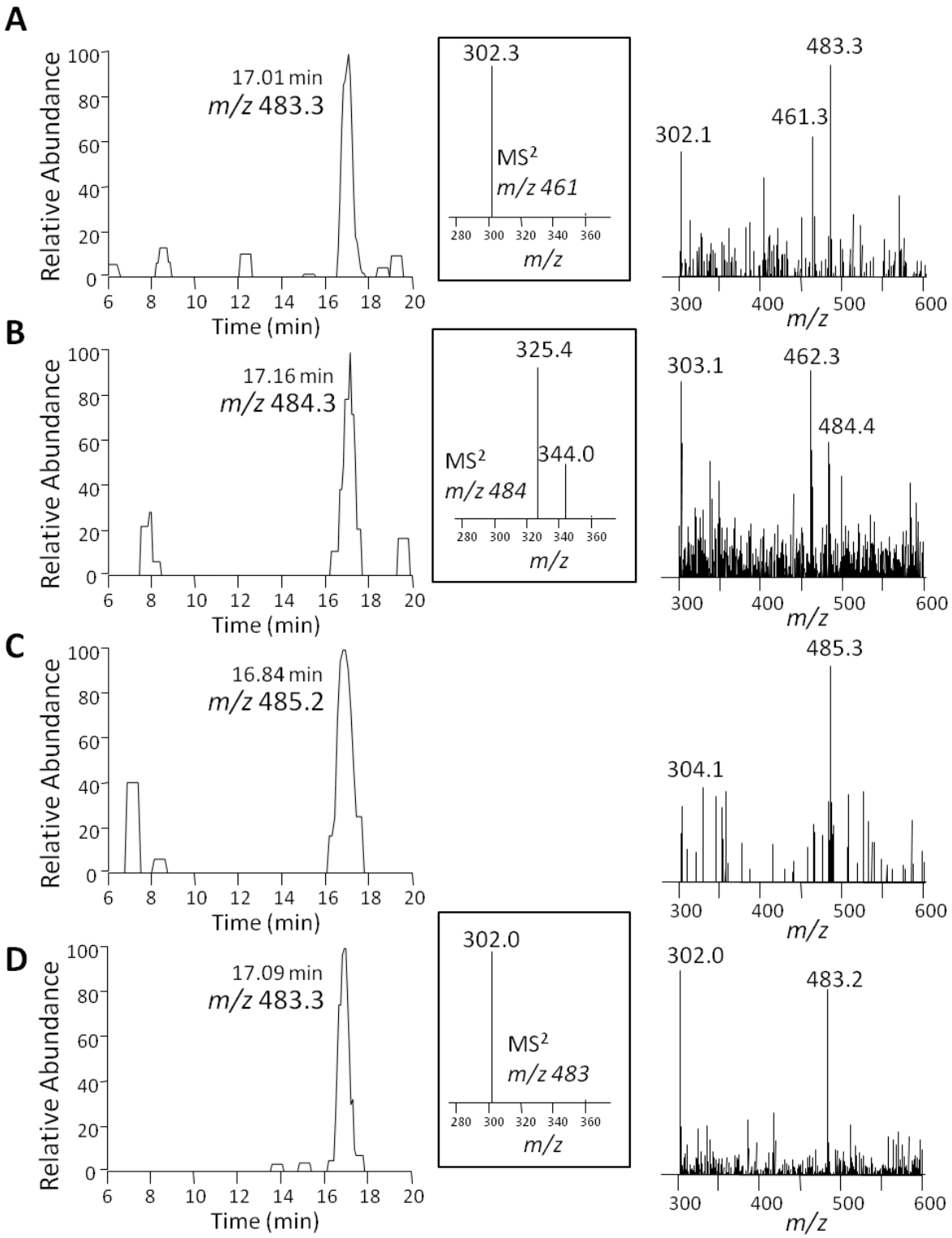

Figure 5.14 Observed products of Pi-JI-20b reaction with recombinant GenB3 protein in D_2O. (A) Reaction of GenB3 with Pi-JI-20b in water; LC-MS chromatogram showing selected ion monitoring of the compound (left), MS:MS ion fragments of the peak (middle, *m/z* 320 to 420), and ion spectrum [*m/z* 300 to 600] of the selected peak. (b and c) products of reaction of GenB3 with Pi-JI-20b in heavy water; (D) keto-verdamicin standard.

5.5 Discussion

Analysis of gentamicin intermediates produced by Δ*genB3 M. echinospora* mutant suggests that the PLP-dependent aminotransferase GenB3 could be responsible for catalysing di-dehydroxylation steps on Pi-JI-20a and Pi-JI-20b. *In vitro* assays showed that this enzyme alone is capable and sufficient for the 3'-phospho and 4'-hydroxyl groups removal of phosphorylated JI-20 compounds, making it a phospho-lyase and a dehydroxylase.

Sisomicin and verdamicin have been thought of as highly-related compounds to gentamicins. The reaction of GenB3 is the first suggestion of 4',5'-unsaturated compounds being true intermediates in the gentamicin biosynthetic pathway. A final reductase enzyme is needed to convert these products of GenB3 to gentamicins C1a and C2b.

6

Di-dehydroxylation: reduction by GenB4

6.1 Sisomicin and verdamicin as gentamicin biosynthesis intermediates

For a long time sisomicins and verdamicins were thought to be a separate class of antibiotics, closely related to gentamicin. Sisomicin, the major product of *Micromonospora inyoensis*, was discovered by Weinstein and co-workers in 1970 (Weinstein et al., 1970). Sisomicin is like gentamicin C1a, but has a 4'-5' double bond, which changes the purpurosamine ring conformation from a normal chair to a half-chair. Sisomicin has a similar spectrum of antibiotic activity to gentamicin C1a but is more potent (Nagabhushan et al., 1982). The *sis* cluster was sequenced and annotated in 2011, and many *sis* genes possess high similarity to *gen* genes. The near-identity of the two biosynthetic pathways has been known since the biotransformation experiments by Testa and Tilley (Testa and Tilley, 1976, Testa and Tilley, 1975). It is also known that feeding sisomicin to *M. echinospora* mutants, blocked early in the gentamicin pathway, leads to its conversion to gentamicins C1a and C2b (Lee et al., 1977).

Verdamicin is the major product of *Micromonospora grisea* and was discovered in 1975 (Weinstein et al., 1975). Conversion of verdamicin to gentamicin C2a by a gentamicin C2b producer *Micromonospora sagamiensis* has been reported (Kase et al., 1982c). The genome of *M. grisea* is currently being sequenced by the PFL group to discover the similarities and differences of *ver* and *gen* biosynthetic clusters.

Sisomicin and verdamicin have been shown to be products of the GenB3-catalysed reaction, together with their keto versions. A final reductase enzyme is necessary to convert the two to the first gentamicin C complex components, gentamicins C1a and C2a, respectively.

6.2 Double bond reduction

A reduction of a double bond requires introduction of two hydrogen atoms to the molecule. Various hydrogen atom donors are used as cofactors by biosynthetic reductases. For example, enoyl-acyl carrier protein (ACP) reductase enzymes catalyse the reduction of a double bond in and are essential for the elongation step of fatty acid biosynthesis, and can use either NADH, NADPH, or reduced flavin as a reductant (Massengo-Tiassé and Cronan, 2009). Enoyl reductases are also used in polyketide biosynthesis for double bond reduction in a NADH- or NADPH-dependent manner (Bumpus et al., 2008).

6.2.1 *gen* cluster: *genD3*

The *gen* cluster possesses five genes that encode oxidoreductase enzymes: *genE, genW, genD2, genD3, genQ* (Figure 6.1A). Out of these five, only the products of *genW* and *genD3* have not been characterised. GenE is involved in paromamine biosynthesis, GenD2 – in gentamicin A2 biosynthesis, and GenQ is necessary for biosynthesis of JI-20a and JI-20b. GenD3 dehydrogenase has not been assigned a function. Putative reductase *genW* was cloned into pET-28a (+), and the expressed protein showed no activity on verdamicin.

In the apramycin biosynthetic pathway, AprD3 is the catalytic reductase involved in the 3' dehydroxylation step (Figure 6.1B). Alignment of protein sequences by BLAST revealed that GenD3 is 60% identical to AprD3 (Figure 6.1C). GenD3 was expressed using protocol described in Section 2.4.3.1.1, and

showed no activity on verdamicin or sisomicin. The reductase catalysing the last step of di-dehydroxylation was not found amongst the five obvious candidates.

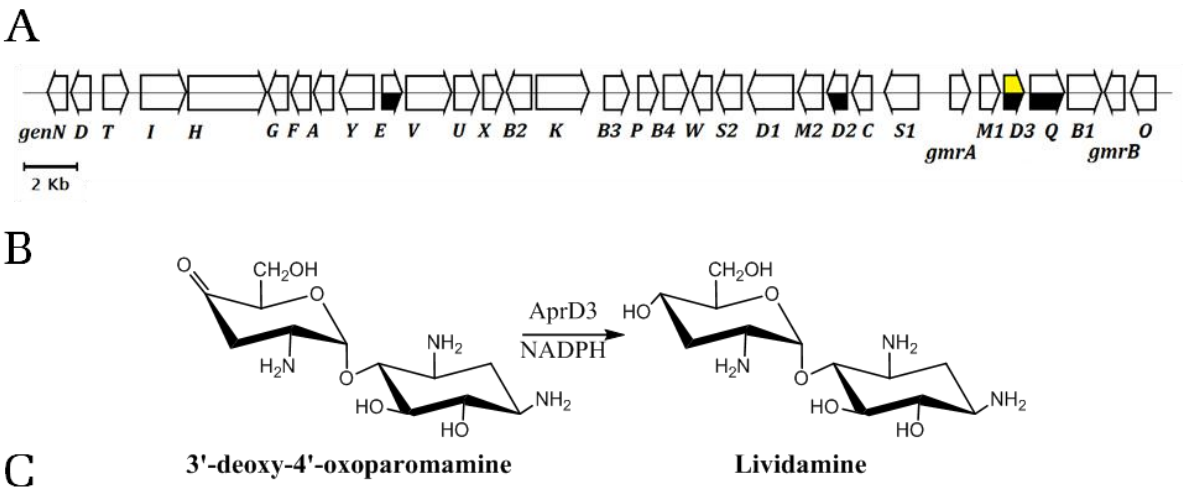


```
GenD3      MDTAPANTHVRPRRGHVLVTGGNRGLGLATATLLVDDGWSVLLGCRDERRGAAAAEALRR 60
AprD3      ----------MEQRYVLVTGASRGLGRRSAEELAGRGWTVVLACRDVADVASLLATVRG 49
                      .: :*****..****  :*  *.. **:*:*.***    *:   ::*

GenD3      RGGRAAHVPLEVTSPASIAAAVDLVADRTGGRLAGLVNNAGVFLDERDADLESVTAEAVH 120
AprD3      RGARAHAVPMDVTDPDSVAAAVDAVR-EVGGRLHALVNNAGVFRHAEE-RFPGLTPGDAL 107
           **.**  **::**.* *:***** *  ..**** .******** . .:  : .:*   .

GenD3      ELLAVNAVGPLLVTRAMVPLLRAAAGAAVVNVTADDADPATADGEATGYRMSKAALNIMT 180
AprD3      DILLTNTYGPLVVTRAFLPLLRAAGGAAVVNVTSRDADEDTFDGEFTCYRASKAALNAMT 167
           ::* .*: ***:****::******.********: ***  * *** * ** ****** **

GenD3      VNLAVALREQDVVVNAVDPGWIPTDMGGPEAPDDTAAAARLVAWAVTAAREHGTTGQVLS 240
AprD3      RNLAVALRPDRIVVNAVDPGWIPTDMGGPEAPDSLDAAVTAVVDAVELAGS-DRTGVLLR 226
            ****** : :********************.  **.  *. **  * . . ** :*

GenD3      VRQPPD---GLRADPVTVGAPPTVVPPHGQPQ---- 269
AprD3      AGRDPAPPVAAPSEPNQRHQP--DLPPPPVPRWSAS 260
           . : *    .  ::*     *   :**   *:
```

Figure 6.1 The *gen* cluster: reductase enzymes. (A) Gentamicin biosynthetic cluster contains genes four encoding reductase enzymes; (B) AprD3-catalysed reaction; (C) GenD3 is 60% identical to AprD3, a dehydrogenase catalysing a deoxygenation step in apramycin biosynthesis.

An * (asterisk) indicates a fully conserved residue, a : (colon) indicates groups with similar properties, a . (period) indicates weakly similar groups.

6.2.2 Δ*genB4 M. echinospora*

PLP-dependent enzymes are able to catalyse a wide variety of reactions (Toney, 2011). PLP-dependent enzymes can act as oxidases: a PLP-dependent enzyme

Ind4, that is involved in indolmycin biosynthesis, is able to oxidise an non-activated carbon-carbon bond (Du et al., 2016); they can also catalyse reductive reactions such as transamination.

Single knock-out mutants of GenB enzymes, two of which - GenB3 and GenB4 - are PLP-binding aminotransferases, were generated by Dr Chuan Huang in Wuhan, including a Δ*genB4 M. echinospora* (Guo et al., 2014). Analysis of the fermentation products of the mutants showed accumulation of verdamicin and keto-verdamicin (Figure 6.2). As described in Chapter 3, the mixture contained two verdamicin molecules with different retention times, which are probably stereoisomers of each other.

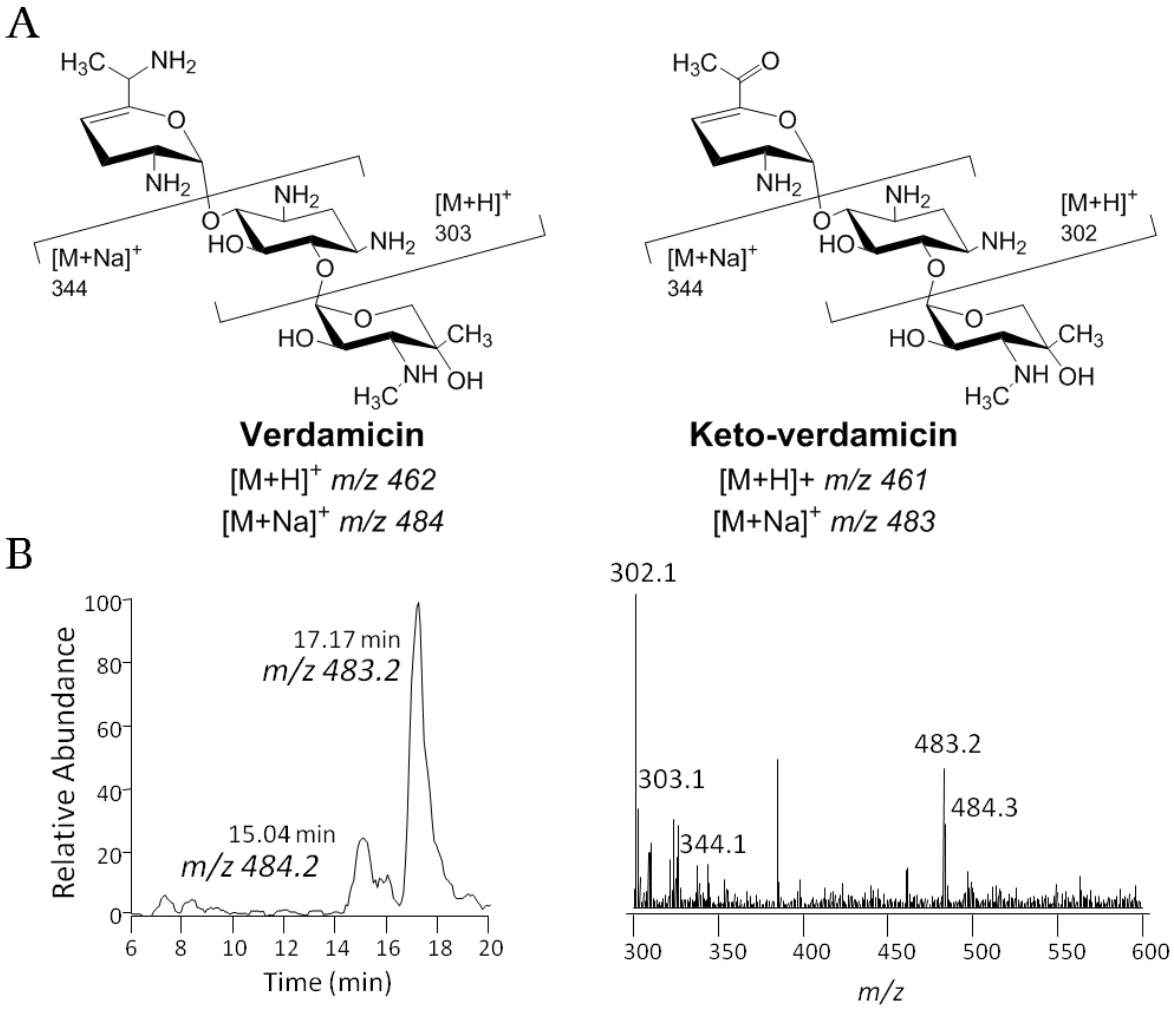

Figure 6.2 Products of Δ*genB4* mutant *M. echinospora*. Δ*genB4 M. echinospora* produces verdamicin and keto-verdamicin, gentamicin intermediates with 4'-5' double bond. Sisomicin and keto-sisomicin are also present in small amounts. No gentamicin C complex components were detected. (A) Fragmentation patterns of more abundant products: verdamicin and keto-verdamicin; (B) LC-MS chromatogram showing selected ion monitoring of verdamicin (left), MS:MS ion fragments of the verdamicin peak (middle, *m/z* 320 to 420), and ion spectrum [*m/z* 300 to 600] of the selected peak. (C) Keto-verdamicin.

6.3 GenB4 enzyme

To study the activity of GenB4 on 4',5'-unsaturated substrates *in vitro* the gene was cloned into pET-28a (+), transformed into BLR *E. coli*, and over-expressed and purified as described in Chapter 2 (Figure 6.3). Recombinant GenB4 protein has a yellow colour.

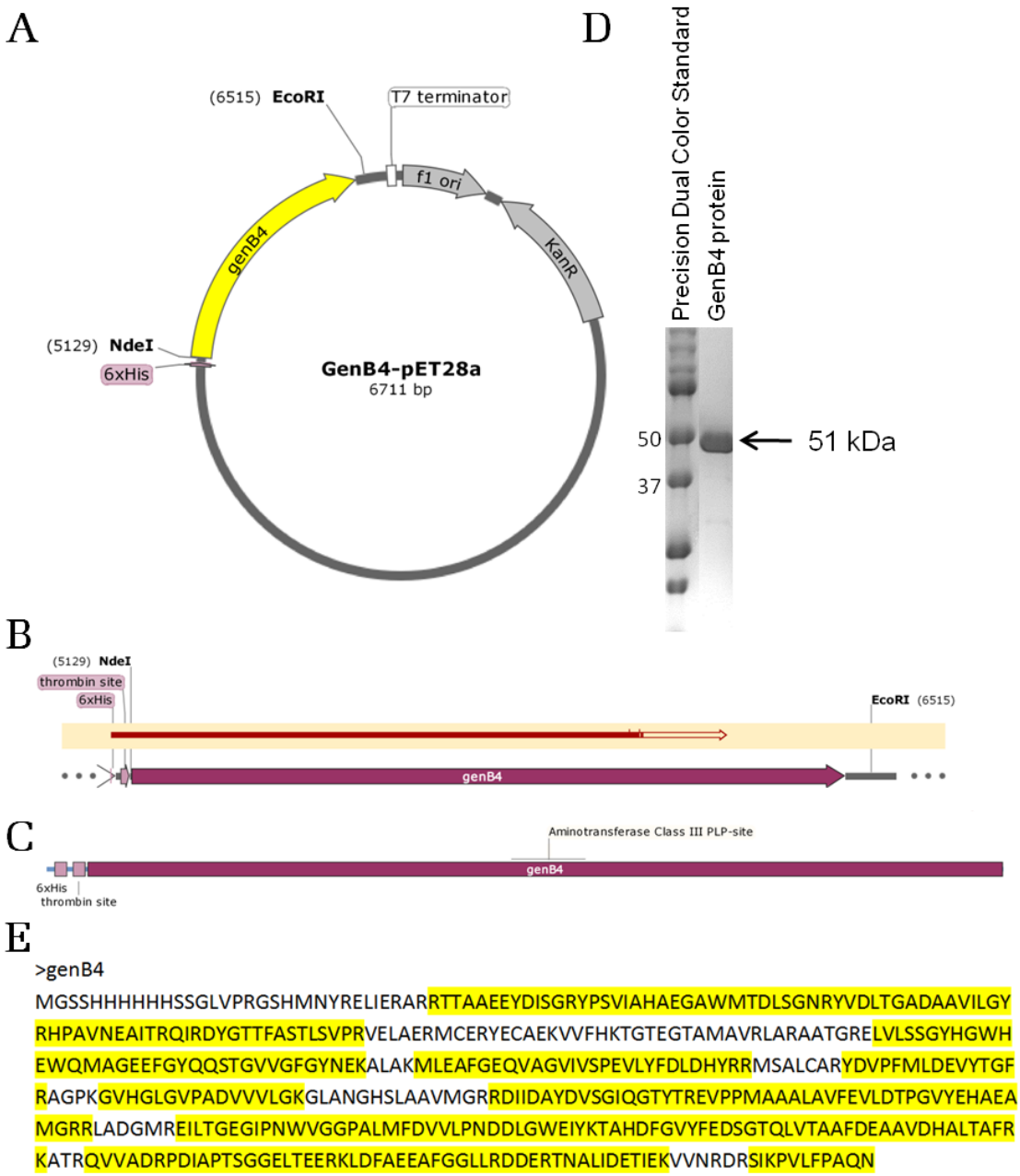

Figure 6.3 Recombinant GenB4 protein profile. (A) *genB4*-pET-28a (+) vector map; (B) confirmation of *genB4* sequence by DNA sequencing with T7 and T7t primers; (C) GenB4 protein map; (D) SDS-PAGE gel of recombinant GenB4 purified by Co^{2+} affinity chromatography; (E) MALDI fingerprinting analysis showing detected protein fragments in yellow.

6.3.1 *In vitro* assays of GenB4 with 4',5'–unsaturated substrates (Dr Fanglu Huang)

The *in vitro* activity of recombinant GenB4 (and other GenB enzymes) has been tested on sisomicin, verdamicin, and keto-verdamicin (Dr Fanglu Huang, personal communication). Conversion of sisomicin to gentamicin C1a was

achieved with GenB4 (Figure 6.4). Small amounts of gentamicin C1a could also be detected with GenB3.

Conversion of verdamicin to gentamicin C2a was achieved only when two GenB enzymes were used together: GenB4-GenB2, GenB4-GenB3, and GenB2-GenB3. Verdamicin possesses a chiral centre at the 6' position. Therefore, two possible conformations and stereoisomers are possible: verdamicins C2 (*R* conformation) and C2a (*S* conformation). Synthetic verdamicins C2 (*R* conformation) and C2a (*S* conformation) were prepared and kindly donated by Professor Steven Hanessian (Hanessian et al., 2009). Both stereoisomers of verdamicin were converted *in vitro.* The highest conversion was achieved by GenB4-GenB3. Keto-verdamicin was not converted by any combination of GenB enzymes. It is predicted that a transaminase enzyme elsewhere in the cell or one of the GenB enzymes recycles keto-verdamicin back to verdamicin in the presence of an appropriate amino donor.

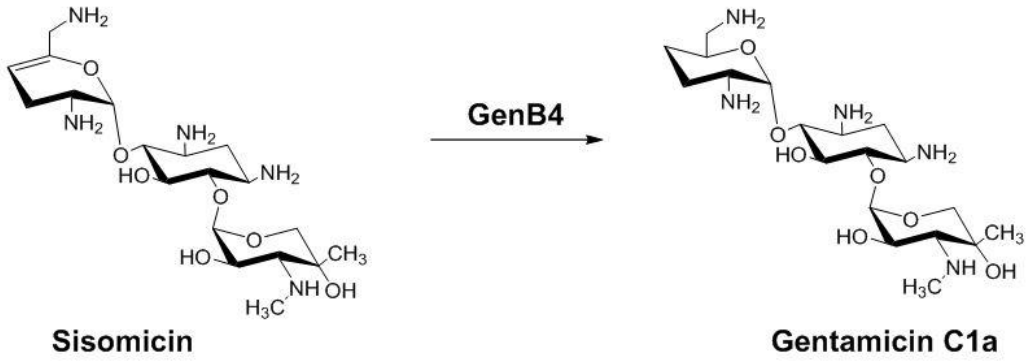

Figure 6.4 Reaction of sisomicin catalysed by GenB4. GenB4 accepts sisomicin as a substrate and is able to reduce the 4',5' double bond to give gentamicin C1a.

6.3.2 Minimal cluster experiments (Wuhan)

A *M. echinospora* mutant was constructed in Wuhan, where the entire *gen* cluster was deleted, and self-resistance gene *grmA* was re-introduced: Δ*genBN*. This mutant provided a platform for cloning in genes of interest individually or in batches. In this way the activity of Gen proteins could be tested *in vivo* without any gentamicin background.

Feeding experiments on various mutants were conducted by Mr Sicong Lee in Wuhan. Feeding JI-20 complex to *M. echinospora* Δ*genN-gmrB::gmrA*

containing *genB3* produced two verdamicin products and keto-verdamicin. Feeding JI-20a to *M. echinospora* Δ*genN-gmrB::gmrA* containing *genB3* and *genB4* led to accumulation of gentamicins C1a and C2b. The yield was improved by addition of the *genB2* gene to the mini-cluster.

Feeding of keto-verdamicin, verdamicins C2a or C2 to *M. echinospora* Δ*genN-gmrB::gmrA* with *genB4* showed that only verdamicin C2a was accepted as a substrate *in vivo*. No other enzyme outside of the cluster could reduce the 4',5' double bond *in vivo.* The feeding experiments helped compare the activity of GenB enzymes *in vitro* and *in vivo.*

6.3.3 *In vitro* assays of Pi–JI–20 with GenB3 and GenB4

Phosphorylated JI-20b was used as a substrate for an *in vitro* assay containing GenB3 and GenB4. Gentamicin C2a was observed (Figure 6.5).

Phosphorylated JI-20a was used as a substrate for an *in vitro* assay containing GenB3 and GenB4. Gentamicin C1a was observed (Figure 6.6).

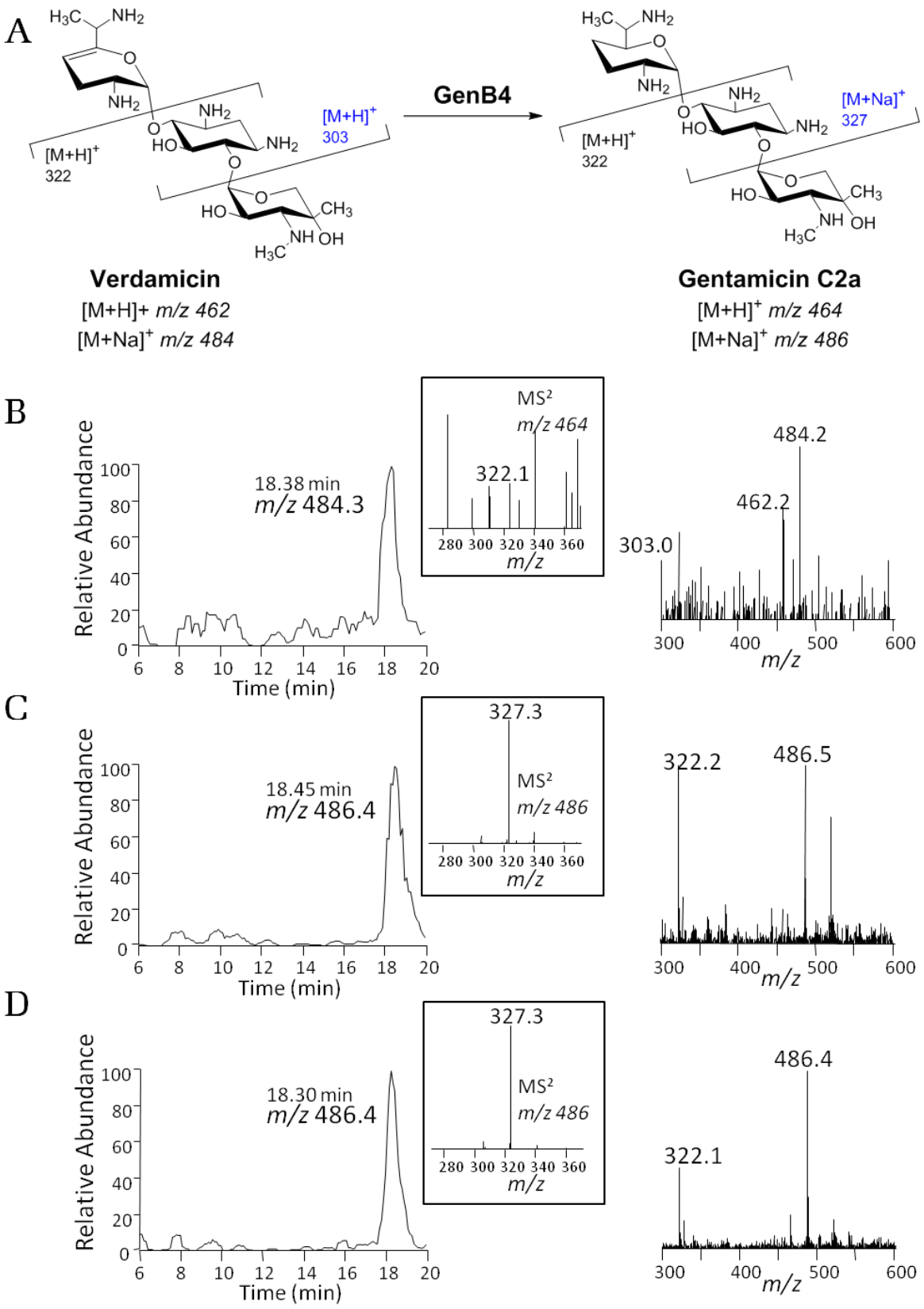

Figure 6.5 Reaction of verdamicin catalysed by GenB4. (A) GenB4 accepts verdamicin C2a as a substrate and is able to reduce the 4',5' double bond to give gentamicin C2a; (B) LC-MS chromatogram showing selected ion monitoring of substrate: verdamicin (left), MS:MS ion fragments of the verdamicin peak (middle, *m/z* 320 to 420), and ion spectrum [*m/z* 300 to 600] of the selected peak. (C) product, gentamicin C2a; (D) gentamicin C2a standard.

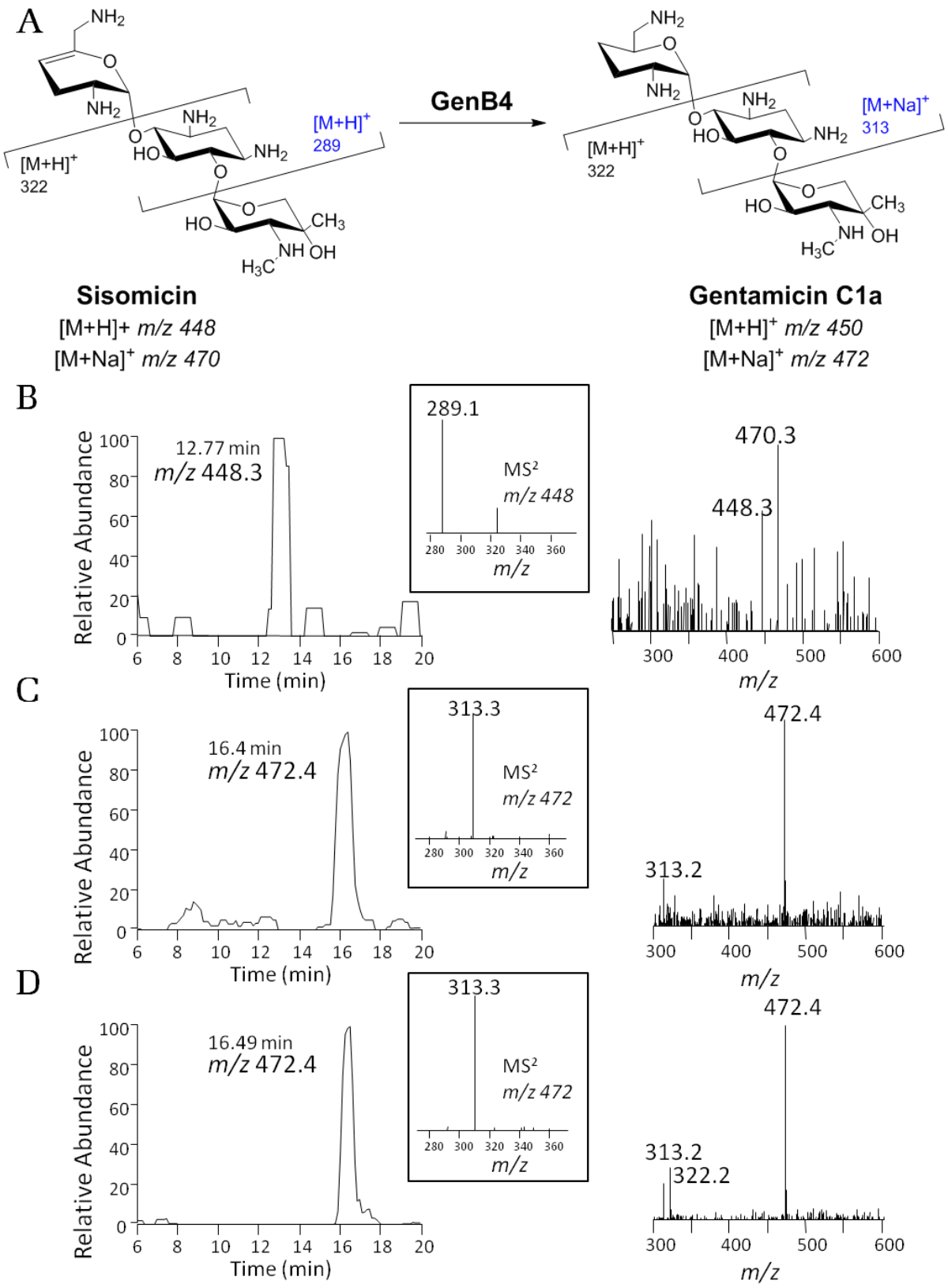

Figure 6.6 Reaction of GenB4 with sisomicin. (A) GenB4 accepts sisomicin as a substrate and is able to reduce the 4',5' double bond to give gentamicin C1a; selected ion monitoring of (B) LC-MS chromatogram showing selected ion monitoring of substrate: sisomicin (left), MS:MS ion fragments of the sisomicin peak (middle, *m/z* 320 to 420), and ion spectrum [*m/z* 300 to 600] of the selected peak. (C) product, gentamicin C1a; (D) gentamicin C1a standard.

6.3.4 *In vitro* reconstitution of di-dehydroxylation reaction

Various combinations of recombinant GenP, GenB2, GenB3, and GenB4 proteins were used on JI-20b to test for the progression of di-dehydroxylation reaction *in vitro*. GenP could fully convert JI-20b to Pi-JI-20b. GenP and GenB3 were able to convert JI-20b to a 3:1 mixture of keto-verdamicin and verdamicin. GenP, GenB3, and GenB4 together could convert JI-20b to gentamicin C2a (with verdamicin, keto-verdamicin, and keto-gentamicin C2a), but the efficiency was much improved on addition of GenB2 (even inactive GenB2 C9A mutant) to the mixture.

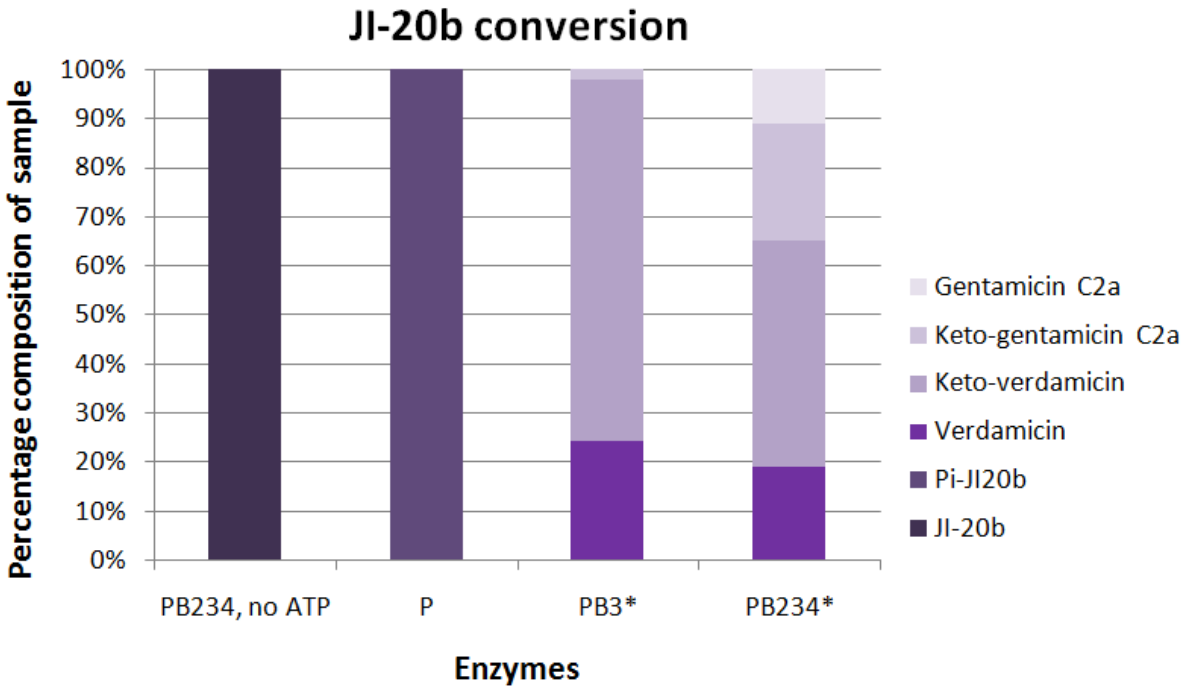

Enzymes	JI-20b	Pi-JI20b	Verdamicin	Keto-verdamicin	Keto-gentamicin C2a	Gentamicin C2a
PB234, no ATP	100.0	0.0	0.0	0.0	0.0	0.0
P	0.0	100.0	0.0	0.0	0.0	0.0
PB3*	0.0	0.0	24.4±4.7	73.3±3.9	2.3±3.1	0.0
PB234*	0.0	0.0	19.0±2.6	46.1±23.5	23.8±18.2	11.0±5.7

Figure 6.7 Conversion of JI-20b. *In vitro* reactions were set up containing described mixtures of enzymes and JI-20b (with ATP and $MgCl_2$) incubated at 37˚C for 1 hour. Five replicates were performed. GenP fully phosphorylates JI-20b in the presence of ATP. GenB3 produces keto-verdamicin and verdamicin in a 3 to 1 ratio. In combination with GenB4, di-dehydroxylation of JI-20b occurs to give gentamicin C2a.

Therefore, GenP, GenB3, and GenB4 comprise the minimal set of enzymes required for the di-dehydroxylation step in the gentamicin biosynthetic pathway. Interestingly, the three enzymes are co-located within the *gen* cluster (Figure 6.8).

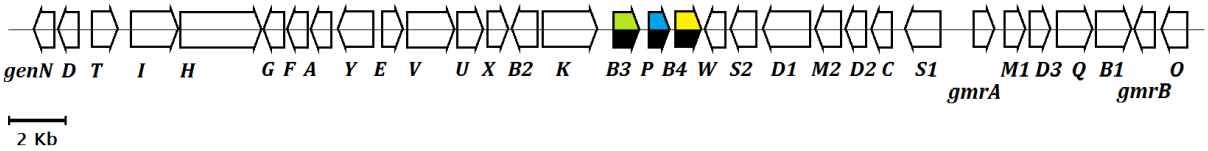

Figure 6.8 *genB3, genP, genB4* within *gen* cluster. The genes encoding the minimal set of enzymes required for di-dehydroxylation of JI-20a and JI-20b is co-located within the *gen* cluster.

6.3.5 Possible mechanism for PLP-dependent transamination

GenB4 is a PLP-dependent enzyme. No other cofactors were required or could improve the efficiency of the 4',5' double bond reduction (NADH, NADPH, various amino acids tested). Based on these facts, and the presence of multiple products in the reaction mixture, a disproportionation transamination mechanism was proposed by Dr Finian Leeper from the Department of Chemistry (Figure 6.9).

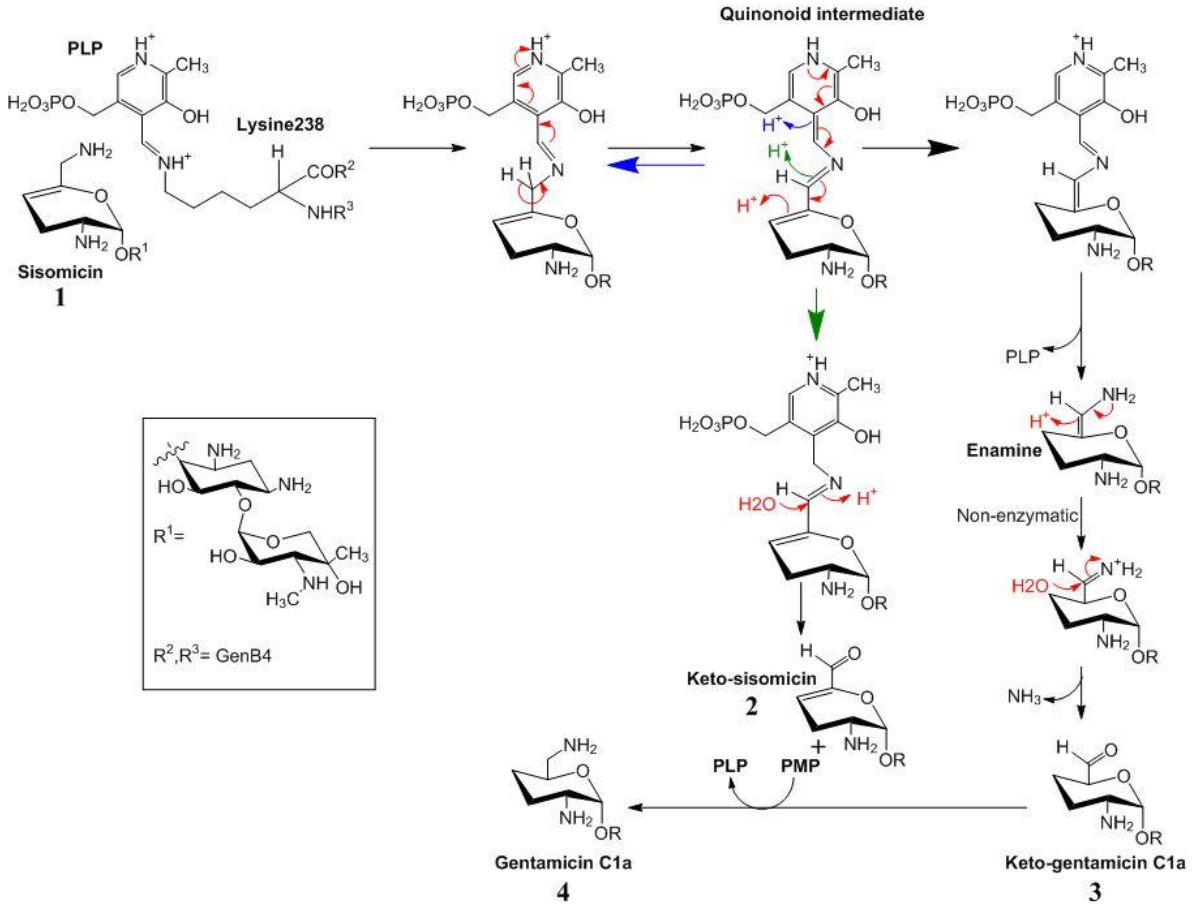

Figure 6.9 Proposed mechanism of PLP-dependent GenB4 catalysis. The reaction of sisomicin (1) with GenB3 proceeds through a keto-gentamicin C1a (3) to give gentamicin C1a (4). Keto-sisomicin (2) has to be reduced into sisomicin by another mechanism.

It was proposed that PLP-dependent transamination by GenB4 occurs through a quinonoid intermediate. There are three possible sites of protonation on the intermediate, indicated on Figure 6.9 by the blue, green and black arrows. Protonation via the blue route reverses the reaction to give sisomicin. Protonation by the green route will give keto-sisomicin (2) and PMP-GenB4. Protonation by the black arrow will be followed by an imine exchange with the active site lysine (residue 238), which will result in an imine-bound PLP and an enamine product. The enamine product will spontaneously hydrolyse in water to give ammonia and keto-gentamicin C1a (3). Transamination of keto-gentamicin C1a by a PMP-dependent enzyme would restore the PLP inside the active site and generate gentamicin C1a (4). This mechanism explains why all three products - keto-sisomicin, keto-gentamicin C1a, and gentamicin C1a - are observed. Furthermore, a mechanism to transaminate keto-sisomicin to

sisomicin using an amino group donor should also be present in the cell (by an unknown enzyme).

6.3.6 Pull-down assays with GenB enzymes

Protein complexes, consisting of the same or different species, tend to have enhanced thermodynamic and biochemical stability (Foit et al., 2009). Substrate channelling, to enhance reaction rate, is another advantage of protein interactions (Spivey and Ovádi, 1999, You et al., 2012). Because of the improved observed yield of product when inactive GenB2 protein C9A was added to *in vitro* assays containing other GenB enzymes, pull-down assays were performed to check if GenB2 could form hetero-complexes with other enzymes involved in the di-dehydroxylation reactions to stabilise them.

Genes encoding GenB2 and GenB3 were cloned into pET-28a (+) using *Nco*I and *Bam*HI and *Eco*RI restriction sites respectively (Figures 6.10 and 6.11). Use of *Nco*I removed the His-tag, creating tag-less versions of both proteins.

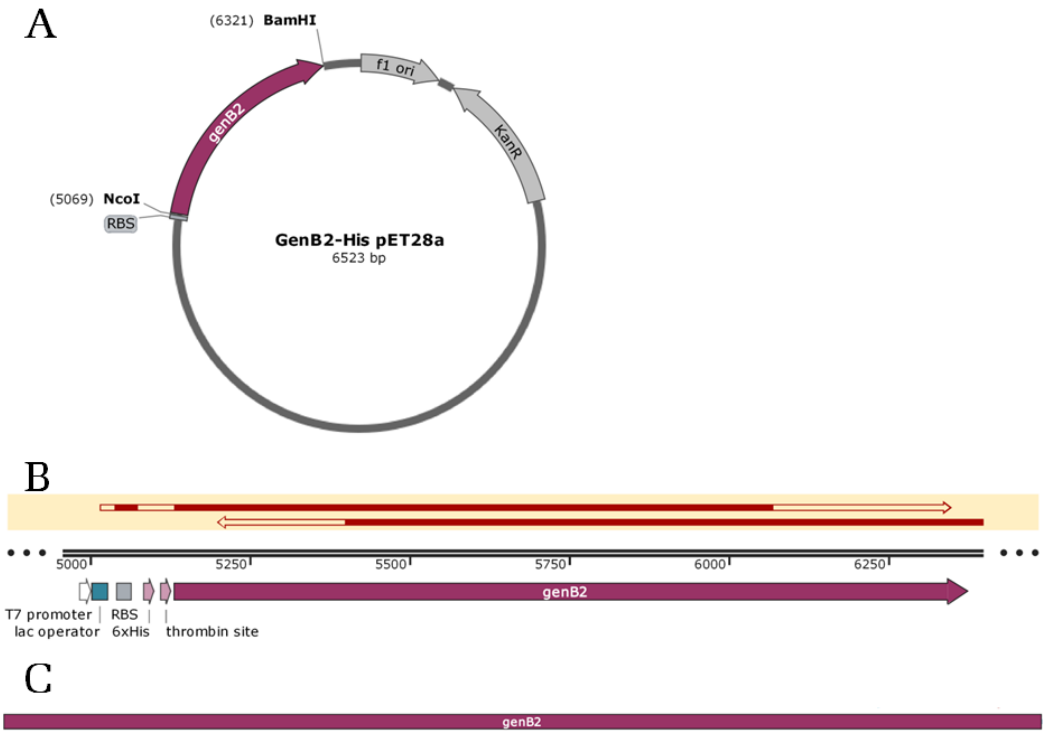

Figure 6.10 Constructs of untagged *genB2*-pET-28a (+). (A) *genB2*-pET-28a (+) vector map; (B) confirmation of deletion of His-tag within the *genB2* sequence by DNA sequencing with T7 and T7t primers; (C) GenB2 protein map without N-terminal His-tag.

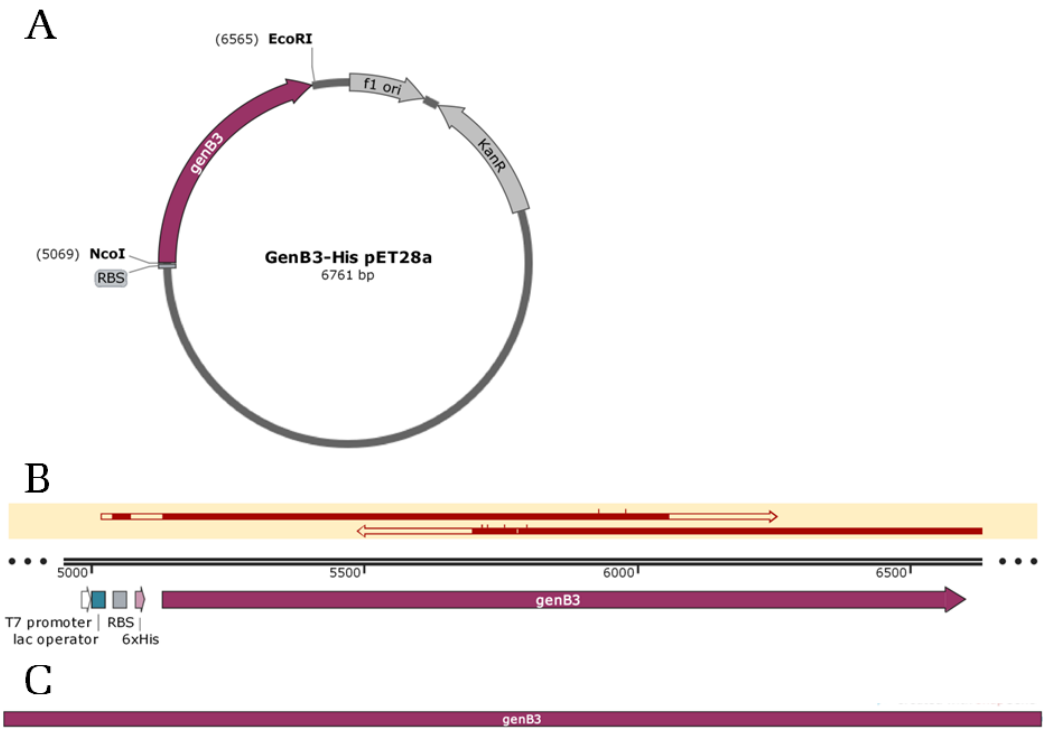

Figure 6.11 Constructs of untagged *genB3*-pET-28a (+). (A) *genB3*-pET-28a (+) vector map; (B) confirmation of deletion of His-tag within the *genB3* sequence by DNA sequencing with T7 and T7t primers; (C) GenB3 protein map without N-terminal His-tag.

The Thermo Scientific Pull-down protocol was followed. Recombinant His-tagged proteins (GenB2, GenB3, and GenB4) were purified first as previously described. They were buffer-exchanged into a buffer containing no imidazole and bound onto a Co^{2+} affinity chromatography column.

Tag-less GenB2 and GenB3 proteins were expressed in *E. coli* BLR cells. The cells were collected by centrifugation at 3600 RCF for 10 minutes. The cell pellet was resuspended in Binding buffer. An Emulsiflex homogenizer was used to lyse the cells. Supernatant was separated from cell debris by centrifugation at 48000 RCF for 1 hour at 4˚C and filtering through a 5µm membrane. The column containing the immobilised bait protein was capped, and the supernatant (5 mL) containing the un-tagged prey protein was incubated with the beads for an hour at 4˚C. Following that, the unbound protein could flow through the column. The resin was washed with Binding Buffer and 10 mM imidazole Wash Buffer before being eluted with the normal Elution Buffer for the bait protein. All the fractions were analysed by performing SDS-PAGE with a 12% (v/v) polyacrylamide gel.

Interaction was detected between GenB2 and GenB3, and GenB2 and GenB4. A pull-down consisting of His-tagged GenB4 and un-tagged GenB2 and GenB3 resulted in all three proteins co-eluting from the Co^{2+} column suggesting an interaction. The results are summarised in Table 6.1 and Figure 6.12.

Table 6.1 GenB protein pull-down experiment

Immobilised bait protein	Untagged prey protein (s)	Interaction observed
GenB2	GenB3	Yes
GenB3	GenB2	No*
GenB4	GenB2	Yes
GenB4	GenB3	No
GenB4	GenB2, GenB3	Yes

*The interaction surface may have been obstructed by the His-tag.

Interactions were observed between GenB2 and GenB3, and GenB2 and GenB4, but not GenB3 and GenB4 (Figure 6.12). However, the His-tag may not be the best choice of tag for a pull-down experiment, and a more specific tag, such as GST, is recommended for further experiments.

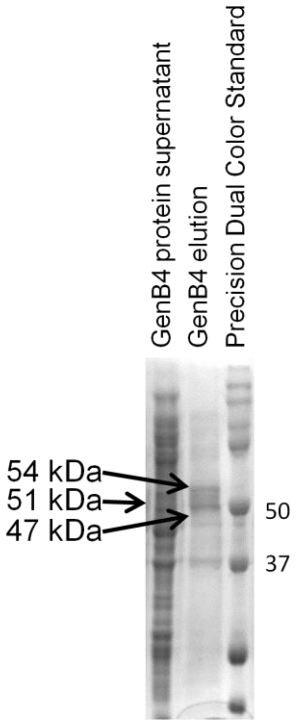

Figure 6.12 Pull-down experiment with GenB enzymes. His-tagged GenB4 protein was used as bait for untagged GenB2 and GenB3. The elution fraction contained all three proteins suggesting their interaction to form a catalytic complex**.** This result may explain why *M. echinospora* Δ*genB3* produces only one JI-20b stereoisomer despite GenB2 presence in the cells.

6.4 Discussion

In this Chapter I have shown the identity of the third enzyme required for the di-dehydroxylation step, GenB4. The minimal set of enzymes for this reaction is therefore defined. There is potential for these enzymes to be used to remove the hydroxyl groups of other aminoglycosides, particularly ones that suffer from issues of pathogen resistance development via 3' phosphorylation and 4' adenylation. Of course, in addition to biosynthetic removal of a hydroxyl groups, other routes can also be used. Chemical dehydroxylation often involves converting a *trans*-diol into dimesylate, followed by zinc-mediated elimination (Suami et al., 1977). However, the complicated nature of the structures, the presence of many unprotected groups, and the need to use biological starting material all render chemical synthesis a poor strategy for modification of aminoglycosides.

On the other hand, semisynthesis can be used to remove the hydroxyl groups with relative specificity and ease. Dibekacin (3',4'-dideoxykanamycin B) was developed using kanamycin B as starting material (Miyake et al., 1976). It could completely overcome resistance caused by 3' phosphorylating enzymes. Detailed knowledge of the catalytic mechanism, as well as developments of dynamic CCC, will allow access to new intermediates, which can be used as starting material for semi-synthetic development of new aminoglycosides.

6.4.1 The GenB enzymes

The *gen* cluster possesses four related PLP/PMP-dependent *genB* genes: *genB1, genB2, genB3,* and *genB4.* These can be separated by similarity, as *genB1/genB2* and *genB3/genB4* are more like each other than to others (Figure 6.13). Recombinant GenB1 and GenB2 proteins are pink, whereas recombinant GenB3 and GenB4 are yellow from PLP or PMP cofactors. These four aminotransferase enzymes have essential roles in catalysing the late steps of gentamicin biosynthesis: GenB1 catalyses the transamination of 6'-dehydroxy-6'-oxo-G418 and 6'-dehydroxy-6'-oxo-gentamicin X2, with the other GenB enzymes being able to complement the Δ*genB1* deletion mutant to a certain extent showing redundancy in the pathway (Table 6.2). GenB2 is an essential epimerase and a gentamicin C2 synthase. GenB3 has been shown here to be a Pi-JI-20a and Pi-JI-

20b phospho-lyase and deoxygenase. Finally, in this Chapter the role of GenB4 as the enzyme responsible for sisomicin and verdamicin reduction into gentamicins C1a and C2a respectively was described. The GenB enzymes are all essential for the biosynthesis of and are responsible for the wide variety of gentamicin components produced by the branched end pathway.

Table 6.2 GenB enzymes

Protein	Substrate	Product	Function	Complemented by
GenB1	6'-DOX and 6'-DOG	JI-20a and JI-20b	Aminotransferase	GenB2, GenB3, GenB4
GenB2	Gentamicin C2a*	Gentamicin C2	Epimerase	
GenB3	Pi-JI-20a and Pi-JI-20b	Sisomicin, keto-sisomicin, verdamicin, keto-verdamicin	Phospho-lyase, deoxygenase	
GenB4	Sisomicin, verdamicin	Gentamicins C1a and C2a	Reductase	**

**In vitro* GenB2 accepts a variety of substrates.
***In vitro* GenB2 and GenB3 together can convert verdamicin.

```
GenB3      MAVADHRSSEPSWRAGRTARRRSRWHSWARVKSAREGSQDMDSANLTNRGLVERARRVTA 60
GenB4      ---------------------------------------------MNYRELIERARRTTA 15
GenB1      -------------------------------------MTIDIGAGKLLAQEPT--- 16
GenB2      -----------------------------------------------MIIANADG--- 8
                                                            :: .

GenB3      AENYDIGTRFSAMIQSGEGAWLTDVEGNRYVDLTASSGTIILGHRNQAVTEAITRQIRDF 120
GenB4      AEEYDISGRYPSVIAHAEGAWMTDLSGNRYVDLTGADAAVILGYRHPAVNEAITRQIRDY 75
GenB1      CPRD--ADGRPRVFVEGSGAYLTDPDGRRWIDFDNARGSVVLGHGDEEVAEAIARAARGR 74
GenB2      CTPY--EVARGVTIVRGEGAYVYDAEGRGLIDLSNSFGSVMLGHQDPVVTEAVLKTVRS- 65
           .           :  ..**:: * .*.  :*:  : .:::**: .  * **: :  *.

GenB3      GTAFASTLSVPRVELAERLCERYECAEKVVFHKTGSEGTAMAARLARAATGRELILSCGY 180
GenB4      GTTFASTLSVPRVELAERMCERYECAEKVVFHKTGTEGTAMAVRLARAATGRELVLSSGY 135
GenB1      SGVGTAWSPVLDS-LLGQ-LQEVCGGDVVGLYRTGTAALRSVTCAVRDARDRSIVLSSGY 132
GenB2      -GVPAAASLDLQNHLAEQIAGDLPGDQRVAFFKTGTAATRAAASAARQVTGKRLIASCGY 124
             . ::       *  :       : * :.:**: .   ..  .* . .: :: *.**

GenB3      HGWHEWQLAGETFGYQQTTGVVGFGYNEKALAKMLEAFGNEVAGVLISPELLYFDVEFYQ 240
GenB4      HGWHEWQMAGEEFGYQQSTGVVGFGYNEKALAKMLEAFGEQVAGVIVSPEVLYFDLDHYR 195
GenB1      HGYDPMWHCDEP-FTPNQHGIVEFLFDLDVLAEWLS-RPEQVAAVVISPDHMHLGERWYT 190
GenB2      HGYDLMWEFTPP-GQPNSEDVLHCYHLPELIDQVLDKHAHELAAVIIAPDYIHVSPEYIA 183
           **:.           :  .::   .  . : : *.   .::*.*:::*: ::..

GenB3      RMYALCARYDVPFMMDEVYTGFRAGPKG-VHGLGVPADVVVVSKGLANGHSLAAVMGRRD 299
GenB4      RMSALCARYDVPFMLDEVYTGFRAGPKG-VHGLGVPADVVVLGKGLANGHSLAAVMGRRD 254
GenB1      EFTRLTKEADVPVIADEVKVGLRYRAGLSTP--LLDPAVWIVAKCLANGSPVAAVGGDAH 248
GenB2      DLFERCERVGVVTIADEVKHGYRLRQGASVTEASVVADMYTYAKGISNGWPLSCVAGDER 243
            :    . .*  : ***  * *      .   :   :   .* ::**  ::.* *

GenB3      IIDAYDVSGIQGTYTREVPPMAAAMAVLDVLDTPGVYEHAEAMGRRLADGMREILTGEGI 359
GenB4      IIDAYDVSGIQGTYTREVPPMAAALAVFEVLDTPGVYEHAEAMGRRLADGMREILTGEGI 314
GenB1      LLAALE--DVSFTSYFEPTAMAAATTTLRRMATGEPQQAIRAAGDRFIAHTRAAFANAGV 306
GenB2      FLKPLA--EFVSTLTFEAPSFAAASATLDRLAELDVQAQLAIDGARFVSEAAKMISTRDL 301
           ::       .  *   *   :*** :.:  :           * *:       ::  .:

GenB3      PNWVGGPALMFDTVLPNDDLGWEIYKTAHDFGVYFEDSGTQLVTTAFDEAAVDHALTAFR 419
GenB4      PNWVGGPALMFDVVLPNDDLGWEIYKTAHDFGVYFEDSGTQLVTAAFDEAAVDHALTAFR 374
GenB1      PIDLAGNGNLFQFVCADDEVADAFHAAAAAEGLLFFEGDNQTPSAAFTDEVVEDACGRID 366
GenB2      PIEMAGTGAAFQFVCAEE-VEEVLLPHALAEGLILEPSDQQYPSACFRGEVVDDALERLD 360
           *  :.* .  *: *  :: :   :   *   *: :  .. *  ::.*   .*:.*   :

GenB3      KATRQVIADRPDIAPTSGGELTEERKLDFAEEAFGGLLRDDERTNALIDETIEKVVNRDR 479
GenB4      KATRQVVADRPDIAPTSGGELTEERKLDFAEEAFGGLLRDDERTNALIDETIEKVVNRDR 434
GenB1      RVSAALTG---RFT---DRELTEESWYASAWGAMDGLADRPRT--REETTAI---VERLW 415
GenB2      RALTTMAAARPDLV---GREVTQLDRVNAAFCQMDGLPGRPDG--WSLDQCVEYVTAQL- 414
           :.   : .    :.   . *:*:      *   :.**             :   . :

GenB3      SIKPVLIPAQN  490
GenB4      SIKPVLFPAQN  445
GenB1      ED---------  417
GenB2      -----------  414
```

Figure 6.13 Alignment of GenB protein sequences. Clustal Omega software was used to align the four GenB protein sequences. GenB3 and GenB4 showed high degree of similarity to each other. The PLP-binding motif of GenB4 is highlighted in orange, with the PLP-binding lysine residue shown in a purple box.

6.4.2 Stereochemistry at the 6' position

Gentamicin pathway intermediate JI-20b contains a chiral centre at the 6' position due to the presence of a 6'-*C*-methyl group. The stereochemistry of G418, a JI-20b precursor, is known to be *R.* Δ*genB3 M. echinospora* produces only one JI-20b stereoisomer, but its stereochemistry is unknown at present. However, the product of the di-dehydroxylation reaction of this JI-20b stereoisomer, gentamicin C2a, possesses an *S* stereochemistry at the 6' position. The mechanisms described in this work proceed through several 6'-keto intermediates, which would cancel out the previous stereochemical layout. Therefore, only the transaminase GenB4, which catalyses the final reduction of keto-gentamicin C2a to gentamicin C2a, determines the stereochemistry of the final product. When verdamicin produced by the Δ*genB4 M. echinospora* was separated by dynamic CCC, two peaks of identical mass but with different retention time were observed, possibly corresponding to two stereoisomers of verdamicin being produced (made by GenB3 or converted by GenB2).

The active site of the transaminase enzyme determines the stereochemistry of the product (Dunathan et al., 1968). As the Δ*genB4* mutant of *M. echinospora* potentially produces two stereoisomers of verdamicin, for which GenB3 has been shown to be responsible, and the product of the GenB4 reaction (or the 6'-*C*-methylated product of Δ*genB2 M. echinospora*) is only gentamicin C2a, the PLP-binding motif of the proteins can be compared to see the reason for the difference. Surprisingly, only two residues are different between the GenB3 and GenB4 PLP-binding motifs: the pair of amino acids immediately prior to the PLP-binding lysine in GenB3 (residues 281 - 282) is valine - serine, but in GenB4 (residues 236 - 237) it is leucine - glycine (Figure 6.12). The aminoglycoside binding site, which should be located near the PLP-binding site, is also important for stereochemistry determination. To help find out why these differences can produce two different isomers and to confirm the stereochemistry of the transaminations, crystal structures of GenB3 and GenB4 with bound intermediates will be necessary. It would also be interesting to see if by mutating the active site (PLP-binding motif) of GenB3 or GenB4 a preference for synthesis of a specific stereoisomer could be achieved.

6.4.3 GenB2 enzyme

GenB2 enzyme has been described by our lab as an essential epimerase and gentamicin C2 synthase (Guo et al., 2014). The reaction is reversible. Mutant Δ*genB2 M. echinospora* does not produce gentamicins C2 and C1. GenB2 has been expressed and is a bright pink protein (Figure 6.14). *In vitro* this enzyme can interconvert two stereoisomers of JI-20b, verdamicin, and gentamicin C2, always producing a mixture of two stereoisomers (Figures 6.15, 6.16, 6.17). Therefore, GenB2 is essential for generation of 6'-methylated stereoisomer pairs: JI-20b and JI-20ba, verdamicins C2 and C2a, and gentamicins C2 and C2a.

One observation that does not fit in with the above description of GenB2 is that *in vivo* only one JI-20b stereoisomer is present in the fermentation mixture of Δ*genB3 M. echinospora*. GenB3 has not shown any epimerase activity *in vitro*.

Only one verdamicin, verdamicin C2a (*S* conformation), is accepted as substrate for GenB4. Only one gentamicin C2 stereoisomer, gentamicin C2 (*R* stereoisomer) is further methylated at the 6'-*N* position to give gentamicin C1. GenB2 enzyme is, therefore, essential for inter-conversion of gentamicin stereoisomers, but the conformation is selected for by other enzymes.

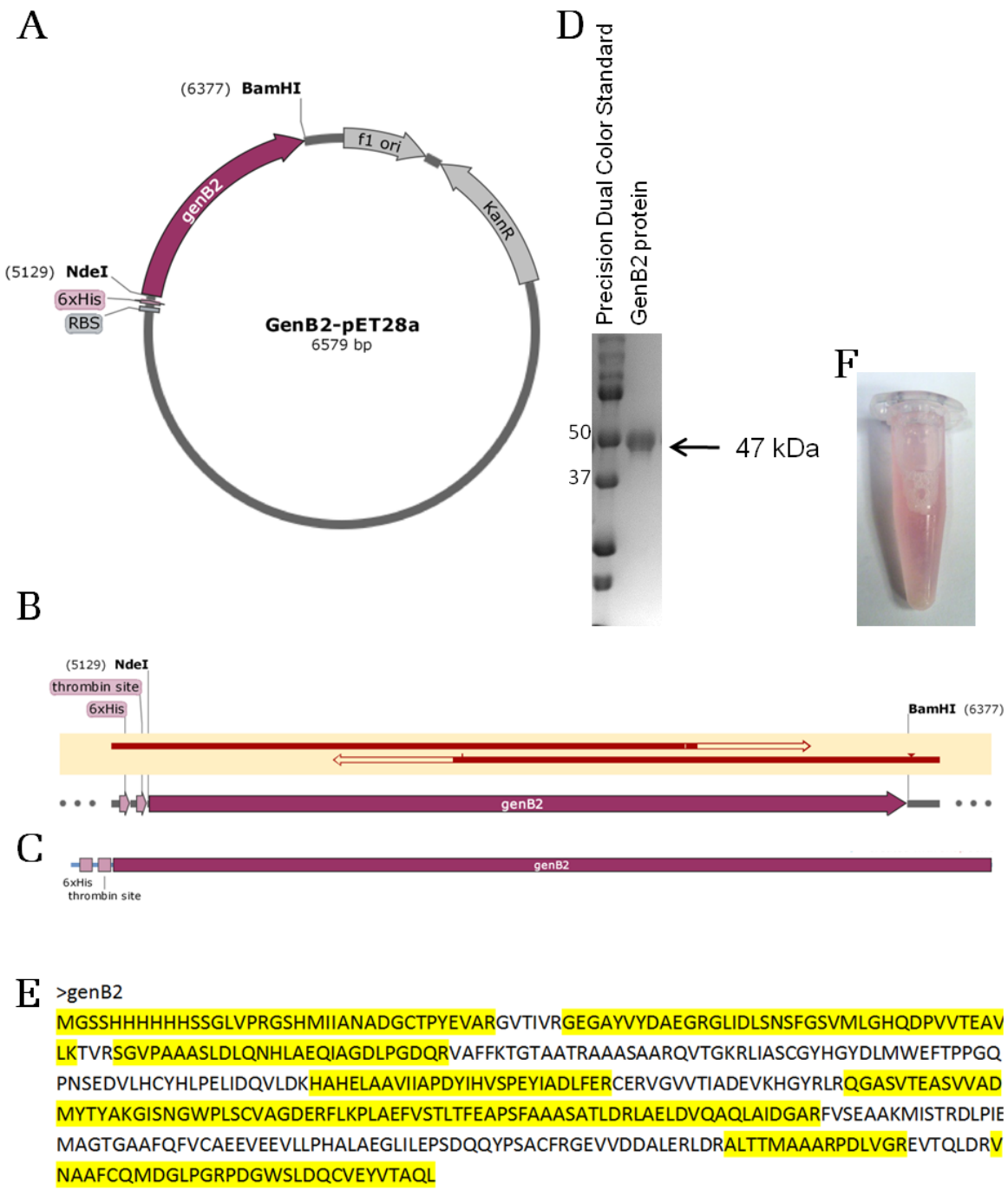

Figure 6.14 Recombinant GenB2 protein profile. (A) *genB2*-pET-28a (+) vector map; (B) confirmation of *genB2* sequence by DNA sequencing with T7 and T7t primers; (C) GenB2 protein map; (d) MALDI fingerprinting analysis showing detected protein fragments in yellow; (E) SDS-PAGE of recombinant GenB2 purified by Co^{2+} affinity chromatography.

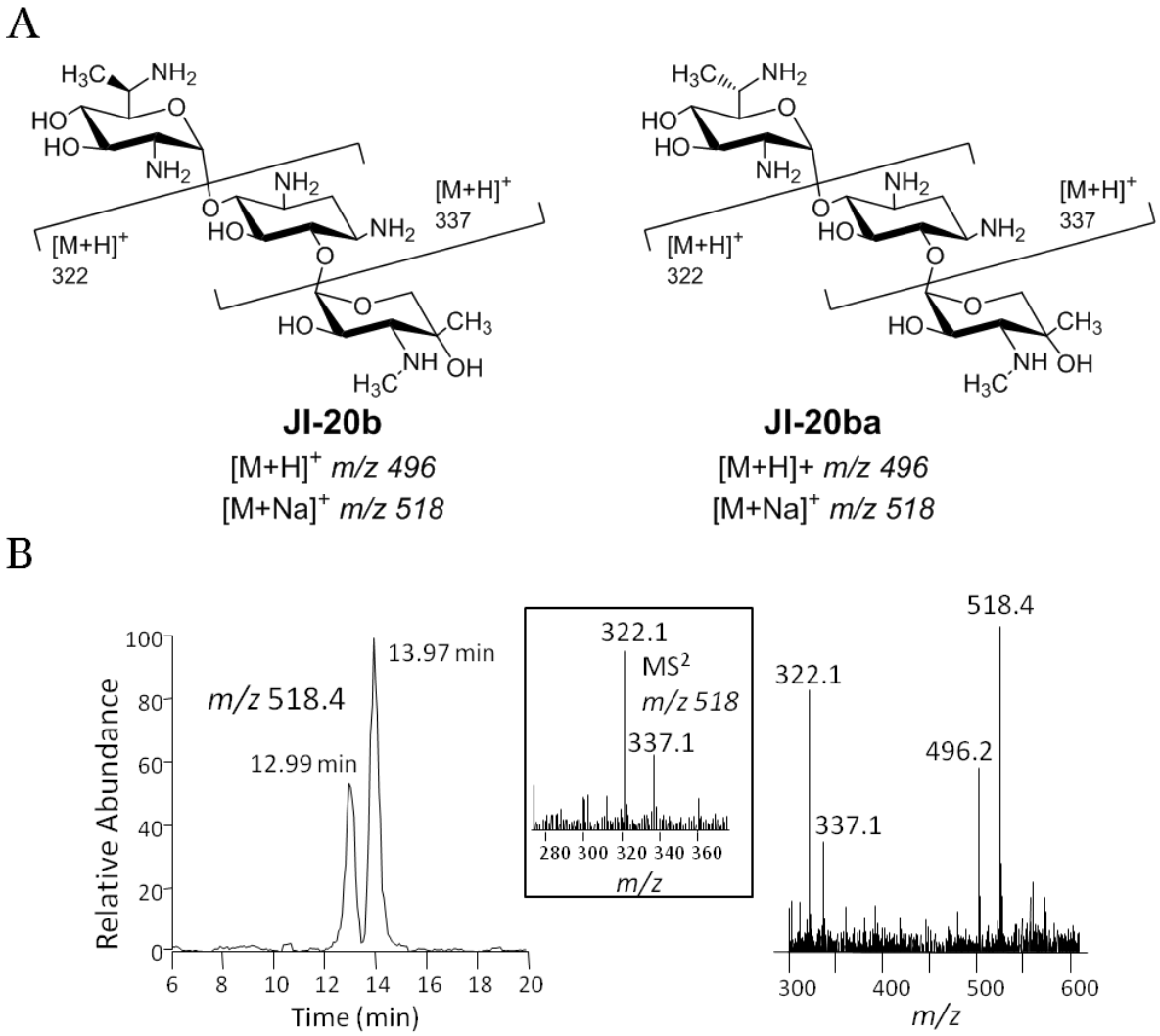

Figure 6.15 *In vitro* reaction of GenB2 with JI-20b. (A) GenB2 produces two stereoisomers, JI-20b and JI-20ba; (B) when analysed by LC-MS, their mass (and *m/z* - left) and ion fragmentation patterns (right) are identical, but the retention time differs. Similarly, the ms/ms fragmentation pattern (middle) is the same.

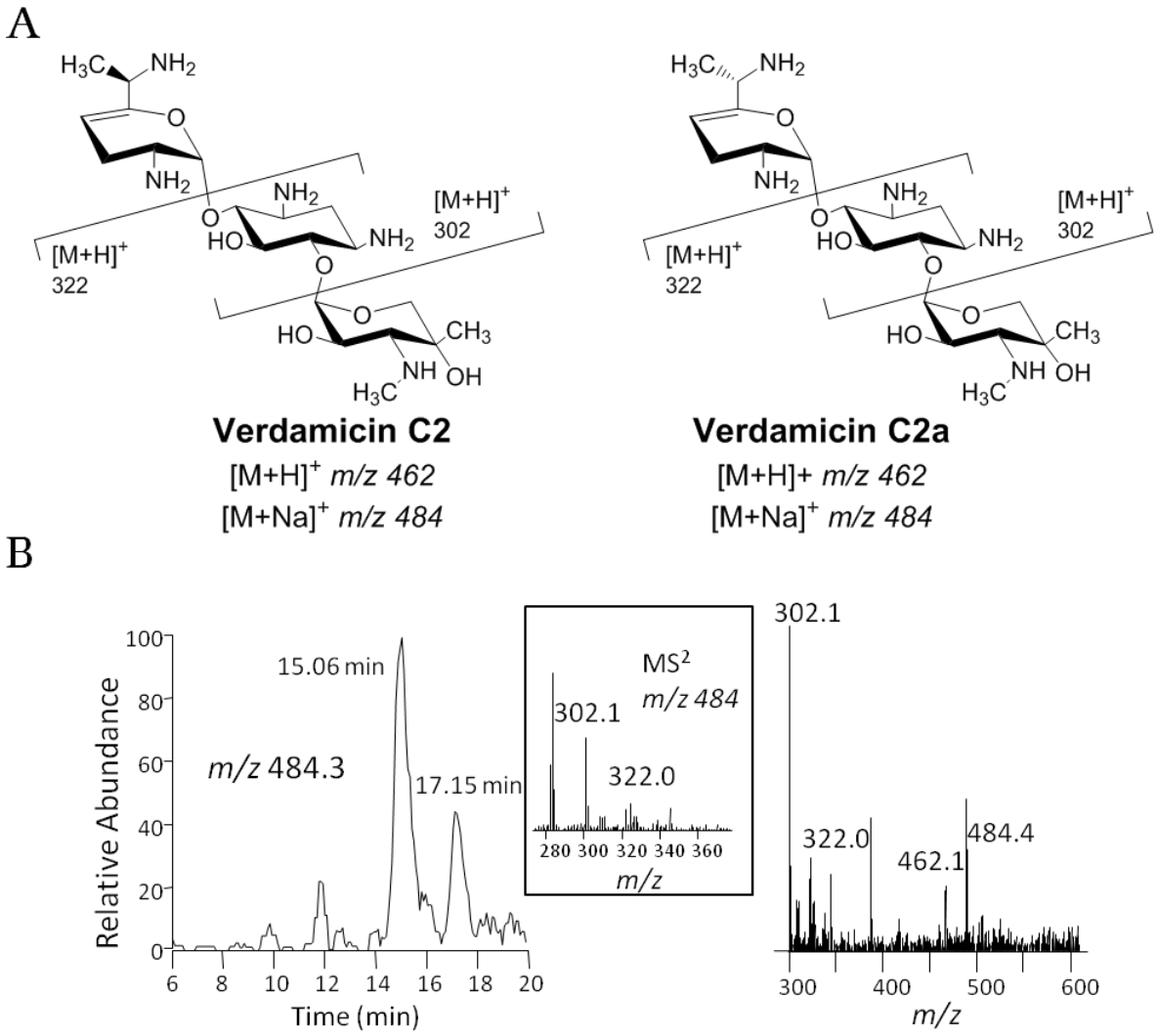

Figure 6.16 *In vitro* reaction of GenB2 with verdamicin C2. (A) GenB2 produces two stereoisomers, verdamicins C2 and C2a; (B) when analysed by LC-MS, their mass (and *m/z* - left) and ion fragmentation patterns (right) are identical, but the retention time differs. Similarly, the ms/ms fragmentation pattern (middle) is the same.

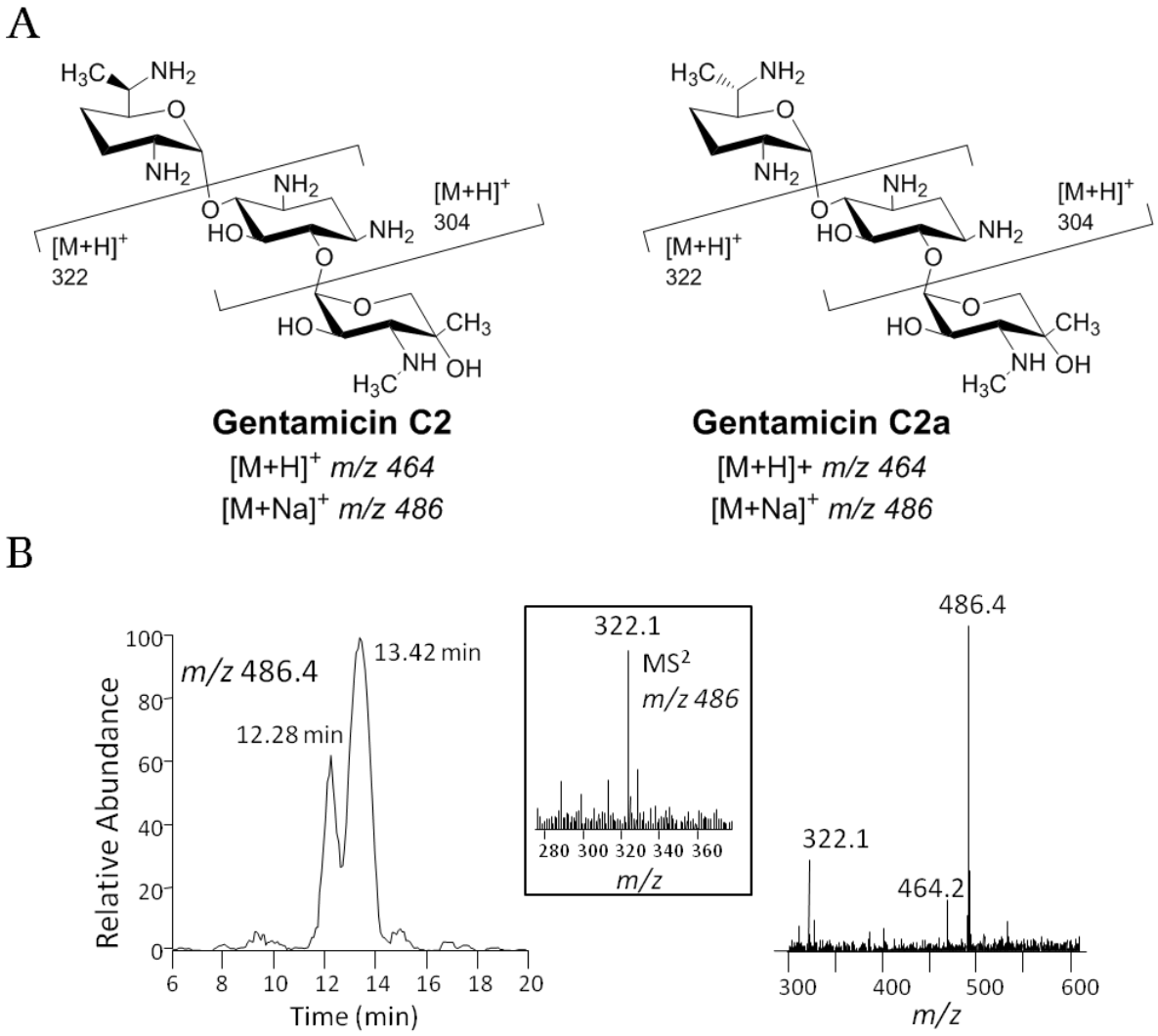

Figure 6.17 *In vitro* reaction of GenB2 with C2. (A) GenB2 produces two stereisomers, gentamicins C2 and C2a; (B) when analysed by LC-MS, their mass (and *m/z* - left) and ion fragmentation patterns (right) are identical, but the retention time differs. Similarly, the ms/ms fragmentation pattern (middle) is the same.

7

Methylation of gentamicins C1a and C2

Gentamicin C complex is made of five components which differ in their 6'-C- and 6'-*N*-methylation patterns (Figure 7.1) (Byrne et al., 1977). Gentamicins C2a, C2, and C1 have a methyl group at 6'-*C*, and gentamicins C2b and C1 have a 6'-*N*-methyl group. Furthermore, gentamicins C2 and C2a are 6'-*C* epimers of each other, and gentamicins C2 and C1 both possess 6'-*R* stereochemistry at the amine centre (Byrne et al., 1977). The gentamicin C complex is obtained by fermentation; thus, the composition of the mixture varies, but in general, gentamicin C1 is the major component (around 30+%), followed by gentamicin C1a (around 30%), gentamicin C2 (around 25%), gentamicin C2a (less than 10%), and gentamicin C2b (less than 5%) (Vydrin et al., 2003, Byrne et al., 1977).

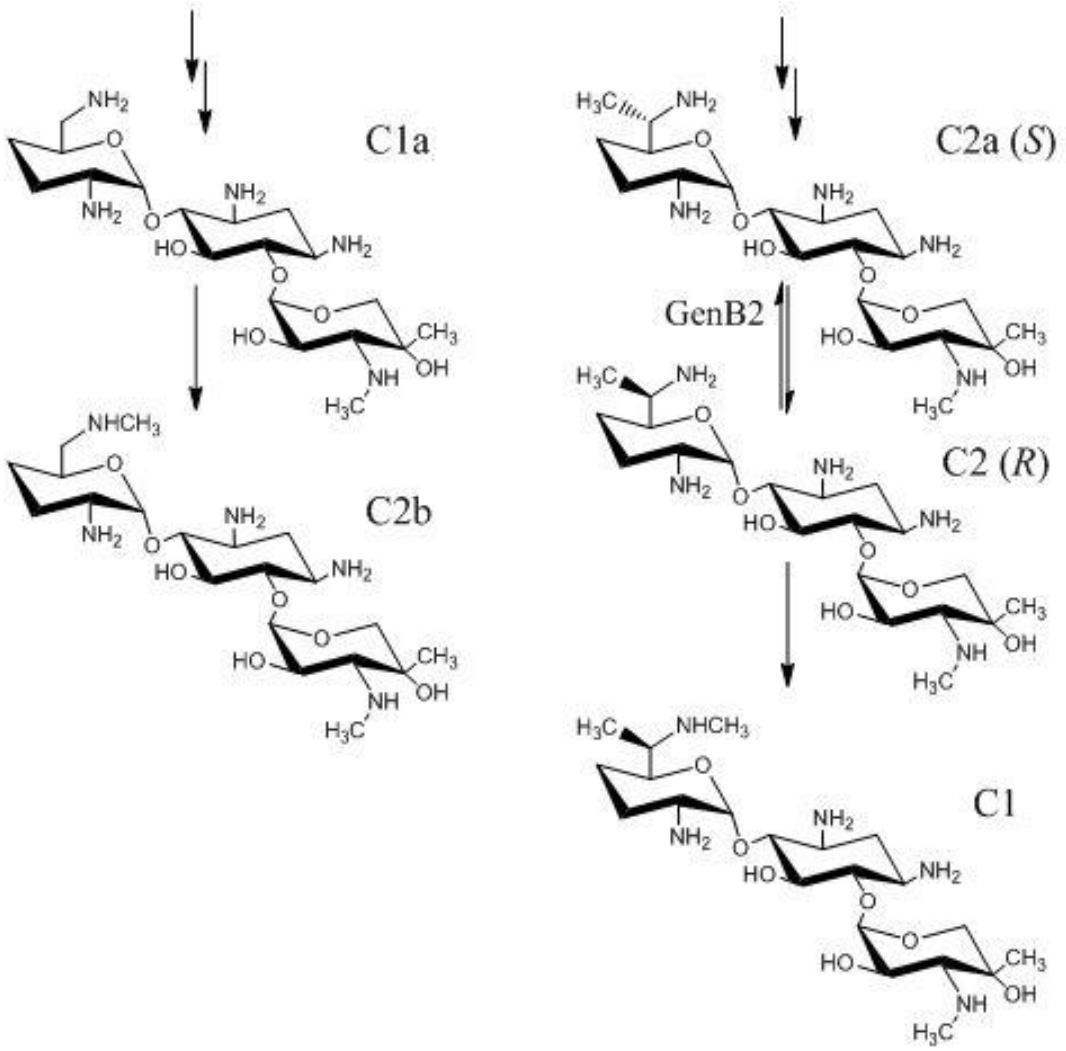

Figure 7.1 Gentamicin C complex. The final reactions of the biosynthesis generate the 5 gentamicin C complex components. Gentamicin C1a does not have any methyl groups on the purpurosamine ring; gentamicin C2b is 6'-*N*-methylated gentamicin C1a, while gentamicin C2a is 6'-*C*-methylated gentamicin C1a; gentamicin C2 is a 6'-epimer of gentamicin C2a, and gentamicin C1 is 6'-*N*-methylated gentamicin C2 or 6'-*C,N*-dimethylated gentamicin C1a.

Two methylation reactions are therefore required to generate the different C complex components: 6'-*C* and/or 6'-*N*. GenK was identified as the 6'-*C*-methyltransferase responsible for one of the two methylation reactions at the purpurosamine ring (ring B) (Kim et al., 2013). GenK is a SAM- and cobalamine-dependent enzyme, and is a relative of ForK, an equivalent enzyme in the fortimicin cluster. Testa and Tilley suggested two parallel branches of gentamicin biosynthesis, created by the GenK reaction (Piepersberg et al., 2007b, Testa and Tilley, 1976); Guo *et al* confirmed this by showing that both gentamicins X2 (GenK substrate) and G418 (GenK product, 6'-*C*-methyl-

gentamicin X2) could be catalysed further by the same enzymes (Guo et al., 2014).

Within the gentamicin structure, the purpurosamine ring (Ring II) contains essential points of contact with 16S rRNA in the bacterial ribosome, the aminoglycoside target. The groups bound to the 6' carbon interact with A1408 and C1409 of helix 44 (Yoshizawa et al., 1998). This part of the molecule is thought to be subject to an ongoing evolution, to produce complex mixtures of antibacterial compounds (Piepersberg et al., 2007a).

The identity of the 6'-*N*-methyltransferase has long remained a mystery. From the composition of the C complex several predictions about it can be made. Firstly, the discovery of parallel branches in gentamicin and kanamycin biosynthetic pathways leads to the idea that there is a single enzyme which can catalyse both pathway branches (Guo et al., 2014, Park et al., 2011). This is further supported by work done by Kase *et al*, that presented a mutant of *M. sagamiensis* (gentamicin C2b-producing strain, DSM 43912), KY 11566, that produced only un-6'-*N*-methylated C complex, increasing the probability that a single enzyme catalyses both of the reactions (Kase et al., 1982b). Secondly, the ability of this enzyme to catalyse reactions of the 6'-*C*-methylated branch (gentamicin C1 branch) is greater, as indicated by the much higher levels of gentamicin C1 as compared to gentamicin C2b in the final mixture. Thirdly, the lack of an epimer of gentamicin C1 shows that this methyltransferase is stereo-specific. And finally, 6'-*N*-methyltransferase should be a SAM-dependent enzyme, as all the methyl groups of the gentamicin structure were shown to be derived from methionine in a labelling experiment performed by Lee *et al*; Deguchi *et al* also showed this specifically for gentamicin C1a to C2b conversion (Lee et al., 1973, Deguchi et al., 1977). Another mutant of *M. sagamiensis,* KY 11564, produced gentamicins C1a, C2b, and C2a only, presumably because the gentamicin C2 synthase (now known to be GenB2) was absent from it (Kase et al., 1982b).

In addition, as the ultimate step of gentamicin biosynthesis and a crucial one for generating the complete gentamicin C complex, this 6'-*N*-methyltransferase enzyme is predicted to be located within the *gen* gene cluster.

All the enzymes needed to catalyse post-gentamicin X2 steps have evolved from fortimicin gene cluster, however, fortimicin itself does not possess a 6'-*N*-methyl group (Piepersberg et al., 2007b).

In this chapter the identity of the 6'-*N*-methyltransferase is revealed, with functional and structural studies of the enzyme.

7.1 Genetic characterization of *Micromonospora echinospora* ATCC 15835

The initial targets of our investigation were the six methyltransferases present in the gentamicin cluster (Figure 7.2).

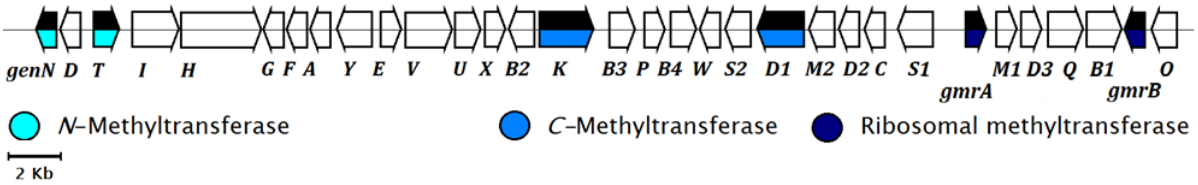

Figure 7.2 Methyltransferases of the *gen* cluster. Genes for six methyltransferases are present in the GEN cluster: two *C*-methyltransferase genes, *genK* and *genD1*, two ribosomal methyltransferase genes, *gmrA* and *gmrB*, and two *N*-methyltransferase genes, *genN* and *genT.*

These were cloned and investigated *in vitro* by Dr Fanglu Huang and by feeding studies of deletion mutants by our collaborators in Wuhan, with no positive result. However, to be able to feed antibiotics to the mutants, *gmrA* methyltransferase resistance gene had to be kept in. To make sure that the recombinant gmrA protein (Figure 7.3A) was active *in vitro*, a feeding experiment with *gmrA*-pET-28a (+) BLR *E. coli* was performed. *E. coli* cells were grown in 4 x 10 mL of LB medium and gmrA expression was induced with IPTG at A_{600} = 0.6 in tubes 1 and 3. The cells were incubated for an hour at room temperature, then 0.5 mg of gentamicin C1a or C2 was added to tube 1 and 2, and 3 and 4 respectively. The cells were grown overnight, spun, and disrupted by sonication. Gentamicins were purified using the standard protocol. No conversion of gentamicins C1a or C2 was observed.

For another closely-related aminoglycoside, istamycin, the equivalent reaction is performed by IstU methyltransferase (Kudo and Eguchi, 2009). A synthetic and codon-optimized gene of *istU* was transformed into *E. coli* BLR

cells and expressed (Figure 7.3B). Purified IstU showed no activity in an *in vitro* assay on either gentamicin C1a or C2.

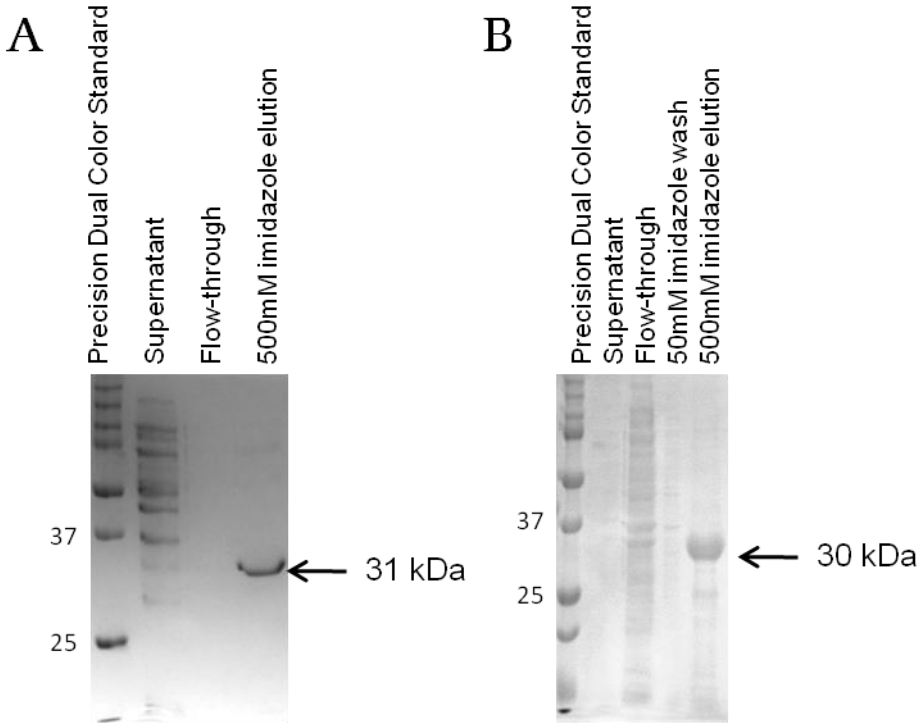

Figure 7.3 Expression of gmrA and IstU. Affinity chromatography was used to purify both recombinant gmrA (SDS-PAGE performed - left) and synthetic IstU (SDS-PAGE performed - right).

7.2 6'-*N*-Methyltransferase isolation

Another feeding experiment was performed in Wuhan, where ΔBN::*gmrA M. echinospora* (with the entire gentamicin cluster deleted) was shown to still be able to convert gentamicins C1a and C2, but not C2a, *in vivo.* This increased the probability of the 6'-*N*-methyltransferase gene being outside of the cluster, despite its importance for the biosynthesis. To investigate this possibility two parallel approaches were undertaken: ammonium sulphate fractionation of *M. echinospora* proteins and a homology-based search through its genome.

7.2.1 Ammonium sulphate fractionation of proteins in *M. echinospora*

Ammonium sulfate fractionation is one of the oldest and most common methods for protein purification. By interacting with polar and ionic groups on the surface of the protein, the ammonium and sulfate ions prevent the protein's interaction with the aqueous buffer, causing the protein to precipitate.

Depending on the surface area and charge, different proteins can be separated by increasing concentrations of the salt (Duong-Ly and Gabelli, 2014).

A protein fractionation protocol from Park *et al* was used (Park et al., 2008b). *M. echinospora* WT (ATCC® 15835) cells were grown in production medium F50 for 5 days to ensure 6'-*N*-methyltransferase presence (as a control, a small portion of the cells was subjected to the normal gentamicin purification protocol; both gentamicins C1 and C2b were detected). A cell pellet (71 g) was obtained by centrifuging at 4000 RCF for 20 minutes. The pellet was resuspended in Buffer (50 mM Tris-HCl, pH 7.5) to a total volume 250 mL. SIGMAFAST protease inhibitor cocktail and DNaseI were added. The cells were disrupted by sonication (30 minutes, 5 seconds on, 5 seconds off; with stirring every 5 minutes) on ice. The cell lysate was spun at 48000 RCF for 20 minutes at 4˚C. The supernatant was subjected to $(NH_4)_2SO_4$ fractionation in 20% increments until complete saturation, with precipitated protein separated and measured at every stage by centrifugation - all at 4˚C. The mass of ammonium sulfate to be added at each stage was calculated using EnCor Biotechnology Inc.'s Ammonium Sulfate Calculator. The fractions containing precipitated protein were dialysed against 5 L of Buffer C three times. The proteins were then used in an *in vitro* assay with gentamicin C2. Fraction 40-60% showed activity and was used for further purification with SAH-resin.

7.2.2 Capture of 6'-*N*-methyltransferase using SAH-sepharose resin

Kim *et al* described a fast new affinity chromatography technique, designed specifically to capture SAM-dependent methyltransferases (Kim et al., 1978). In this method, sepharose was functionalized with one of the products of the methyltransferase, SAH, to "fish out" methyltransferases from a cell lysate. Increasing the concentrations of salt or a buffer containing a substrate, SAM, would disassociate the enzyme.

To further purify the 6'-*N*-methyltransferase, SAH-sepharose resin was prepared and used. NHS sepharose (5 mL, 80-115 µmol NHS) was washed with 75 mL cold 1 mM HCl. A solution of SAH was prepared by adding 250 µL of 1 M HCl to 5 mg of SAH to form0.07 M solution. A volume of 7.14 µL was added to

2.5 mL of coupling buffer (0.2 M $NaHCO_3$, pH 7.5, 0.5 M NaCl), and mixed with the sepharose. The pH of the sepharose was adjusted to 7.5 with 1 M HCl. The beads were left at 4˚C overnight. Buffer (2.5 mL of 0.1 M Tris-HCl, pH 8.5) was added and incubated with sepharose for 2 hours. To block any un-reacted groups the resin was washed with a) 15 mL of 0.1 M Na acetate, pH 4.5, 0.5 M NaCl, and b) 15 mL of 0.1 M Tris-HCl, pH 8.5. The wash step was repeated 5 times each. The beads (structure shown in Figure 7.4) were stored in 70% ethanol at 4˚C.

The column was equilibrated with exchange buffer (20 mM Tris-HCl, pH 7.8, 0.5 M NaCl) before the supernatant from the fraction was passed through the column; the column was then washed with 50 mL of exchange buffer. Proteins were eluted off the column in 10 mL fractions of buffer with increasing NaCl concentrations (0.5 M, 1 M, 2.5 M, 5 M), followed by a 10 mL fraction of buffer containing 1 mM SAM, and 10 mL fractions of decreasing pH (6, 4.5, 3, 2.4). The proteins in each fraction were concentrated and used in *in vitro* assays. The fraction eluted with 1 mM SAM showed activity on gentamicin C2 (data not shown).

The homology-based approach for identifying the missing methyltransferase undertaken by our collaborators in Wuhan yielded a positive match: the clone of one of the *genN* homologues could convert gentamicin C2 *in vitro* in a cell-free assay. Therefore, a further purification by ammonium sulfate precipitation (as well as amino acid sequencing of the protein bands on an SDS-PAGE gel) was unnecessary, and instead efforts were made into expressing the novel protein.

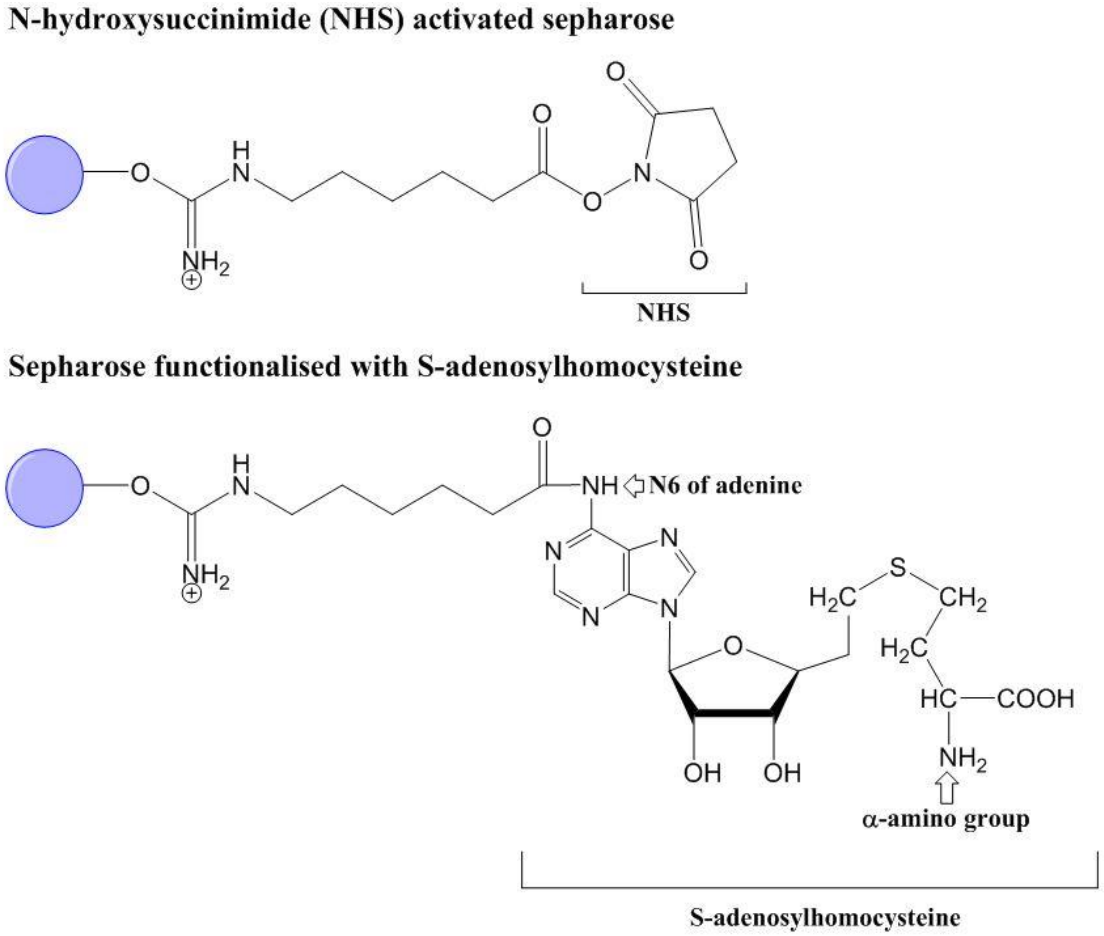

Figure 7.4 Structure of SAH-sepharose resin. (A) NHS-Activated sepharose was reacted with SAH to give (B) SAM-dependent methyltransferase-affinity resin: sepharose bound to *S*-adenosylhomocysteine (SAH) (Kim et al., 1978). The SAH molecule has two primary amines which are able to react with NHS. The choice of the coupling amine group is determined by the pH of the reaction. At pH 9, the more reactive α-amino group of homocysteine reacts with NHS, at lower pH amino group at N6 of adenine reacts instead (Matuszewska and Borchardt, 1983). Due to the importance of the methionine/homocysteine part for the binding of GenL, pH 6 was used.

7.3 GenL enzyme

Our collaborator Sicong Li from Wuhan University in China took an *in silico* approach, and used genome BLAST to identify methyltransferase candidates using *genN* and *istU* as probes.

Several promising candidates were identified this way. These were cloned and expressed in *E. coli* by Dr Huang and myself. None of the cloned, expressed, and tested proteins (orf_82, orf_1566, orf_2195, orf2_904, X1-X18) showed any activity on gentamicin C2 in an *in vitro* assay, until GenL (Table 7.1).

Table 7.1 PSI-BLAST analysis of candidate 6'-*N*-methyltransferase genes. The GenN protein sequence was used as a probe for PSI-BLAST of *Micromonospora echinospora* ATCC 15835 genome sequence. Twenty candidate genes were identified and cloned into pET-28a (+) for expression in *E. coli*. Candidate 6 (= GenL) showed catalytic activity in a cell-free assay with gentamicin C2 and SAM.

No.	ORFs	Amino acids	Identity to GenN (%)	E-value
	genN	321	100	1.00E-174
1	orf04864_1	493	30.6	8.00E-07
2	orf05573_1	246	26.67	7.00E-05
3	orf00639_1	215	37.31	8.00E-04
4	orf05344_1	264	37.5	0.008
5	orf02298_1	201	32.58	0.019
6	**orf05365_1**	**239**	**37.84**	**0.023**
7	orf05664_1	257	40.35	0.025
8	orf01520_1	266	33.33	0.025
9	orf05560_1	394	36.21	0.06
10	orf00475_1	482	29.77	0.18
11	orf05598_1	267	51.85	0.22
12	orf03626_1	283	38	0.25
13	orf02148_1	219	27.78	0.29
14	orf00088_1	263	31.43	0.41
15	orf00283_1	295	38.1	0.99
16	orf06656_1	525	39.62	1.4
17	orf02746_1	250	37.78	2
18	orf03388_1	347	35.29	3.7
19	orf05907_1	207	37.84	4.6
20	orf04521_1	326	34.04	9.1

7.3.1 Discovery of GenL (Wuhan)

Another round of PSI-BLAST for candidate methyltransferases was performed in Wuhan and gave 20 new genes. One (orf03626_1) was identified as an IstU homologue. The candidates were cloned into a pET-28a (+) vector and expressed in *E. coli* BL21 (DE3). The cells were collected by centrifugation, resuspended in 50 mM Tris-HCl, pH 8.0, 200 mM NaCl, and disrupted by ultrasonication. Cell debris was removed by centrifugation. Gentamicin C2 and SAM were added to the supernatant, and the cell-free system was then incubated at 30˚C for 6 hours. The products were purified using the normal gentamicin purification procedure and analysed by LC-MS. Orf05365_1 - later named GenL - showed conversion of gentamicin C2 to C1 (Li et al., 2018). Boiled supernatant showed no conversion confirming that any activity was due to the protein.

7.3.2 Generation of *M. echinospora* Δ*genL* Δ*genK* strain

In parallel to the mutant generation undergoing in Wuhan, a Δ*genL* Δ*genK* deletion mutant of *M. echinospora* was generated *in situ*. Deletion of *genK* results in non-6'-*C*-methylated gentamicins only, while deletion of *genL* results in non-6'-*N*-methylated gentamicins. Out of the gentamicin C complex components, only one can satisfy both of these: gentamicin C1a.

The Wuhan protocol of gene deletion in *Micromonospora* was followed (Guo et al., 2014), which is described in Section 3.1.4.1. Successful *genL* deletion was obtained in Δ*genK M. echinospora*, generating a double mutant. Of the C complex components, only gentamicin C1a could be detected by LC-MS analysis (data shown in Chapter 3).

7.3.3 *In silico* analysis of *genL*

A Δ*genL M. echinospora* mutant created in Wuhan stopped producing any 6'-*N*-methylated gentamicins, proving the essential and unique function of GenL as the catalyst of gentamicins C2b and C1 synthesis. However, the sequence of *genL* is located 2.5 MBp away from the rest of the cluster (Figure 7.5).

An alignment of protein sequences of GenL, GenN, and IstU showed very little identity between the three (Figure 7.6). The only highly conserved motif between the three was the SAM binding motif, GxGxG.

The GenL protein sequence was used as a probe for PSI-BLAST of Non-redundant protein sequences (nr) databaseof Actinomycetes (taxid: 1760; on 05/05/2017). Only two similar sequences were found in *M. pallida* (89% identical) and sisomicin-producing *M. inyoensis* (92% identical). Surprisingly, no similar gene was found in either *M. olivasterospora*, the fortimicin producer, or *Streptomyces tenjimariensis*, the istamycin producer, perhaps owing to incomplete genomes submitted.

The *genL* gene sequence was also used as a probe against the nucleotide collection (nr/nt) of Actinomycetes (taxid: 1760) genes (on 05/05/2017). Only one sequence – LT60741.1 - was identified as highly similar, belonging to another strain of *Micromonospora echinospora*; the protein sequence of GenL used in this study was aligned with the protein product of LT607413.1, SCF41374.1. Six positions had different amino acids in place. The origin of this crucial gene, therefore, remains unclear.

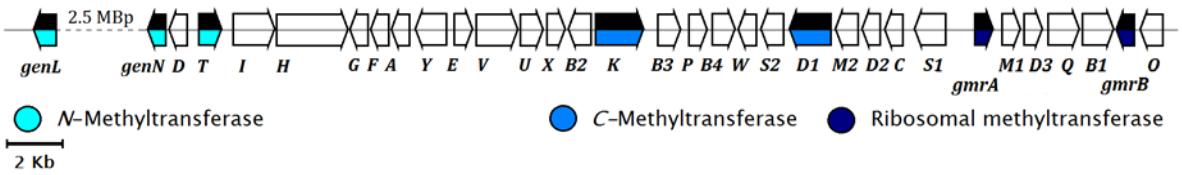

Figure 7.5 Gentamicin biosynthetic cluster and *genL*. The highlighted genes comprise all the methyltransferase genes within the cluster or needed for the biosynthesis of gentamicins.

```
CLUSTAL O(1.2.4) multiple sequence alignment

GenL      -MLSISD---LRTDWKIFRQ---TMRD-----------STLKEALVDSAEYIRIRRH-ER  41
GenN      MIVGGSTIQPERVDAAALRQLGDAMRKVVGSADPTPLADLLSGTPVDPDELTREVGADGR  60
IstU      -MIG---------------------------------GLSANGPSGPGG---PHGPNGR  22
           ::.                                 .       .           *

GenL      RERFDER-------------FGTETNGIVGLADIDSIGTHQEEASHYLPTRKQEFDRMMA  88
GenN      QALLDSGMAVDDGTTFSSPLRGHQLHGVVVLSDPDVEE---EVQHRWYVDPL--WEADLL  115
IstU      GSG------AK-------P-----SHAYAA--WGDYWA---GVLDDWIGGE---IDADCL  56
                                  :. .     *          :        :

GenL      TVGELDHGEHVFVDLGCGKGRVVLLAAEKPYKKVIGVDFSPSFISQAKENVERYTGPVAT  148
GenN      IRLMLRRGGARALDMGCGSGVLSLVLA-DRYESVLGVDVNPRAVALSRLNAALNGLTNVT  174
IstU      AVLCDLADGGDVLELGIGTGRVAIPLA-RSGLTVHGFELSDAMIE--KLREKPYGDKITV  113
                 .    :::* *.* : :  *     .* *.:..   :   : .        ..

GenL      HEIELLAIDAVDFVVPPENL---IVYL------------FSPFGPPVFDTVMRNLVAATK  193
GenN      FRE-------GDMFEPAEGRFSRIVFNSPTNEEGNEFVDLLEAGEPILETFFRNVPRKLE  227
IstU      FQE-------NYVDVAVEGTYRLVPWI--------DWGPVLLHSQEEQLTCFRNVAKCLE  158
          ..          .    *.    : :             .   .     * :**:    :

GenL      KRKQ---KITIVYY-SPDYDDV-----------VREAGFT--LVAQGKGDHWPWSVYSVG  236
GenN      SGGIVEVNLAMNDYPGDPFRERLADWLGLTENGLRVQIFTSQRRATESGGEWKRGWLV--  285
IstU      PGGHFVIEMPTRL--------PLPDGRGN---GDGNEHLVVESINPSSVGLWAVDYNPVD  207
                 ::                                :.       . . *  .

GenL      ESA-----------------------------------------------------------  239
GenN      ---------VAPGPVGLTEVEWPYHDRYEEDPDALLDGTDRLLRG---------------  321
IstU      QTMFTQQVLLEDGSVTVKPVRMRYASASELDLMARMAGLELCHRWADWRRSPISSSSPAH  267


GenL      ----------    239
GenN      ----------    321
IstU      ISVYRKPPSS    277
```

Figure 7.6 Clutal Omega alignment of GenL, GenN, and IstU protein sequences. GenL, GenN, and IstU protein sequences were aligned using Clustal Omega. Poor identity and similarity were observed. The red box shows conserved GxGxG SAM-binding motif in the three sequences.

An * (asterisk) indicates a fully conserved residue, a : (colon) indicates groups with similar properties, a . (period) indicates weakly similar groups.

Phylogenetic trees for all the candidate 6'-*N*-methyltransferase genes were constructed by Miss Cassandra L Smith. Briefly, the sequences were aligned with MUSCLE on default settings, and checked manually in Jalview. The tree was created using PhyML (Guindon et al., 2010) and visualized using iTOL (Letunic and Bork, 2016). The sequence comparison showed that *genL* was unique and dissimilar to the rest (Figure 7.7).

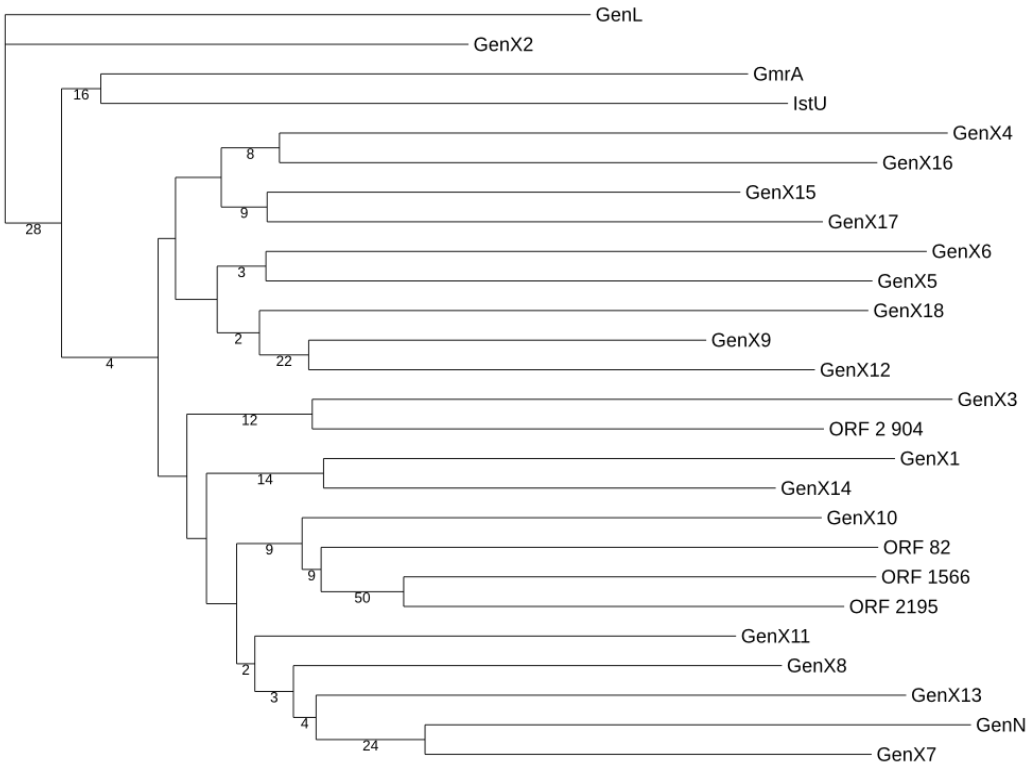

Figure 7.7 Phylogenetic tree of all 6'-*N*-methyltransferase candidate genes. The phylogenetic tree shows how different the *genL* sequence is when compared to the other candidate methyltransferases. This work was performed by Cassandra L Smith, MSc.

7.3.4 Confirmation of GenL function as a SAM-dependent 6'-*N* methyltransferase

The GenL enzyme catalyses a methyl group transfer in the presence of SAM (Figure 7.8).

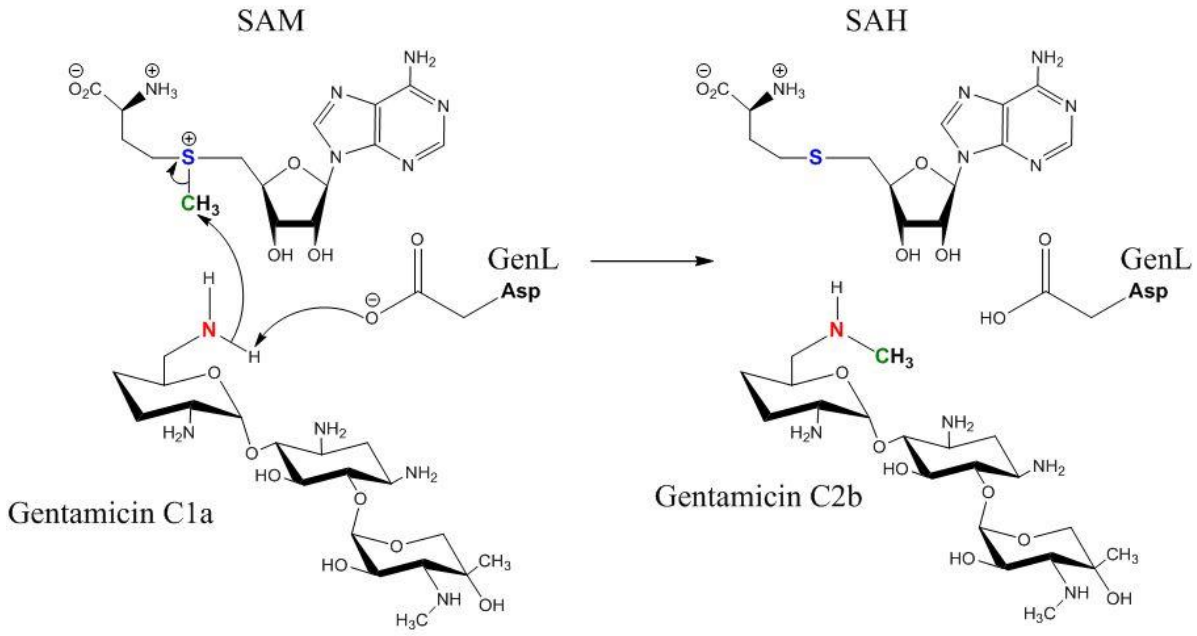

Figure 7.8 6'-*N*-Methylation mechanism. A key aspartic residue in the active site of GenL is predicted to initiate the reaction via a nucleophilic attack of the amino group on gentamicin C1a (shown) or C2.

In vitro reactions were performed with purified recombinant GenL protein. The un-6'-*N*-methylated gentamicin C complex components: gentamicins C1a, C2, and C2a, were used as substrates for these reactions (Figure 7.9). In the presence of GenL and SAM only gentamicins C1a and C2 could be converted to gentamicins C2b and C1 respectively (Figures 7.10 and 7.11). Gentamicin C2a was not accepted as a substrate, and had to be converted to gentamicin C2 by GenB2 epimerase before GenL could catalyse it. Relative conversion was a lot greater if gentamicin C2 rather than C1a was used as a substrate.

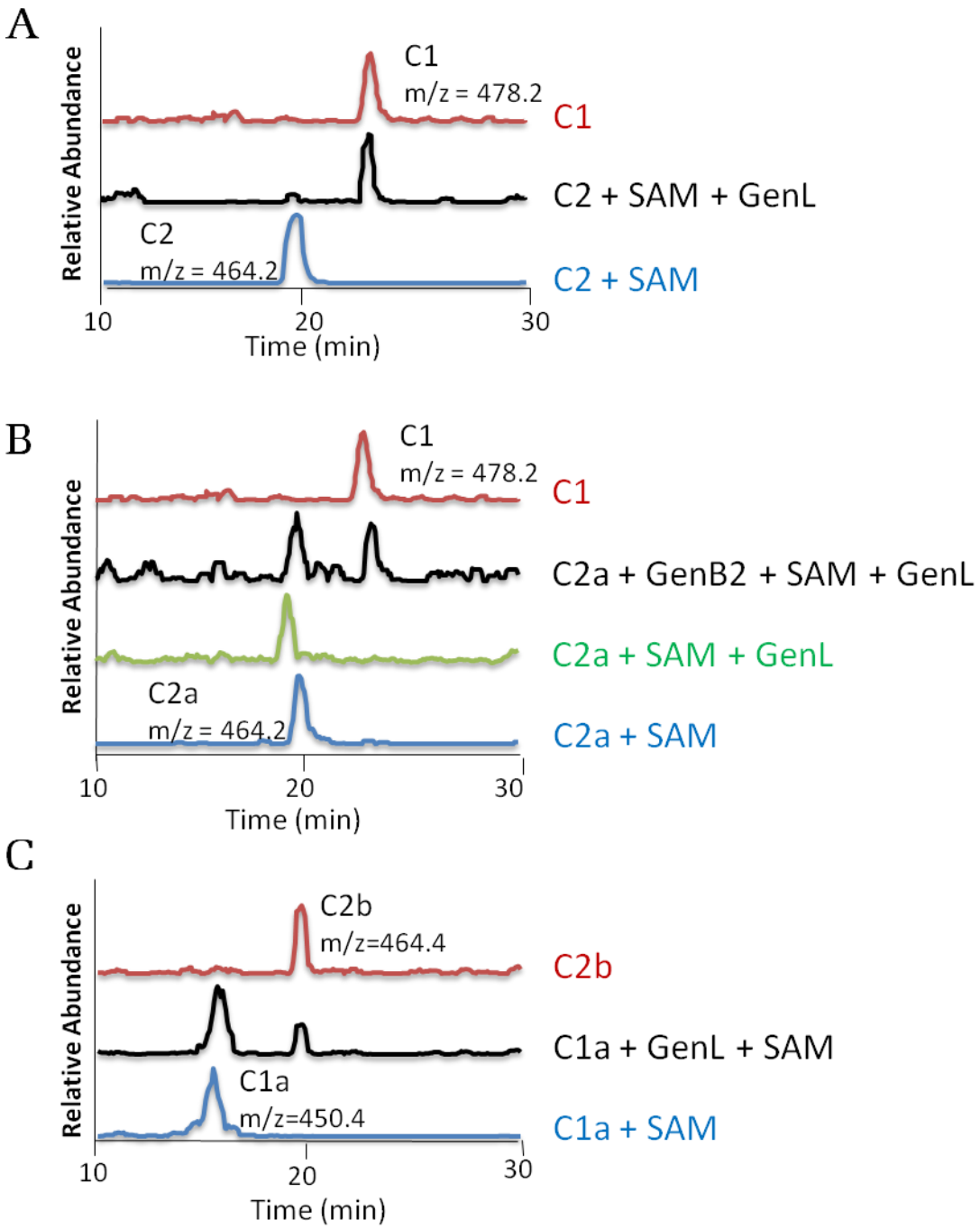

Figure 7.9 Conversion of 6'-*N*-unmethylated C complex components. LC-MS chromatogram showing specific ion monitoring of gentamicin C complex components: GenL SAM-dependent methyltransferase catalyses the conversion of (A) gentamicin C1a and C2 to (C) C2b and C1 respectively. (B) Gentamicin C2 stereoisomer, C2a, cannot be converted either *in vitro* or *in vivo*. Instead, epimerase GenB2 inter-converts the two stereoisomers.
Red: standards, black and green: *in vitro* reaction components, blue: *in vitro* reaction controls.

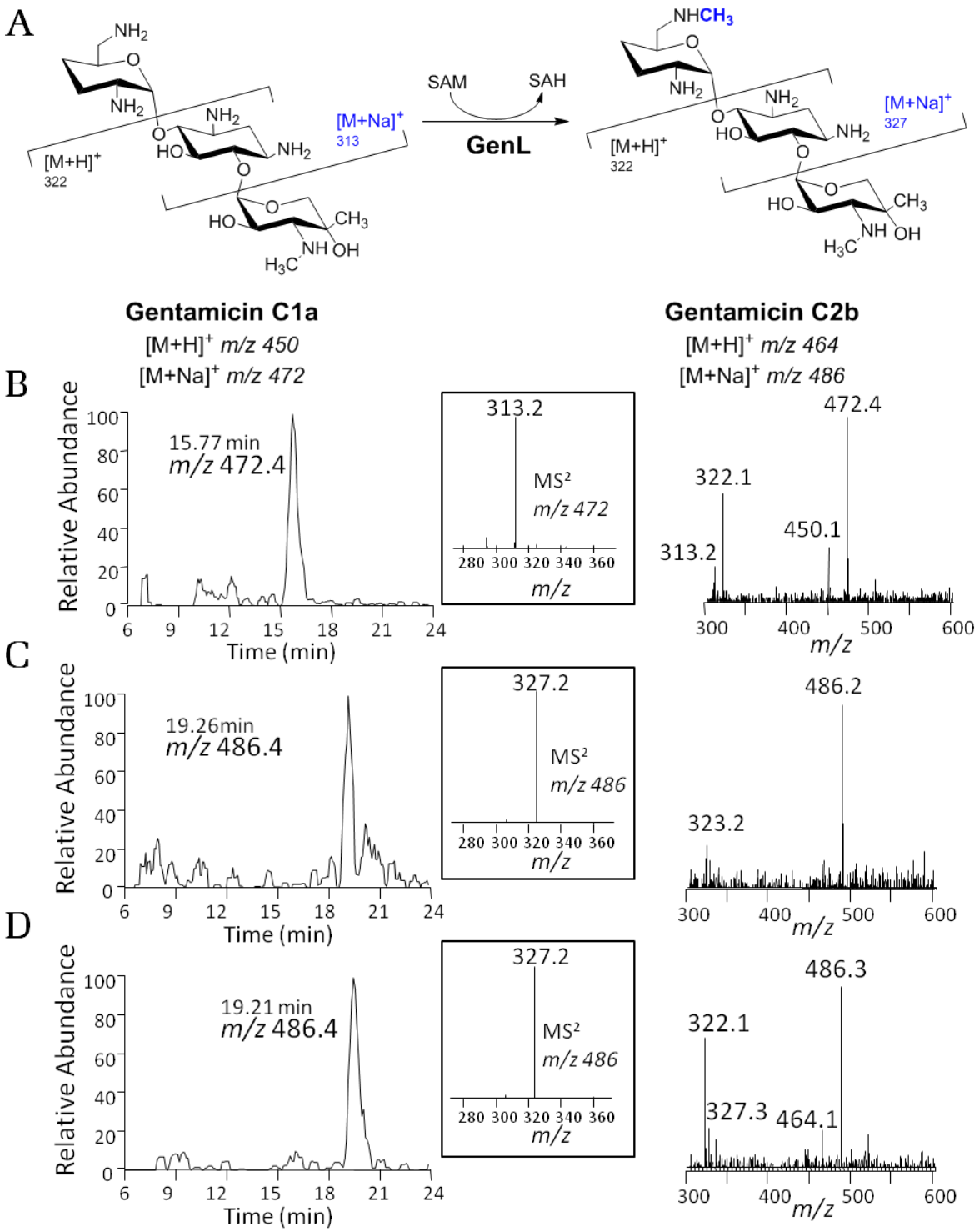

Figure 7.10 GenL-catalysed methylation of gentamicin C1a. LC-MS chromatogram showing selected ion monitoring of gentamicin C complex component (left), MS:MS ion fragments of the selected peak (middle, *m/z* 280 to 420), and ion spectrum [*m/z* 300 to 600] of the selected peak. (A) GenL accepts gentamicin C1a as a substrate; (B) gentamicin C1a; (C) product, gentamicin C2b; (D) gentamicin C2b standard.

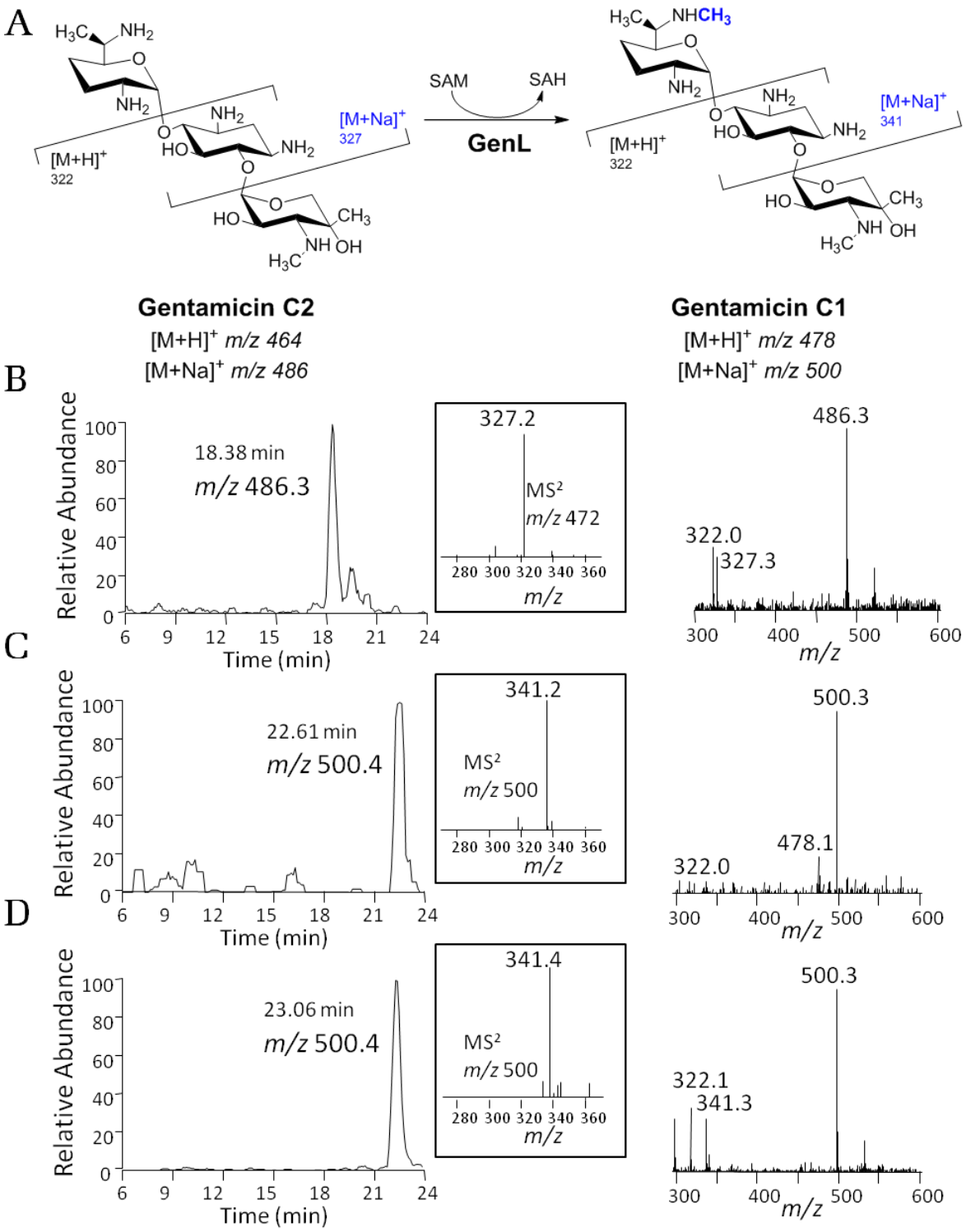

Figure 7.11 GenL-catalysed methylation of gentamicin C2. LC-MS chromatogram showing selected ion monitoring of gentamicin C complex component (left), MS:MS ion fragments of the selected peak (middle, *m/z* 280 to 420), and ion spectrum [*m/z* 300 to 600] of the selected peak. (A) GenL accepts gentamicin C2 as a substrate; (B) gentamicin C2; (C) product, gentamicin C1; (D) gentamicin C1 standard.

7.4 Improving GenL solubility and protein yield

The yield of monomeric recombinant GenL after cobalt affinity and gel filtration chromatography was very poor, and further structural and kinetic studies required this issue to be addressed. Several strategies were tried before a successful and reproducible purification protocol was developed.

7.4.1 Modificationof the pET-28a (+) ribosome binding site

Efficient protein synthesis requires good understanding of promoters for gene transcription, and ribosome binding site (RBS) for mRNA translation. Both control elements are located upstream of the gene of interest. Promoter strength determines the number of mRNA copies of the gene, while the RBS affects the translation rate and mRNA stability (Bernstein et al., 2002, Gold and Stormo, 1990).

A traditional *E. coli* expression vector possesses a strong promoter, a strong RBS, and an antibiotic selective marker to maintain the plasmid (Olins et al., 1988). Recent work by Ceroni *et al* has shown mathematically and practically that a reduced-burden vector, i.e. one possessing a much weaker RBS (4000 or less arbitrary units), improved cell viability, reduced the rate of vector mutation, and improved both the solubility and stability of expressed proteins (Ceroni et al., 2015). These phenomena are explained by lower cell stress levels via reduced ribosome stalling, as translation is the most energetically-costly part of metabolism (Li et al., 2012, Ma et al., 2002).

Variations in ribosome binding site strength were introduced by the double primer method (Zheng et al., 2004) of site-directed mutagenesis. The Salis lab RBS strength calculator (Salis, 2011) was used to estimate the strength of the native pET-28a RBS (Table 7.2).

Table 7.2 Ribosome binding sites' sequences

RBS name	Vector	RBS sequence	% GC content	RBS strength*/au
WT	pET-28a (+)	AAGAAGGAGA	40	28855.06
RBS1	pAR1	ACTACGACGT	50	3707.47
RBS2	pAR2	AATTAAGGAC	30	3543.36
RBS3	pAR3	AGGAGGCACA	60	71362.74

Three new vectors were generated: two variants of pET-28a (pAR1 and pAR2) with weaker RBSs and a variant with super-strong RBS (pAR3). pET-28a (+) vector was digested with *Sal*I and *Sph*I/*Pae*I restriction endonucleases. The generated fragment (411 bp) was cloned into pUC19 vector using T4 ligase. "RBS1", "RBS2", and "RBS3" primers were used to perform site directed mutagenesis on RBS-pUC19 using Phusion High-Fidelity MasterMix with GC buffer (Figure 7.12). DNA sequencing was used to confirm the vectors isolated from transformed NovaBlue cells grown on ampicillin-containing LB agar. After a restriction digest with *Sal*I and *Sph*I/*Pae*I endonucleases, a DNA Clean & Concentrator™ kit was used to create fragments of DNA for T4 ligation. NovaBlue *E. coli* cells were transformed with the ligation product and grown on kanamycin-containing LB agar plates. The vectors were confirmed by DNA sequencing.

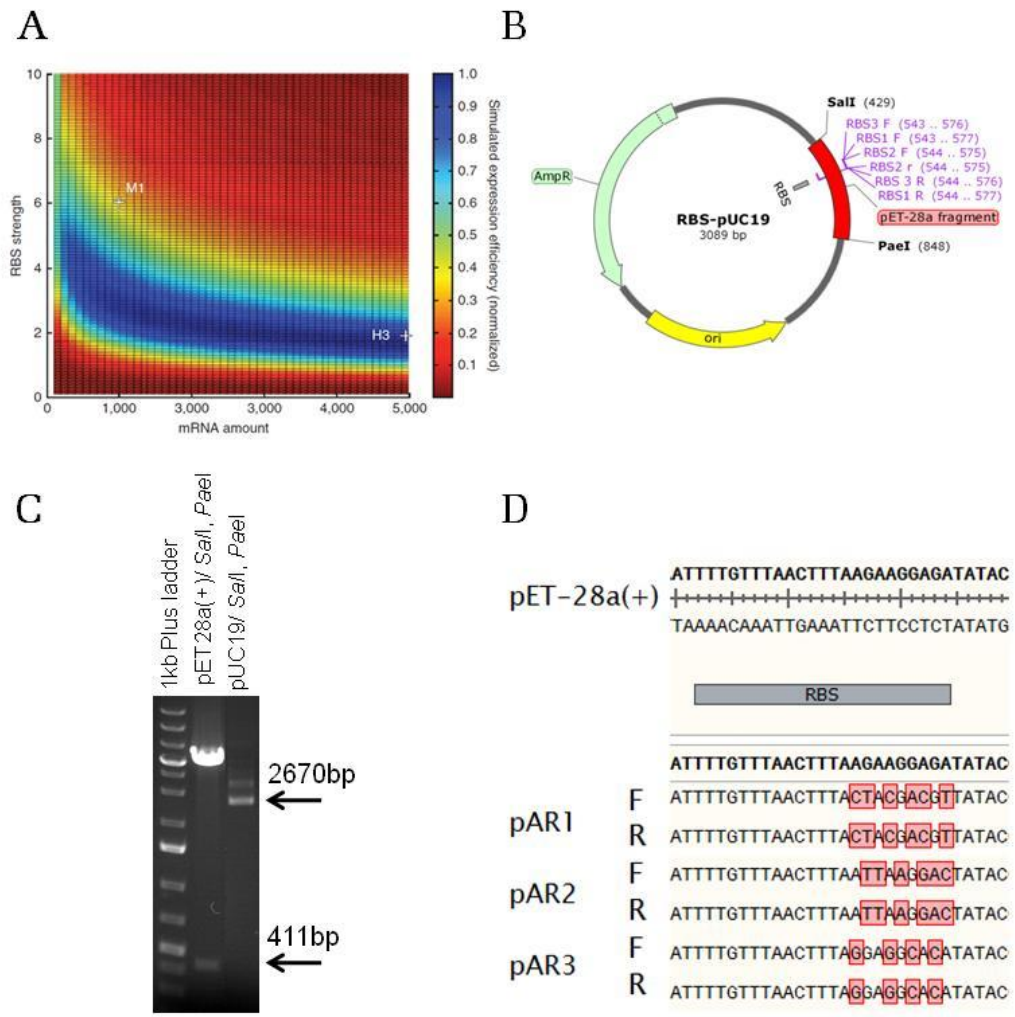

Figure 7.12 pET-28a (+) Ribosome binding site cloning. (A) Figure 2d from Ceroni *et al.*, 2015: Ribosome binding site strength versus protein expression efficiency; (B) the *Sal*I- and *Pae*I-digested fragment of pET-28a (+) was cloned into pUC19 for double-primer SDM; (C) 411 bp pET-28a (+) fragment containing RBS and 2670 bp pUC19 vector to be ligated; (D) sequences of strong (pET-28a), weak RBS (pAR1 and pAR2), and super-strong (pAR3).

Cells were transformed with *genL*-pAR1 or *genL*-pET-28a (+) vector. Their growth, final cell mass, and protein yield were compared. Cells, containing *genL*-pAR1, produced more, but still very little of, the protein in a non-aggregated state (Figure 7.13). Cells containing *genL*-pAR2 behaved similarly, but cells with super strong-RBS *genL*-pAR3 failed to grow at all.

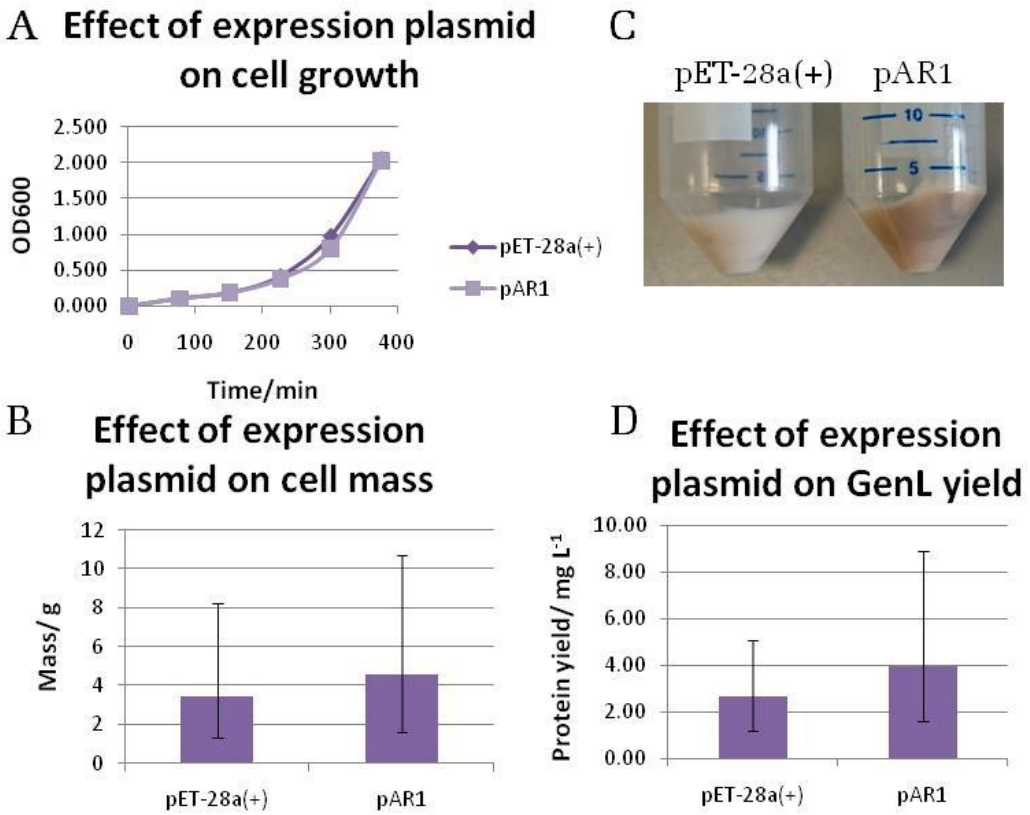

Figure 7.13 Comparison of parameters affected by RBS. (A) New pET-28a (+)-based vectors possess no effect on cell growth rate as monitored by measuring the increase in absorbance at 600 nm per unit time, however (B and C) the final cell mass is increased for lower RBS-strength pAR1, and (D) more protein is produced.

7.4.2 Expression in *Streptomyces coelicolor* CH999

A *genL*-pCJW93 vector was generated using a restriction digest and T4 ligase cloning as described in Chapter 2. *E. coli* ET12567/pUZ8002 cells were transformed with the vector and plated on 2xTY agar containing chloramphenicol (25 µg/mL for ET12567), kanamycin (50 µg/mL for pUZ8002), and apramycin (50 µg/mL for pCJW93).

Streptomyces coelicolor CH999 cells from a glycerol stock kept at -80˚C were grown on TSBY plates until an actively-growing culture was obtained. The cells were then inoculated into 25 mL of liquid TSBY medium in 250 mL flask with a spring. The cells were incubated at 30˚C, shaking at 200 RPM for 2 days.

E. coli cells were grown at 37˚C in 5 mL 2xTY medium until A_{600} reached 0.3. Both *E. coli* and *S. coelicolor* cells were spun at 4000 RCF for 10 minutes at 4˚C and washed twice with antibiotic-free 2xTY. *S. coelicolor* cells (100 µL) were carefully mixed with 100 µL of *E. coli,* and plated out on plated of ABB agar with 10 mM $MgCl_2$. The dried plates were incubated at 30˚C for 10 hours.

The plate was overlaid with 1 mL of MQ H_2O containing nalidixic acid (25 µg/mL) and apramycin (25 µg/mL) per mL of agar, i.e. a 30 mL agar plate required 500 µg of nalidixic acid and 500 µg of thiostrepton. The plates were incubated at 30˚C for 4-5 days until the exconjugants could be observed

The exconjugants were re-plated twice on ABB plates with nalidixic acid (25 µg/mL) and apramycin (25 µg/mL). The presence of vector was checked by PCR.

To create a primary culture, actively-growing cells were inoculated into 30 mL Super-YEME medium with apramycin (25 µg/mL) in a 250-mL flask with a spring. The cells were shaken at 30˚C, 200 RPM, for 4 days. A secondary culture (3 mL of primary culture in 30 mL Super-YEME medium with apramycin (25 µg/mL)) was grown at 30˚C, 200 RPM, for 2 days.

The secondary culture (5 mL) was inoculated into 100 mL Super-YEME medium containing apramycin (25 µg/mL) and grown at 30˚C, 200 RPM, for 2

days. Protein expression was induced by adding thiostrepton to a final concentration of 10 µg/mL. The culture was grown for 2 more days.

Streptomyces coelicolor CH999:*genL*-pCJW93 cells were collected by centrifugation at 3600 RCF for 20 minutes. The cell pellet was resuspended in Binding buffer. Sonication was used to disrupt the cell membrane (t_{total} = 15 minutes, t_{on} = 5 seconds, t_{off} = 10 seconds). Supernatant was separated from cell debris by centrifugation at 48000 RCF for 30 minutes at 4˚C and filtering through a 5µm membrane. The supernatant was then passed through a 1mL Co^{2+} His-Select resin. After washing the column with 10 mL of Binding and Wash buffers each, the protein was eluted off the column with Elution buffer. A CentriPure P25 desalting column was used to buffer-exchange the protein into Exchange buffer. The protein was then concentrated using a 10 kDa VivaSpin PES concentrator. The protein solution was stored in 10% glycerol at -20˚C. Very little non-aggregated protein was collected from the *Streptomyces* cells, making this purification strategy non-viable (Figure 7.17).

7.4.3 Refolding experiments

Protein purification from inclusion bodies was attempted as full-length protein was present in the insoluble fraction. The *E. coli* BLR:*genL*-pET-28a (+) cells were collected by centrifugation at 3600 RCF for 10 minutes. The cell pellet was resuspended in Lysis buffer (20 mM Tris-HCl, pH 7.8, 0.5 M NaCl, 1 mM DTT, 1% (w/v) SDS). Emulsiflex homogenizer was used to further lyse the cells. Supernatant was separated from cell debris by centrifugation at 48000 RCF for 20 minutes at 4˚C. The supernatant was discarded, and the cell pellet was resuspended in 1 M guanidine hydrochloride solution, broken down by sonication (t_{total} = 5 minutes, t_{on} = 5 seconds, t_{off} = 10 seconds) and centrifuged at 20000 RCF for 10 minutes. This guanidine hydrochloride wash procedure was repeated 3 more times. Finally, the inclusion body pellet was resuspended with 10 mL Exchange buffer. A 6 M solution of guanidine hydrochloride was added drop-wise to the inclusion bodies until a clear solution was obtained (about 40 mL). The solution was left stirring at room temperature for 1 hour. Denatured protein was then separated from other particles by centrifugation at 48000 RCF for 30 minutes at 4˚C. The denatured protein was added drop-wise to various

refolding buffers (approximately 5 mL per buffer). The refolded protein was filtered through a 0.45 µm membrane before the supernatant was passed through a 1mL Co^{2+}His-Select resin. After washing the column with 10 mL of Binding and Wash buffers each, the protein was eluted off the column with Elution buffer. A CentriPure P25 desalting column was used to buffer-exchange the protein into Exchange buffer. The protein was then concentrated using a VivaSpin PES concentrator of appropriate pore size. Gel filtration chromatography was performed to assess the oligomeric state of the refolded protein. *In vitro* assays were performed to assess activity. No activity was found from refolded proteins despite their apparent monomeric state (Figure 7.18).

7.4.4 Alternative construct generation

The 5' region of the *genL* gene originally cloned in Wuhan contained several features inconsistent with a normal *Streptomyces* gene (Starmer et al., 2006). The first residue was encoded by GTG (valine) codon and was changed to ATG (methionine) during cloning. The -10 (GAGCAG) and -35 (GCATCC) promoter sequences were also inconsistent with TANART and TTGACN normally found in *Streptomyces* (Strohl, 1992, Labes et al., 1997, Wang et al., 2013). An alternative start codon was found that better satisfied these parameters, and a shorter version of *genL*, *sgenL*, was cloned into pET-28a (+). sGenL protein expressed better and with less aggregation, however, the activity of the enzyme was lower (Figures 7.14 and 7.17).

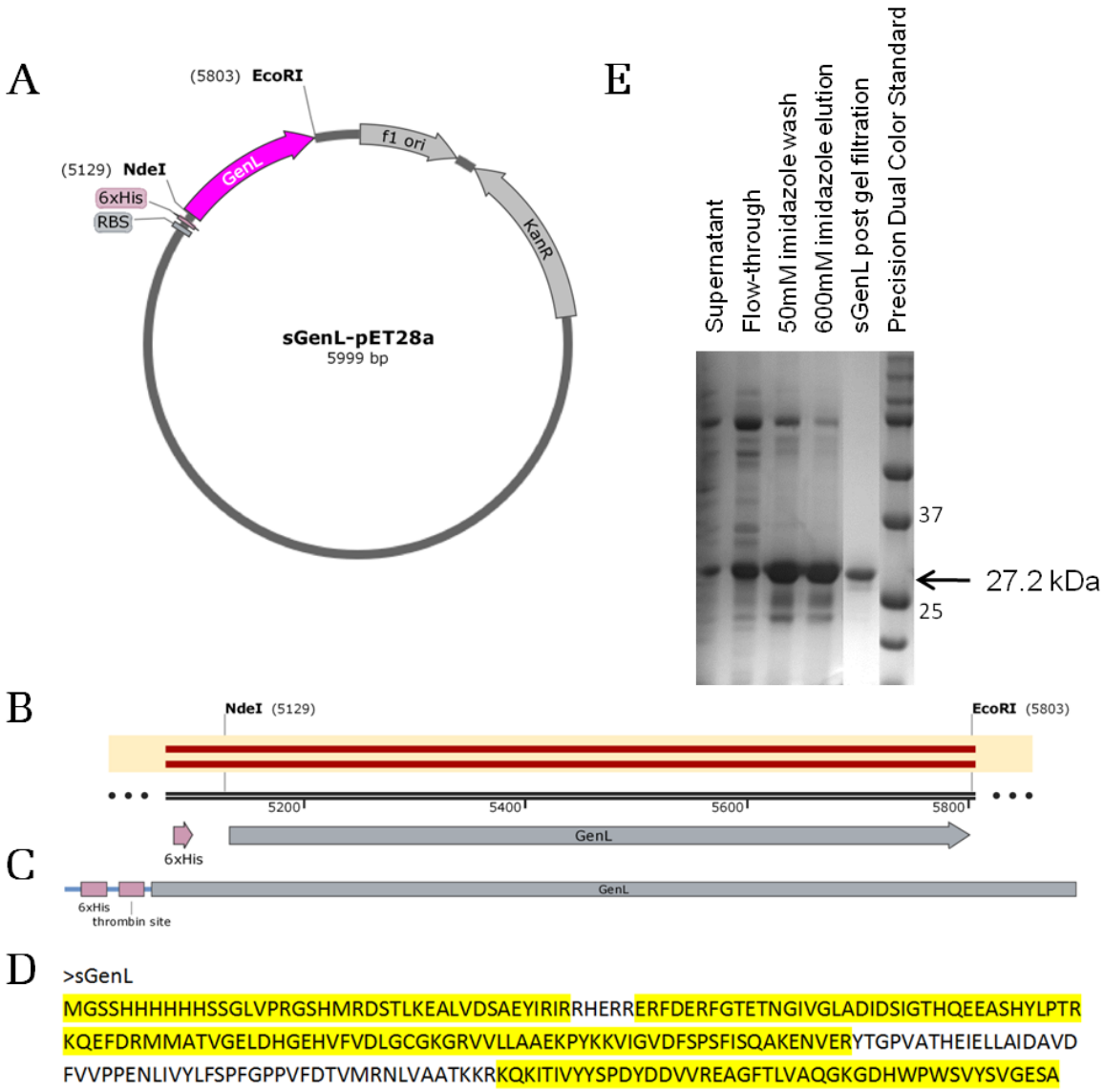

Figure 7.14 sGenL protein profile. (A) *sgenL*-pET-28a (+) vector map; (B) confirmation of *sgenL* sequence by DNA sequencing with T7 and T7t primers; (C) sGenL protein map; (D) MALDI fingerprinting analysis showing detected protein fragments in yellow; (E)SDS-PAGE of the recombinant sGenL purification by Co^{2+} affinity chromatography.

A C-terminal His-tagged version of *genL* was also cloned into pET-28a (+), *lgenL.* This protein expressed at similar low levels as GenL, showing that it wasn't an N-terminal tag that was interfering with folding (Figures 7.15 and 7.17).

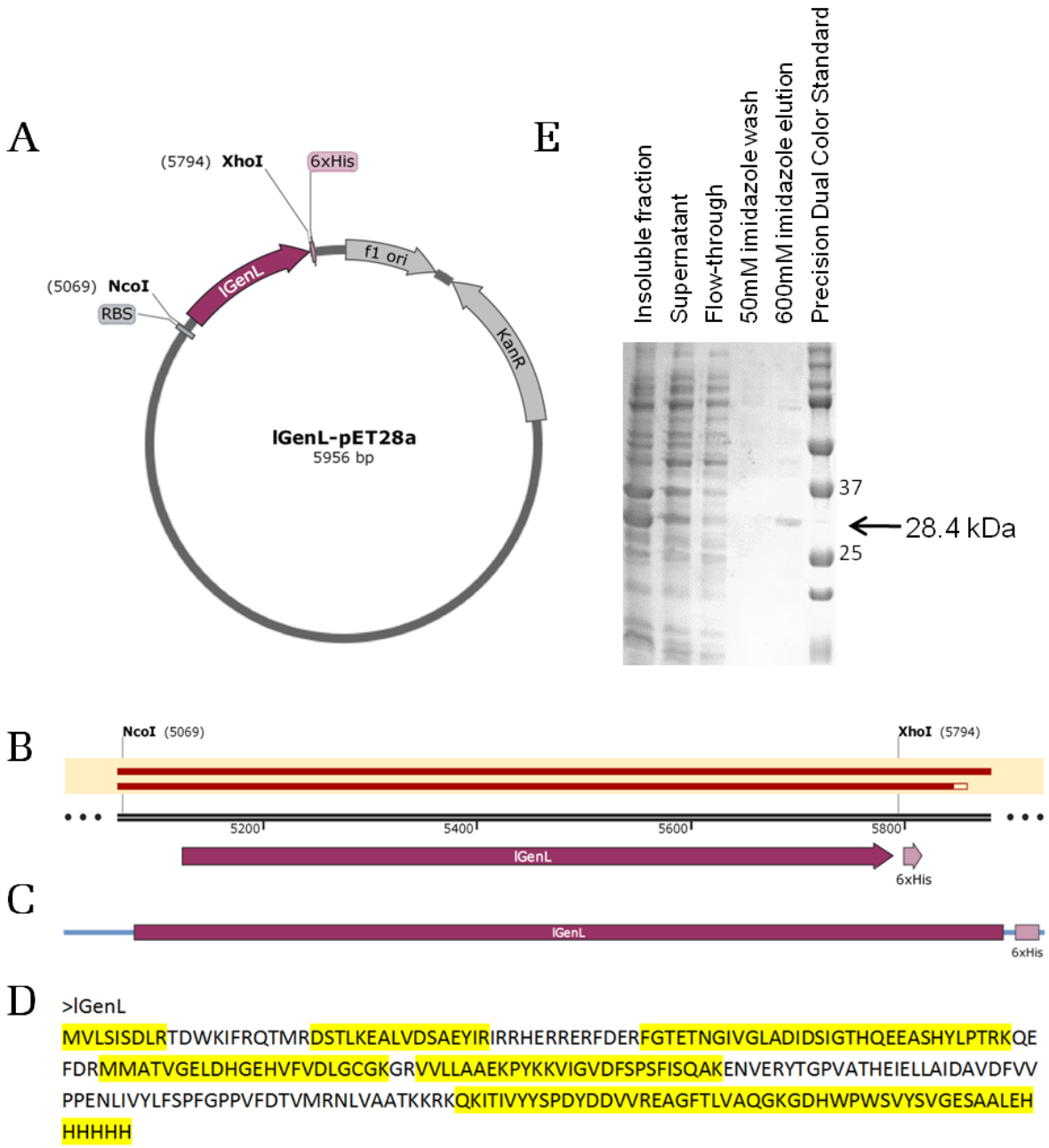

Figure 7.15 lGenL protein profile. (A) *lgenL*-pET-28a (+) vector map; (B) confirmation of *lgenL* sequence by DNA sequencing with T7 and T7t primers; (C) lGenL protein map; (D) MALDI fingerprinting analysis showing detected protein fragments in yellow; (E) SDS-PAGE of the recombinant lGenL purification by Co^{2+} affinity chromatography.

7.4.5 GenL purification protocol

Most of the GenL protein expressed in *E. coli* or *S. coelicolor* was full-length and insoluble in the normal buffer system used for all other gentamicin proteins' purification. However, *genL* is not in the cluster and is unlike many other SAM-dependent methyltransferases. Furthermore, GenL possesses a very positively-

charged amino acid stretch, and its activity seems to be improved by addition of inactive GenB2 (C9A mutant) implying an interaction between the two proteins. This lead to a new buffer system (Table 7.3) developed specifically for GenL. All buffers contained 10% (v/v) glycerol and 0.5% (v/v) non-ionic detergent Tween® 20 to help stabilize the protein. Tween® 20 is known to prevent protein aggregation and has been used for membrane protein stabilization for many years (Chou et al., 2005).

Table 7.3 Binding buffers for recombinant GenL purification

Buffer	Application	Chemical composition
Binding buffer 2	Metal affinity chromatography	50 mM K_2HPO_4/KH_2PO_4, pH 8 (i.e. 94% 1 M K_2HPO_4, 6% 1 M KH_2PO_4), 0.1 M NaCl, 10% (v/v) glycerol, 10 mM imidazole, 0.5% (v/v) Tween® 20
Elution buffer 2	Metal affinity chromatography	50 mM K_2HPO_4/KH_2PO_4, pH 8, 0.1 M NaCl, 10% (v/v) glycerol, 500 mM imidazole, 0.5% (v/v) Tween® 20
Exchange buffer 2	Metal affinity chromatography	50 mM K_2HPO_4/KH_2PO_4, pH 8, 0.1 M NaCl, 10% (v/v) glycerol, 0.5% (v/v) Tween® 20
Wash buffer 2	Metal affinity chromatography	50 mM K_2HPO_4/KH_2PO_4, pH 8, 0.1 M NaCl, 10% (v/v) glycerol, 40 mM imidazole, 0.5% (v/v) Tween® 20

Using the new system, a small but consistingly pure, active, and homogeneous sample was obtained (Figures 7.16 and 7.17).

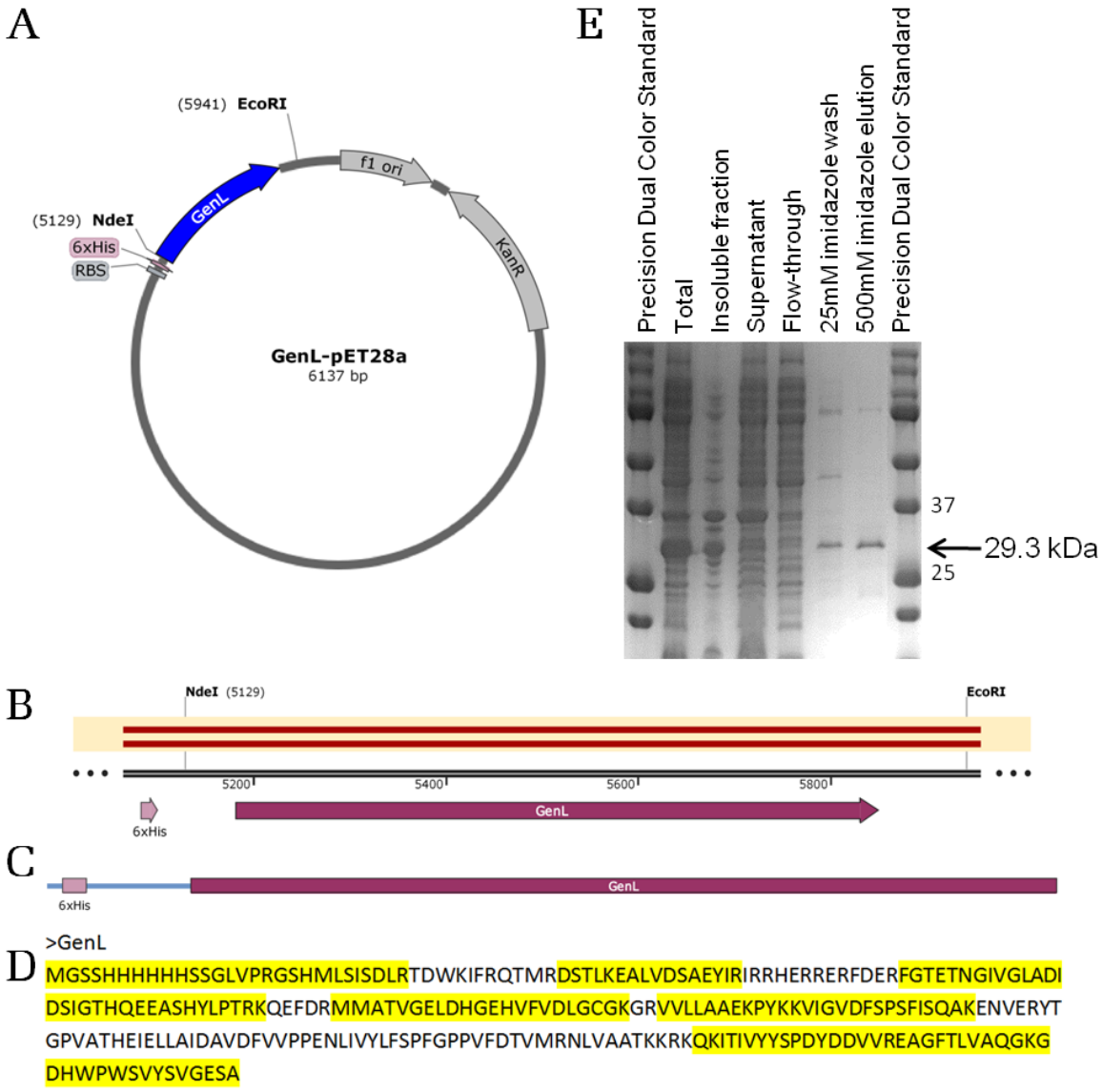

Figure 7.16 GenL protein profile. (A) *genL*-pET-28a (+) vector map; (B) confirmation of *genL* sequence by DNA sequencing with T7 and T7t primers; (C) MALDI fingerprinting analysis showing detected protein fragments in yellow; (E) SDS-PAGE of the recombinant GenL purification by Co^{2+} affinity chromatography.

The comparison of the gel filtration traces of all the protein expression and solubilisation techniques are shown below in Figure 7.17. In general, TB medium, lower expression temperature and shorter expression time, as well as a vector with weaker RBS (e.g. pAR1 or pAR2), produced more of the monomeric protein.

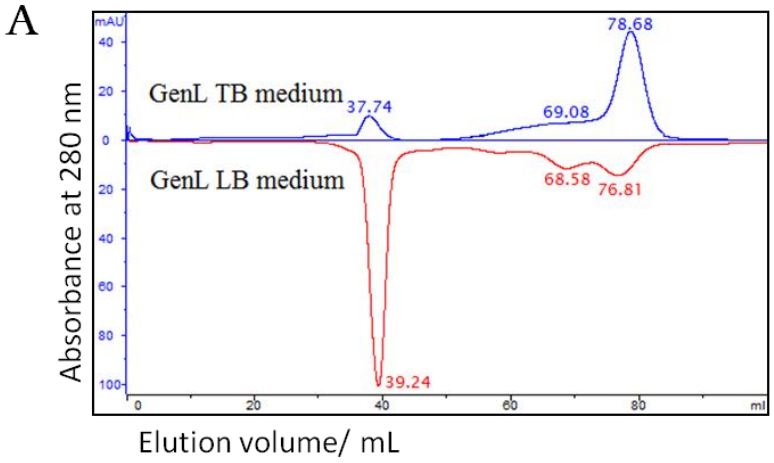
A
mAU
GenL TB medium
GenL LB medium
37.74
69.08
78.68
68.58
76.81
39.24
Absorbance at 280 nm
Elution volume/ mL

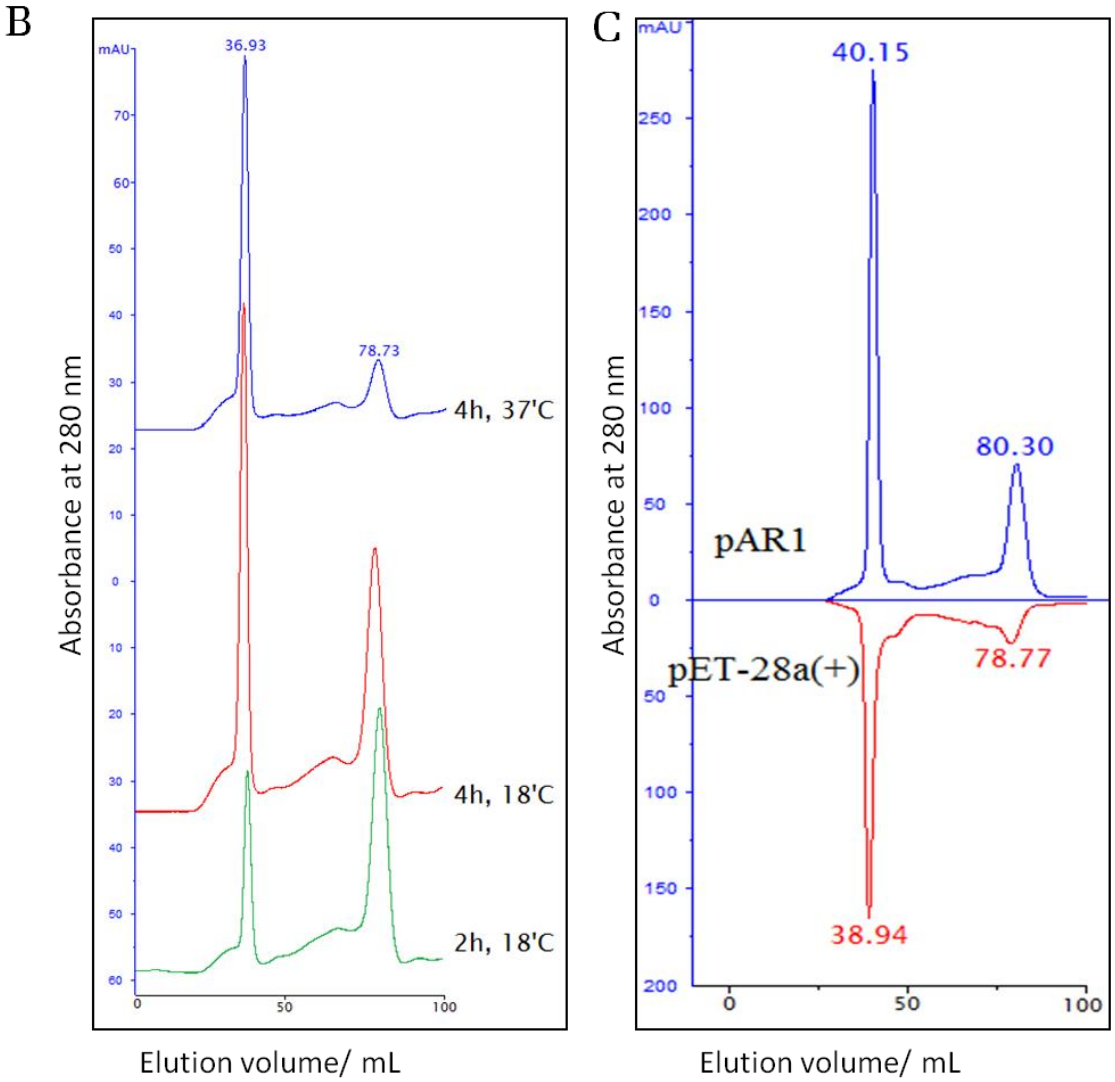
B
mAU
36.93
78.73
4h, 37'C
4h, 18'C
2h, 18'C
Absorbance at 280 nm
Elution volume/ mL
C
mAU
40.15
80.30
pAR1
pET-28a(+)
78.77
38.94
Absorbance at 280 nm
Elution volume/ mL

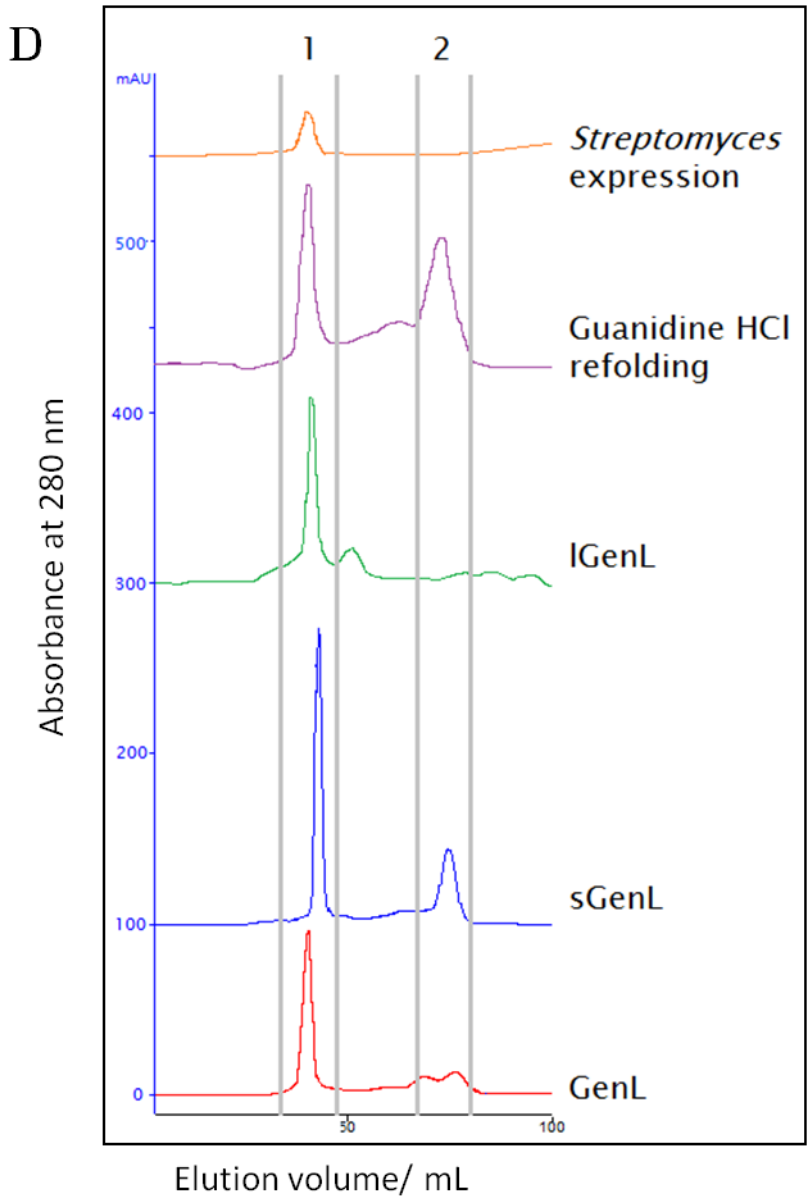

Figure 7.17 Gel filtration traces showing expression-purification protocol evolution. (A) Cells grown in TB medium show more of predicted monomer and less aggregation; (B) low expression temperature (18˚C) improved monomer yields. However, this amount is low and cannot be improved upon by longer expression time; (C) pAR1 vector, with weak RBS, improved total yield of protein and of monomer; (D) all the different ways of expressing GenL protein give a large aggregation peak (1) and a small monomer peak (2).

7.5 GenL structure elucidation

7.5.1 Biophysical methods

To ascertain the oligomeric state of GenL, analytical centrifugation was performed on the protein. GenL in Exchange Buffer 2 (400 µL of 1 mg/mL solution) was slowly loaded into cell 1 using a 200 µL pipette with a gel-loading tip. Two serial dilutions (0.33 mg/mL and 0.11 mg/mL) were loaded into cells 2 and 3. In all cases, a blank of Exchange Buffer 2 was used. The cells were sealed.

Optimisation of the protein detection was performed by determining the maximum-absorbance wavelength; it was carried out at 3000 RPM (λ_{min}= 220 nm, λ_{max}= 300 nm; single scan). A wavelength of 264 nm was used. Absorbance and interference readings were performed (R_{min}= 5.9, R_{max}= 7.2, w = 264 nm, s = 40000 RPM, T = 20.0˚C; 300 scans). GenL protein was found to be monomeric (Figure 7.18a).

A sample of GenL protein (400 µL of 0.01 mg/mL; concentration determined by Amino Acid Analysis performed by Mr Sharratt) in CD buffer (10 mM K_2HPO_4/KH_2PO_4 pH 8.0, 10% (v/v) glycerol, 0.5% (v/v) Tween® 20) was loaded into a 1 mm path-length stain-free QS quartz cuvette, and wavelengths readings were performed at 195-250 nm, with 1 nm steps, 5 seconds average reading, and 3 repeats. Protein concentrator flow-through was used as a blank. The smoothed average of the 3 reads was then created. The secondary structure of GenL was predicted to be mostly α-helical (78%), with expected dips at 222 and 208 nm (Figure 7.18b).

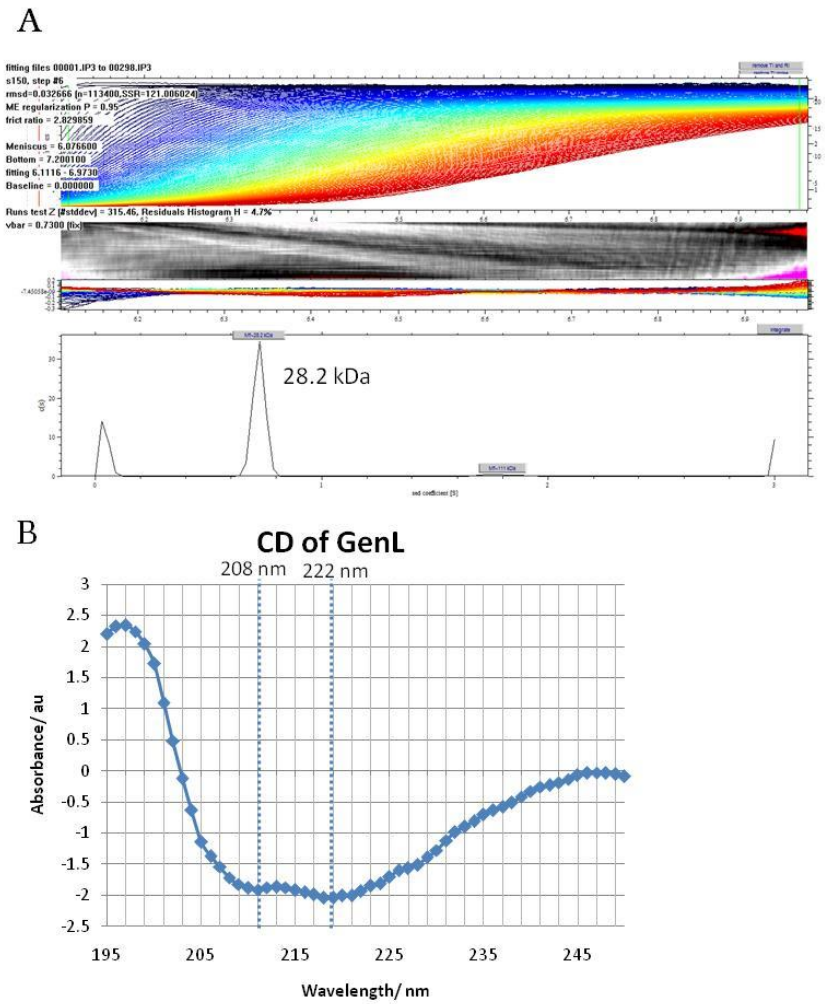

Figure 7.18 GenL analysis. (A) Analytical centrifugation was performed on a 1mg/mL sample of GenL protein to determine its oligomeric state. A peak of 28.2 kDa corresponding to a GenL monomer was observed, however, the observed signal was poor; (B) GenL protein was subjected to circular dichroism spectroscopy measurements, and was revealed to be mostly α-helical, as indicated by the dips at 208 and 222nm.

A thermal denaturation experiment was performed on a sample of GenL protein (400 µL of 0.01 mg/mL) in CD buffer. The solution was heated from 5 to 95˚C in 1˚C increments, with 20 seconds of equilibrium allowed at each step. Absorption at 222 nm was monitored. The protein was denatured at 74˚C showing it was stable in the selected buffer (Figure 7.19).

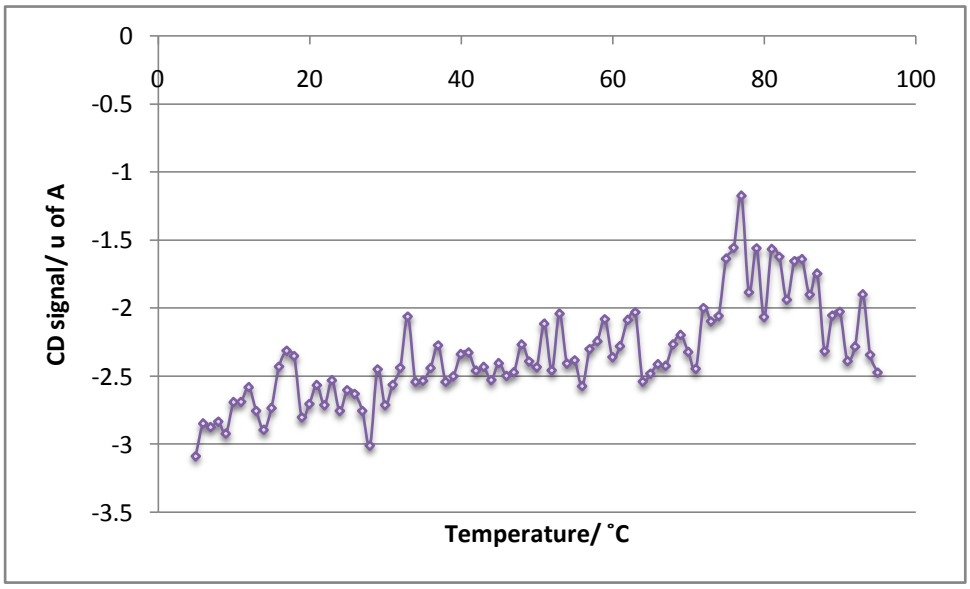

Figure 7.19 Thermal melt of GenL. A GenL sample was heated in 1 degree Celsius increments to assess its stability in buffer. A peak of units of absorbance at 74˚C was observed, indicating denaturation.

7.5.2 X-ray crystallography

Psipred online software was used to predict secondary structure of GenL protein. Based on the result, GenL is a Class I/Rossman-like methyltransferase, as it possesses a conserved GxGxG SAM-binding motif at the end of the first beta strand and a single acidic residue (Asp) at the end of the second beta strand. The structure of the core of Class I methyltransferases, consisting of about 150 amino acids, is highly conserved (Schubert et al., 2003), so tertiary structure prediction can be performed using PHYRE 2.

A pre-crystallization screen (Watson and O'Callaghan, 2005) was used to narrow down the conditions necessary for GenL crystal formation. Reservoirs on a VDX plate were filled with 1 mL of reagent A1, B1, A2, or B2 (Table 7.4). Protein sample (1 µL, 10 mg/mL) was added to a sample (1 µL) of a reagent solution on a circular glass cover slide. The slide was inverted over the reservoir with the corresponding reagent solution. Grease was used to seal the well. The plate was kept at room temperature for a minimum of 30 minutes, after which the slides were inspected under a microscope. Light precipitate or needles were indicative of good protein buffer (protein, salt, and additive concentrations) composition, whereas heavy amorphous precipitate indicated a poor system.

Table 7.4 Pre-crystallization test reagents

Buffer	Application	Chemical composition
Reagent A1	Pre-crystallization test	0.1 M Tris-HCl, pH 8.5, 2.0 M $(NH_4)_2SO_4$
Reagent B1	Pre-crystallization test	0.1 M Tris-HCl, pH 8.5, 1.0 M $(NH_4)_2SO_4$
Reagent A2	Pre-crystallization test	0.1 M Tris-HCl, pH 8.5, 0.2 M $MgCl_2$ x 6 H_2O, 30% (w/v) polyethylene glycol 4000
Reagent B2	Pre-crystallization test	0.1 M Tris-HCl, pH 8.5, 0.2 M $MgCl_2$ x 6 H_2O, 15% (w/v) polyethylene glycol 4000

In addition to setting up hanging drops, a Mosquito robot was used to aliquot protein and precipitant solutions into wells for sitting drop crystallization. The plates used are listed in Table 7.5.

Table 7.5 Crystallization kits used

Screen	Company	Description
Cryos	Qiagen®	Various precipitants, glycerol
JCSG+	Molecular Dimensions	PEG and others, salts
Morpheus	Molecular Dimensions	Various precipitants
PACT	Molecular Dimensions	PEG 3350, buffer and salts
PEG I	Qiagen®	PEG, buffer or salts
PEG II	Qiagen®	PEG, buffer and salts
pH Clear I	Qiagen®	Various precipitants
Wizard 1&2	Molecular Dimensions	PEG and others, salts
Wizard 3&4	Molecular Dimensions	PEG and others, salts

Typically, a 0.2 µL droplet of buffer was mixed with 0.2 µL (10 mg/mL) of protein in buffer with SAM and gentamicin C2. The plates were sealed and kept at 19˚C.

Crystals were obtained in suspension drops with pre-crystallization reagents A2 and B2, containing PEG 4000 (Figure 7.20). Identical conditions in sitting drops yielded no crystals. Twenty-four crystals of various shapes were mounted, frozen in liquid nitrogen and sent for analysis. Sadly, GenL crystals did not diffract well, with prediction of the best resolution at 5 Å (0.3 mg/mL GenL in 50 mM K_2HPO_4/KH_2PO_4, pH 8.0, 0.1 M NaCl, 10% (v/v) glycerol, 0.5 % (v/v) Tween® 20; final concentration of additives: 10mM SAM and 1 mM gentamicin C2; precipitant: reagent B2. Crystal shape: clump of rods). No further optimisation was undertaken.

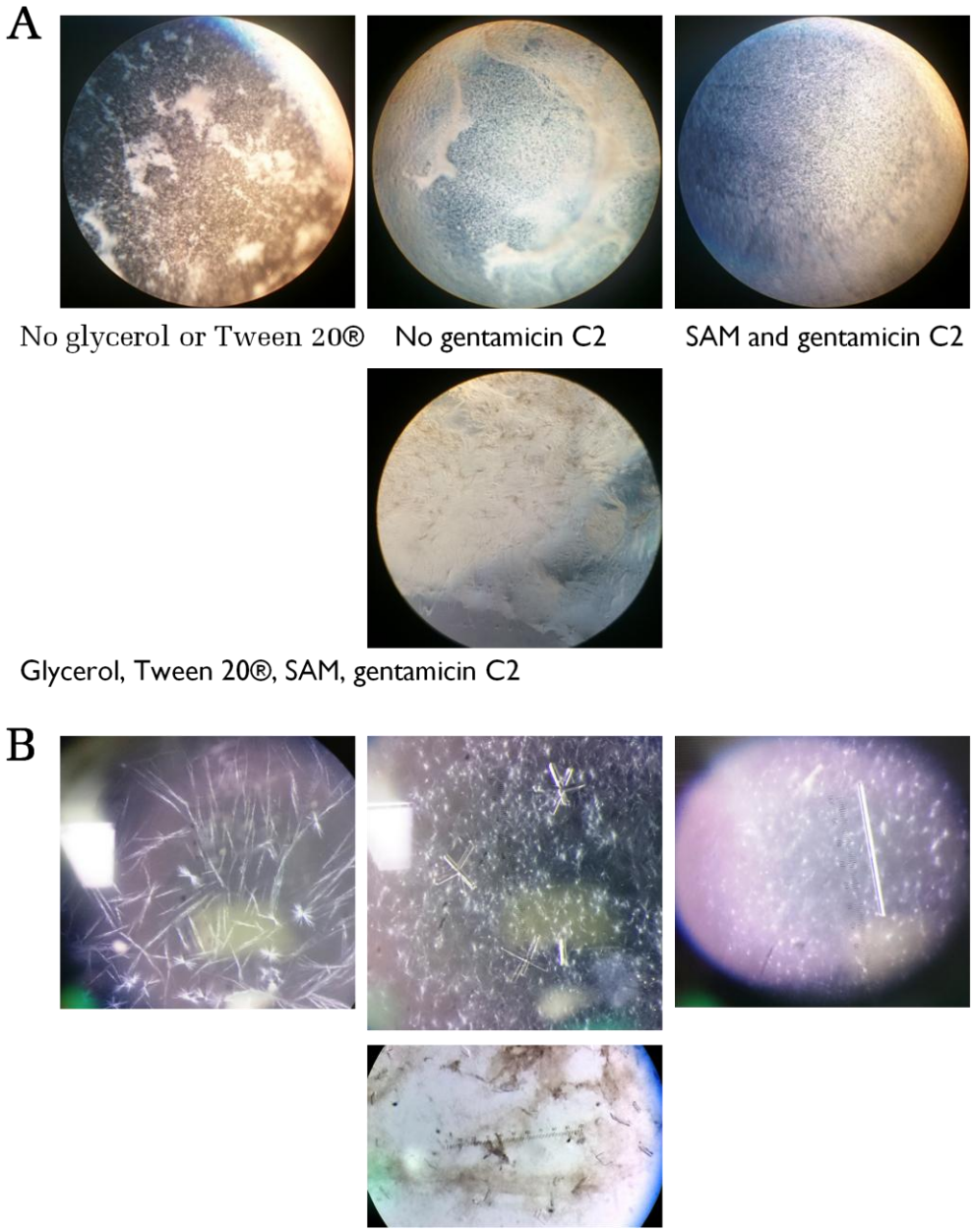

Figure 7.20 Recombinant GenL crystallisation. Crystals as seen by visible light microscopy (X50 magnification). (A) Various buffers and presence of substrates were tested using the protein a pre-crystallization kit. Protein in 20 mM Tris-HCl, pH 8, 0.1 M NaCl, 10% glycerol, 0.5% Tween 20®, 10 µM SAM and 5 µM gentamicin C2 appears to form needles with Reagent A2 and B2 (PEG 4000). (B) Variously shaped crystals in suspension drops with Reagents A2 and B2 (PEG 4000).

Co-crystallisation with GenB2 was also attempted. A different crystal form - rhombus - was obtained. The crystal diffracted very well, and a GenB2 protein structure was obtained at a final resolution of 1.6 Å (10 mM K_2HPO_4/KH_2PO_4, 10% (v/v) glycerol, 0.5 % (v/v) Tween® 20; final concentration of additives: 10 mM SAM and 1 mM gentamicin C2; precipitant: Reagent A2 (Figure 7.21).

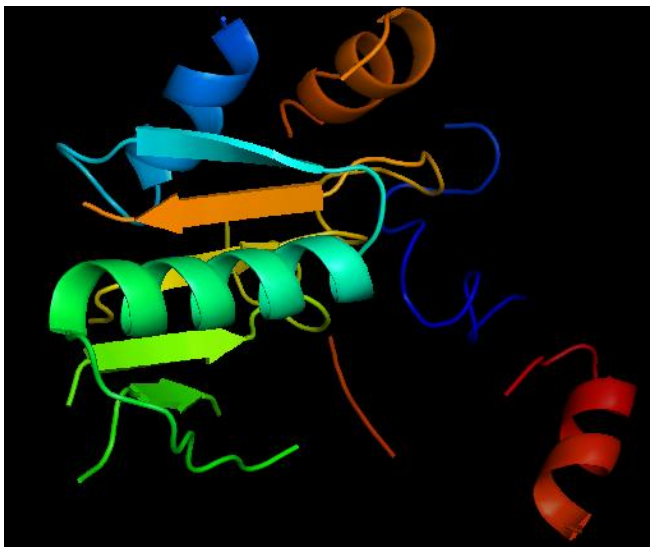

Figure 7.21 Epimerase GenB2 structure. Recombinant GenB2 protein was purified and crystallised with pre-crystallization reagents. The electron density map was analysed and the structure fitted by Dr Paul Brear.

7.6 Kinetic studies of GenL

GenL is a monomeric SAM-dependent methyltransferase. The catalytic activity of GenL can be studied further if a coupled colorimetric assay is used. Determination of K_M and k_{cat} parameters of GenL can help explain the preference of the enzyme towards specific substrates.

A continuous Methyltransferase Colorimetric Assay Kit (Dorgan et al., 2006) was used to follow GenL activity in real time. Transfer of the methyl group from S-adenosylmethionine (SAM) to gentamicins C2 or C1a was linked to a series of hydrolysis reactions to yield hydrogen peroxide, which then reacts with 3,5-dichloro-2-hydroxybenzenesulfonic acid to form a coloured (pink, absorbs at 500-520 nm) product (Figure 7.22). All the reactions downstream of GenL were non- rate-limiting. The protocol of the assay was followed. Briefly, to a mixture (total volume 10 µL) of recombinant GenL in Exchange buffer 2 and various concentrations (50-800 µM) of gentamicins C2 or C1a, a reaction mix consisting of SAM (final concentration 0.175 mM), detection system enzymes and chemicals, and buffer, was added. The plate (half-area, flat-bottom wells) was shaken for 10 seconds, and absorbance at 510 nm was recorded every 30 seconds or 1 minute over 1 hour using a BMG Pherastar spectrophotometer. These reactions were performed at 30˚C, in triplicate. A negative control was used to generate the background signal. A positive control with SAH was used to test system efficacy.

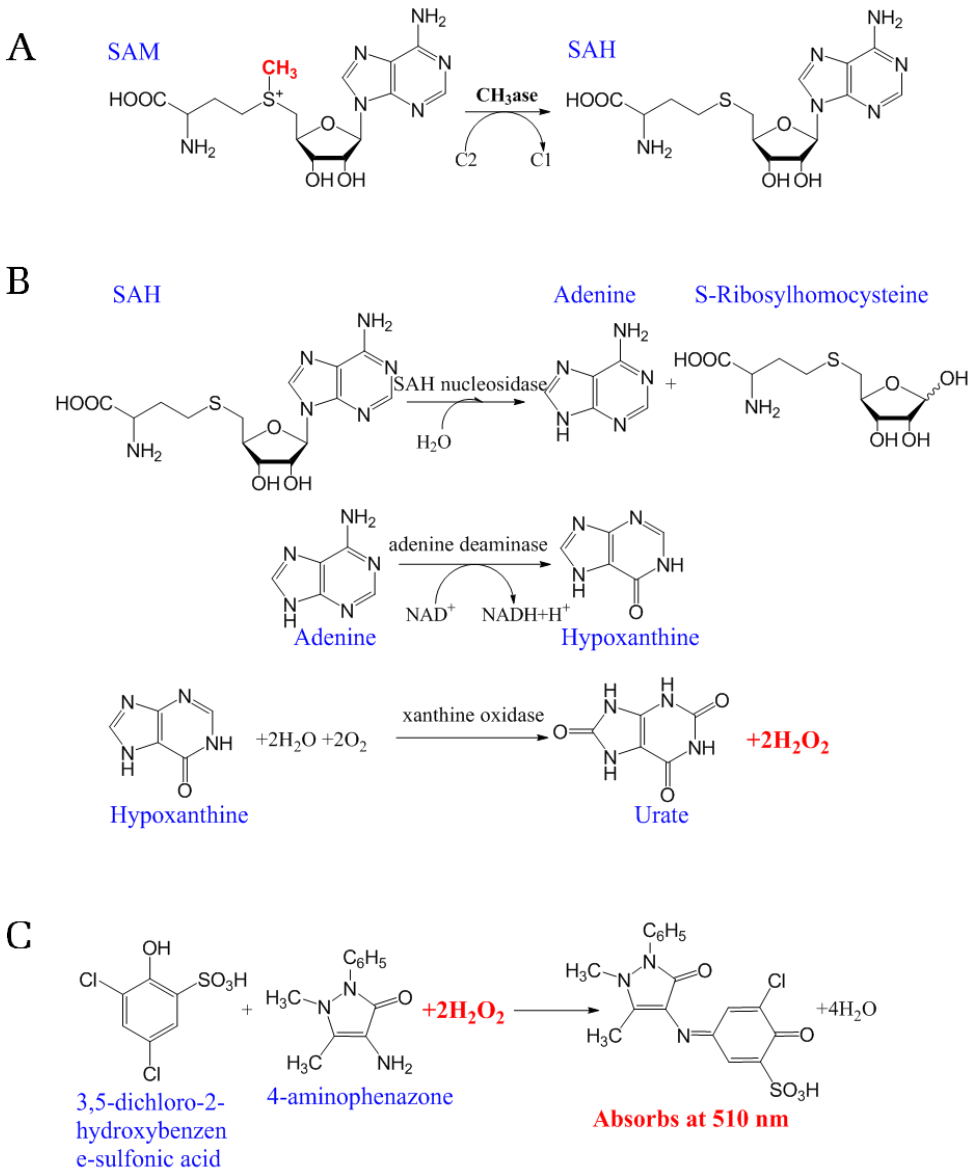

Figure 7.22 Methyltransferase Colorimetric Kit. (A) GenL reaction with SAM and gentamicin C2 producing SAH and gentamicin C1; (B) three enzymes present in the colorimetric kit degrade SAH to give 2 molar equivalents of hydrogen peroxide; (C) Chemicals in the kit react in the presence of hydrogen peroxide to give a coloured compound (pink) that absorbs at 510 nm.

The data was analysed using GraphPad Prism 7. Absorbance at 510 nm was plotted against time in minutes. The linear part of the curve was used to determine the rate of change of absorbance per minute, $\Delta A/t$ (min^{-1}). The background signal was subtracted before the data was converted to reaction rate, v ($\mu M\ s^{-1}$), by the following equation:

$$v = \Delta c = \frac{\Delta A}{\epsilon \times l} \times \frac{1000}{60} = \frac{\Delta A \times 1000}{26 \times 1 \times 60} = \Delta A \times 0.641$$

where v is reaction rate (μM s^{-1}), Δc is change in substrate concentration (μM s^{-1}), ΔA is change of absorbance at 510 nm of the linear portion of the curve (min^{-1}), ε is the extinction coefficient of 3,5-dichloro-2-hydroxybenzenesulfonic acid (the coloured product of the assay, mM^{-1} cm^{-1}), l is path length (= 1 cm due to in-built path correction of a BMG Pherastar FS spectrophotometer), 1000 is the factor for converting mM to μM, and 1/60 is the factor for converting second to minutes.

The reaction rate (μM s^{-1}) was plotted against the substrate concentration (μM), and fitted to the Michaelis-Menten equation. Parameters for the maximum rate, V_{max} (μM s^{-1}) and the Michaelis constant, K_m apparent (μM; at final concentration of SAM - 0.175 mM), were obtained. The following equation was used to calculate k_{cat}:

$$k_{cat} = \frac{V_{max}}{[E]}$$

where [E] is the enzyme concentration (μM) in the reaction.

The values, obtained for gentamicin C2 (Figure 7.23) and C1a (Figure 7.24), are shown in Table 7.6. GenL shows preference for gentamicin C2 over C1a as a substrate, as a smaller concentration of it is needed to reach half of the maximum rate, V_{max}. This explains why *in vivo* the ratio of gentamicin C1 to C2 is much greater than gentamicin C2b to C1a, and gentamicin C1 is the major component of the complex. The catalytic rate constant, k_{cat}, is the same for both accepted substrates, and is low for a methyltransferase, perhaps explaining the incomplete conversion of gentamicins C1a and C2 *in vivo.*

Table 7.6 Kinetic parameters of GenL

Substrate	K_M apparent/ μM	k_{cat}/ s^{-1}
Gentamicin C2	77.8 ± 8	0.043
Gentamicin C1a	347.8 ± 86	0.040

Some catalytic activity was also observed on sisomicin. The predicted product would be 6'-*N*-sisomicin, or antibiotic G-52, a minor component of *M. inyoensis* fermentation (Nagabhushan et al., 1982, Daniels et al., 1976). It is also a major product of *M. zionensis* (Leitner and Price, 1982, Marquez et al., 1976), which might possess a mutated version of *genL*. None of the other tested substrates (gentamicin C2a, pathway intermediates: G418, JI-20a, JI-20b; pathway

intermediates: verdamicins C2 and C2a, and related aminoglycosides: kanamycins A and B, tobramycin) showed any activity at all (Figure 7.25).

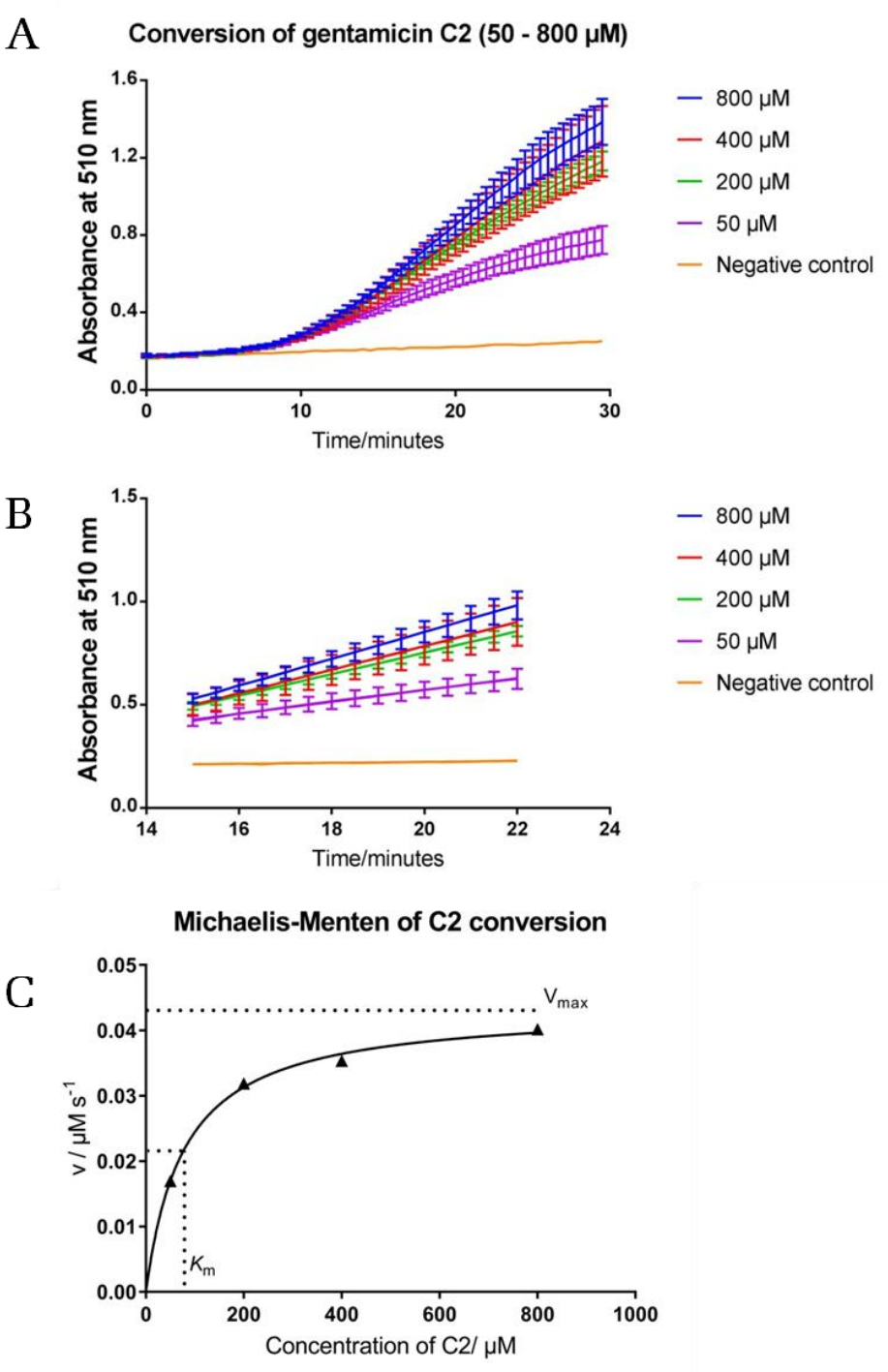

Figure 7.23 Conversion of gentamicin C2 by GenL methyltransferase. (A) Gentamicin C2 to C1 conversion can be followed by a continuous colorimetric assay; (B) the linear portion of the graph used to calculate change of absorbance per minute (slope) values; (C) calculated *v* values fitted to the Michaelis-Menten equation.

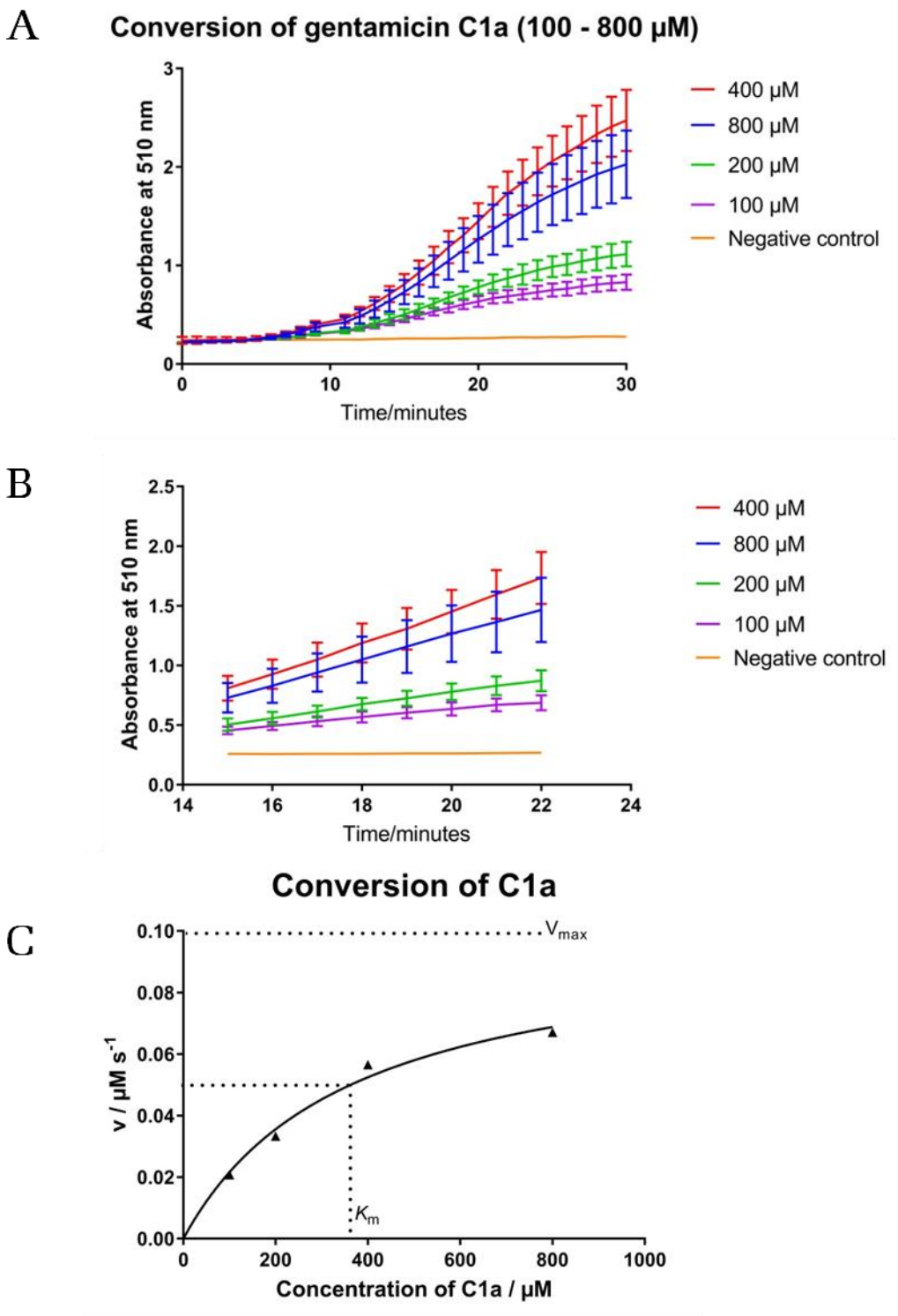

Figure 7.24 Conversion of gentamicin C1a by GenL methyltransferase. (A) Gentamicin C1a to C2b conversion can be followed by a continuous colorimetric assay; (B) the linear portion of the graph used to calculate change of absorbance per minute (slope) values; (C) calculated *v* values fitted to the Michaelis-Menten equation.

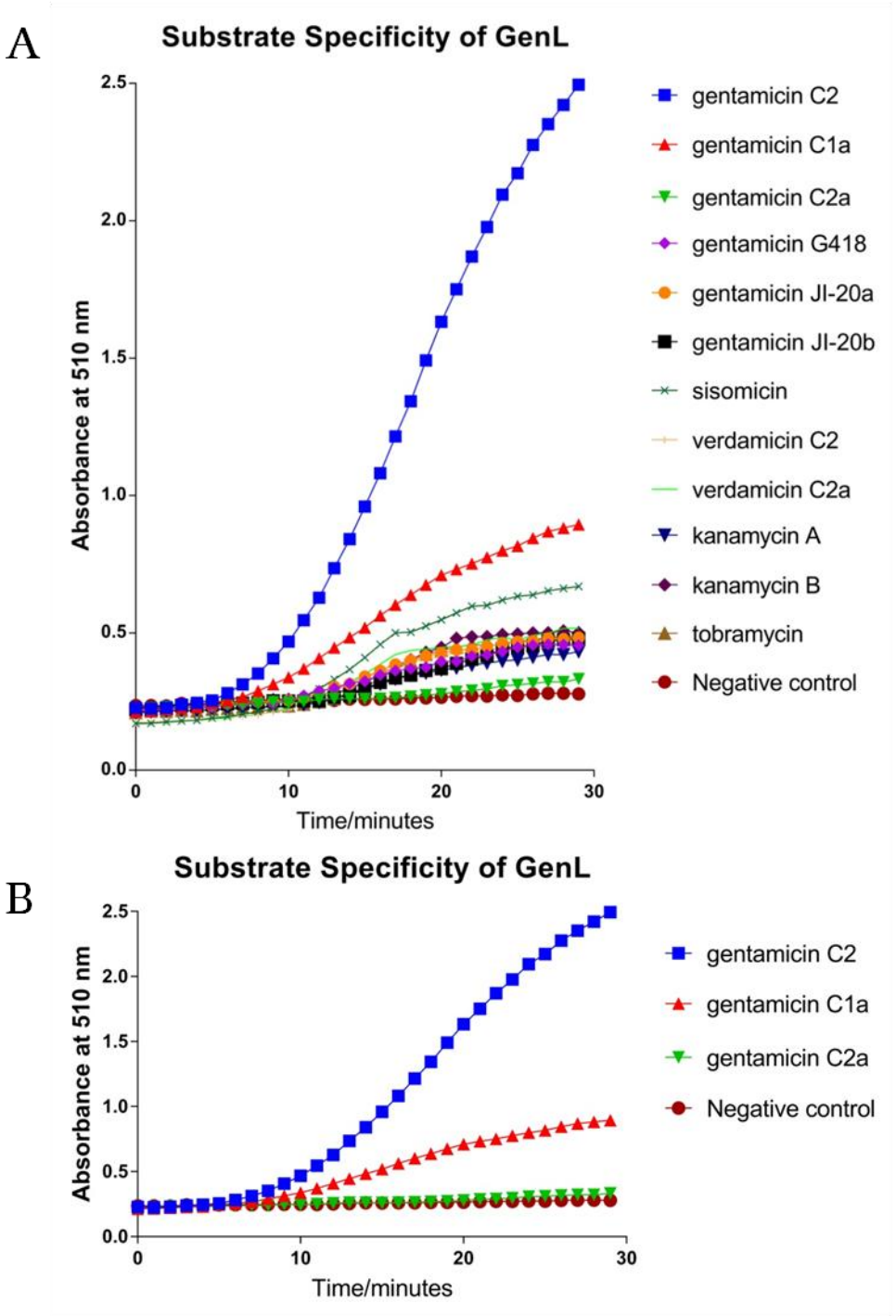

Figure 7.25 Substrate specificity of GenL methyltransferase. (A) Un-6'-*N*-methylated gentamicin C components (C1a, C2, C2a), pathway intermediates (G418, JI-20b, JI-20a), putative pathway intermediates (sisomicin, verdamicins C2 and C2a) , and related aminoglycosides (kanamycins A and B, tobramycin) were tested for conversion by GenL. Only C2, C1a, and sisomicin exhibited significant activity. (B) Reactions of un-6'-*N*-methylated gentamicin C components (C1a, C2, C2a) with GenL, showing stereochemical selectivity of GenL.

7.7 Discussion

GenL is responsible for synthesis of 2 out of 5 components of the C complex, gentamicins C2b and C1. GenL substrate, gentamicin C2, has been previously shown to be less nephrotoxic in rats, when compared to the other components of the mixture (Sandoval et al., 2006). Another GenL substrate, gentamicin C1a, and a GenL product, gentamicin C1, cause less damage to the inner ear, reducing the irreversible hearing-loss side effect (Fox et al., 1980, Kobayashi et al., 2008). By discovering the identity of the terminal methyltransferase of the pathway, bioengineering of new strains has led to mutant *M. echinospora* fermentation mixtures, enriched in specific products.

7.7.1 The role of metal ions in gentamicin biosynthesis

Cobalt is an important metal for gentamicin biosynthesis for several reasons. Addition of cobalt to the production medium was found to enhance the levels of gentamicins, probably via supplying the PLP-dependent synthesis of methionine with an essential cofactor (Krasnova et al., 1978). Methionine is a source of not only methyl groups but also amino groups for gentamicin (Guo et al., 2014). A few steps of the gentamicin biosynthetic pathway proposed by Testa and Tilley in 1976 required cobalt, such as GenD1-catalysed methylation of gentamicin A to X2 and GenK-catalysed methylation of gentamicin X2 to G418 (Testa and Tilley, 1976, Kim et al., 2013, Huang et al., 2015). Both methyltransferases are radical SAM- and cobalt-dependent enzymes.

Interestingly, Testa and Tilley suggested that all *C*-methylation and *N*-methylation reactions of gentamicin biosynthesis, including the 6'-*N*-methylation catalysed by GenL, should require cobalt. GenL can catalyse the reaction without the addition of cobalt to the *in vitro* reaction mixture, however, the recombinant enzyme was purified by Co^{2+} affinity chromatography which may have supplied the necessary ions. Magnesium is another metal ion which is essential for the activity of phosphotransferase GenP.

8

Conclusions, Discussion, and Future Work

8.1 Conclusions

For the first time since the discovery of gentamicin, the complete pathway of its biosynthesis is proposed here, with all the enzymes necessary for individual steps from glucose-6-phosphate to final gentamicin C complex components identified. Mainly, the late steps of biosynthesis, 3',4'-di-dehydroxylation and 6'-*N*-methylation are discussed.

Phosphotransferase GenP is essential for the activation of the hydroxyl group on gentamicin intermediates JI-20a and JI-20b for subsequent 3',4'-di-dehydroxylation. The work described in this Thesis shows the activity of the GenP on its native substrates, confirming the 3' hydroxyl being phosphorylated and calculating the kinetic parameters for gentamicin intermediates and kanamycins.

Phospho-lyase GenB3 acts on Pi-JI-20a and Pi-JI-20b to remove the 3' phosphate and the 4' hydroxyl groups in a series of PLP-dependent reactions. Reaction with GenB3 showed that only a single phosphorylation reaction by GenP was necessary for di-dehydroxylation. The importance of PLP-dependent reactions for di-dehydroxylation is further proven by the last step of di-dehydroxylation, a 4',5' double bond reduction, catalysed by PLP-dependent GenB4. Together, GenP, GenB3, and GenB4 make up the minimal set of enzymes necessary for *in vitro* and *in vivo* reconstitution of the di-dehydroxylation step.

The identity of the 6'-*N*-methyltransferase has been determined and the relevant enzyme, GenL, has been characterised. It acts in the pathway as a gentamicins C2b and C1 synthase. The enzyme was studied here using kinetic, biophysical, and crystallographic approaches.

Therefore, the absolute minimal set of enzymes necessary to synthesise the complete gentamicin C complex is now complete. The function of some of the Gen proteins, however, is predicted from their close identity to other aminoglycoside biosynthetic enzymes.

For the first time dynamic CCC was performed on gentamicin samples using a planetary centrifuge. The technique shows a lot of promise as a cheap, scalable, and fast method for a complete separation of gentamicin C complex components. A novel solvent system has also been developed for the purification of gentamicin intermediates.

All together the findings described in this Thesis provide a stronger platform for development of novel aminoglycoside antibiotics, as well as safer gentamicins for clinical use.

8.2 Discussion: the *gen* cluster

Although most biosynthetic genes tend to be clustered together in a particular portion of the genome, *genL* is not the first example of a gene to be located outside of a cluster. In some cases essential - resistance - genes are located away from the rest of biosynthetic genes, or borrowed from a separate cluster also present in the producer, like the genes necessary for tobramycin biosynthesis being located in the apramycin cluster (Piepersberg et al., 2007a).

Out of the 32 ORFs present in the gentamicin cluster and *genL* outside of it, only 18 genes are essential for generating gentamicin from precursors obtained from primary metabolism (although a resistance gene, *gmrA,* also must be present to protect the host). GenC, GenS1, GenE, GenM2, GenD, and GenM1 are needed to synthesise gentamicin A2. GenD2, GenS2, GenN, and GenD1 catalyse the formation of gentamicin X2, the last common precursor of all five gentamicin C complex components. GenK methyltransferase creates a branch point in the pathway, and GenQ and GenB1 generate the JI-20 complex. Work described here showed that the GenP, GenB3, and GenB4 enzymes are sufficient to form *in vitro* the first two gentamicin C complex components, gentamicin C1a and gentamicin C2a. GenB2 is gentamicin C2 synthase, and GenL catalyses the last step of the pathway, generating gentamicins C1 and C2b. Thus, for the first time, the

minimal set of enzymes necessary to catalyse the formation of gentamicin has been identified, with every reaction proven *in vitro* (Figure 8.1).

Looking back to the probable evolutionary origin of the *gen* genes, from the *kan* and *for* gene clusters, the genes encoding proteins that catalyse kanamycin-like transformations are important for the early steps of gentamicin biosynthesis. The proteins catalysing the later steps of gentamicin biosynthesis, with fortimicin-like reactions, are encoded by genes homologous to components of the *for* cluster.

In addition to the 18 genes required for the synthesis of gentamicin, the *gen* cluster also contains two genes involved in resistance (*gmrA* and *gmrB*), four genes for transport (*genH, genI, genV,* and *genY*), and two genes involved in regulation (*genA* and *genU*). Table 8.1 summarises the functions of the *gen* genes, including the newly-assigned ones described here. Although expressed and purified in our lab (data not shown), the functions of GenT, GenG, GenF, GenD3, and GenO, as well as identity of GenX and GenW as proteins, were not confirmed.

Figure 8.1 Complete gentamicin biosynthetic pathway. (A) Biosynthetic genes responsible for the formation of indicated products are highlighted in the *gen* cluster and *genL*; (B) The gentamicin pathway was reconstituted step-by-step *in vitro* with purified substrates and proteins. The functions of the proteins were further confirmed by mutant generation and fermentation.

Table 8.1 The *gen* cluster analysis

gen Name	*gnt* Name	*gac/gtm* Name	Function of protein	Product of catalysis
genL	-	-	*N*-methyltransferase	Gentamicins C2b and C1
genN	-	-	*N*-methyltransferase	gentamicinA
genD	-	*gtmM*	deacylase	paromamine
genT	-	-	*N*-methyltransferase	?
genI	-	-	exporter	-
genH	-	-	exporter	-
genG	-	-	6-pyruvoyl	?

			tetrahydropterin synthase	
genF	*gntS*	-	production protein	?
genA	*gntR*	-	regulator	-
genY	*gntQ*	*gacI*	cation antiporter	-
genE	*gntP*	*gacH*	dehydrogenase	3-amino-2,3-dideoxy-*scyllo*-inosose
genV	*gntO*	*gtmK*	efflux protein	-
genU	*gntN*	*gacG*	regulator	-
genX	*gntM*	*gacF*	hypothetical protein	?
genB2	*gntL*	*gacE*	aminotransferase	Gentamicin C2
genK	*gntK*	*gacD*	*C*-methyltransferase	G418
genB3	*gntW*	*gacC*	aminotransferase	Sisomicin, verdamicin
genP	*gntI*	*gtmJ*	phosphotransferase, resistance	Pi-JI-20a, Pi-JI-20b
genB4	*gntL*	*gacB*	aminotransferase	Gentamicins C1a and C2a
genW	*gntG*	*gacA*	GTP cyclohydrolase I	?
genS2	*gntF*	*gtmD*	aminotransferase	3''-dehydro-3''-amino-gentamicin A2
genD1	*gntE*	*gtmI*	*C*-methyltransferase	Gentamicin X2
genM2	*gntD*	*gtmE*	glycosyltransferase	Gentamicin A2
genD2	*gntC*	*gtmC*	NAD-dependent dehydrogenase	3''-dehydro-3''-oxo-gentamicin A2
genC	*gntB*	*gtmA*	2-deoxy-*scyllo*-inosose synthase	2-deoxy-*scyllo*-inosose
genS1	*gntA*	*gtmB*	2-deoxy-*scyllo*-inosose aminotransferase	2-deoxy-*scyllo*-inososamine, 2-deoxystreptamine
gmrA	*grmA*	*gtmF*	ribosomal RNA-methyltransferase, resistance	-
genM1	*gntZ*	*gtmG*	glycosyltransferase	2'-*N*-acetylparomamine
genD3	*gntY*	*gtmH*	dehydrogenase	?
genQ	*gntX*	*gacJ*	dehydrogenase	6'-dehydro-6'-oxo-gentamicin X2, 6'-dehydro-6'-oxo-gentamicin G418
genB1	*gntW*	*gacK*	aminotransferase	JI-20A, JI-20B
gmrB	*grmO*	*gtmL*	ribosomal RNA-methyltransferase, resistance	-
genO	*gntV*	*gacL*	tRNA ribosyltransferase	?

Some of the genes with yet unconfirmed functions (*genO, genW, genA, genF, genG*) form a set of highly conserved genes, also present in fortimicin producers, *M. olivasterospora* and *Francia* sp. CcI3. Homologous proteins have

been shown to be involved in the modification of guanine residues in the wobble position of tRNAs with anticodons specific for Asp, Asn, His, and Tyr (Reader et al., 2004). In those, the guanine is modified into queuine (Q). A gene encoding a second 16S rRNA methyltransferase resistance gene, *gmrB,* is also found within the *gen* cluster.

Overall, the *gen* cluster is both typical and unusual. The presence of multiple copies of the "same" gene - like the GenB enzymes - is common amongst aminoglycoside gene clusters. Re-using the same enzyme in multiple parts of the pathway is also standard. The GenB enzymes themselves are unusual as GenB2, GenB3, and GenB4 can all substitute for GenB1 function, but they have also evolved to catalyse other essential steps in the pathway. Perhaps the most unusual aspect of the cluster is that the gene encoding an essential 6'-*N*-methyltransferase is located 2.5 Mbp away from the rest of the *gen* genes.

8.3 Future Work

8.3.1 NMR of intermediates

The availability of gentamicin intermediates and the products of the feeding studies can be used to confirm the structure of keto-sisomicin, keto-gentamicin C1a and keto-gentamicin C2a.

NMR spectra of gentamicin molecules could also be used to confirm the proposed mechanisms for the catalysis by GenB3 and GenB4. Large-scale reactions with D_2O, and analysis by NMR of the products from these reactions, could show the absolute position of incorporated deuterium atoms.

8.3.2 Crystal structures of Gen proteins

Our collaborator Dr Marcio Dias from the University of Sao Paulo has already crystallised and solved the structures of all four GenB aminotransferases (personal communication). The new *Micromonospora* mutants provide access to genuine gentamicin intermediates, which could be used to soak the crystallised protein to visualise the position of the aminoglycoside within the active site of the protein. There are examples of crystals of PLP-dependent enzymes showing the quinonoid intermediate within the protein structure (Romo and Liu, 2011, Smith et al., 2008, Schneider et al., 2000). This would help confirm the proposed mechanisms for GenB3 and GenB4.

8.3.3 Stereochemistry elucidation

Stereoisomers of JI-20b, verdamicin, and gentamicin C2 could be made *in vitro* by a reaction with recombinant GenB2 epimerase or *in vivo* by feeding them to a *M. echinospora* mutant containing only the *genB2* and *gmrA* genes. The various stereoisomers could then be separated by different solvent systems using CCC. The compounds could be subjected to the Kuhn-Roth oxidation and Marfey's analysis for characterization before using them as substrates for *in vitro* reactions or *in vivo* feeding experiments (Figure 8.2).

During stereochemistry elucidation by the Kuhn-Roth oxidation, individual *S* and *R* components were degraded to L-alanine and D-alanine respectively, using Kuhn-Roth type chromic acid oxidation (Rognstad et al.,

1968). The improved Marfey's reagent, Nα-(2,4-dinitro-5-fluorophenyl)-L-valinamide, was reacted with the product of the oxidation to produce one of the diastereomers (Bhushan and Brückner, 2011). The differences between the diastereomers were analysed using TLC and LC-MS. Commercial L- and D-alanine were used to create standards.

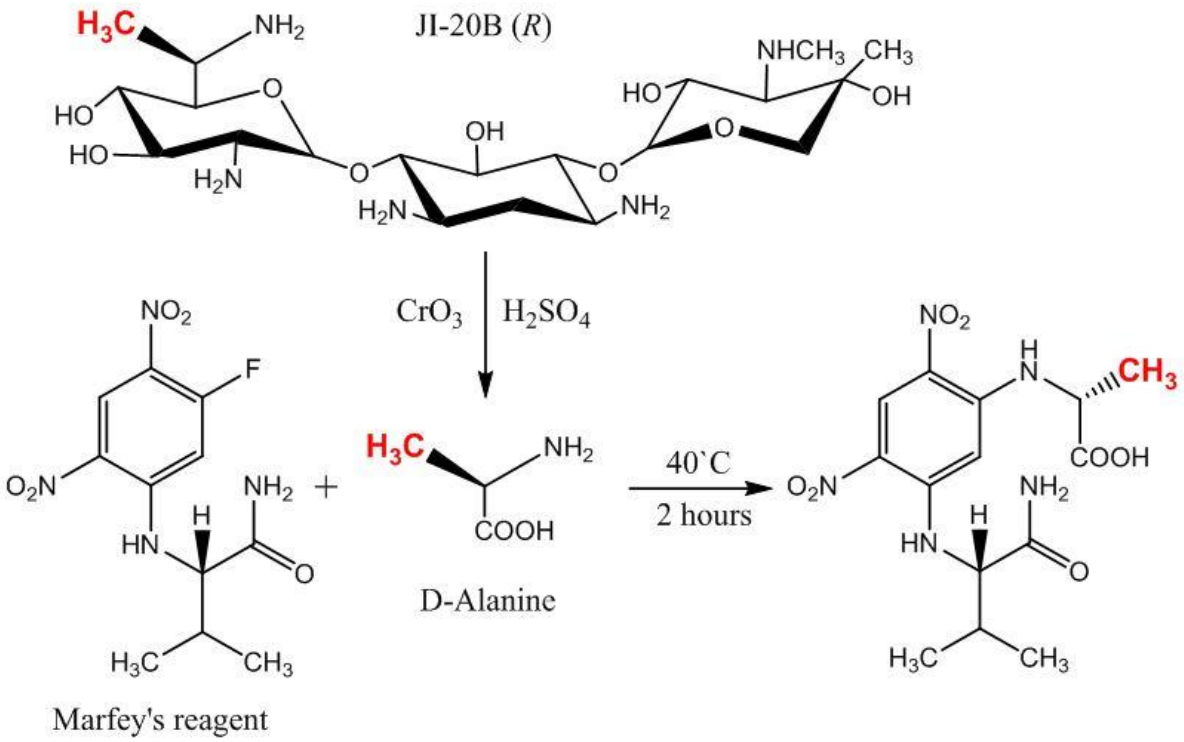

Figure 8.2 Kuhn-Roth oxidation and Marfey's analysis. Absolute stereochemistry determination can be achieved through acid hydrolysis of gentamicins and subsequent reaction of the produced amino acid with Marfey's reagent. Standards of both amino acid conformations are then used to determine the stereochemistry of the 6' group.

8.3.4 *M. inyoensis* and *M. grisea*

Sisomicin producer *M. inyoensis* and verdamicin producer *M. grisea* are separate *Micromonospora* species that nevertheless produce gentamicin pathway intermediates. They could be used as a source of intermediates for semi-synthesis or as gentamicin C complex producers with fewer components. The *sis* cluster has been sequenced, whereas the *ver* cluster is currently being sequenced and assembled in our lab. *In silico* analysis will reveal what genes the *ver* cluster possesses, specifically, if *genB4* is absent. *GenB4* could be used to complement the two species and provide further proof of GenB4 function.

8.3.5 Potential use of gentamicin enzymes as other aminoglycoside modifiers

The wide specificity of gentamicin enzymes has been known for a long time. Feeding of kanamycin B to *M. echinospora* generated compound I-B_1, 3''-*N*-methyl-4''-*C*-methyl-3',4'-dideoxy-6'-*N*-methylkanamycin B (Figure 8.3) (Oka et al., 1979).

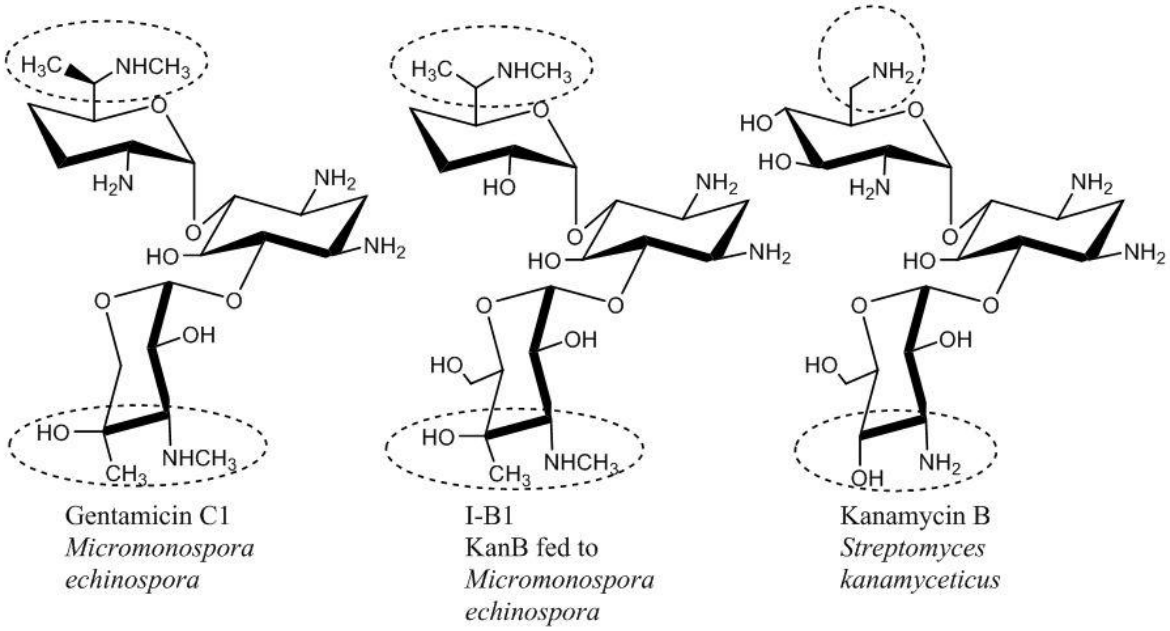

Figure 8.3 Biosynthesis of neoglycosides . *M. echinospora* mutants have been used previously to create a novel kanamycin compound. The identification of enzyme catalysts involved in di-dehydroxylation step could lead to more new structures.

The identification of the enzymes involved in the di-dehydroxylation step could allow for creation of novel aminoglycosides or neoglycosides by cloning these genes into other aminoglycoside-producing strains.

References

Aboshanab, K. M. A. (2005) Genetic studies on the biosynthesis of the major aminoglycoside antibiotics: Isolation, analysis and comparison of the biosynthetic gene clusters for 12 aminoglycoside antibiotics. Doctor of Natural Sciences, Bergische Wuppertal University, Wuppertal.

Aggen, J. B., Armstrong, E. S., Goldblum, A. A., Dozzo, P., Linsell, M. S., Gliedt, M. J., Hildebrandt, D. J., Feeney, L. A., Kubo, A., Matias, R. D., Lopez, S., Gomez, M., Wlasichuk, K. B., Diokno, R., Miller, G. H. and Moser, H. E. (2010) 'Synthesis and spectrum of the neoglycoside ACHN-490', *Antimicrob Agents Chemother,* 54(11), pp. 4636-42.

Agnihotri, G. and Liu, H. W. (2001) 'PLP and PMP radicals: a new paradigm in coenzyme B6 chemistry', *Bioorg Chem,* 29(4), pp. 234-57.

Akiyama, T., Tanaka, K. and Tanaka, N. (1978) 'Interaction of viomycin and aminoglycoside antibiotics with tubulin and microtubules', *J Antibiot (Tokyo),* 31(12), pp. 1306-9.

Aldridge, S. 1999. The Discovery and Development of Penicillin, 1928-1945. London, UK: American Chemical Society.

Anchaogen (2017) Plazomicin: the first clinical candidate from our gram-negative antibiotic discovery engine. Available at: http://www.achaogen.com/plazomicin/.

Arrow, A. S. and Taber, H. W. (1986) 'Streptomycin accumulation by *Bacillus subtilis* requires both a membrane potential and cytochrome aa3', *Antimicrob Agents Chemother,* 29(1), pp. 141-6.

Baddour, L. M., Wilson, W. R., Bayer, A. S., Fowler, V. G., Bolger, A. F., Levison, M. E., Ferrieri, P., Gerber, M. A., Tani, L. Y., Gewitz, M. H., Tong, D. C., Steckelberg, J. M., Baltimore, R. S., Shulman, S. T., Burns, J. C., Falace, D. A., Newburger, J. W., Pallasch, T. J., Takahashi, M., Taubert, K. A., Committee on Rheumatic Fever, E. d., and Kawasaki Disease, Young, C. o. C. D. i. t., Councils on Clinical Cardiology, S. r., and Cardiovascular Surgery and Anesthesia, Association, A. H. and America, I. D. S. o. (2005) 'Infective endocarditis: diagnosis, antimicrobial therapy, and management of complications: a statement for healthcare professionals from the Committee on Rheumatic Fever, Endocarditis, and Kawasaki Disease, Council on Cardiovascular Disease in the Young, and the Councils on Clinical Cardiology, Stroke, and Cardiovascular Surgery and Anesthesia, American Heart Association: endorsed by the Infectious Diseases Society of America', *Circulation,* 111(23), pp. e394-434.

Barka, E. A., Vatsa, P., Sanchez, L., Gaveau-Vaillant, N., Jacquard, C., Klenk, H. P., Clément, C., Ouhdouch, Y. and van Wezel, G. P. (2016) 'Taxonomy, Physiology, and Natural Products of Actinobacteria', *Microbiol Mol Biol Rev,* 80(1), pp. 1-43.

Barton-Davis, E. R., Cordier, L., Shoturma, D. I., Leland, S. E. and Sweeney, H. L. (1999) 'Aminoglycoside antibiotics restore dystrophin function to skeletal muscles of mdx mice', *J Clin Invest,* 104(4), pp. 375-81.

Bekiesch, P., Basitta, P. and Apel, A. K. (2016) 'Challenges in the Heterologous Production of Antibiotics in Streptomyces', *Arch Pharm (Weinheim),* 349(8), pp. 594-601.

Bentley, S. D., Chater, K. F., Cerdeño-Tárraga, A. M., Challis, G. L., Thomson, N. R., James, K. D., Harris, D. E., Quail, M. A., Kieser, H., Harper, D., Bateman, A., Brown, S., Chandra, G., Chen, C. W., Collins, M., Cronin, A., Fraser, A., Goble, A., Hidalgo, J., Hornsby, T., Howarth, S., Huang, C. H., Kieser, T., Larke, L., Murphy, L., Oliver, K., O'Neil, S., Rabbinowitsch, E., Rajandream, M. A., Rutherford, K., Rutter, S., Seeger, K., Saunders, D., Sharp, S., Squares, R., Squares, S., Taylor, K., Warren, T., Wietzorrek, A., Woodward, J., Barrell, B. G., Parkhill, J. and Hopwood, D. A. (2002) 'Complete genome sequence of the model actinomycete *Streptomyces coelicolor* A3(2)', *Nature,* 417(6885), pp. 141-7.

Benveniste, R. and Davies, J. (1971a) 'Enzymatic acetylation of aminoglycoside antibiotics by *Escherichia coli* carrying an R factor', *Biochemistry,* 10(10), pp. 1787-96.

Benveniste, R. and Davies, J. (1971b) 'R-factor mediated gentamicin resistance: A new enzyme which modifies aminoglycoside antibiotics', *FEBS Lett,* 14(5), pp. 293-296.

Bergmans, H. E., van Die, I. M. and Hoekstra, W. P. (1981) 'Transformation in Escherichia coli: stages in the process', *J Bacteriol,* 146(2), pp. 564-70.

Bernstein, J. A., Khodursky, A. B., Lin, P. H., Lin-Chao, S. and Cohen, S. N. (2002) 'Global analysis of mRNA decay and abundance in *Escherichia coli* at single-gene resolution using two-color fluorescent DNA microarrays', *Proc Natl Acad Sci U S A,* 99(15), pp. 9697-702.

Betancor, L. (2009) *Final Report,* PFL Lab: University of Cambridge.

Betancor, L., Hidalgo, A., Fernández-Lorente, G., Mateo, C., Fernández-Lafuente, R. and Guisan, J. M. (2003) 'Preparation of a stable biocatalyst of bovine liver catalase using immobilization and postimmobilization techniques', *Biotechnol Prog,* 19(3), pp. 763-7.

Betancor, L. and Luckarift, H. R. (2008) 'Bioinspired enzyme encapsulation for biocatalysis', *Trends Biotechnol,* 26(10), pp. 566-72.

Betancor, L., Luckarift, H. R., Seo, J. H., Brand, O. and Spain, J. C. (2008) 'Three-dimensional immobilization of beta-galactosidase on a silicon surface', *Biotechnol Bioeng,* 99(2), pp. 261-7.

Beyer, N., Alam, J., Hallis, T. M., Guo, Z. and Liu, H. W. (2003) 'The biosynthesis of GDP-L-colitose: C-3 deoxygenation is catalyzed by a unique coenzyme B6-dependent enzyme', *J Am Chem Soc,* 125(19), pp. 5584-5.

Bhushan, R. and Brückner, H. (2011) 'Use of Marfey's reagent and analogs for chiral amino acid analysis: assessment and applications to natural products and biological systems', *J Chromatogr B Analyt Technol Biomed Life Sci,* 879(29), pp. 3148-61.

Bibb, M. J. (2005) 'Regulation of secondary metabolism in Streptomycetes', *Curr Opin Microbiol,* 8(2), pp. 208-15.

Bibb, M. J. (2013) 'Understanding and manipulating antibiotic production in actinomycetes', *Biochem Soc Trans,* 41(6), pp. 1355-64.

Bonomo, R. A. and Szabo, D. (2006) 'Mechanisms of multidrug resistance in Acinetobacter species and Pseudomonas aeruginosa', *Clin Infect Dis,* 43 Suppl 2, pp. S49-56.

Boxerbaum, B., Pittman, S., Doershuk, C. F., Stern, R. C. and Matthews, L. W. (1971) 'Use of gentamicin in children with cystic fibrosis', *J Infect Dis,* 124 Suppl, pp. S293-95.

Bradow, J., Riley, F., Philippe, L., Yan, Q., Schuff, B. and Harris, G. H. (2015) 'Automated solvent system screening for the preparative countercurrent chromatography of pharmaceutical discovery compounds', *J Sep Sci,* 38(23), pp. 3983-91.

Bretscher, M. S. (1968) 'Direct translation of a circular messenger DNA', *Nature,* 220(5172), pp. 1088-91.

Brummett, R. E. and Fox, K. E. (1977) 'Comparative ototoxicity of BB-K8 (amikacin), gentamicin, sisomicin and tobramycin in the guinea pig', *Proc West Pharmacol Soc,* 20, pp. 449-53.

Brummett, R. E. and Fox, K. E. (1982) 'Studies of aminoglycoside toxicity in animal models', in Whelton, A. & Neu, H.C. (eds.) *The aminoglycosides: microbiology, clinical use, and toxicology.* New York: Marcel Dekker, Inc., pp. 419-451.

Brummett, R. E., Fox, K. E., Bendrick, T. W. and Himes, D. L. (1978) 'Ototoxicity of tobramycin, gentamicin, amikacin and sisomicin in the guinea pig', *J Antimicrob Chemother,* 4 Suppl A, pp. 73-83.

Brummett, R. E., Himes, D., Saine, B. and Vernon, J. (1972) 'A comparative study of the ototoxicity of tobramycin and gentamicin', *Arch Otolaryngol,* 96(6), pp. 505-12.

Bryan, L. E. and Kwan, S. (1983) 'Roles of ribosomal binding, membrane potential, and electron transport in bacterial uptake of streptomycin and gentamicin', *Antimicrob Agents Chemother,* 23(6), pp. 835-45.

Bumpus, S. B., Magarvey, N. A., Kelleher, N. L., Walsh, C. T. and Calderone, C. T. (2008) 'Polyunsaturated fatty-acid-like trans-enoyl reductases utilized in polyketide biosynthesis', *J Am Chem Soc,* 130(35), pp. 11614-6.

Butler, M. S., Blaskovich, M. A. and Cooper, M. A. (2013) 'Antibiotics in the clinical pipeline in 2013', *J Antibiot (Tokyo),* 66(10), pp. 571-91.

Byrne, K. M., Kershner, A. S., Maehr, H., Marquez, J. A. and Schaffner, C. P. (1977) 'Separation of gentamicin C-complex into five components by Craig distribution', *J Chromatogr,* 131, pp. 191-203.

Carter, A. P., Clemons, W. M., Brodersen, D. E., Morgan-Warren, R. J., Wimberly, B. T. and Ramakrishnan, V. (2000) 'Functional insights from the structure of the 30S ribosomal subunit and its interactions with antibiotics', *Nature,* 407(6802), pp. 340-8.

Center for Disease Control and Prevention (1999) 'Achievements in Public Health, 1900-1999: Control of Infectious Diseases', *Morbidity and Mortality Weekly Report,* 48(29), pp. 621-629.

Ceroni, F., Algar, R., Stan, G. B. and Ellis, T. (2015) 'Quantifying cellular capacity identifies gene expression designs with reduced burden', *Nat Methods,* 12(5), pp. 415-8.

Chen, Y., Deng, W., Wu, J., Qian, J., Chu, J., Zhuang, Y., Zhang, S. and Liu, W. (2008) 'Genetic modulation of the overexpression of tailoring genes eryK and eryG leading to the improvement of erythromycin A purity and production in *Saccharopolyspora erythraea* fermentation', *Appl Environ Microbiol,* 74(6), pp. 1820-8.

Chisholm, G. D. (1974) 'The use of gentamicin in urinary tract infections with special reference to drug levels in complicated (urological) infections', *Postgrad Med J,* 50 Suppl 7, pp. 23-31.

Chiu, P. J. and Long, J. F. (1978) 'Effects of hydration on gentamicin excretion and renal accumulation in furosemide-treated rats', *Antimicrob Agents Chemother,* 14(2), pp. 214-7.

Chou, D. K., Krishnamurthy, R., Randolph, T. W., Carpenter, J. F. and Manning, M. C. (2005) 'Effects of Tween 20 and Tween 80 on the stability of Albutropin during agitation', *J Pharm Sci,* 94(6), pp. 1368-81.

Chu, J., Li, B., Zhang, S. and Li, Y. (2000) 'On-line ultrasound stimulates the secretion and production of gentamicin by *Micromonospora echinospora*', *Process Biochemistry,* 35(6), pp. 569-572.

Chu, J., Niu, W., Zhang, A., Zhuang, Y., Hu, H. and Li, Y. (2004) 'Effect of metal ions on the binding of gentamicin to the peptidoglycan of *Micromonospora echinospora*', *Process Biochemistry,* 39, pp. 1145-1150.

Cooper, D. J., Daniels, P. J. L., Yudis, M. D., Marigliano, H. M., Guthrie, R. D. and Bukhari, S. T. K. (1971a) 'The gentamicin antibiotics. 3. The gross structures of gentamicin C components.', *Journal of the Chemical Society C: Organic,* (0), pp. 3126-3129.

Cooper, D. J., Yudis, M. D., Marigliano, H. M. and Traubel, T. (1971b) 'The gentamicin antibiotics. II. Separation and degradation of the gentamicin C components. The purpurosamines, a new class of naturally occurring 2,6-diaminomonosaccharides', *J Chem Soc Perkin 1,* 17, pp. 2876-9.

Craig, L. C. and Golumbic, C. (1945) 'Identification of small amounts of organic compounds by distribution studies; the use of buffers in counter-current distribution', *J Biol Chem,* 161, pp. 321-32.

Cuccarese, M. F., Singh, A., Amiji, M. and O'Doherty, G. A. (2013) 'A novel use of gentamicin in the ROS-mediated sensitization of NCI-H460 lung cancer cells to various anticancer agents', *ACS Chem Biol,* 8(12), pp. 2771-7.

Dairi, T., Ohta, T., Hashimoto, E. and Hasegawa, M. (1992) 'Organization and nature of fortimicin A (astromicin) biosynthetic genes studied using a cosmid library of *Micromonospora olivasterospora* DNA', *Mol Gen Genet,* 236(1), pp. 39-48.

Daniels, P. J., Jaret, R. S., Nagabhushan, T. L. and Turner, W. N. (1976) 'The structure of antibiotic G-52, a new aminocyclitol-aminoglycoside antibiotic produced by *Micromonospora zionensis*', *J Antibiot (Tokyo),* 29(5), pp. 488-91.

Daniels, P. J., Luce, C. and Nagabhushan, T. L. (1975) 'The gentamicin antibiotics. 6. Gentamicin C2b, an aminoglycoside antibiotic produced by *Micromonospora purpurea* mutant JI-33', *J Antibiot (Tokyo),* 28(1), pp. 35-41.

Daniels, P. J. L. (1975) 'The elucidation of the structures of gentamicin and sisomicin and the current status of clinical resistance to these antibiotics.', *Aminoglycoside antibiotics*. Tokyo: University Park Press, pp. 77-111.

Daniels, P. J. L. and Marquez, J. A. (1976) Method of isolating gentamicin C2a. [Online].

Daum, S. J., Rosi, D. and Goss, W. (1977) 'Production of antibiotics by biotransformation of 2,4,6/3,5-pentahydroxycyclohexanone and 2,4/3,5-tetrahydroxycyclohexanone by a deoxystreptamine-negative mutant of *Micromonospora purpurea*', *J Am Chem Soc,* 99(1), pp. 283-4.

Davies, J. (2006) 'Where have All the Antibiotics Gone?', *Can J Infect Dis Med Microbiol,* 17(5), pp. 287-90.

Davies, J. and Davies, D. (2010) 'Origins and evolution of antibiotic resistance', *Microbiol Mol Biol Rev,* 74(3), pp. 417-33.

Davies, J., von Ahsen, U., Wank, H. and Schroeder, R. (1992) 'Evolution of secondary metabolite production: potential roles for antibiotics as prebiotic effectors of catalytic RNA reactions', *Ciba Found Symp,* 171, pp. 24-32; discussion 32-44.

Davies, J. E. (1964) 'Studies on the ribosomes of streptomycin-sensitive and resistant strains of *Escherichia coli*', *Proc Natl Acad Sci U S A,* 51, pp. 659-64.

Deguchi, T., Okumura, S., Ishii, A. and Tanaka, M. (1977) 'Synthesis of carbon-14 and tritium labeled sagamicin', *J Antibiot (Tokyo),* 30(11), pp. 993-8.

Dorgan, K. M., Wooderchak, W. L., Wynn, D. P., Karschner, E. L., Alfaro, J. F., Cui, Y., Zhou, Z. S. and Hevel, J. M. (2006) 'An enzyme-coupled continuous spectrophotometric assay for S-adenosylmethionine-dependent methyltransferases', *Anal Biochem,* 350(2), pp. 249-55.

Driscoll, R. S. (2003) *War Casualties*. Dictionary of American History: The Gale Group, Inc. Available at: http://www.encyclopedia.com/history/dictionaries-thesauruses-pictures-and-press-releases/war-casualties.

Drusano, G. L. (1990) 'Human pharmacodynamics of beta-lactams, aminoglycosides and their combination', *Scand J Infect Dis Suppl,* 74, pp. 235-48.

Du, Y. L., Singh, R., Alkhalaf, L. M., Kuatsjah, E., He, H. Y., Eltis, L. D. and Ryan, K. S. (2016) 'A pyridoxal phosphate-dependent enzyme that oxidizes an unactivated carbon-carbon bond', *Nat Chem Biol,* 12(3), pp. 194-9.

Dubin, D. T., Hancock, R. and Davis, B. D. (1963) 'The sequence of some effects of streptomycin in *Escherichia coli*', *Biochim Biophys Acta,* 74, pp. 476-89.

Dunathan, H. C., Davis, L., Kury, P. G. and Kaplan, M. (1968) 'The stereochemistry of enzymatic transamination', *Biochemistry,* 7(12), pp. 4532-7.

Duong-Ly, K. C. and Gabelli, S. B. (2014) 'Salting out of proteins using ammonium sulfate precipitation', *Methods Enzymol,* 541, pp. 85-94.

Durante-Mangoni, E., Grammatikos, A., Utili, R. and Falagas, M. E. (2009) 'Do we still need the aminoglycosides?', *Int J Antimicrob Agents,* 33(3), pp. 201-5.

Endimiani, A., Hujer, K. M., Hujer, A. M., Armstrong, E. S., Choudhary, Y., Aggen, J. B. and Bonomo, R. A. (2009) 'ACHN-490, a neoglycoside with potent in vitro activity against multidrug-resistant *Klebsiella pneumoniae* isolates', *Antimicrob Agents Chemother,* 53(10), pp. 4504-7.

Erdos, T. and Ullmann, A. (1959) 'Effect of streptomycin on the incorporation of amino-acids labelled with carbon-14 into ribonucleic acid and protein in a cell-free system of a *Mycobacterium*', *Nature,* 183(4661), pp. 618-9.

Evans, W. E., Feldman, S., Ossi, M., Taylor, R. H., Chaudhary, S., Melton, E. T. and Barker, L. F. (1979) 'Gentamicin dosage in children: a randomized prospective comparison of body weight and body surface area as dose determinants', *J Pediatr,* 94(1), pp. 139-43.

Fair, R. J. and Tor, Y. (2014) 'Antibiotics and bacterial resistance in the 21st century', *Perspect Medicin Chem,* 6, pp. 25-64.

Fan, Q., Huang, F., Leadlay, P. F. and Spencer, J. B. (2008) 'The neomycin biosynthetic gene cluster of *Streptomyces fradiae* NCIMB 8233: genetic and biochemical evidence for the roles of two glycosyltransferases and a deacetylase', *Org Biomol Chem,* 6(18), pp. 3306-14.

Feldman, M. B., Terry, D. S., Altman, R. B. and Blanchard, S. C. (2010) 'Aminoglycoside activity observed on single pre-translocation ribosome complexes', *Nat Chem Biol,* 6(1), pp. 54-62.

Fernandes, P. and Martens, E. (2017) 'Antibiotics in late clinical development', *Biochem Pharmacol,* 133, pp. 152-163.

Firn, R. D. and Jones, C. G. (2000) 'The evolution of secondary metabolism - a unifying model', *Mol Microbiol,* 37(5), pp. 989-94.

Flatt, P. M. and Mahmud, T. (2007) 'Biosynthesis of aminocyclitol-aminoglycoside antibiotics and related compounds', *Nat Prod Rep,* 24(2), pp. 358-92.

Foit, L., Morgan, G. J., Kern, M. J., Steimer, L. R., von Hacht, A. A., Titchmarsh, J., Warriner, S. L., Radford, S. E. and Bardwell, J. C. (2009) 'Optimizing protein stability in vivo', *Mol Cell,* 36(5), pp. 861-71.

Forge, A., Li, L., Corwin, J. T. and Nevill, G. (1993) 'Ultrastructural evidence for hair cell regeneration in the mammalian inner ear', *Science,* 259(5101), pp. 1616-9.

Forge, A. and Schacht, J. (2000) 'Aminoglycoside antibiotics', *Audiol Neurootol,* 5(1), pp. 3-22.

Fourmy, D., Recht, M. I., Blanchard, S. C. and Puglisi, J. D. (1996) 'Structure of the A site of *Escherichia coli* 16S ribosomal RNA complexed with an aminoglycoside antibiotic', *Science,* 274(5291), pp. 1367-71.

Fox, K. E., Brummett, R. E., Brown, R. and Himes, D. (1980) 'A comparative study of the ototoxicity of gentamicin and gentamicin C1', *Arch Otolaryngol,* 106(1), pp. 44-9.

Galani, I., Souli, M., Daikos, G. L., Chrysouli, Z., Poulakou, G., Psichogiou, M., Panagea, T., Argyropoulou, A., Stefanou, I., Plakias, G., Giamarellou, H. and Petrikkos, G. (2012) 'Activity of plazomicin (ACHN-490) against MDR clinical isolates of *Klebsiella pneumoniae, Escherichia coli,* and *Enterobacter* spp. from Athens, Greece', *J Chemother,* 24(4), pp. 191-4.

Galimand, M., Courvalin, P. and Lambert, T. (2003) 'Plasmid-mediated high-level resistance to aminoglycosides in *Enterobacteriaceae* due to 16S rRNA methylation', *Antimicrob Agents Chemother,* 47(8), pp. 2565-71.

Garrard, I. J., Fisher, D. and Sutherland, I. A. (2008) 'Dynamic Extraction: A High Speed, High Capacity Purification Process that is Rapidly Scaleable', *LCGC North America,* 26(5), pp. 1-7.

Gibson, D. G. (2011) 'Enzymatic assembly of overlapping DNA fragments', *Methods Enzymol,* 498, pp. 349-61.

Goh, E. B., Yim, G., Tsui, W., McClure, J., Surette, M. G. and Davies, J. (2002) 'Transcriptional modulation of bacterial gene expression by subinhibitory concentrations of antibiotics', *Proc Natl Acad Sci U S A,* 99(26), pp. 17025-30.

Gold, L. and Stormo, G. D. (1990) 'High-level translation initiation', *Methods Enzymol,* 185, pp. 89-93.

Grahek, R. and Zupancic-Kralj, L. (2009) 'Identification of gentamicin impurities by liquid chromatography tandem mass spectrometry', *J Pharm Biomed Anal,* 50(5), pp. 1037-43.

Gregory, M. A., Petkovic, H., Lill, R. E., Moss, S. J., Wilkinson, B., Gaisser, S., Leadlay, P. F. and Sheridan, R. M. (2005) 'Mutasynthesis of rapamycin analogues through the manipulation of a gene governing starter unit biosynthesis', *Angew Chem Int Ed Engl,* 44(30), pp. 4757-60.

Grisebach, H. (1978) 'Biosynthesis of sugar components of antibiotic substances.', *Advances in carbohydrate chemistry,* 35, pp. 81-126.

Grossman, T. H., Fyfe, C., O'Brien, W., Hackel, M., Minyard, M. B., Waites, K. B., Dubois, J., Murphy, T. M., Slee, A. M., Weiss, W. J. and Sutcliffe, J. A. (2017) 'Fluorocycline TP-271 Is Potent against Complicated Community-Acquired Bacterial Pneumonia Pathogens', *mSphere,* 2(1).

Gu, Y., Ni, X., Ren, J., Gao, H., Wang, D. and Xia, H. (2015) 'Biosynthesis of Epimers C2 and C2a in the Gentamicin C Complex', *Chembiochem.*

Guan, M. X., Fischel-Ghodsian, N. and Attardi, G. (2000) 'A biochemical basis for the inherited susceptibility to aminoglycoside ototoxicity', *Hum Mol Genet,* 9(12), pp. 1787-93.

Guindon, S., Dufayard, J. F., Lefort, V., Anisimova, M., Hordijk, W. and Gascuel, O. (2010) 'New algorithms and methods to estimate maximum-likelihood phylogenies: assessing the performance of PhyML 3.0', *Syst Biol,* 59(3), pp. 307-21.

Guo, J., Huang, F., Huang, C., Duan, X., Jian, X., Leeper, F., Deng, Z., Leadlay, P. F. and Sun, Y. (2014) 'Specificity and promiscuity at the branch point in gentamicin biosynthesis', *Chem Biol,* 21(5), pp. 608-18.

Hamilton-Miller, J. M. and Shah, S. (1995) 'Activity of the semi-synthetic kanamycin B derivative, arbekacin against methicillin-resistant *Staphylococcus aureus*', *J Antimicrob Chemother,* 35(6), pp. 865-8.

Hanessian, S., Szychowski, J. and Maianti, J. P. (2009) 'Synthesis and comparative antibacterial activity of verdamicin C2 and C2a. A new oxidation of primary allylic azides in dihydro[2H]pyrans', *Org Lett,* 11(2), pp. 429-32.

Hasegawa, M. (1991) 'A gene cloning system in *Micromonospora* which revealed the organization of biosynthetic genes of fortimicin A (astromicin)', *Actinomycetologica,* 5(2), pp. 126-131.

Haslam, E. (1995) 'Secondary metabolism - evolution and function: products or processes?', *Chemoecology,* 5(2), pp. 89-95.

He, K. Y., Zhang, C., Duan, Y. R., Huang, G. L., Yang, C. Y., Lu, X. R., Zheng, C. J. and Chen, G. Y. (2017) 'New chlorinated xanthone and anthraquinone produced by a mangrove-derived fungus *Penicillium citrinum* HL-5126', *J Antibiot (Tokyo),* 70(7), pp. 823-827.

Hede, K. (2014) 'Antibiotic resistance: an infectious arms race', *Nature,* 509(7498), pp. S2-3.

Hertweck, C. (2009) 'The biosynthetic logic of polyketide diversity', *Angew Chem Int Ed Engl,* 48(26), pp. 4688-716.

Hesketh, A., Chen, W. J., Ryding, J., Chang, S. and Bibb, M. (2007) 'The global role of ppGpp synthesis in morphological differentiation and antibiotic production in *Streptomyces coelicolor* A3(2)', *Genome Biol,* 8(8), pp. R161.

Himabindu, M. and Jetty, A. (2006) 'Optimization of nutritional requirements for gentamicin production by *Micromonospora echinospora*', *Indian J Exp Biol,* 44(10), pp. 842-8.

Himabindu, M., Potumarthi, R. and Jetty, A. (2007) 'Enhancement of gentamicin production by mutagenesis and non-nutritional stress conditions of *Micromonospora echinospora*', *Process Biochemistry,* 42, pp. 352-356.

Hodges, G. R. and Saslaw, S. (1972) 'Gentamicin in the treatment of respiratory tract infections', *Ohio State Med J,* 68(5), pp. 475-80.

Hong, L., Zhao, Z. and Liu, H. W. (2006) 'Characterization of SpnQ from the spinosyn biosynthetic pathway of *Saccharopolyspora spinosa*: mechanistic and evolutionary implications for C-3 deoxygenation in deoxysugar biosynthesis', *J Am Chem Soc,* 128(44), pp. 14262-3.

Hopwood, D. A. (2007) 'How do antibiotic-producing bacteria ensure their self-resistance before antibiotic biosynthesis incapacitates them?', *Mol Microbiol,* 63(4), pp. 937-40.

Houghton, J. L., Green, K. D., Chen, W. and Garneau-Tsodikova, S. (2010) 'The future of aminoglycosides: the end or renaissance?', *Chembiochem,* 11(7), pp. 880-902.

Huang, C., Huang, F., Moison, E., Guo, J., Jian, X., Duan, X., Deng, Z., Leadlay, P. F. and Sun, Y. (2015) 'Delineating the biosynthesis of gentamicin x2, the common precursor of the gentamicin C antibiotic complex', *Chem Biol,* 22(2), pp. 251-61.

Huang, F., Haydock, S. F., Mironenko, T., Spiteller, D., Li, Y. and Spencer, J. B. (2005) 'The neomycin biosynthetic gene cluster of *Streptomyces fradiae* NCIMB 8233: characterisation of an aminotransferase involved in the formation of 2-deoxystreptamine', *Org Biomol Chem,* 3(8), pp. 1410-8.

Huang, F., Li, Y., Yu, J. and Spencer, J. B. (2002) 'Biosynthesis of aminoglycoside antibiotics: cloning, expression and characterisation of an aminotransferase involved in the pathway to 2-deoxystreptamine', *Chem Commun (Camb),* (23), pp. 2860-1.

Huang, F., Spiteller, D., Koorbanally, N. A., Li, Y., Llewellyn, N. M. and Spencer, J. B. (2007) 'Elaboration of neosamine rings in the biosynthesis of neomycin and butirosin', *Chembiochem,* 8(3), pp. 283-8.

Ikeda, H., Ishikawa, J., Hanamoto, A., Shinose, M., Kikuchi, H., Shiba, T., Sakaki, Y., Hattori, M. and Omura, S. (2003) 'Complete genome sequence and comparative analysis of the industrial microorganism *Streptomyces avermitilis*', *Nat Biotechnol,* 21(5), pp. 526-31.

Ilavsky, J., Bayan, A. P., Charney, W. and Reimann, H. (1975) *Antibiotics from Micromonospora purpurea*. [Online].

Isoherranen, N., Lavy, E. and Soback, S. (2000) 'Pharmacokinetics of gentamicin C(1), C(1a), and C(2) in beagles after a single intravenous dose', *Antimicrob Agents Chemother,* 44(6), pp. 1443-7.

Ito, Y. (1981) 'Countercurrent chromatography', *J Biochem Biophys Methods,* 5(2), pp. 105-29.

Ito, Y. and Bowman, R. L. (1970) 'Countercurrent chromatography: liquid-liquid partition chromatography without solid support', *Science,* 167(3916), pp. 281-3.

Ito, Y. and Bowman, R. L. (1971) 'Countercurrent chromatography with flow-through coil planet centrifuge', *Science,* 173(3995), pp. 420-2.

Ito, Y., Namba, M., Nagahama, N., Yamaguchi, T. and Okuda, T. (1964) 'Thin layer chromatography of the basic water-soluble antibiotics', *J Antibiot (Tokyo),* 17, pp. 218-9.

Ito, Y., Weinstein, M., Aoki, I., Harada, R., Kimura, E. and Nunogaki, K. (1966) 'The coil planet centrifuge', *Nature,* 212(5066), pp. 985-7.

James, P. D., Raut, S., Rivard, G. E., Poon, M. C., Warner, M., McKenna, S., Leggo, J. and Lillicrap, D. (2005) 'Aminoglycoside suppression of nonsense mutations in severe hemophilia', *Blood,* 106(9), pp. 3043-8.

Jenkins, W. T. (1991) 'The pyruvate kinase-coupled assay for ATPases: a critical analysis', *Anal Biochem,* 194(1), pp. 136-9.

Jiang, H., Sha, S. H. and Schacht, J. (2006) 'Rac/Rho pathway regulates actin depolymerization induced by aminoglycoside antibiotics', *J Neurosci Res,* 83(8), pp. 1544-51.

Kala, R. (2000) *Microbial production of antibiotics from mangrove ecosystem*. Doctor of Philosophy, COCHIN UNIVERSITY OF SCIENCE AND TECHNOLOGY.

Kamjam, M., Sivalingam, P., Deng, Z. and Hong, K. (2017) 'Deep Sea Actinomycetes and Their Secondary Metabolites', *Front Microbiol,* 8, pp. 760.

Kantor, N. and Selzer, G. (1968) 'Chromatographic separation and bioassay of the gentamicin complex', *J Pharm Sci,* 57(12), pp. 2170-1.

Karpiuk, I. and Tyski, S. (2015) 'Looking for new preparations for antibacterial therapy. IV. New antimicrobial agents from the aminoglycoside, macrolide and tetracycline groups in clinical trials', *Przegl Epidemiol,* 69(4), pp. 723-9, 865-70.

Kase, H., Odakura, Y. and Nakayama, K. (1982b) 'Sagamicin and the related aminoglycosides: fermentation and biosynthesis. I. Biosynthetic studies with the blocked mutants of *Micromonospora sagamiensis*', *J Antibiot (Tokyo),* 35(1), pp. 1-9.

Kase, H., Shimura, G., Iida, T. and Nakayama, K. (1982c) 'Biotransformation of sisomicin and verdamicin by *Micromonospora sagamiensis*', *Agricultural and Biological Chemistry,* 46, pp. 515-522.

Kawamoto, I., Oka, T. and Nara, T. (1981) 'Cell wall composition of *Micromonospora olivoasterospora, Micromonospora sagamiensis*, and related organisms', *J Bacteriol,* 146(2), pp. 527-34.

Kawamoto, K., Sha, S. H., Minoda, R., Izumikawa, M., Kuriyama, H., Schacht, J. and Raphael, Y. (2004) 'Antioxidant gene therapy can protect hearing and hair cells from ototoxicity', *Mol Ther,* 9(2), pp. 173-81.

Kharel, M. K., Basnet, D. B., Lee, H. C., Liou, K., Moon, Y. H., Kim, J. J., Woo, J. S. and Sohng, J. K. (2004) 'Molecular cloning and characterization of a 2-deoxystreptamine biosynthetic gene cluster in gentamicin-producing *Micromonospora echinospora* ATCC15835', *Mol Cells,* 18(1), pp. 71-8.

Khosla, C., Herschlag, D., Cane, D. E. and Walsh, C. T. (2014) 'Assembly line polyketide synthases: mechanistic insights and unsolved problems', *Biochemistry,* 53(18), pp. 2875-83.

Kieser, T., Bibb, M. J., Buttner, M. J., Chater, K. F. and Hopwood, D. A. (2000) *Practical Streptomyces genetics*. Norwich: John Innes Foundation.

Kim, H. J., LeVieux, J., Yeh, Y. C. and Liu, H. W. (2016) 'C3'-Deoxygenation of Paromamine Catalyzed by a Radical S-Adenosylmethionine Enzyme: Characterization of the Enzyme AprD4 and Its Reductase Partner AprD3', *Angew Chem Int Ed Engl,* 55(11), pp. 3724-8.

Kim, H. J., McCarty, R. M., Ogasawara, Y., Liu, Y. N., Mansoorabadi, S. O., LeVieux, J. and Liu, H. W. (2013) 'GenK-catalyzed C-6' methylation in the biosynthesis of gentamicin: isolation and characterization of a cobalamin-dependent radical SAM enzyme', *J Am Chem Soc,* 135(22), pp. 8093-6.

Kim, J. Y., Suh, J. W., Kang, S. H., Phan, T. H., Park, S. H. and Kwon, H. J. (2008) 'Gene inactivation study of gntE reveals its role in the first step of pseudotrisaccharide modifications in gentamicin biosynthesis', *Biochem Biophys Res Commun,* 372(4), pp. 730-4.

Kim, S., Nochumson, S., Chin, W. and Paik, W. K. (1978) 'A rapid method for the purification of S-adenosylmethionine: protein-carboxyl O-methyltransferase by affinity chromatography', *Anal Biochem,* 84(2), pp. 415-22.

Kobayashi, M., Sone, M., Umemura, M., Nabeshima, T., Nakashima, T. and Hellström, S. (2008) 'Comparisons of cochleotoxicity among three gentamicin compounds following intratympanic application', *Acta Otolaryngol,* 128(3), pp. 245-9.

Kohanski, M. A., Dwyer, D. J. and Collins, J. J. (2010) 'How antibiotics kill bacteria: from targets to networks', *Nat Rev Microbiol,* 8(6), pp. 423-35.

Krasnova, T. P., Laznikova, T. N., Likina, E. V. and Orlova, N. V. (1978) '[Role of cobalt in the biosynthesis of the components of the gentamicin complex]', *Antibiotiki,* 23(1), pp. 12-8.

Kudo, F. and Eguchi, T. (2009) 'Biosynthetic genes for aminoglycoside antibiotics', *J Antibiot (Tokyo),* 62(9), pp. 471-81.

Kudo, F., Hosomi, Y., Tamegai, H. and Kakinuma, K. (1999a) 'Purification and characterization of 2-deoxy-scyllo-inosose synthase derived from Bacillus circulans. A crucial carbocyclization enzyme in the biosynthesis of 2-deoxystreptamine-containing aminoglycoside antibiotics', *J Antibiot (Tokyo),* 52(2), pp. 81-8.

Kudo, F., Numakura, M., Tamegai, H., Yamamoto, H., Eguchi, T. and Kakinuma, K. (2005) 'Extended sequence and functional analysis of the butirosin biosynthetic gene cluster in Bacillus circulans SANK 72073', *J Antibiot (Tokyo),* 58(6), pp. 373-9.

Kudo, F., Tamegai, H., Fujiwara, T., Tagami, U., Hirayama, K. and Kakinuma, K. (1999b) 'Molecular cloning of the gene for the key carbocycle-forming enzyme in the biosynthesis of 2-deoxystreptamine-containing aminocyclitol antibiotics and its comparison with dehydroquinate synthase', *J Antibiot (Tokyo),* 52(6), pp. 559-71.

Labes, G., Bibb, M. and Wohlleben, W. (1997) 'Isolation and characterization of a strong promoter element from the *Streptomyces ghanaensis* phage I19 using the gentamicin resistance gene (aacC1) of Tn 1696 as reporter', *Microbiology,* 143 (Pt 5), pp. 1503-12.

Lee, B. K., Bailey, J. V., Condon, R. G., Marquez, J. A., Wagman, G. H. and Weinstein, M. J. (1977) 'Biotransformation of sisomicin to gentamicin C2b', *Antimicrob Agents Chemother,* 12(3), pp. 335-8.

Lee, B. K., Testa, R. T., Wagman, G. H., Liu, C. M., McDaniel, L. and Schaffner, C. (1973) 'Incorporation of L-methionine-methyl-14C into gentamicins', *J Antibiot (Tokyo),* 26(12), pp. 728-31.

Leekha, S., Terrell, C. L. and Edson, R. S. (2011) 'General principles of antimicrobial therapy', *Mayo Clin Proc,* 86(2), pp. 156-67.

Leitner, F. and Price, K. E. (1982) 'Aminoglycosides under development', in Whelton, A. & Neu, H.C. (eds.) *The aminoglycosides: microbiology, clinical use, and toxicology*. New York: marcel Dekker, Inc., pp. 29-64.

Lepape, A., Monnet, D. L. and participating members, E. r. S. o. I. C. M. (2009) 'Experience of European intensive care physicians with infections due to antibiotic-resistant bacteria, 2009', *Euro Surveill,* 14(45).

Lesniak, W., Pecoraro, V. L. and Schacht, J. (2005) 'Ternary complexes of gentamicin with iron and lipid catalyze formation of reactive oxygen species', *Chem Res Toxicol,* 18(2), pp. 357-64.

Letunic, I. and Bork, P. (2016) 'Interactive tree of life (iTOL) v3: an online tool for the display and annotation of phylogenetic and other trees', *Nucleic Acids Res,* 44(W1), pp. W242-5.

Li, D., Li, H., Ni, X., Zhang, H. and Xia, H. (2013) 'Construction of a gentamicin C1a-overproducing strain of *Micromonospora purpurea* by inactivation of the gacD gene', *Microbiol Res,* 168(5), pp. 263-7.

Li, G. W., Oh, E. and Weissman, J. S. (2012) 'The anti-Shine-Dalgarno sequence drives translational pausing and codon choice in bacteria', *Nature,* 484(7395), pp. 538-41.

Li, L., Nevill, G. and Forge, A. (1995) 'Two modes of hair cell loss from the vestibular sensory epithelia of the guinea pig inner ear', *J Comp Neurol,* 355(3), pp. 405-17.

Li, S., Guo, J., Reva, A., Huang, F., Xiong, B., Liu, Y., Deng, Z., Leadlay, P. F. and Sun, Y. (2018) 'Methyltransferases of gentamicin biosynthesis', *Proc Natl Acad Sci U S A,* 115(6), pp. 1340-1345.

Ling, L. L., Schneider, T., Peoples, A. J., Spoering, A. L., Engels, I., Conlon, B. P., Mueller, A., Schäberle, T. F., Hughes, D. E., Epstein, S., Jones, M., Lazarides, L., Steadman, V. A., Cohen, D. R., Felix, C. R., Fetterman, K. A., Millett, W. P., Nitti, A. G., Zullo, A. M., Chen, C. and Lewis, K. (2015) 'A new antibiotic kills pathogens without detectable resistance', *Nature,* 517(7535), pp. 455-9.

Liu, G., Chater, K. F., Chandra, G., Niu, G. and Tan, H. (2013) 'Molecular regulation of antibiotic biosynthesis in *Streptomyces*', *Microbiol Mol Biol Rev,* 77(1), pp. 112-43.

Liu, Y., Friesen, J. B., Klein, L. L., McAlpine, J. B., Lankin, D. C., Pauli, G. F. and Chen, S. N. (2015a) 'The Generally Useful Estimate of Solvent Systems (GUESS) method enables the rapid purification of methylpyridoxine regioisomers by countercurrent chromatography', *J Chromatogr A,* 1426, pp. 248-51.

Liu, Y., Friesen, J. B., McAlpine, J. B. and Pauli, G. F. (2015b) 'Solvent System Selection Strategies in Countercurrent Separation', *Planta Med,* 81(17), pp. 1582-91.

Liu, Y. Y., Wang, Y., Walsh, T. R., Yi, L. X., Zhang, R., Spencer, J., Doi, Y., Tian, G., Dong, B., Huang, X., Yu, L. F., Gu, D., Ren, H., Chen, X., Lv, L., He, D., Zhou, H., Liang, Z., Liu, J. H. and Shen, J. (2016) 'Emergence of plasmid-mediated colistin resistance mechanism MCR-1 in animals and human beings in China: a microbiological and molecular biological study', *Lancet Infect Dis,* 16(2), pp. 161-8.

Llewellyn, N. M. and Spencer, J. B. (2006) 'Biosynthesis of 2-deoxystreptamine-containing aminoglycoside antibiotics', *Nat Prod Rep,* 23(6), pp. 864-74.

Lv, M., Ji, X., Zhao, J., Li, Y., Zhang, C., Su, L., Ding, W., Deng, Z., Yu, Y. and Zhang, Q. (2016) 'Characterization of a C3 Deoxygenation Pathway Reveals a Key Branch Point in Aminoglycoside Biosynthesis', *J Am Chem Soc,* 138(20), pp. 6427-35.

Lynch, S. R. and Puglisi, J. D. (2001a) 'Structural origins of aminoglycoside specificity for prokaryotic ribosomes', *J Mol Biol,* 306(5), pp. 1037-58.

Lynch, S. R. and Puglisi, J. D. (2001b) 'Structure of a eukaryotic decoding region A-site RNA', *J Mol Biol,* 306(5), pp. 1023-35.

Lynch, S. R., Recht, M. I. and Puglisi, J. D. (2000) 'Biochemical and nuclear magnetic resonance studies of aminoglycoside-RNA complexes', *Methods Enzymol,* 317, pp. 240-61.

Ma, J., Campbell, A. and Karlin, S. (2002) 'Correlations between Shine-Dalgarno sequences and gene features such as predicted expression levels and operon structures', *J Bacteriol,* 184(20), pp. 5733-45.

MacNeil, D. J. (1988) 'Characterization of a unique methyl-specific restriction system in *Streptomyces avermitilis*', *J Bacteriol,* 170(12), pp. 5607-12.

Macone, A. B., Caruso, B. K., Leahy, R. G., Donatelli, J., Weir, S., Draper, M. P., Tanaka, S. K. and Levy, S. B. (2014) 'In vitro and in vivo antibacterial activities of omadacycline, a novel aminomethylcycline', *Antimicrob Agents Chemother,* 58(2), pp. 1127-35.

Maehr, H. and Schaffner, C. P. (1967) 'The separation and differentiation of the gentamicin complex', *J Chromatogr,* 30(2), pp. 572-8.

Magnet, S. and Blanchard, J. S. (2005) 'Molecular insights into aminoglycoside action and resistance', *Chem Rev,* 105(2), pp. 477-98.

Mandt, C. (2008) *Biosynthesen von Aminoglycosidantibiotika: Glycosyltransferasen und Deacetylasen*. Doctor rerum naturalium, Bergischen Universität Wuppertal, Wuppertal.

Marquez, J. A., Wagman, G. H., Testa, R. T., Waitz, J. A. and Weinstein, M. J. (1976) 'A new broad spectrum aminoglycoside antibiotic, G-52, produced by *Micromonospora zionensis*', *J Antibiot (Tokyo),* 29(5), pp. 483-7.

Martin, C. M., Ikari, N. S., Zimmerman, J. and Waitz, J. A. (1971) 'A virulent nosocomial *Klebsiella* with a transferable R factor for gentamicin: emergence and suppression', *J Infect Dis,* 124 Suppl, pp. S24-9.

Martín, J. F., Casqueiro, J. and Liras, P. (2005) 'Secretion systems for secondary metabolites: how producer cells send out messages of intercellular communication', *Curr Opin Microbiol,* 8(3), pp. 282-93.

Martínez-Hidalgo, P., Galindo-Villardón, P., Trujillo, M. E., Igual, J. M. and Martínez-Molina, E. (2014) '*Micromonospora* from nitrogen fixing nodules of alfalfa (Medicago sativa L.). A new promising Plant Probiotic Bacteria', *Sci Rep,* 4, pp. 6389.

Martínez-Hidalgo, P., García, J. M. and Pozo, M. J. (2015) 'Induced systemic resistance against *Botrytis cinerea* by *Micromonospora* strains isolated from root nodules', *Front Microbiol,* 6, pp. 922.

Massengo-Tiassé, R. P. and Cronan, J. E. (2009) 'Diversity in enoyl-acyl carrier protein reductases', *Cell Mol Life Sci,* 66(9), pp. 1507-17.

Mathalone, B. (1974) 'Gentamicin in eye infection', *Postgrad Med J,* 50 Suppl 7, pp. 38-9.

Matsui, J. I., Ogilvie, J. M. and Warchol, M. E. (2002) 'Inhibition of caspases prevents ototoxic and ongoing hair cell death', *J Neurosci,* 22(4), pp. 1218-27.

Matuszewska, B. and Borchardt, R. T. (1983) 'Guinea pig brain histamine N-methyltransferase: purification and partial characterization', *J Neurochem,* 41(1), pp. 113-8.

McCormick, G. C., Weinberg, E., Szot, R. J. and Schwartz, E. (1985) 'Comparative ototoxicity of netilmicin, gentamicin, and tobramycin in cats', *Toxicol Appl Pharmacol,* 77(3), pp. 479-89.

Medema, M. H., Trefzer, A., Kovalchuk, A., van den Berg, M., Müller, U., Heijne, W., Wu, L., Alam, M. T., Ronning, C. M., Nierman, W. C., Bovenberg, R. A., Breitling, R. and Takano, E. (2010) 'The sequence of a 1.8-mb bacterial linear plasmid reveals a rich evolutionary reservoir of secondary metabolic pathways', *Genome Biol Evol,* 2, pp. 212-24.

Mitsuhashi, S. (1982) 'Antibacterial activity of aminoglycoside antibiotics', in Umezawa, H. & Hooper, I.R. (eds.) *Aminoglycoside antibiotics.* Berlin: Springer-Verlag.

Miyake, T., Tsuchiya, T., Umezawa, S. and Umezawa, H. (1976) 'A synthesis of 3',4'-dideoxykanamycin B', *Carbohydr Res,* 49, pp. 141-51.

Moazed, D. and Noller, H. F. (1987) 'Interaction of antibiotics with functional sites in 16S ribosomal RNA', *Nature,* 327(6121), pp. 389-94.

Moellering, R. C. (1982) 'Clinical microbiology and the in vitro activity of aminoglycosides', in Whelton, A. & Neu, H.C. (eds.) *The aminoglycosides: microbiology, clinical use, and toxicology.* New York: Marcel Dekker, pp. 65-96.

Moore, S. (1968) 'Amino acid analysis: aqueous dimethyl sulfoxide as solvent for the ninhydrin reaction', *J Biol Chem,* 243(23), pp. 6281-3.

Méndez, C. and Salas, J. A. (2001) 'The role of ABC transporters in antibiotic-producing organisms: drug secretion and resistance mechanisms', *Res Microbiol,* 152(3-4), pp. 341-50.

Nagabhushan, T. L., Miller, G. H. and Weinstein, M. J. (1982) *The Aminoglycosides: Microbiology, Cinical Use, and Toxicology. Nephrology:* Marcel Dekker, Inc.

Ni, X., Li, D., Yang, L., Huang, T., Li, H. and Xia, H. (2011) 'Construction of kanamycin B overproducing strain by genetic engineering of *Streptomyces tenebrarius*', *Appl Microbiol Biotechnol,* 89(3), pp. 723-31.

Ni, X., Sun, Z., Zhang, H., He, H., Ji, Z. and Xia, H. (2014) 'Genetic engineering combined with random mutagenesis to enhance G418 production in *Micromonospora echinospora*', *J Ind Microbiol Biotechnol,* 41(9), pp. 1383-90.

Nichols, D., Cahoon, N., Trakhtenberg, E. M., Pham, L., Mehta, A., Belanger, A., Kanigan, T., Lewis, K. and Epstein, S. S. (2010) 'Use of ichip for high-throughput in situ cultivation of "uncultivable" microbial species', *Appl Environ Microbiol,* 76(8), pp. 2445-50.

Noone, P., Pattison, J. R. and Davies, D. G. (1974) 'The effective use of gentamicin in life-threatening sepsis', *Postgrad Med J,* 50 Suppl 7, pp. 9-16.

Oishi, M. and Cosloy, S. D. (1972) 'The genetic and biochemical basis of the transformability of *Escherichia coli* K12', *Biochem Biophys Res Commun,* 49(6), pp. 1568-72.

Oka, Y., Ishida, H., Morioka, M., Numazaki, Y., Yamafugi, T., Ozono, T. and Umezawa, H. (1979) 'New antibiotics and production thereof', *Japan Kokai,* 741, pp. 54-98.

Okuyama, A. and Tanaka, N. (1972) 'Differential effects of aminoglycosides on cistron-specific initiation of protein synthesis', *Biochem Biophys Res Commun,* 49(4), pp. 951-7.

Olano, C., Wilkinson, B., Sánchez, C., Moss, S. J., Sheridan, R., Math, V., Weston, A. J., Braña, A. F., Martin, C. J., Oliynyk, M., Méndez, C., Leadlay, P. F. and Salas, J. A. (2004) 'Biosynthesis of the angiogenesis inhibitor borrelidin by *Streptomyces parvulus* Tü4055: cluster analysis and assignment of functions', *Chem Biol,* 11(1), pp. 87-97.

Olins, P. O., Devine, C. S., Rangwala, S. H. and Kavka, K. S. (1988) 'The T7 phage gene 10 leader RNA, a ribosome-binding site that dramatically enhances the expression of foreign genes in *Escherichia coli*', *Gene,* 73(1), pp. 227-35.

Oliynyk, M., Samborskyy, M., Lester, J. B., Mironenko, T., Scott, N., Dickens, S., Haydock, S. F. and Leadlay, P. F. (2007) 'Complete genome sequence of the erythromycin-producing bacterium *Saccharopolyspora erythraea* NRRL23338', *Nat Biotechnol,* 25(4), pp. 447-53.

Ota, Y., Tamegai, H., Kudo, F., Kuriki, H., Koike-Takeshita, A., Eguchi, T. and Kakinuma, K. (2000) 'Butirosin-biosynthetic gene cluster from *Bacillus circulans*', *J Antibiot (Tokyo),* 53(10), pp. 1158-67.

Palumbi, S. R. (2001) 'Humans as the world's greatest evolutionary force', *Science,* 293(5536), pp. 1786-90.

Park, J. W., Ban, Y. H., Nam, S. J., Cha, S. S. and Yoon, Y. J. (2017) 'Biosynthetic pathways of aminoglycosides and their engineering', *Curr Opin Biotechnol,* 48, pp. 33-41.

Park, J. W., Hong, J. S., Parajuli, N., Jung, W. S., Park, S. R., Lim, S. K., Sohng, J. K. and Yoon, Y. J. (2008a) 'Genetic dissection of the biosynthetic route to gentamicin A2 by heterologous expression of its minimal gene set', *Proc Natl Acad Sci U S A,* 105(24), pp. 8399-404.

Park, J. W., Lee, S. G., Song, J. Y., Joo, J. S., Chung, M. J., Kim, S. C., Youn, H. S., Kang, H. L., Baik, S. C., Lee, W. K., Cho, M. J. and Rhee, K. H. (2008b) 'Proteomic analysis of *Helicobacter pylori* cellular proteins fractionated by ammonium sulfate precipitation', *Electrophoresis,* 29(13), pp. 2891-903.

Park, J. W., Park, S. R., Nepal, K. K., Han, A. R., Ban, Y. H., Yoo, Y. J., Kim, E. J., Kim, E. M., Kim, D., Sohng, J. K. and Yoon, Y. J. (2011) 'Discovery of parallel pathways of kanamycin biosynthesis allows antibiotic manipulation', *Nat Chem Biol,* 7(11), pp. 843-52.

Park, S. R., Park, J. W., Ban, Y. H., Sohng, J. K. and Yoon, Y. J. (2013) '2-Deoxystreptamine-containing aminoglycoside antibiotics: recent advances in the characterization and manipulation of their biosynthetic pathways', *Nat Prod Rep,* 30(1), pp. 11-20.

Peyman, G. A. and Herbst, R. (1974) 'Bacterial endophthalmitis. Treatment with intraocular injection of gentamicin and dexamethasone', *Arch Ophthalmol,* 91(5), pp. 416-8.

Piepersberg, W., Aboshanab, K. M., Schmidt-Beissner, H. and Wehmeier, U. F. (2007a) *Aminoglycoside Antibiotics: From Chemical Biology to Drug Discovery. Wiley series in drug discovery and development* New Jersey: John Wiley & Sons, Inc.

Piepersberg, W., Aboshanab, K. M., Schmidt-Beissner, H. and Wehmeier, U. F. (2007b) 'The biochemistry and genetics of aminoglyside producers', in Arya, D.P. (ed.) *Aminoglycoside antibiotics*. USA: John Wlley & Sons, Inc., pp. 68-75.

Pokrovskaya, V., Nudelman, I., Kandasamy, J. and Baasov, T. (2010) 'Aminoglycosides redesign strategies for improved antibiotics and compounds for treatment of human genetic diseases', *Methods Enzymol,* 478, pp. 437-62.

Prezant, R. T., Shohat, M., Jaber, L., Pressman, S. and Fischel-Ghodsian, N. (1992) 'Biochemical characterization of a pedigree with mitochondrially inherited deafness', *Am J Med Genet,* 44(4), pp. 465-72.

Price, K. E., Pursiano, T. A. and DeFuria, M. D. (1974) 'Activity of BB-K8 (amikacin) against clinical isolates resistant to one or more aminoglycoside antibiotics', *Antimicrob Agents Chemother,* 5(2), pp. 143-52.

Priuska, E. M., Clark-Baldwin, K., Pecoraro, V. and Schacht, J. (1998) 'NMR studies of iron-gentamicin complexes and the implications for aminoglycoside toxicity', *Inorganica Chimica Acta,* 273(1-2), pp. 85-91.

Priuska, E. M. and Schacht, J. (1995) 'Formation of free radicals by gentamicin and iron and evidence for an iron/gentamicin complex', *Biochem Pharmacol,* 50(11), pp. 1749-52.

Reader, J. S., Metzgar, D., Schimmel, P. and de Crécy-Lagard, V. (2004) 'Identification of four genes necessary for biosynthesis of the modified nucleoside queuosine', *J Biol Chem,* 279(8), pp. 6280-5.

Reiblein, W. J., Watkins, P. D. and Wagman, G. H. (1973) 'Binding of gentamicin and other aminoglycoside antibiotics to mycelium of various actinomycetes', *Antimicrob Agents Chemother,* 4(6), pp. 602-6.

Rice, N. M., Irving, H. M. N. H. and Leonard, M. A. (1993) 'Nomenclature for liquid-liquid distribution (solvent extraction)', *Pure & Applied Chemistry,* 65(11), pp. 2373-2396.

Rigali, S., Nothaft, H., Noens, E. E., Schlicht, M., Colson, S., Müller, M., Joris, B., Koerten, H. K., Hopwood, D. A., Titgemeyer, F. and van Wezel, G. P. (2006) 'The sugar phosphotransferase system of *Streptomyces coelicolor* is regulated by the GntR-family regulator DasR and links N-acetylglucosamine metabolism to the control of development', *Mol Microbiol,* 61(5), pp. 1237-51.

Rinehart, K. L. and Stroshane, R. M. (1976) 'Biosynthesis of aminocyclitol antibiotics', *J Antibiot (Tokyo),* 29(4), pp. 319-53.

Rognstad, R., Woronsberg, J. and Katz, J. (1968) 'Acetyl group transfer in lipogenesis. I. Studies involving the degradation of fatty acids by the Kuhn-Roth and related methods', *Arch Biochem Biophys,* 127(1), pp. 429-36.

Romo, A. J. and Liu, H. W. (2011) 'Mechanisms and structures of vitamin B(6)-dependent enzymes involved in deoxy sugar biosynthesis', *Biochim Biophys Acta,* 1814(11), pp. 1534-47.

Sairio, E., Kasanen, A., Kangas, L., Nieminen, A. L. and Nieminen, L. (1978) 'The nephrotoxicity of renal accumulation of amikacin, tobramycin and gentamicin in rats, rabbits and guinea pigs.', *International Journal of Experimental Pathology,* 15, pp. 370-375.

Salis, H. M. (2011) 'The ribosome binding site calculator', *Methods Enzymol,* 498, pp. 19-42.

Sandoval, R. M., Reilly, J. P., Running, W., Campos, S. B., Santos, J. R., Phillips, C. L. and Molitoris, B. A. (2006) 'A non-nephrotoxic gentamicin congener that retains antimicrobial efficacy', *J Am Soc Nephrol,* 17(10), pp. 2697-705.

Sat, B., Hazan, R., Fisher, T., Khaner, H., Glaser, G. and Engelberg-Kulka, H. (2001) 'Programmed cell death in *Escherichia coli*: some antibiotics can trigger mazEF lethality', *J Bacteriol,* 183(6), pp. 2041-5.

Savic, M., Lovric, J., Tomic, T. I., Vasiljevic, B. and Conn, G. L. (2009) 'Determination of the target nucleosides for members of two families of 16S rRNA methyltransferases that confer resistance to partially overlapping groups of aminoglycoside antibiotics', *Nucleic Acids Res,* 37(16), pp. 5420-31.

Schatz, A., Bugie, E. and Waksman, S. (1944) 'Streptomycin: A Substance Exhibiting Antibiotic Activity Against Gram-Positive and Gram-Negative Bacteria.', *Proceedings of the Society for Experimental and Biological Medicine,* 55, pp. 66-69.

Schentag, J. J. (1982) 'Aminoglycoside pharmacokinetics as a guide to therapy and toxicology', in Whelton, A. & Neu, H.C. (eds.) *The aminoglycosides: microbiology, clinical use, and toxicology.* New York: Marcel Dekker, Inc., pp. 143-167.

Schneider, G., Käck, H. and Lindqvist, Y. (2000) 'The manifold of vitamin B6 dependent enzymes', *Structure,* 8(1), pp. R1-6.

Schubert, H. L., Blumenthal, R. M. and Cheng, X. (2003) 'Many paths to methyltransfer: a chronicle of convergence', *Trends Biochem Sci,* 28(6), pp. 329-35.

Sha, S. H., Qiu, J. H. and Schacht, J. (2006) 'Aspirin to prevent gentamicin-induced hearing loss', *N Engl J Med,* 354(17), pp. 1856-7.

Shao, L., Chen, J., Wang, C., Li, J. A., Tang, Y., Chen, D. and Liu, W. (2013) 'Characterization of a key aminoglycoside phosphotransferase in gentamicin biosynthesis', *Bioorg Med Chem Lett,* 23(5), pp. 1438-41.

Shirling, E. B. and Gottlieb, D. (1966) 'Methods for characterization of *Streptomyces* species', *International Journal of Systematic and Evolutionary Microbiology,* 16, pp. 313-340.

Smith, P., Szu, P. H., Bui, C., Liu, H. W. and Tsai, S. C. (2008) 'Structure and mutagenic conversion of E1 dehydrase: at the crossroads of dehydration, amino transfer, and epimerization', *Biochemistry,* 47(24), pp. 6329-41.

Someya, A. and Tanaka, N. (1979) 'Interaction of aminoglycosides and other antibiotics with actin', *J Antibiot (Tokyo),* 32(2), pp. 156-60.

Song, B. B. and Schacht, J. (1996) 'Variable efficacy of radical scavengers and iron chelators to attenuate gentamicin ototoxicity in guinea pig in vivo', *Hear Res,* 94(1-2), pp. 87-93.

Spivey, H. O. and Ovádi, J. (1999) 'Substrate channeling', *Methods,* 19(2), pp. 306-21.

Stark, W. M., Hoehn, M. M. and Knox, N. G. (1967) 'Nebramycin, a new broad-spectrum antibiotic complex. I. Detection and biosynthesis', *Antimicrob Agents Chemother (Bethesda),* 7, pp. 314-23.

Starmer, J., Stomp, A., Vouk, M. and Bitzer, D. (2006) 'Predicting Shine-Dalgarno sequence locations exposes genome annotation errors', *PLoS Comput Biol,* 2(5), pp. e57.

Staunton, J. and Weissman, K. J. (2001) 'Polyketide biosynthesis: a millennium review', *Nat Prod Rep,* 18(4), pp. 380-416.

Stegmann, E., Frasch, H. J., Kilian, R. and Pozzi, R. (2015) 'Self-resistance mechanisms of actinomycetes producing lipid II-targeting antibiotics', *Int J Med Microbiol,* 305(2), pp. 190-5.

Steinman, A., Isoherranen, N., Ashoach, O. and Soback, S. (2010) 'Pharmacokinetics of gentamicin C1, C1a and C2 in horses after single intravenous dose.', *Equine Veterinary Journal,* 34(6), pp. 615-618.

Strohl, W. R. (1992) 'Compilation and analysis of DNA sequences associated with apparent streptomycete promoters', *Nucleic Acids Res,* 20(5), pp. 961-74.

Suami, T., Nishiyama, S., Ishikawa, Y. and Katsura, S. (1977) 'Chemical modification of neamine', *Carbohydr Res,* 53(2), pp. 239-46.

Sucipto, H., Kudo, F. and Eguchi, T. (2012) 'The last step of kanamycin biosynthesis: unique deamination reaction catalyzed by the α-ketoglutarate-dependent nonheme iron dioxygenase KanJ and the NADPH-dependent reductase KanK', *Angew Chem Int Ed Engl,* 51(14), pp. 3428-31.

Sugiyama, M. (2015) 'Structural biological study of self-resistance determinants in antibiotic-producing actinomycetes', *J Antibiot (Tokyo),* 68(9), pp. 543-50.

Sugiyama, M., Sakamoto, M., Mochizuki, H., Nimi, O. and Nomi, R. (1983) 'Purification and characterization of streptomycin 6-kinase, an enzyme implicated in self-protection of a streptomycin-producing micro-organism', *J Gen Microbiol,* 129(6), pp. 1683-7.

Sutherland, I., Hewitson, P. and Ignatova, S. (2009) 'New 18-l process-scale counter-current chromatography centrifuge', *J Chromatogr A,* 1216(19), pp. 4201-5.

Swan, S. K. (1997) 'Role of lipids in chronic renal allograft rejection', *Contrib Nephrol,* 120, pp. 62-7.

Takeishi, R., Kudo, F., Numakura, M. and Eguchi, T. (2015) 'Epimerization at C-3" in butirosin biosynthesis by an NAD(+) -dependent dehydrogenase BtrE and an NADPH-dependent reductase BtrF', *Chembiochem,* 16(3), pp. 487-95.

Tamegai, H., Nango, E., Kuwahara, M., Yamamoto, H., Ota, Y., Kuriki, H., Eguchi, T. and Kakinuma, K. (2002) 'Identification of L-glutamine: 2-deoxy-scyllo-inosose aminotransferase required for the biosynthesis of butirosin in *Bacillus circulans*', *J Antibiot (Tokyo),* 55(8), pp. 707-14.

Tang, X., Li, J., Millán-Aguiñaga, N., Zhang, J. J., O'Neill, E. C., Ugalde, J. A., Jensen, P. R., Mantovani, S. M. and Moore, B. S. (2015) 'Identification of Thiotetronic Acid Antibiotic Biosynthetic Pathways by Target-directed Genome Mining', *ACS Chem Biol,* 10(12), pp. 2841-2849.

Taniyama, H., Sawada, Y., Okuno, T. and Hashimoto, K. (1972) '[Separation and purification of water-soluble basic antibiotics by using microcrystalline cellulose "Avicel"]', *Jpn J Antibiot,* 25(2), pp. 84-90.

Tao, W., Yurkovich, M. E., Wen, S., Lebe, K. E., Samborskyy, M., Liu, Y., Yang, A., Ju, Y., Deng, Z., Tosin, M., Sun, Y. and Leadlay, P. F. (2016) 'A genomics-led approach to deciphering the mechanism of thiotetronate antibiotic biosynthesis', *Chem Sci,* 7(1), pp. 376-385.

Testa, R. T. and Tilley, B. C. (1975) 'Biotransformation, a new approach to aminoglycoside biosynthesis. I. Sisomicin', *J Antibiot (Tokyo),* 28(8), pp. 573-9.

Testa, R. T. and Tilley, B. C. (1976) 'Biotransformation, a new approach to aminoglycoside biosynthesis: II. Gentamicin', *J Antibiot (Tokyo),* 29(2), pp. 140-6.

Thomas, A. H. and Tappin, S. D. (1974) 'Separation of gentamicin complex by ion-exchange column chromatography', *J Chromatogr,* 97(2), pp. 280-3.

Toney, M. D. (2011) 'Controlling reaction specificity in pyridoxal phosphate enzymes', *Biochim Biophys Acta,* 1814(11), pp. 1407-18.

Torok, E., Moran, E. and Cooke, F. (2009) *Oxford Handbook of Infectious Diseases and Microbiology.* Oxford: OUP Oxford, p. Chapter 2 Antimicrobials.

Trujillo, M. E., Bacigalupe, R., Pujic, P., Igarashi, Y., Benito, P., Riesco, R., Médigue, C. and Normand, P. (2014) 'Genome features of the endophytic actinobacterium *Micromonospora lupini* strain Lupac 08: on the process of adaptation to an endophytic life style?', *PLoS One,* 9(9), pp. e108522.

Umemura, E., Sakamoto, Y., Takahashi, Y. and Miyake, T. (2015) 'Synthesis and antibacterial activity of 1-N-[(S)-ω-amino-2-hydroxyalkyl] derivatives of dibekacin, 5-deoxydibekacin, 3'-deoxykanamycin A and gentamicin B', *J Antibiot (Tokyo),* 68(6), pp. 421-3.

Unwin, J., Standage, S., Alexander, D., Hosted, T., Horan, A. C. and Wellington, E. M. (2004) 'Gene cluster in *Micromonospora echinospora* ATCC15835 for the biosynthesis of the gentamicin C complex', *J Antibiot (Tokyo),* 57(7), pp. 436-45.

Varley, A. J., Sule, J. and Absalom, A. R. (2009a) 'Principles of antibiotic therapy', *Continuing Education in Anaesthesia Critical Care & Pain,* 9(6), pp. 184-188.

Varley, A. J., Sule, J. and Absalom, A. R. (2009b) 'Principles of antibiotic therapy', *Continuing Education in Anaesthesia Critical Care & Pain,* 9(6), pp. 184-188.

Velayati, A. A., Masjedi, M. R., Farnia, P., Tabarsi, P., Ghanavi, J., ZiaZarifi, A. H. and Hoffner, S. E. (2009) 'Emergence of new forms of totally drug-resistant tuberculosis bacilli: super extensively drug-resistant tuberculosis or totally drug-resistant strains in iran', *Chest,* 136(2), pp. 420-425.

Vicens, Q. and Westhof, E. (2003) 'Crystal structure of geneticin bound to a bacterial 16S ribosomal RNA A site oligonucleotide', *J Mol Biol,* 326(4), pp. 1175-88.

Villano, S., Steenbergen, J. and Loh, E. (2016) 'Omadacycline: development of a novel aminomethylcycline antibiotic for treating drug-resistant bacterial infections', *Future Microbiol,* 11, pp. 1421-1434.

Vydrin, A. F., Shikhaleev, I. V., Makhortov, V. L., Shcherenko, N. N. and Kolchanova, N. V. (2003) 'Component Composition of Gentamicin Sulfate Preparations. ', *Pharmaceutical Chemistry Journal,* 37(8), pp. 448-450.

Wachino, J. and Arakawa, Y. (2012) 'Exogenously acquired 16S rRNA methyltransferases found in aminoglycoside-resistant pathogenic Gram-negative bacteria: an update', *Drug Resist Updat,* 15(3), pp. 133-48.

Wachino, J., Shibayama, K., Kurokawa, H., Kimura, K., Yamane, K., Suzuki, S., Shibata, N., Ike, Y. and Arakawa, Y. (2007) 'Novel plasmid-mediated 16S rRNA m1A1408 methyltransferase, NpmA, found in a clinically isolated *Escherichia coli* strain resistant to structurally diverse aminoglycosides', *Antimicrob Agents Chemother,* 51(12), pp. 4401-9.

Wagman, G. H., Marquez, J. A., Bailey, J. V., Cooper, D., Weinstein, J., Tkach, R. and Daniels, P. (1972) 'Chromatographic separation of some minor components of the gentamicin complex', *J Chromatogr,* 70(1), pp. 171-3.

Wagman, G. H., Marquez, J. A. and Weinstein, M. J. (1968) 'Chromatographic separation of the components of the gentamicin complex.', *Journal of Chromatography,* 34(2), pp. 210-215.

Wagman, G. H., Testa, R. T., Marquez, J. A. and Weinstein, M. J. (1974) 'Antibiotic G-418, a new *Micromonospora*-produced aminoglycoside with activity against protozoa and helminths: fermentation, isolation, and preliminary characterization', *Antimicrob Agents Chemother,* 6(2), pp. 144-9.

Wagman, G. H. and Weinstein, M. J. (1973) *Chromatography of antibiotics. Journal of Chromatography Library* Amsterdam, London, New York: Elsevier Scientific Publishing Company, p. 79-83.

Waguespack, J. R. and Ricci, A. J. (2005) 'Aminoglycoside ototoxicity: permeant drugs cause permanent hair cell loss', *J Physiol,* 567(Pt 2), pp. 359-60.

Walker, P. D. and Shah, S. V. (1987) 'Gentamicin enhanced production of hydrogen peroxide by renal cortical mitochondria', *Am J Physiol,* 253(4 Pt 1), pp. C495-9.

Walsh, C. T. (2016) 'Insights into the chemical logic and enzymatic machinery of NRPS assembly lines', *Nat Prod Rep,* 33(2), pp. 127-35.

Walsh, F. M. and Amyes, S. G. (2004) 'Microbiology and drug resistance mechanisms of fully resistant pathogens', *Curr Opin Microbiol,* 7(5), pp. 439-44.

Wang, W., Li, X., Wang, J., Xiang, S., Feng, X. and Yang, K. (2013) 'An engineered strong promoter for *Streptomycetes*', *Appl Environ Microbiol,* 79(14), pp. 4484-92.

Watson, A. A. and O'Callaghan, C. A. (2005) 'Crystallization and X-ray diffraction analysis of human CLEC-2', *Acta Crystallogr Sect F Struct Biol Cryst Commun,* 61(Pt 12), pp. 1094-6.

Weinstein, M. J., Luedemann, G. M., Oden, E. M. and Wagman, G. H. (1963) 'GENTAMICIN, A NEW BROAD-SPECTRUM ANTIBIOTIC COMPLEX', *Antimicrob Agents Chemother (Bethesda),* 161, pp. 1-7.

Weinstein, M. J., Marquez, J. A., Testa, R. T., Wagman, G. H., Oden, E. M. and Waitz, J. A. (1970) 'Antibiotic 6640, a new *Micromonospora*-produced aminoglycoside antibiotic', *J Antibiot (Tokyo),* 23(11), pp. 551-4.

Weinstein, M. J., Wagman, G. H., Marquez, J. A., Testa, R. T. and Waitz, J. A. (1975) 'Verdamicin, a new broad spectrum aminoglycoside antibiotic', *Antimicrob Agents Chemother,* 7(3), pp. 246-9.

Weinstein, M. J., Wagman, G. H., Oden, E. M. and Marquez, J. A. (1967) 'Biological activity of the antibiotic components of the gentamicin complex', *J Bacteriol,* 94(3), pp. 789-90.

Weissman, K. J. (2016) 'Genetic engineering of modular PKSs: from combinatorial biosynthesis to synthetic biology', *Nat Prod Rep,* 33(2), pp. 203-30.

WHO (2017) *WHO Model List of Essential Medicines*: World Health Organization. Available at: http://www.who.int/medicines/publications/essentialmedicines/20th_EML2017.pdf?ua=1.

Wilkinson, B. and Micklefield, J. (2007) 'Mining and engineering natural-product biosynthetic pathways', *Nat Chem Biol,* 3(7), pp. 379-86.

Wilschanski, M., Yahav, Y., Yaacov, Y., Blau, H., Bentur, L., Rivlin, J., Aviram, M., Bdolah-Abram, T., Bebok, Z., Shushi, L., Kerem, B. and Kerem, E. (2003) 'Gentamicin-induced correction of CFTR function in patients with cystic fibrosis and *CFTR* stop mutations', *N Engl J Med,* 349(15), pp. 1433-41.

Wu, Q., Liu, Y. N., Chen, H., Molitor, E. J. and Liu, H. W. (2007) 'A retro-evolution study of CDP-6-deoxy-D-glycero-L-threo-4-hexulose-3-dehydrase (E1) from *Yersinia pseudotuberculosis*: implications for C-3 deoxygenation in the biosynthesis of 3,6-dideoxyhexoses', *Biochemistry,* 46(12), pp. 3759-67.

Xu, Z., Wang, Y., Chater, K. F., Ou, H. Y., Xu, H. H., Deng, Z. and Tao, M. (2017) 'Large-Scale Transposition Mutagenesis of *Streptomyces coelicolor* Identifies Hundreds of Genes Influencing Antibiotic Biosynthesis', *Appl Environ Microbiol,* 83(6).

Yamaguchi, T. (1965) 'Comparison of the cell-wall composition of morphologically distinct Actinomycetes', *J Bacteriol,* 89, pp. 444-53.

Yamauchi, N. and Kakinuma, K. (1992) 'Confirmation of in vitro synthesis of 2-deoxy-scyllo-inosose, the earliest intermediate in the biosynthesis of 2-deoxystreptamine, using cell free preparations of *Streptomyces fradiae*', *J Antibiot (Tokyo),* 45(5), pp. 774-80.

Yim, G., Wang, H. H. and Davies, J. (2006) 'The truth about antibiotics', *Int J Med Microbiol,* 296(2-3), pp. 163-70.

Yim, G., Wang, H. H. and Davies, J. (2007) 'Antibiotics as signalling molecules', *Philos Trans R Soc Lond B Biol Sci,* 362(1483), pp. 1195-200.

Yokoyama, K., Numakura, M., Kudo, F., Ohmori, D. and Eguchi, T. (2007) 'Characterization and mechanistic study of a radical SAM dehydrogenase in the biosynthesis of butirosin', *J Am Chem Soc,* 129(49), pp. 15147-55.

Yoshizawa, S., Fourmy, D. and Puglisi, J. D. (1998) 'Structural origins of gentamicin antibiotic action', *EMBO J,* 17(22), pp. 6437-48.

You, C., Myung, S. and Zhang, Y. H. (2012) 'Facilitated substrate channeling in a self-assembled trifunctional enzyme complex', *Angew Chem Int Ed Engl,* 51(35), pp. 8787-90.

Yu, Y., Zhang, Q. and Deng, Z. (2017) 'Parallel pathways in the biosynthesis of aminoglycoside antibiotics', *F1000Res,* 6.

Zapp, M. L., Stern, S. and Green, M. R. (1993) 'Small molecules that selectively block RNA binding of HIV-1 Rev protein inhibit Rev function and viral production', *Cell,* 74(6), pp. 969-78.

Zheng, L., Baumann, U. and Reymond, J. L. (2004) 'An efficient one-step site-directed and site-saturation mutagenesis protocol', *Nucleic Acids Res,* 32(14), pp. e115.